New ongoing commissioning approach of central plants: methodology and case study


Danielle Monfet



A Thesis

In the Department

of

Building, Civil & Environmental Engineering



Presented in Partial Fulfillment of the Requirements

For the Degree of

Doctor of Philosophy (Building Engineering)

Concordia University

Montreal, Quebec, Canada


September 2011


© Danielle Monfet, 2011

**CONCORDIA UNIVERSITY**
**SCHOOL OF GRADUATE STUDIES**

This is to certify that the thesis prepared

By:         Danielle Monfet

Entitled:     New ongoing commissioning approach of central plants: methodology and case study

and submitted in partial fulfillment of the requirements for the degree of

Doctor of Philosophy (Building Engineering)

complies with the regulations of the University and meets the accepted standards with respect to originality and quality.

Signed by the final examining committee:

| | |
|---|---|
| Dr. I.G. Hassan | Chair |
| Dr. T.A. Reddy | External Examiner |
| Dr. M.Y. Chen | External to Program |
| Dr. T. Zayed | Examiner |
| Dr. M. Zaheeruddin | Examiner |
| Dr. R. Zmeureanu | Thesis Supervisor |

Approved by

Chair of Department or Graduate Program Director

Sept. 9, 2011

Dean of Faculty

**ABSTRACT**

**New ongoing commissioning approach of central plants: methodology and case study**

**Danielle Monfet, Ph.D.**

**Concordia University, 2011**

This research project proposes a new methodology and tool to perform ongoing commissioning of central plants. The proposed methodology includes a new approach for the development and use of benchmarking models in the context of ongoing commissioning. Different techniques are explored to establish the benchmarking models: (1) a static approach, which is based on pre-defined training set size and established different models for week days and weekend & holidays, or (2) window techniques, which are either augmented or sliding. Two different types of benchmark models are evaluated: correlation-based and Artificial Neural Network (ANN) models.

The proposed ongoing commissioning methodology is evaluated for two chillers installed in the central plant of the Concordia Sciences Building (CSB). Both chillers have identical capacity and performance characteristics; however, they have quite different operating hours. The results show that models developed with seven days of data monitored at the beginning of the summer season provide accurate results over the remaining of the summer and for the following summer. For the chillers used in the case study, the proposed multivariable polynomial (MP) models provide the most accurate prediction with CV(RMSE) below 7% over the remaining of the summer season, and below 8% for the following summer season.

As part of the ongoing commissioning approach, measured data used to develop the benchmarking models combined with manufacturer's information were also used to develop a calibrated computer model of the CSB central cooling plant in TRNSYS. User input files were modified to reflect the operating characteristics of the equipment installed in the central plant and a control equation was proposed for the cooling towers. The simulation results were in good agreement with the monitored data, with CV(RMSE) that do not exceed 5.5% for water temperature at key locations, 12.5% for the electric power input of the cooling equipment, and 18.6% for the COP of chillers and various groups of equipment. The Relative Error (R.E.) calculated over the summer season for the cooling electricity used is within ±15.6%.

The approach undertaken to calibrate the CSB central cooling plant showed that it is possible to develop a calibrated model using measurements already available from the Monitoring and Data Acquisition System (MDAS) and manufacturer data, without modifying by trial-and-error some variables or using stochastic approaches.

# ACKNOWLEDGMENTS

# TABLE OF CONTENTS

# LIST OF FIGURES

xi

xii

# LIST OF TABLES

xvi

# LIST OF ACRONYMES

| Name | Definition |
|------|------------|
| AHU | Air Handling Unit |
| ANN | Artificial Neural Network |
| CC$^{SM}$ | Continuous Commissioning$^{SM}$ |
| COP | Coefficient Of Performance |
| CSB | Concordia Science Building |
| CV(RSME) | Coefficient of Variance of the Root-Mean Square Error |
| DABO | Diagnostic Agent for Building Operation |
| EMCS | Energy Management Control System |
| FDD | Fault Detection and Diagnostics |
| FDDO | Fault Detection, Diagnostics and Optimization |
| HVAC | Heating, Ventilation, and Air Conditioning |
| MBE | Mean Bias Error |
| MDAS | Monitoring and Data Acquisition System |
| NMBE | Normalized Mean Bias Error |
| ML | Multivariable Linear |
| MP | Multivariable Polynomial |
| OPR | Owner's Project Requirements |
| PF | Power Factor |
| PACRAT | Performance and Continuous Re-commissioning Analysis Tool |
| RBAO | Remote Building Analysis and Optimization |
| R.E. | Relative Error |
| RMSE | Root-Mean Square Error |
| RPM | Rotation Per Minute |
| RLA | Relative Load Amperage |
| TRNSYS | TRaNsient SYstem Simulation |
| VAV | Variable Air Volume |
| VFD | Variable Frequency Drive |
| WBD | Whole-Building Diagnostician |

# NOMENCLATURE

| Symbol | | Units |
|---|---|---|
| **Roman** | | |
| $\dot{m}$ | Mass flow rate | kg/s |
| $\dot{q}$ | Rate of heat transfer | kW |
| $E$ | Electric energy use | kWh |
| $I$ | Electric current | A |
| $P$ | Rated capacity/power | kW |
| $Q$ | Total load | MJ |
| $\tilde{T}$ | Temperature | °C |
| $U$ | Uncertainty | |
| $V$ | Voltage | V |
| $UA$ | Overall heat transfer coefficient | kW/K |
| $C_p$ | Specific heat | kJ/kg ·°C |
| $\dot{E}$ | Instantaneous electric power | kW |
| $\dot{V}$ | Volumetric flow rate | m³/s |
| $\dot{Q}$ | Thermal load | kW |
| **Greek** | | |
| $\rho$ | Density | kg/m³ |
| $\Delta$ | Delta, difference | |
| $\sigma$ | Standard deviation | |
| **Subscript** | | |
| $t$ | Time | |
| $m$ | Logarithmic mean temperature difference | |
| *const.* | Constant speed equipment | |
| *elec.* | Central plant electricity use | |
| *fan* | Fan | |
| *pt* | Setpoint | |
| *pump* | Pump | |
| *rec.* | Recovered | |
| *reject.* | Rejected | |
| *water* | Water | |
| *BE* | Boiler economizer | |
| *CH* | Chiller | |
| *CHW* | Chilled water | |
| *CND* | Condenser | |
| *CT* | Cooling tower | |
| *E* | Evaporator | |
| *HW* | Heating water | |
| *VFD* | Complete with variable frequency drive | |
| **Superscript** | | |
| *CSB* | Concordia Science Building | |
| K | Temperature in Kelvins | |

# 1    INTRODUCTION

## 1.1    Problem statement

Improving building energy performance is becoming a common task in both newly constructed and existing buildings. The terms commissioning, re-commissioning, retro-commissioning, and ongoing commissioning are often used to describe the actions undertaken to verify if the installed building components or systems perform in compliance with the design specifications, current goals and/or Owner's Project Requirements (OPR). For new buildings, commissioning normally takes place before occupancy, and ensures the mechanical systems are checked for performance and system interoperability at part load and design conditions (ASHRAE 2005a). For existing facilities, re-commissioning or retro-commissioning are used to restore the facility's performance to its initial design specifications or to make the mechanical systems work efficiently (Abouzelof 2001). More recently, the new concepts of ongoing commissioning has been proposed for existing buildings to ensure that the strategies implemented continue to meet the current or evolving OPR throughout time (ASHRAE 2005a). Ongoing commissioning is a comprehensive process used to help resolve operation problems, improve comfort, optimize energy use and identify retrofits for existing commercial and institutional buildings and central plant facilities (Liu et al. 2002).

Ongoing commissioning provides great possibility to improve the energy consumption in buildings, which is something that needs to be addressed since the energy consumption of commercial and institutional buildings in Canada has increased by 33% between 1990 and 2005 (Natural Resources Canada 2008). This is particularly true for

the higher education sector (cégep and university establishments) in Québec, which represents 15% of the total floor area of the public sector, while accounting for 20% of the energy use (Roy 2008).

Ongoing commissioning is a complex approach for the monitoring and analysis of operational parameters of heating, ventilation and air conditioning (HVAC) systems and components in order to (1) detect faults and failures, (2) display warnings and recommend remedial actions, and estimate the energy or cost implications of such measures, (3) compare the monitored performance with benchmarking data to detect the deterioration of performance or abnormal operation conditions, and (4) present the relevant indicators of energy performance to help building operators and managers to become aware of the systems performance, and therefore, to undertake the required actions for achieving high performance along the systems useful life.

So far, no detailed or standard approach has been proposed by the industry to establish benchmarking models at the central plant component level in the context of ongoing commissioning. This research project proposes a new approach to develop benchmarking models that characterize the equipment or system performance under normal operation to identify operation problems using benchmarking models.

## 1.2   Scope and methodology

This research project proposes a new approach to perform ongoing commissioning in central plants, which includes a new approach to develop and use benchmarking models in the context of ongoing commissioning. Different techniques are explored to establish the benchmarking models as well as different types of benchmark

models (correlation-based and ANN models). The tool will attempt to periodically report the energy performance of equipment and of the overall central plant in order to maintain the systems operating performance.

The benchmarking models are established using previously monitored data. To illustrate the proposed approach, a case study for developing benchmarking models, in the context of ongoing commissioning, is presented for the electric power input to chillers installed in the central plant of a university building located in Montréal, Canada, the Concordia Sciences Building (CSB). The proposed approach can later on be extended to the other equipment present in the central plant or to the whole central plant.

Also, as part of the ongoing commissioning approach, a new approach is proposed to calibrate the TRNSYS model of the CSB central cooling plant, where measured data used to develop the benchmarking models combined with manufacturer's information are used to identify the TRNSYS user input files to reflect the operating characteristics of the equipment installed in the central plant.

To achieve the scope of this research project, the available literature on ongoing commission and inverse models is first reviewed (Chapter 2) followed by a detailed description of the proposed ongoing commissioning approach (Chapter 3). The following two chapters introduce the case study (Chapter 4) and the evaluation of the benchmarking models (Chapter 5). In Chapter 6, the calibration process and results are described. Finally, conclusions, contributions and future work of this project are presented in Chapter 7.

# 2    LITERATURE REVIEW

Ongoing commissioning is a complex approach to maintain optimum operation by performing constant monitoring of HVAC systems and equipment, data analysis, and sensors calibration and systems tuned up, as needed. Tools for ongoing commissioning can be used to (1) detect faults and failures, (2) display warnings and recommend remedial actions, and estimate the energy or cost implications of such measures, (3) compare the monitored performance with benchmarking data to detect the deterioration of performance or abnormal operation conditions, and (4) present the relevant indicators of energy performance to help building operators and managers to become aware of the systems performance, and therefore, to undertake the required actions for achieving high performance along the systems useful life.

The development of a new approach to perform ongoing commissioning requires a review of the literature to assess the current state of the industry. Available ongoing commissioning techniques, including available commissioning methods and software to assist the building managers developed by manufacturers and control companies, and benchmarking and inverse modeling methods are presented. Based on the review of the published information and the limitations of the presented techniques and tools, the objectives of the thesis are presented.

## 2.1    Commissioning classification and definitions

Improving building energy performance is becoming a common task in both newly constructed and existing buildings. The terms commissioning, re-commissioning, retro-commissioning, continuous commissioning$^{SM}$ and ongoing commissioning are often

used to describe the actions undertaken to verify if the installed building components or systems perform in compliance with the design specifications, current goals and/or Owner's Project Requirements (OPR). Commissioning, in any of its form, ensure and maximize the performance of energy efficiency measures (Mills 2011). It also involves identifying energy efficient strategies in ordinary buildings where no particular effort have been previously made to save energy. The persistence of the savings is often ensured using benchmarking and by revisiting the need to commission the building again.

### 2.1.1 Commissioning

For new buildings, commissioning normally takes place before occupancy, and ensures the mechanical systems are checked for performance and system interoperability at part load and design conditions (ASHRAE 2005a). ASHRAE has published two guidelines on commissioning: "Guideline 0-2005: The Commissioning Process" (ASHRAE 2005a) and "Guideline 1.1-2007: HVAC&R Technical Requirements for the Commissioning Process" (ASHRAE 2007). Both guidelines present the procedures to verify and document that the performance of the systems meets defined objectives and criteria. The major objectives include documenting the owner's requirements, verifying the building installation and performance, coordinating the systems installation and operation, and detecting system problems. Ideally the process starts at the beginning of the design phase, continues throughout the construction phase, and is finalized before occupancy. The contractors, designers, engineers and architects work in collaboration with an independent commissioning agent to perform the commissioning of new constructions.

### 2.1.2 Re-commissioning and retro-commissioning

Re-commissioning and retro-commissioning apply to existing buildings and are one time processes. In the case of re-commissioning, the building has previously been commissioned, while retro-commissioning applies to existing building that were not previously commissioned. The objectives are similar to the commissioning process. Re-commissioning has for goal to restore the facility's performance to its initial design specifications or to make the mechanical systems work efficiently (Abouzelof 2001). In the case of retro-commissioning, the process ensures that the building and its systems are adjusted to meet the current operational needs (Wiggins 2005). The retro-commissioning process include also technical retro-commissioning, where actual flows, temperatures and pressures of the building systems are compared to the actual control sequences to determine energy-efficient control sequences (McFarlane 2010).

### 2.1.3 Continuous and ongoing commissioning

Follow-up consumption tracking and initial commissioning is essential to ensure proper operation of the mechanical systems and perform continuous and ongoing commissioning. Techniques to perform commissioning, retro-commissioning, continuous commissioning[SM] and/or ongoing commissioning have similar objectives: improve the operation of the system based on design or building conditions. Commissioning, in any form, is based on a similar approach. However, continuous and ongoing commissioning ensure that the strategies implemented are maintained throughout time to improve the building performance. Continuous commissioning[SM] is a comprehensive process used to help resolve operation problems, improve comfort, optimize energy use and identify

retrofits for existing commercial and institutional buildings and central plant facilities (Liu et al. 2002). Continuous commissioning$^{SM}$ is performed periodically, usually every three or fourth months, while a much smaller time step, usually between ten minutes and one hour, is selected for ongoing commissioning (Claridge et al. 2004). The continuous and ongoing commissioning processes are a continuation of the initial commissioning process that take places before the occupancy and operation phase.

### 2.1.3.1  *Process description*

During continuous or ongoing commissioning, the project intent is only considered as a reference, not as the performance target, realizing that (1) the building designer rarely specifies the optimal operation of the systems, and (2) the building function and use have often changed significantly from original expectations (Liu et al. 2003a). The processes of continuous or ongoing commissioning are integrated approaches that implement optimal schedules for operating setpoints, and ensure optimal operation of the systems and persistence of the integrated changes. The objective is to maintain optimum operation by performing ongoing monitoring of the systems, data analysis and sensors calibration, and systems tuned up, as needed. However, this process has yet to be automated and only a limited number of applications have been developed, beyond the conventional control of HVAC systems, to automatically assess and maintain the performance of the mechanical systems.

Continuous or ongoing commissioning include different tasks to ensure the performance of the systems is maintained throughout time, which are defined for

different building sub-systems such as the air-handling units (AHU), the central cooling or heating plant or the storage system.

Three different approaches can be used to provide continuous and ongoing commissioning: (1) perform initial commissioning of a new building or retro-commissioning for an existing building, with quarterly follow-up evaluations to assess the energy building performance (typically called Continuous Commissioning[SM]); (2) an ongoing commissioning provider performs off-site continuous data collection of systems operation and use Fault Detection, Diagnostics and Optimization (FDDO) tools to evaluate energy consumption on a monthly basis and recommend measures to be implemented; or (3) the building operator purchases and implements a FDDO tool to continuously collect and analyse data to identify energy savings opportunities (Roth et al. 2008). Ongoing commissioning yields better results for large buildings where opportunities for improving and optimizing the systems interaction are possible.

The "Continuous Commissioning (CC)[SM] Guidebook" prepared by Liu et al. (2002) for the Federal Energy Management Program, US Department of Energy and "Methods for automated and continuous commissioning of building systems" prepared by the Portland Energy Conservation (ARTI 2003) provide examples of measures to be implemented. For instance, in the case of central chiller plants, the measurements needed for calculating the kW electric input per ton of refrigeration and rules-of-thumb to reset the supply chilled water temperature are presented. The ongoing measurement and analysis of energy performance can be used to: (1) identify problems; (2) establish a post-CC[SM] baseline to be used as a reference to which future performance is compared; and (3)

periodically trend some operating parameters and compare with historical levels. Some related developments are presented.

### 2.1.3.2   Case studies

Generally, the measured energy use savings per surface area are strongly dependent on the building type. Liu et al. (1997) performed a study in which the savings generated by $CC^{SM}$ are measured. The average savings are $13.56/m$^2$/yr for seven medical research laboratory buildings, $4.63/m$^2$/yr for six hospitals, $4.63/m$^2$/yr for five university teaching and office buildings, $2.37/m$^2$/yr for seven office buildings, and $1.83/m$^2$/yr for two school buildings.

Deng et al. (2001) developed a $CC^{SM}$ plan that was first applied on the air/water distribution of a building HVAC system, and later extended to central chilled/hot water distribution loops and utilities plants. Several strategies were developed: (1) optimized chiller/boiler operation schedule/sequence based on individual plant conditions and load profile, (2) a chilled/hot water supply temperature reset schedule based on the ambient temperature, (3) a chilled/hot water plant differential pressure (DP) reset schedule based on the ambient temperature or total flow rate, and (4) a condensing water supply temperature reset schedule based on the ambient temperature. The performance of the central plant was then monitored to demonstrate the benefit of $CC^{SM}$.

The $CC^{SM}$ process was also implemented at the South City Campus (Deng et al. 2005). The campus is divided between classrooms, offices, labs, cafeteria, two gymnasiums, an auditorium and a swimming pool. Two 300-ton, one 130-ton chillers, and three low-pressure steam boilers (two at 500 hp and one 150 hp) served 30 major Air

Handling Units (AHUs). To ensure optimal system operation, building data are monitored and compared with benchmark to improve the performance of the central plant. A temperature-based regression model was developed to estimate the energy savings due to the implementation of the different measures. The energy savings were estimated to be in excess of 10% of the utility bill.

Chen et al. (2006) also implemented $CC^{SM}$ for the chilled water cooling systems of a modern Central Utility Plant (CUP) with 935-ton chillers and five 100 hp Variable Frequency Drive (VFD) primary pumps. $CC^{SM}$ was applied to evaluate the already very efficient CUP, to further optimize its operation, and to reduce operation costs. The measures are presented in Table 2.1 and can be used as guidelines to optimize the cooling plant operation.

*Table 2.1: Example of $CC^{SM}$ measures applied to a central cooling plant (Chen, et al. 2006)*

| Item | Chilled water side | Condenser water side |
|---|---|---|
| Staging strategy | Improve so individual chillers are always operated in the high efficiency range | Applied to cooling tower fan |
| Temperature reset control | N/A | Temperature setpoint based on ambient wet-bulb temperature and system load |
| Flow control | N/A | Independent of chillers operation |
| Chiller start/stop control | Reduce electrical spike by spreading the AHU's start-up sequence, stage up chillers earlier, limit the maximum number of chillers running during AHUs start-up period, increase the time span between chillers stage up. | |

The $CC^{SM}$ process is well established; however, the implementation and description of ongoing commissioning approaches and tools still lack detailed methodologies to analyse monitored data.

## 2.2    Available tools for data collection and analysis

The installation of Energy Management Control System (EMCS) in modern buildings allows for the monitoring of operating parameters and energy performance of primary and secondary building system components. However, the analysis, interpretation and visualization of the collected data can still be enhanced, in the context of ongoing commissioning. A few studies and tools that have been developed to assist the evaluation process are presented in this section.

### 2.2.1    Data visualization tools

Various visualization techniques can be used to describe or evaluate the building performance such as line plots, carpet plots, scatter plots, which describe the functionality and performance of building and system in a visual way (Baumann 2004). The use of such techniques simplifies and allows for a rapid identification of errors, malfunctions, deterioration of performance and optimization opportunities.

Trend analysis is a powerful approach for commissioning or continuous commissioning (Seidl 2006). The "offset from setpoint" analysis is often performed on the data collected using the EMCS. This determines how long the component operates outside the boundary conditions and its magnitude above design conditions. The current operating trends are compared with the baseline trends, which are established under normal equipment operation. Once set up and tested, the analysis is done automatically. For example, the Universal Translator (UT) is a free tool that allows filtering, analysis and visualization of large amount of data (Seidl 2007). This tool can read large amount of data, transform trend data into databases with uniform time-stamps, graphically show

trend data in time series and perform limited automatic analysis to evaluate economizer performance and the ability of all equipment to maintain setpoints over time, which is useful to visualize data and perform simple commissioning task and energy tracking. However, the tool does not offer standardized and pre-programmed continuous analysis of mechanical systems and equipment performances.

### 2.2.2 *Data analysis tools*

Different companies have developed data collection/optimization tool. For example, one of the tools advises the plant engineers and/or operators on how to best operate the equipment to achieve the least-cost operation of the system at any time (Fernández-Polanco et al. 2005). The optimizer uses a mixture of plant data and manual data as input. The system generally runs by manual request, but automatic optimization is also possible. To evaluate the plant performance, two types of measurements are proposed: (1) Key Performance Indicators (KPIs) and (2) Energy-Influencing Variables (EIVs). The models are derived from design data, historical data, or thermodynamic principles. The optimization is performed using Mixed Integer Programming (MIP) and Non-Linear Programming (NLP) techniques. The tool finds the least-cost equipment operations that meet the process demand, while taking into consideration physical constraints and equipment availability.

The Remote Building Analysis and Optimization (RBAO) program informs operation managers via monthly reports that state the problems and possible solutions required to optimize the equipment of the building (Lash 2005). The objective of the method is to uncover faults that cannot otherwise be detected or uncovered from a one-

shot survey of a building or addressed with a commercial software product, since, in most cases, commercial software product still require on-site expertise and time to interpret the outputs. The RBAO uses a combination of artificial intelligence and advanced diagnostic methods to perform data analysis (Lash 2005).

The Diagnostic Agent for Building Operation (DABO), the software developed by the Intelligent Buildings Group of the CanmetENERGY Research Centre, provides automatic analysis and reporting of monitored data based on artificial intelligence algorithms, engineering calculations and statistical analysis (Choinière 2004). The software helps to improve the building operation by comparing the operating parameters of HVAC air-handling units, room control devices, heating and cooling circuits and rooftop units with the corresponding setpoint values (CANMET 2007). The analysis is performed in three steps: (1) hourly component analysis, (2) integrated systems analysis where the overall HVAC system is analyzed over a longer period of time, and (3) basic energy auditing (Choinière and Corsi 2003). The integrated systems analysis evaluates if the start up time, supply air temperature, supply air pressure, outdoor air level, and design equipment capacity are optimum. The software includes a data acquisition application that is linked to the building EMCS, a DABO-database (SQL server) and a client application (interface) that assists in the configuration of the building and HVAC systems, system analysis and viewing of results (CANMET 2007).

The Whole-Building Diagnostician (WBD 2008), the modular software developed at the Pacific Northwest National Laboratory, tracks the overall building energy use, monitors the performance of air-handling units, and detects problems with outside-air control. The WBD has two modules: the Whole-Building Energy (WBE) module and the

13

Outdoor Air Economizer (OAE) diagnostic module. The energy analysis of the WBE is based on an Energy Consumption Index (ECI), which is calculated as the ratio of actual energy consumption to the expected energy consumption of the whole building. The expected energy consumption values are estimated using empirical models of the building and systems. Detailed analysis of equipment energy consumption is not yet available. The other diagnostics module, the Outdoor-Air Economizer (OAE) diagnostician, detects air side economizer operation and ventilation problems. Based on the analysis of the recorded information, the OAE module generates a list of possible causes for economizer malfunctioning (Katipamula et al. 2003). The WBD uses graphical representation of the systems parameters, such as air temperature and energy consumption, and database of building energy performance over time to assist the users in identifying major changes in operations and energy consumption.

The HVAC System Assistant (ACRx Palm Pilot$^{TM}$ 2008) records measurements of key variables, and detects fault and degradation of the air conditioning refrigeration system; it informs the service technician of the existence of these conditions, the impact of these faults on energy consumption and the available savings potential. It also calculates the Efficiency Index (EI) and Capacity Index (CI) of the system. Data is transmitted from the databases and accessed via the online web service. Reports are generated including, for instance, the efficiency of the system, the priority of retro-commissioning or tune-up measures, and the estimation of electricity use when the tune-up is completed.

ENFORMA (2009) is an internet-based application that utilizes data from existing building automation system to continuously and automatically identify energy

14

inefficiencies of HVAC systems, by using rule-based fault detection and diagnostic techniques. The system displays the variation in time of selected parameters and evaluates the financial impact of faults.

Performance and Continuous Re-commissioning Analysis Tool (PACRAT 2009) is a tool for monitored data mining to improve facility management. It diagnoses system problems and poor performance, manages and summarizes monitored data, produces extensive reporting and visualization of system operational parameters, documents important operational parameters, provides interoperability for different automation systems, and summarizes/formats the data for effective visualization. It combines historical data from various sources, such as data collected via EMCS and data loggers into one format. It is designed to complement the EMCS, not duplicate its functions. The tool includes modules for AHU as well as chillers and hydronic components. Boiler and VAV box modules are under development (Santos et al. 2008). For each module, standard or user-defined characterization modules help in determining the cost of energy waste or anomalies.

Although the tools presented above have useful features assessing the performance of HVAC systems and the detection of eventual faults, they cannot be used directly in the ongoing commissioning of central cooling plant.

### 2.2.3   *Assessing the energy performance of buildings*

One approach to assess the monitored energy performance of buildings and their systems is to compare the measured data to benchmark data. The benchmark information is often determined using baseline models. Since the 1970s energy crisis, different tools,

techniques and approaches have been proposed to develop baseline models. Although the extensive review of all those developments is beyond the goal of this thesis, a few examples related to the development of baseline models or benchmark data are presented in this section. Spielvogel et al. (1977) developed several energy indices by using statistical analysis of simulation and actual building data. Sud and Wiggins (1983) developed simplified graphical procedure to estimate heating, cooling and electricity energy usage. Other studies on the development of base case energy consumption were presented by Wulfinghoff (1984), Sullivan et al. (1985) and MacArthur et al. (1989). Fels (1986) used the heating energy signature of a house to develop its weather-normalized baseline energy consumption (pre-retrofit value) to be used as a reference value for assessing the annual energy savings due to retrofits. Extensive research was carried out at Texas A&M University: one example is presented in Haberl and Claridge (1987).

Haves et al. (2001) presented different options for baseline analysis, such as previous or current performance of comparable buildings and/or previous or intended performance of the building in question. Typically, simple regression models are used to correct for differences between the conditions under which the actual performance is observed and the conditions for the baseline. Examples include weather and occupancy normalizations.

Baseline energy models, which are used to document energy savings, are developed using one of the following: (1) short-term measured data, (2) long-term hourly or 15-minute whole building energy data, such as building electricity, cooling and heating consumption, and/or (3) utility bills for electricity, gas and/or chilled or hot water (Liu et al. 2002). Most models are expressed as a function of outside air temperature since both

cooling and heating loads are normally weather dependent. Short-term data are useful to determine the baseline for specific pieces of equipment, while long-term data are more reliable to portray the whole building energy use. Models developed using long-term data also improve the detection of system faults during commissioning follow-up. It is recommended to include chilled water energy use or chiller electricity use, hot water/steam energy use or gas consumption, and overall building energy consumption in the baseline models.

Beasley et al. (2002) discussed a procedure to create a baseline of the daily performance of multi-building facilities served by a central plant. The statistical models predict the energy usage, utilizing historical daily data, and are normalized for weather and occupancy effects. Each component is empirically modeled based on past conditions. A comparison module determines the difference between the energy use prediction from the model and the consumption data.

Pattern recognition (Seem 2005) combined with statistical approach (Seem 2007) were also used to determine if the energy consumption of building components was significantly different than previously monitored energy consumption. The method accounted for weekly variation in energy consumption by grouping days of the week with similar power consumption. The method combines an outlier identification method that determines inconsistent numbers, for example energy consumption value, from a set, with additional statistical criteria used to determine if there are any outliers and quantify how many are present. The implementation in real buildings showed that when the appropriate day type is selected, abnormal operations can easily be detected.

Clustering techniques can also be used to identify performance issues in buildings (Santamouris et al. 2007). Simpler models have also been proposed, such as the used of change point multiple linear regression models (Jacob et al. 2010) and the use ANN with Heating and Cooling Degree Day (Yan and Yao 2010) to assess building performances.

Recent research on lifetime commissioning stated that quality control on building energy performances needed to be addressed and compared with design value (Djuric and Novakovic 2010). To address the issue on how to manage monitored data, Ahmed et al. (2010) proposed a data warehouse structure to visualize performance data, where the current data are compared with previously monitored data of the previous year. This approach was also explored by Torrens et al. (2011) to automate the comparison process and evaluate project alternatives.

The use of benchmarking data to detect abnormal operation conditions or performance deterioration is becoming more common. Two different benchmarking systems have been identified: public benchmarking and internal benchmarking (Chung 2011). Public benchmark models are developed using various methods and uses indices of performance from a large number of reference buildings to build benchmarking data; public benchmark models can be used to assess if a building performs poorer, similar or better than comparable buildings in the same region. On the other hand, internal benchmarking models are building specific: the benchmark model, simulation-based or ANN for example, cannot be directly used to establish the score for other buildings. So far, few studies have focus on developing a benchmark model for a particular building and then using it to identify variation of its energy performance over time (Kreider and

Haberl 1994; Haberl and Thamilseran 1996; Beasley et al. 2002; Paris et al. 2009; Ginestet and Marchio 2010).

### *2.2.4 Limitations*

All the tools related to continuous or ongoing commissioning used to evaluate building performance are often limited to the secondary (air-side) HVAC systems and whole building energy consumption. A limited number of tools have the capabilities to perform detailed system analysis. In most cases, the equipment specific analysis tools are not integrated to a complete continuous analysis tool. Furthermore, no detail procedure as to the quantity of monitored data required to establish the benchmark models are provided. Therefore, the evaluation of different techniques to establish benchmark models to perform ongoing commissioning of central plant equipment is required to enhance the currently existing models.

### 2.3 Inverse modeling

Benchmarking models are inverse models developed using monitored or simulated data used to evaluate the energy consumption or demand of the main building equipment (AHUs, fans, boilers, chillers, cooling tower and pumps) and the overall performance of the building or energy use.

Inverse or data-driven models are developed to estimate the systems energy use output (dependent) variables with the support of known and measured input (independent variables). Two different sets of data can be used to achieve this goal: intrusive and non-intrusive data. Intrusive data (or active data) are collected by operating the systems under predetermined or planned conditions for a broad range of system operating conditions

19

(ASHRAE 2001). By setting some restrictions on the system conditions, a more accurate model can be developed since a wider range of inputs and outputs is available to identify the system parameters. Non-intrusive data (or passive data) are collected under normal system operations and can include information such as temperature, pressure differential, metering data and utility bills. In most cases, the mathematical models (inverse models) are developed using non-intrusive data since they use available historical data and are directly monitored using the monitoring and data acquisition system (MDAS) used to control the operation of the building.

From the list of inverse models available in the literature, only two are selected, the analytical and ANN because they are the most commonly use, are relatively simple and flexible for ongoing commissioning purposes.

### 2.3.1   *Analytical models*

Different analytical inverse models have been used to predict the building performance. PRISM, the Princeton Scorekeeping Method, is an example of data-driven approach (Fels et al. 1986). The method uses information from past utility bills and weather data to evaluate energy savings due to renovations, for instance the replacement of a boiler. The Normalized Annual Consumption (NAC) index is calculated for the pre- and post-retrofit periods to evaluate the energy savings.

The ASHRAE HVAC 1 and 2 toolkits present component based models used to model primary and secondary HVAC components (Lebrun et al. 1994 and Brandemuehi et al. 1993). Primary system components are modeled using either regression methods, first-principle methods or a combination of both. The regression analysis is developed

20

using exponential forms, Fourier series, and second- or third-degree polynomials. Manufacturer data combined with one of the above mentioned functional forms allow the estimation of the equipment energy consumption at total and partial load (Lebrun et al. 1994).

Beck and Woodbury (1998) presented an overview of the general procedures and concepts used for parameters or functions identification by inverse techniques. The challenge in developing a good inverse model is to overcome two main difficulties: (1) to find the best correlation between different parameters and (2) the non-linearity and sensitivity of the solution to a number of variables. The developed model is considered satisfactory when the difference between the measured values and the predictions of the corresponding physical model is below a user-defined convergence criterion.

ASHRAE has presented algorithms that can be used to develop inverse models (Kissock et al. 2003). Numerical algorithms are presented for (1) general least-squares regression, for example linear, non-linear, multi-linear regressions, (2) variable-base degree-day (VBDD), (3) change-point, which capture the nonlinear relationship between heating and cooling energy use and ambient temperature caused by system effects such as control and latent loads, and (4) combination change-point multivariable regression models in the inverse modeling toolkit documentation. The proposed models were later on evaluated for different cases by Haberl et al. (2003).

At the component level, different models have been proposed for cooling and heating equipment. For example, models combining first-principles, manufacturer's data and/or thermodynamic correlations are presented in the references (Braun 1988, Brandemuehi et al. 1993, Lebrun et al. 1994, Bechtler et al. 2001, Chen et al. 2003, Solati

et al. 2003, Swider 2003, Saththasivam and Ng 2008). In all cases, the measurements are performed in laboratory settings, under steady-state conditions. Three models from the literature, pertinent to the topic of this study, are selected and presented below.

The York and Cappiello (Y&C) model (1982) estimates the electric power input $E_{CH}$ with a triquadratic polynomial (Equation (2.1)):

$$\dot{E}_{CH} = a + b \cdot Q_E + c \cdot T_{CNDR} + d \cdot T_{CHWS} + e \cdot Q_E^2 + f \cdot T_{CNDR}^2 + g \cdot T_{CHWS}^2 \\ + h \cdot Q_E \cdot T_{CNDR} + i \cdot Q_E \cdot T_{CHWS} + j \cdot T_{CNDR} \cdot T_{CHWS} + k \cdot Q_E \cdot T_{CNDR} \\ \cdot T_{CHWS} \tag{2.1}$$

where the coefficients $a$ to $k$ are indentified with available data points.

In the early nineties, Gordon and Ng presented and tested a chiller model relating the COP to the cooling load (Gordon and Ng 1994, Gordon and Ng 1995, Gordon and al. 1995). Later on, the model was refined into a three-parameter model (Gordon and Ng 2000) defined by Equation (2.2):

$$\left(\frac{1}{COP}+1\right)\frac{T_{CHWR}^K}{T_{CNDR}^K} - 1 = a_1 \frac{T_{CHWR}^K}{Q_E} + a_2 \frac{(T_{CNDR}^K - T_{CHWR}^K)}{(T_{CNDR}^K \cdot Q_E)} + a_3 \frac{(1/COP + 1) \cdot Q_E}{T_{CNDR}^K} \tag{2.2}$$

where $a_1$ (ΔS) is the total entropy production in chiller, $a_2$ ($Q_{leak}$) is the heat losses (or gains) from (or into) chiller, and $a_3$ (R) is the total heat exchanger thermal resistance.

Swider (2003) proposed a simple model to estimate the COP of chillers (Equation (2.3)).

$$COP = \alpha_1 \cdot Q_E + \alpha_2 \cdot T_{CHWR} + \alpha_3 \cdot T_{CNDR} \tag{2.3}$$

### 2.3.2 Artificial neural network (ANN) models

Different neural networks have been developed to predict building energy use (Kreider et al. 1995; Dodier and Henze 2004; Ben-Nakhi et al. 2004). Neural networks are models that determine the output by using compositions of basics functions of the

22

inputs. For example, the feed-forward approach is based on two steps: (1) prior determination of dependencies in the data set by using δ-test, and (2) feed-forward artificial neural networks for model building (system identification) (Ohlsson et al. 1994). The δ-test is used to determine dependency, assuming an underlying continuous function, by constructing conditional probabilities. A dependability index is defined to quantify the dependency on each of the variables. The system identification is then performed by realizing a function mapping for the input values to the output values.

The neural network with pre- and post-processing consisted of three parts: (1) an input vector, which consisted of independent variables, (2) an output vector, which consisted of dependent variables, and (3) an algorithm that maps the inputs to the outputs (Feuston and Thurtell 1994). The data were prepared using scaling transforms and principal component analysis, and a conjugate gradient method was employed to determine the model coefficients.

Some studies presented models to estimate energy savings for building retrofits (Krarti et al. 1998), while others try to predict future building energy use based on weather variables and building characteristics. In general, the training consists of adjusting the weights to minimize the error over a set of data. The case studies used to evaluate the performance of ANN showed that the cooling and heating loads could be predicted quite accurately without referencing to actual loads from the previous few hours.

### 2.3.3    *Great predictor SHOOTOUT*

The great energy predictor SHOOTOUT I competition was organized to evaluate various approaches that are available to perform data analysis and prediction. The objective was to identify the most accurate method to predict hourly energy use based on a limited amount of measured data using empirical models (Kreider and Haberl 1994). To predict the hourly energy use, the contestants were provided with a training set consisting of whole-building electricity (lights and receptacles), chilled water, hot water, and environmental data (ambient temperature, absolute humidity ratio, wind, and horizontal insolation). Two statistical measures were used to evaluate the predictions made with the various model: the coefficient of variation of the root mean square error (Equation (2.4)) and the mean bias error (Equation (2.5)).

$$CV(RMSE) = \frac{\sqrt{\frac{\sum_{i=1}^{n}(\hat{y}_i - y_i)^2}{n}}}{\bar{y}} \tag{2.4}$$

$$MBE = \frac{\sum_{i=1}^{n}(\hat{y}_i - y_i)}{n \cdot \bar{y}} \tag{2.5}$$

where *CV(RMSE)* is the coefficient of variance of the root mean squared error; *MBE* is the mean bias error; where $\hat{y}_i$ is the predicted value. $y_i$ is the measured value, $\bar{y}$ is the mean of the measured value sample data, and $n$ is the number of records of data in the testing set.

The Bayesian non-linear modeling, the feed-forward multilayer perceptron and the neural network with pre- and post-processing were the models that provided the best predictions (Kreider and Haberl 1994). The results from the three models had an average CV(RMSE) and MBE below 0.205 and 0.146, respectively for the prediction of whole-building electricity use, chilled water load and heating water load.

24

The great energy predictor SHOOTOUT II involved developing the most effective model to simulate energy baselines for the purposed of evaluating energy savings from retrofits (Haberl and Thamilseran 1996). Two buildings that received retrofits were used as case studies. The first building was an engineering building of 30,000 m$^2$ that contained classrooms, offices, a computer centre, laboratories facilities and an unconditioned underground parking garage. The second building was a business building, with a floor area of 12,925 m$^2$, which consisted of six stories of classrooms, offices and lecture halls. For both buildings, data sets were provided in different files for pre- and post-retrofit periods. Each file included independent variables (weather data and calendar time stamp) and corresponding dependent variables, such as whole-building energy use.

The winner of the contest used a combination of 10 neural networks with two hidden layers of 25 units each (Haberl and Thamilseran 1998). The runner-up of the contest, in contrast to the other participants, used a non-neural-net-based statistical day type routine for weather-dependent independent variables and weekday-weekend, hourly multiple regressions for the weather dependent data. The third place participant used a Bayesian non-linear regression with multiple hyper-parameters after removal of outliers. For all three models, the CV(RMSE) and the MBE were below 0.20 and 0.35 respectively.

### 2.3.4   Inverse models for ongoing commissioning

Inverse models are often used to develop baseline energy use in buildings. Baseline energy uses are frequently referred to benchmarking in an ongoing

commissioning context. The development of the inverse model allows the establishment of the benchmark model that can later on be used to evaluate the current performance of the building by comparisons (current performance versus benchmark performance). The benchmark model can also be used to evaluate the impact of optimization measures for the systems and equipment present in the building.

Different challenges must be overcome to evaluate techniques to identify model coefficients for benchmarking using monitored data. For example, Reddy et al. (2003a) looked at different initial length of data set for adaptive on-line training, techniques to determine when monitored data do not provide new information to the model parameters, and if the selected model influences the initial length of data set required for training. Two indices, the trace of a matrix of regressors (the sum of the diagonal elements) and the log of the mean of the determinant of regressors, were proposed to assess the length of data set required for training.

Reddy et al. (2003b) compared the use of four model types for the assessment of the prediction accuracy and their ability to evaluate the model parameter. They evaluate the models for on-line training for two different approaches: (1) by re-estimating the parameters or (2) by incrementally adjusting the parameters as newer monitored data are available. Two different field operated chiller data sets are used to evaluate the approaches and model types. The first data set consist of hourly data over five months, while the second data set consists of 1126 data sets of 15-minute data. The results obtained from the analysis showed that the CV(RMSE) varies widely for the sliding window approach. Also, for the evaluated correlation-based models, about 300 to 400 points is required to reach model stability. The final conclusion recommended the use of

the Gordon-Ng model for FD using model parameter tracking sets. The black-box multivariate polynomial model and the multilayer perceptron ANN model also showed good model prediction accuracy. In the study by Reddy et al. (2003b), the proposed approaches and models were evaluated for FDD using adaptive on-line training for steady-state performance. They also concluded that there is no significant difference between the internal and external predictive accuracy. The former refers to the model identification using data of the training set, while the letter refers to data of the testing set.

However, further evaluation of techniques and models must still be overcome to obtain a close representation of building or system behaviours: (1) the inputs relevant to the prediction must be determined, (2) the appropriate model structure for a given set of inputs must be selected, (3) the appropriate time lag must be selected, and (4) ensure the model excludes the noise from the data set (Dodier and Henze 2004).

The use of inverse or data-driven models for benchmarking is becoming more common. New rating systems, such as the Building Energy Quotient (Building EQ) proposed by ASHRAE requires two rating components: (1) an asset rating (as design) and (2) an operational rating (in operation) to assist owners and operators in understanding their building and identifying potential energy improvement measures (Colker 2009, Jarnagin 2009, Nall 2009). Currently, the Building EQ is calculated as the ratio between the Energy Use Index (EUI) for the subject building, divided by the median source EUI for that type of building in the same climate zone. For the operational rating, the calculation of Building EQ is based on actual utility bills over one full year; however the use of benchmarking models at the equipment level could lead to more complete assessment of the energy performance of buildings.

27

## 2.4 Objective of the thesis

The concept of ongoing commissioning is becoming more popular given the continual increase in energy costs. To reduce the energy use in buildings the current performance and operating conditions need to be continuously monitored and analysed, which also includes the comparison of measured data with benchmarking data to detect abnormal operation conditions or performance deterioration.

So far, no detailed or standard approach has been proposed by the industry to establish benchmarking models at the component and central plant level in the context of ongoing commissioning. This thesis proposes a new approach to develop benchmarking models that characterize the equipment or system performance under normal operation and to identify operation problems using benchmarking models. The benchmarking models are established using previously monitored data. This thesis is a contribution to the development of the ongoing commissioning approach, and focuses on discussing and presenting results for different training and retraining approaches to establish the benchmarking models. To illustrate the proposed approach, a case study for developing benchmarking models, in the context of ongoing commissioning, is presented for the electric power input to chillers of an existing central cooling and heating plant that serves several buildings.

The main objectives of the thesis are

1. To develop an ongoing commissioning approach to evaluate the energy performance of central plant for buildings, including an approach to establish benchmark models using monitored data;

2. To develop new benchmarking correlation-based and ANN models from the monitored data and assess their ability to be used to perform ongoing commissioning compared to existing models;

3. To test the proposed approach using a case study; and

4. To propose a calibration technique using a sub-set of monitored data and to calibrate a TRNSYS model of the central cooling plant.

The central cooling plant of the Concordia Sciences Building (CSB) is used to evaluate the proposed ongoing commissioning and benchmarking approaches.

Various tools and models have been developed to evaluate the performance of the secondary systems. Therefore, the focus of this study will be on the current building load used to perform ongoing commissioning of the central plant.

# 3   PROPOSED ONGOING COMMISSIONING APPROACH

The literature review (Chapter 2) presented different approaches and techniques to evaluate and predict the energy-related performance of buildings, including commissioning, re- and retro-commissioning and ongoing commissioning. Ongoing commissioning is a complex approach for the monitoring and analysis of operational parameters of HVAC systems and components in order to (1) detect faults and failures, (2) display warnings and recommend remedial actions, and estimate the energy or cost implications of such measures, (3) compare the monitored performance with benchmarking data to detect the deterioration of performance or abnormal operation conditions, and (4) present the relevant indicators of energy performance to help building operators and managers to become aware of the systems performance, and therefore, to undertake the required actions for achieving high performance along the systems useful life.

This research project proposes a new methodology to perform ongoing commissioning in central plants. The proposed methodology includes a new approach for the development and use of benchmarking models in the context of ongoing commissioning and a prototype tool to display the results and provide operating performance information to the building operators. So far, no detailed or standard approach has been proposed by the industry to establish benchmarking models at the component and central plant level in the context of ongoing commissioning.

The benchmarking models, which are energy baseline models, are obtained and updated using monitored data. This research proposes guidelines and recommendations for equipment and central plant benchmarking. This includes exploring different

techniques as well as different types of model, such as correlation-based and Artificial Neural Network (ANN) models that are suitable for benchmarking and ongoing commissioning.

The benchmarking models are established using previously monitored data. The proposed approach can be applied to any piece of equipment present in the central plant or to the whole central plant. The proposed approach can be used in buildings of different sizes; however it should be more cost effective in large buildings with complex systems and operating strategies. The remediation tasks to be performed, once operation problems have been identified, are beyond the purpose of this thesis. For specific action that could be undertaken to address the identified problems, refer to the Continuous Commissioning (CC)$^{SM}$ Guidebook (Liu et al. 2002) and the Methods for Automated and Continuous Commissioning of Building Systems (ARTI 2003) (Monfet and Zmeureanu 2011).

The new ongoing commissioning prototype tool is also presented and will periodically evaluate and compare the energy performance of heating and cooling central plants of large commercial and institutional buildings. This approach will ensure that no changes (e.g. degradation of equipment performances) occur throughout time without being noticed by the building operators. To help the building operators to detect changes, the current system performances is displayed continuously and reports and warnings are periodically transmitted to the operators. The proposed approach will also help maintain the performance of the systems.

31

## 3.1 Overview of the proposed ongoing commissioning methodology

Figure 3.1 presents a flow chart of the proposed methodology, including the main components used to develop the ongoing commissioning tool. The proposed ongoing commissioning methodology, which is to be integrated in the Monitoring and Data Acquisition System (MDAS) of large commercial and institutional buildings, is composed of (1) the preliminary phase, in which data are monitored and archived in a database, and benchmarking models (inverse models) of the energy performance of the central cooling and heating plan are developed and tested, based on past normal operation conditions, and (2) the ongoing commissioning phase, in which the actual performance of the central plant is compared with the results from the benchmarking models; finally, reports and warnings are sent to the building operators.
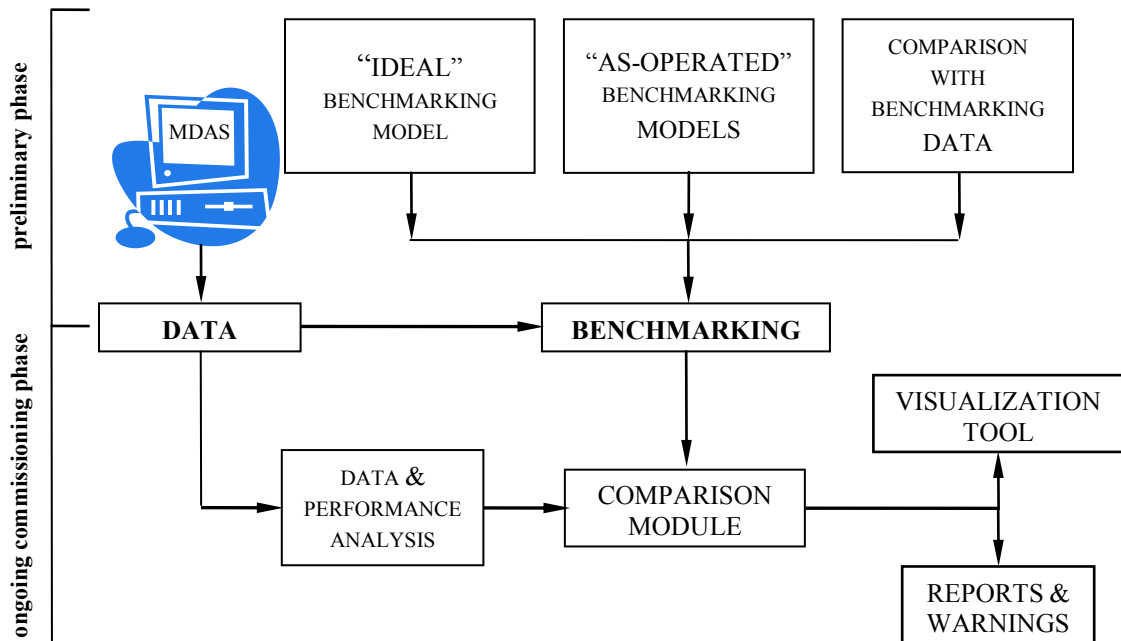


*Figure 3.1: Overview of the new ongoing commissioning concept (Monfet and Zmeureanu 2011)*

### 3.1.1 Preliminary phase

During the preliminary phase, the benchmarking models of the central plant energy performance under normal operating conditions, without known problems, are established. The benchmarking models are developed using monitored data, collected via the Monitoring and Data Acquisition Systems (MDAS), at the beginning of the ongoing commissioning process, and used as reference for future measurements. Normally, the data set used to establish the benchmarking models is composed of data monitored at the beginning of the ongoing commissioning process, which is supposed to be representative of the equipment operating conditions; however, this is not always the case since the equipment operation might be in a lower or higher range than normal operation. Thus, the minimum amount of data required to establish accurate benchmarking models and the frequency of retraining the models should be evaluated.

A library of benchmarking models contains; for instance, about 10 correlation-based models and 12 Artificial Neural Network (ANN) models for the electric power input (E, in kW) and Coefficient of Performance (COP). Correlation-based models and ANN models predict the value of a dependent variable (e.g., electric power input to a chiller) in terms of known input independent variables (e.g., outdoor air temperature $T$). The correlation-based models can be as simple as $E = a + b \cdot T$, where the coefficients $a$ and $b$ are identified from the data measured in the past (ASHRAE 2001). The ANN models are more complex as they mimic the information transfer in the human brain. In order to select the most appropriate benchmarking model, a large number of benchmarking models need to be developed and tested using several samples of monitored data. The central plant manager or consultant does not need to be familiar with

the benchmarking models, with the details about the model development, or mathematical background. The model development and application could be automatically controlled by the software that would be implemented in the MDAS, which is not part of this research project. However, the application software would include a feature to provide the user with the opportunity to select one particular model out of many available as well as to select the training data set from the database of monitored data.

For simplification, only one model is used to show the proposed step-by-step approach:

i. Select a set of monitored variables from a list of available sensors, and the recording time and duration: start recording the selected data via the MDAS in the database. It is assumed that during the monitoring and recording of data, the HVAC systems are in normal operation mode, without known problems or failures.

ii. Data monitored during the preliminary phase are used to calculate the weekly or daily benchmarking performance indices. For instance, the following indices should be calculated: total energy consumption, in $kWh/m^2$ per conditioned floor area of buildings supplied with chilled water by the central plant; peak or average electrical demand in kW or $kW/m^2$; average COP of chillers or of the overall central plant; and average thermal efficiency of heat exchangers ($\eta$). The benchmarking performance indices are compared with values from the central plant archive, if available, and with published values from similar central plants. The comparison enables the central plant operators to determine if the

performance of the systems before the beginning of the ongoing commissioning process is poorer, comparable or better than that of the same central plant in the recent past or with that of similar facilities.

iii.  Develop the benchmarking model, i.e., identify the coefficients of independent variables if a correlation-based model is selected, or train the ANN model by using a training set (a sub-set of the selected monitored data set from the database). Different training data sets are used of different lengths and from different acquisition periods. The accuracy of the model is evaluated by using a testing data set, which is the remaining sub-set of the selected monitored data set; and statistical indices such as the coefficient of determination ($R^2$) and the Coefficient of Variance of the Root-Mean-Square-Error (CV(RMSE)), in %. Normally, the training data set should be composed of data monitored at the beginning of the commissioning process, which might not be fully representative of the equipment operating conditions. Hence, different training and retraining techniques using static or dynamic windows (sliding window versus augmented window) are used and the results compared. This includes evaluating different acquisition periods as new data become available in the database, and the need for periodic or "when needed" retraining of the selected model. *This research project evaluates some existing models in terms of accuracy and proposes new models to assess the performance of the equipment and the central plant. The proposed research also studies the best selection of monitored data for the purpose of developing benchmark models, which includes determining the most*

35

*advantageous data acquisition period (when in time) as well as its duration (how long in time) for various existing and new models.*

**iv.** Repeat step (3) for each model of the library of benchmarking models.

**v.** Finally, one benchmarking model is selected based on the accuracy of the results over the testing set, the number of sensors needed, and the training and retraining time.

### 3.1.2 Ongoing commissioning phase

Once the initial/training data acquisition period is over and the benchmark models have been established, the following steps are followed:

**i.** The performance indices of major equipment and of the whole central plant, based on actual monitored data beyond the training set, are compared with the benchmarking targets such as electric power and COP. For this purpose, a statistical approach is used. If the measured index has a value outside the prediction interval, the equipment or the central plant as a whole has an abnormal performance, and a warning is sent to the building operators (Equations (3.5) and (3.6)).

**ii.** The results are presented via the ongoing commissioning prototype tool, which consists mainly of a visualization dashboard. Also, if the comparison shows deterioration in the performance, i.e. if the equipment is performing below its benchmark value, warnings and reports are sent to the building operator that specifies the problem area (Section 3.4).

**iii.** The ongoing commissioning prototype tool can later on be integrated into an existing program, such as DABO, to automatically perform ongoing commissioning of central plants.

## 3.2 Performance evaluation of the system

As part of the proposed ongoing commissioning methodology, data monitored during the preliminary phase are used to compare the current conditions with the design conditions to determine the operation changes that have occurred since the start-up of the systems and their impact on the equipment performances. The analysis could include for example: (1) the chilled and heating water demand, (2) the central plant electricity demand and the overall Coefficient of Performance, and (3) the electricity demand for each piece of equipment. Various daily, weekly and seasonal indices can be calculated to evaluate the performance of the central plant equipment: the peak electric demand in kW, the energy consumption (kWh and kWh/m$^2$ of the building conditioned floor area), the Coefficient of Performance (COP) at the equipment level, and the heat exchangers effectiveness ($\eta$). The indices are used to evaluate the performance of the central plant when compared with values from the central plant archive, if available, with published values from similar central plants, and as a reference point for future comparison.

## 3.3 Benchmarking

Ongoing commissioning helps to maintain and even improve system energy performance throughout time. The process requires the development of performance baselines, which are targets that must be met to maintain the operation of the systems. The performance baselines are energy baseline models that normally include models for

whole building electricity, cooling energy, and heating energy that are either based on regression models or a calibrated simulation (Liu et al. 2003a). For the new concept, the performance baseline is referred to as a benchmarking model, i.e. as the reference model for future comparison. This project proposes and evaluates different approaches and model types to develop the benchmarks.

The benchmarking models are developed using monitored data. The models can also be used to estimate benchmark indices (e.g. COP or electricity use), which might not be directly available through the MDAS.

### 3.3.1 Methodology

As presented in the literature, several different mathematical models are available to evaluate central plant or equipment performances (Chapter 2). However, information on required data set size to develop the models or the period/operating characteristics for which the models are applicable is rarely available. Hence, the effectiveness of different approaches to establish the benchmark models is evaluated for different model types.

For each approach, the data set selected for developing the benchmarking model is divided in two sub-sets: (1) a training data set and (2) a testing data set. Different methods of dividing the selected data set into training and testing data sets (e.g., random selection) can be considered. In this research project, the training data set uses two-thirds of the benchmarking data set (Kreider and Haberl 1994), and the testing data set uses the balance of the data set to verify the correctness of the models before it is used for benchmarking. Different training and retraining techniques using static windows or dynamic windows (sliding window or augmented window) are used, and the results

compared. An example of the application of such training techniques for the prediction of electric input for HVAC systems using ANN models is presented in Yang et al. (2005).

### 3.3.1.1 Static approach

The static technique is used to train the selected model based on a pre-defined training set size, such as the first month of summer or as soon as the data are available from the MDAS; the model is not retrained when new data become available. The static benchmarking model can be developed for various day types, i.e. for different load patterns (week days versus weekend and/or holidays, or week days with different activity types).

In order to determine the minimum amount of monitored data required to establish the benchmark models, testing is performed by varying the training set size and the period for which it applies to determine which combinations provide the most accurate results for each model. Therefore, different scenarios are tested. For example, the training set uses data of the first week of the summer, or the first month of the summer to establish the model for the next days, weeks or the entire summer or cooling season. The analysis is also used to determine the minimum training data set size required at the beginning of the ongoing commissioning process, when only a limited amount of data is available to establish the benchmark. Recommendations are then drawn from the analysis and made available to the user to select the appropriate training data set (how much and when) at the beginning of the ongoing commissioning process.

### 3.3.1.2 Window approach

The dynamically-trained benchmarking model can adapt itself to changes in the energy consumption pattern. For the window technique, the model is retrained periodically using new monitored data. Two different window types are evaluated: the augmented window and the sliding window. In the case of the augmented window technique (Figure 3.2), the initial benchmarking model is developed (trained and tested), for example, by using the window composed of three data sets (no.1 to no.3). Once the model is developed, the new monitored data sets (no.4 to no.9) are compared with the predicted values from the benchmarking model. The window is increased as new data are collected, and is composed now of five data sets (no.1 to no.5). The benchmarking model is retrained using the new enlarged window. The monitored data sets (no.6 to no.9) are compared with the predicted values from the retrained benchmarking model.

The new collected data are added in to the initial training set periodically (daily, weekly, bi-weekly or monthly), thus enlarging the window size, before retraining occurs. At the end of summer season, for instance, the augmented window data set is large and covers the whole spectrum of operating and weather conditions; however, it requires large data storage capacity, and the training/retraining time of benchmarking models could become of concern.
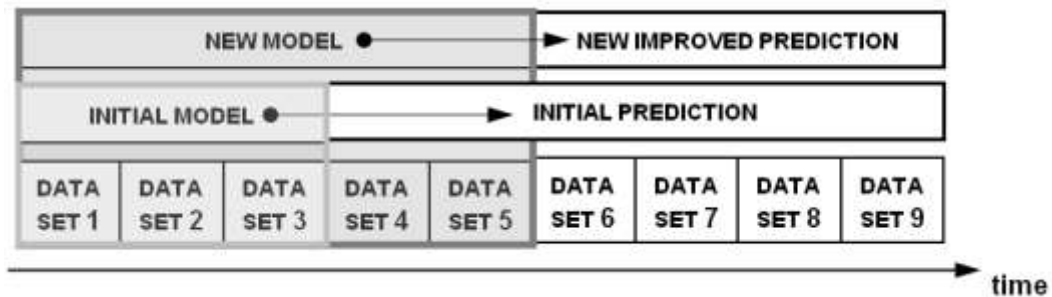


*Figure 3.2: Example of the augmented window process*

In the case of the sliding window (Figure 3.3), the window size is kept constant throughout the evaluation season. The initial benchmarking model is developed (trained and tested) by using the window composed of three data sets (no.1 to no.3). When data set no.4 becomes available, it is added to the data set, while the data set no.1 is dropped from the data, before retraining occurs. Once the model is developed, the new monitored data sets (no.5 to no.9) are compared with the predicted values from the benchmarking model, which is based on the window data sets (no.2 to no.4). The sliding window technique does not increase the need for storage capacity nor the training time as the amount of data used for training remains the same; however, it predicts well the energy performance when the actual operation conditions are in the range of those covered by the reduced training window.
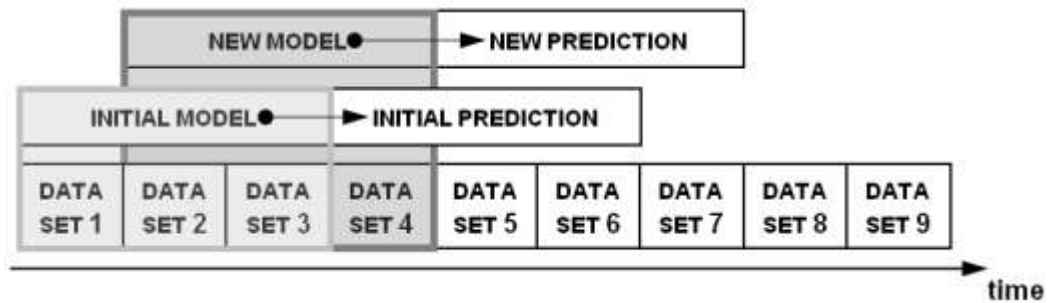


*Figure 3.3: Example of the sliding window process*

For both cases, the integration of the window approach in an ongoing commissioning scheme might increase the complexity of the problem and computing time. Both approaches are analyzed in terms of performance and accuracy and based on the results; guidelines will be proposed to establish accurate benchmark models.

41

### 3.3.2  Model types

The different window approaches proposed to establish the benchmark models at the equipment and the central plant level are evaluated for two different model types: (1) correlation-based models, and (2) ANN models. The performance of each model type is evaluated with the same training data set. The analysis will determine which models are more appropriate to establish the benchmark models in an ongoing commissioning perspective.

### 3.3.2.1  Correlation-based models

A number of models are available to evaluate the performance of the main equipment installed in central plants (Chapter 2). For example, models combining first-principles and correlations are presented in the ASHRAE Toolkits (ASHRAE Toolkits 1 (1994) and 2 (1993)). Other models have been proposed that use and/or combine first-principle, manufacturer data and correlations based on measurements for chillers and cooling towers (Braun 1988, Chen et al. 2003, Solati et al. 2003, and Saththasovam and Ng 2008). In all cases, the input variables are defined, but the required training data set characteristics, e.g. the quantity of data required, are not presented.

Identification of the model coefficients

For the correlation-based models, the model coefficients are identified using least-square regression in STATGRAPHICS (2008). For example, in its general form, a multiple linear regression model or correlation-based model is written according to Equation (3.1):

$$y = a_0 + a_1 \cdot x_1 + a_2 \cdot x_2 + \cdots + a_p \cdot x_p + e \qquad (3.1)$$

where $y$ is the dependent variable, $x$ are the independent variables, $a$ are the unknown regression coefficients, and $e$ is the error or residual. The parameter $p$ denotes the number of independent variables.

To identify the coefficients, the sum of the squares (SS) of the residuals (Equation (3.2)) between the measured and calculated dependent variable is differentiated with respect to each coefficient and set equal to zero. The problem can then be rewritten in matrix form (Equation (3.3)) or in simple form as described by Equation (3.4). The coefficients [A] are then identified by solving Equation (3.4).

$$SS = \sum_{i=1}^{n} \left( y_i - a_0 - a_1 \cdot x_{1i} - a_2 \cdot x_{2i} - \cdots - a_p \cdot x_{pi} \right)^2 \tag{3.2}$$

$$\begin{Bmatrix} 1 & x_{11} & x_{12} & \cdots & x_{1p} \\ 1 & x_{21} & x_{22} & \cdots & x_{2p} \\ \vdots & \vdots & \vdots & & \vdots \\ 1 & x_{n1} & x_{n2} & \cdots & x_{np} \end{Bmatrix} \begin{bmatrix} a_0 \\ a_1 \\ a_2 \\ \vdots \\ a_n \end{bmatrix} = \begin{bmatrix} y_1 \\ y_2 \\ y_3 \\ \vdots \\ y_n \end{bmatrix} \tag{3.3}$$

$$\{X\}\,[A] = [Y] \tag{3.4}$$

Once the model coefficients are identified, the model is tested and can then be used to perform ongoing commissioning.

Prediction interval

The tested model is used to perform ongoing commissioning where the performance indices of major equipment and of the whole central plant, based on actual monitored data beyond the training set, are compared with the benchmarking targets. For this purpose, a statistical approach is used where a warning is sent to the building operators if the measured index has a value outside the prediction interval.

The confidence limit of the forecast is given by Equation (3.5):

$$\hat{y}_i \pm t_{\alpha/2,n-p} \sqrt{\mathrm{MSE}(X_i{}'(X'WX)^{-1}X_i)} \tag{3.5}$$

where $t_{\alpha/2,n\text{-}p}$ is the *t*-value with *n-p* sample size, leaving an area of *α/2* to right and left, and the expression $\sqrt{\text{MSE}(X_i{}'(X'WX)^{-1}X_i)}$ is the standard error for the forecast. For a sample size greater than 30 for a 95% confidence interval, the prediction interval can be estimated by Equation (3.6):

$$\hat{y}_i \pm 1.96 \cdot \text{RMSE} \tag{3.6}$$

where 1.96 represents the *t*-value and RMSE is the Root-Mean-Square-Error calculated using Equation (3.7):

$$RMSE = \sqrt{\frac{\sum_{i=1}^{n}(y_i - \hat{y}_i)^2}{n - p}} \tag{3.7}$$

The prediction interval is used in the ongoing commissioning prototype tool: if the measured values/index falls outside the computed interval, an operating performance issue has been identified.

### 3.3.2.2 ANN models

Artificial neural networks (ANN) benchmarking models of the central plant equipment, developed using the same set of monitored data, are also proposed and tested.

The general model for the proposed ANN includes an input layer with $x_i$ neurons, one or more hidden layers with $h_{j,i}$ neurons, and an output layer with $y_i$ neurons, where *i* defines the number of neurons and *j* the number of hidden layers. The network is characterized by (1) its architecture, i.e. the pattern of connections between each neuron, (2) its training or learning algorithm, which is the method used to determine the weights on the connections, and (3) its activation or transfer functions (Fausett 1994).

In this study, the proposed benchmark ANN models are feedforward backpropagation networks. The feedforward network consists of one input layer, $N$ hidden layers, and one output layer. For feedforward backpropagation networks, using multi-layers, a hyperbolic tangent sigmoid transfer function provides good results between the input and the hidden layers as well as between hidden layers (Fausset 1994, Krarti et al. 1998, Dodier and Henze 2004, and MATLAB 2008). The hyperbolic tangent sigmoid transfer function (Figure 3.4a) is defined by Equation (3.8) where $H_j$ is described by Equation (3.9). Equation (3.9) presents a set of weights ($w$) and bias ($b$) that are used between each connection (neuron) and adjusted to minimize the error.

$$h_{ij} = f(H_j) = tansig(H_j) = \frac{2}{\left(1 + exp(-2 \cdot H_j)\right)} - 1 \tag{3.8}$$

$$H_j = b_j + \sum_{i=1}^{n} x_i \cdot w_{ji} \tag{3.9}$$

The transfer function used to determine the output is set to linear (Figure 3.4b), which is appropriate for regression problems with continuous real value targets (Dodier and Henze 2004). The transfer function describes a linear relationship between the neurons from the last hidden layer and the neurons of the output layer (MATLAB 2008).
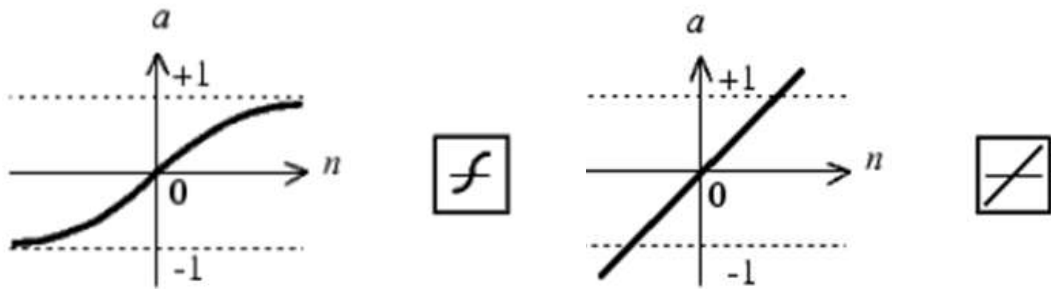


Figure 3.4: Transfer function (MATLAB 2008) - (a) hyperbolic tangent sigmoid, (b) linear

Researchers have used different techniques to train ANN models to predict the energy use of different pieces of equipment or the building loads. For example, building energy use was predicted successfully using the conjugate gradient method (Feuston and Thurtell 1994), the gradient descent backpropagation method (Dodier and Henze 2004), while the generalised radial basis function has been used to predict chiller performances (Bechtler and al. 2001 and Swider 2003).

In this study, the Bayesian regularization backpropagation is selected for training. The Bayesian regularization backpropagation updates the weight and bias values according to Levenberg-Marquardt optimization. This technique minimizes a combination of the sum of the squared errors and weights. The Levenberg-Marquardt algorithm is designed to approach a second order training speed and is an efficient method to train moderate-sized feedforward neural networks (up to several hundred weights). The backpropagation is used to calculate the new performance with respect to the weights and bias variables (MATLAB 2008).

Different training data sets of different sizes are tested in this study as well as different combinations of hidden layers and neurons per layers. The benchmark ANN models are developed using MATLAB (2008). The prediction interval for the ANN model is determined according to Equation (3.6).

## 3.4    Ongoing commissioning prototype tool

The proposed ongoing commissioning tool uses the data available via the MDAS to evaluate the performance and carry out ongoing commissioning of the central plant for the main pieces of equipment that provide cooling and heating to the building. A 15-

minute comparison module, which compares the current data (peak and total demand at that moment) with the benchmark values, is used to assess the performance of the systems. If the comparisons show deterioration in the performance, warnings are sent to the building operators that specify the problem area(s), such as which piece of equipment is performing below the benchmark value.

In addition, a visualization tool is also proposed. The tool includes a graphic representation of the benchmark energy use of the main equipment and central plant as well as the measured energy consumption which is added to the graphic as the information becomes available. Dials for the main indices (COP, η) are also used to provide a better understanding of the current performance of the systems. The dials show the optimum, acceptable and out of range performance criteria in real-time. Figure 3.5 presents an example of the visualization tool. Also, an economic module could also be integrated to the tool.

The proposed approach and techniques can then be integrated to an existing tool, such as DABO, to automatically perform ongoing commissioning of central plants.
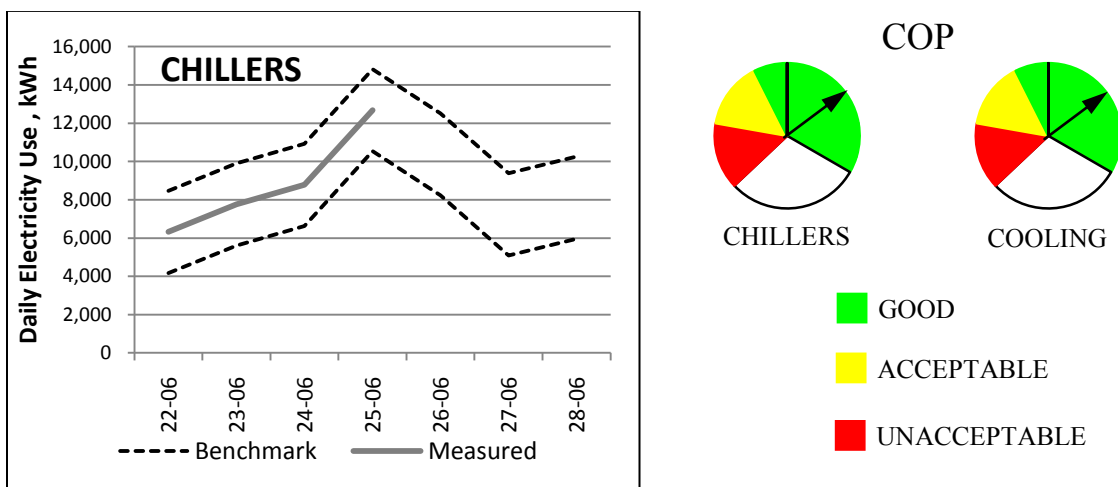


*Figure 3.5: Overview of the proposed visualization tool*

# 4    CASE STUDY: CONCORDIA SCIENCES BUILDING

The Concordia Sciences Building (CSB) is located on the Loyola campus in Montréal and has a total floor area of 32,000 m². The building is divided in three main sectors: sector A, B and C (Figure 4.1). Sector A is the heart of the building and mainly consists of laboratories and offices. Sector B is the Bryan wing, an existing building that is integrated to the CSB, where the majority of the envelope infrastructure has been conserved and the interior has been redesigned to accommodate the new university needs. Sector C is located on the south-west side of the building.
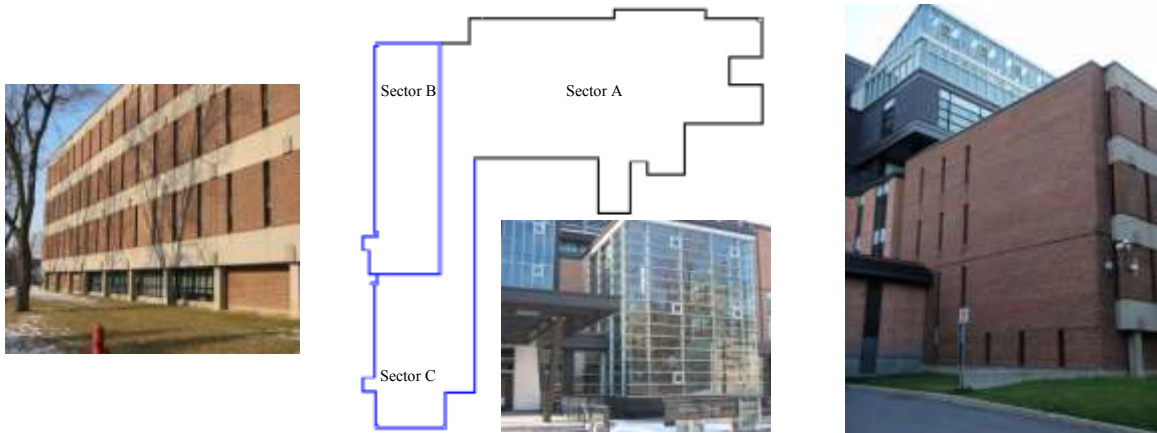


*Figure 4.1: General building layout*

The floor plans of sector A are divided between office spaces and laboratories. Offices are principally located along the south-east and south-west perimeters. The main entrance is along the south façade of the building. The building is eight stories high. There are two basements with storage areas, testing labs and classrooms. Staff offices and teaching areas are located on the five floors above ground. The sixth floor is a mechanical penthouse where most of the HVAC equipment is located. Sector A also includes an atrium located on the west portion of the wing that acts as a transition area between the existing structure and the new structure.

Sector B is the renovated section of the building. The existing Bryan building has been integrated to the new complex. The building is four stories high. There is one basement where offices and lockers are located. The three floors above ground are essentially used for office spaces.

Sector C is the south-west wing of the building. There are four stories above ground and one basement floor. Research labs, computer labs, and machine shops are located in the basement. The fourth floor is a mechanical penthouse where mechanical systems for both sectors B and C are installed. Offices are located along the east façade and labs occupied the remaining of the floor space.

## 4.1    Description of the CSB central plant

A thermal central plant serves all sectors of the building, where different heat recovery systems have been installed to improve the overall performance of the central plant. Chilled water, heating water and steam are supplied to the building to respond to the building load.

### 4.1.1    Cooling systems

Figure 4.2 is a simplified schematic representation of the chilled water components present in the central plant.

#### 4.1.1.1    Cooling equipment for summer design operation

During the summer, two centrifugal chillers, CH-1 and CH-2, provide chilled water to the air-handling units (AHU) installed in the building CSB (point A) and the administrative (AD) building (Point B). The chillers use R-123 refrigerant, have a cooling

capacity of 3165 kW (900 tons) each, and the coefficient of performance (COP) is 5.76 at design conditions. The chilled water leaves at 5.6°C and returns at 13.3ºC, thus providing the cooling required within the CSB (point A) and the AD building (point B) during the summer. When the first chiller is started, the corresponding chilled water and condenser water pumps are started simultaneously. The fans of the cooling towers are started when the condenser pumps are started, if required. The second chiller is only started if the chilled water demand is not meet by the first chiller. In this case, the second set of pumps and cooling tower is also started.

The chillers are cooled down by two perpendicular flow cooling towers, CT-1 and CT-2, having a capacity of 4750 kW (1350 tons) each at design conditions. The condenser water temperature enters the cooling tower at 35.0°C and leaves at 29.4 ºC. During the summer, one of the chillers can operate under heat recovery mode. For that chiller, at design conditions, about 80 % of the condenser water is directed first to a heat exchanger (HX-3) to pre-warm the heating water return, and then mixed with the remaining 20 % before being sent to the cooling tower. The cooling tower fans are turned off whenever the outdoor air conditions allow it. Also, if the chilled water load is low, two smaller chillers, chillers CH-3 and CH-4, are used to provide chilled water to the CSB, while the two large chillers are turned off and the AD building is cooled using outdoor air.

### 4.1.1.2 Cooling equipment for winter design operation

For the CSB, two small chillers, chillers CH-3 and CH-4, installed in the CSB, serve the fan coil units during the winter and part of the shoulder seasons, while cooling

is provided to the AD building using outdoor air. The chillers have a capacity of 352 kW (100 tons) each. The condensers of the smaller chillers (CH-3 and CH-4) are directly connected to the heating water loop to pre-warm the heating water return.

### 4.1.2 Heating systems

Heating water is produced and used for various means, such as specific laboratory applications, heating and humidification (Figure 4.3). During the summer, steam and re-heat water are provided to the CSB, while during the winter, steam and high temperature heating water are provided.

### 4.1.2.1 Heating equipment for summer design operation

During the summer, steam is provided by a high efficiency natural gas boiler (B-1) having a capacity of 815 kW. Steam is used to produce low-, mid- and high-temperature heating water for various purposes as well as being directly used to feed the humidifiers, if required. During this period, the hydronic heating system, which is used for re-heat purposes only, operates on 35ºC supply and 29.4ºC return water temperatures. For that same period, if chillers CH-1 or CH-2 are in operation, the boiler economizer system (S-1) is turned off, and heat is recovered from the cooling towers CT-1 or CT-2 using the heat exchanger HX-3 (Figure 4.3).
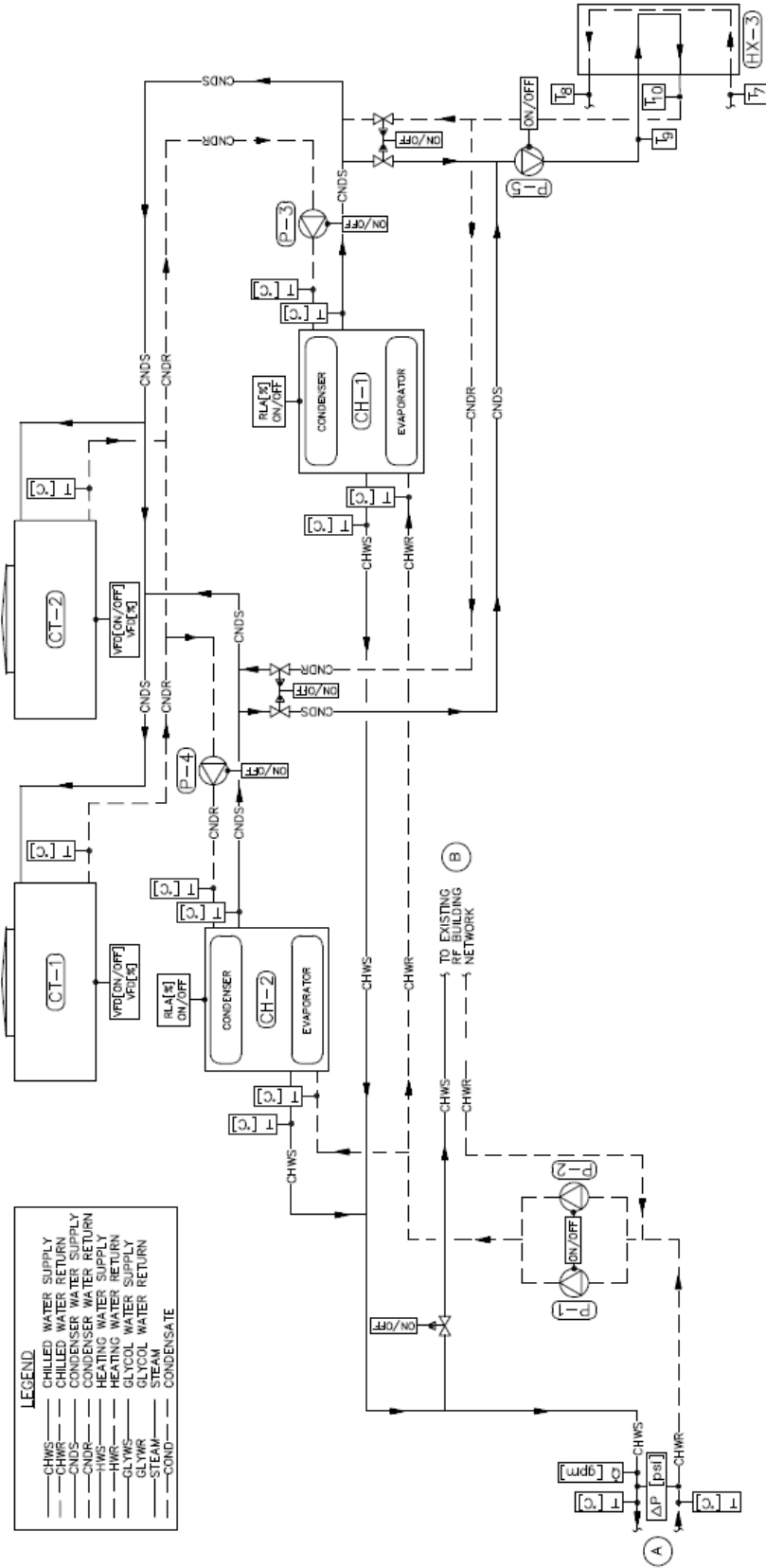
*Figure 4.2: Simplified schematic of the central plant: cooling*

*Figure 4.3: Simplified schematic of the central plant: heating*

During the winter, steam is produced by two existing natural gas boilers. The heat rejected from exhaust gases from the two existing boilers, B-2 and B-3, is recovered using a boiler economizer, S-1, which recuperates heat from the exhaust gases and transfers it to a water stream. The heating water return temperature is increased within the heat recovery heat exchanger (HX-1). If heat recuperated via HX-1 is insufficient to achieve the design heating water supply temperature of 51.7°C, a tube and shell heat exchanger (HX-2) is used to further raise the temperature of the water using steam.

### 4.1.3 Overview of central plant equipment design data

The equipment design conditions and specifications (Table 4.1) are presented to provide an overview of the installed equipment of the thermal central plant.

*Table 4.1: Equipment design information*

| Item | Design information | | Pumps | Design information | |
|---|---|---|---|---|---|
| CH-1 & CH-2 (each) | Power, kW | 549 | P-1 & P-2 | Flow, L/s | 72.6 |
| | RLA, A | 587 | (each) | Power, kW | 75 |
| | Evaporator $T_{in}/T_{out}$,° C | 13.3/5.6 | P-3 & P-4 | Flow, L/s | 131.5 |
| | Evaporator flow, L/s | 97 | (each) | Power, kW | 56 |
| | Condenser $T_{in}/T_{out}$, °C | 29.4/35.0 | P-5 & P-6 | Flow, L/s | 107.3 |
| | Condenser flow, L/s | 162 | (each) | Power, kW | 30 |
| | HCFC 123 charge, kg | 612 | P-7 to P-9 | Flow, L/s | 53.6 |
| | COP | 5.76 | (each) | Power, kW | 56 |
| CT-1 & CT-2 (each) | Flow, L/s | 131.5 | P-10 | Flow, L/s | 38.5 |
| | Fan power, kW | 30 | (boiler economizer) | Power, kW | 37.3 |
| | $T_{in}/T_{out}$,°C | 35.0/29.4 | P-11 | Flow, L/s | 95.3 |
| | $T_{WB}$, °C | 24.3 | (condensate) | Power, kW | 15 |
| Boiler economizer fan | Power, kW | 11.2 | | | |
| **Heat exchanger** | | | | | |
| Item | Hot side | | | Cold side | |
| HX-1 | Flow, L/s | 95.5 | | Flow, L/s | 107.3 |
| | $T_{HSS}$,°C | 57.1 | | $T_{CSS}$,°C | 29.4 |
| | $T_{HSR}$, °C | 32.2 | | $T_{CSR}$, °C | 51.7 |
| HX-2 | Steam, kg/h | 12,701 | | Flow, L/s | 107.3 |
| | Pressure, kPa | 414 | | $T_{CSS}/T_{CSR}$,°C | 35.2/51.7 |
| HX-3 | Flow, L/s | 107.3 | | Flow, L/s | 107.3 |
| | $T_{HSS}/T_{HSR}$,°C | 37.8/32.2 | | $T_{CSS}/T_{CSR}$,°C | 29.4/35.0 |

General system characteristics, such as design temperature and related properties, are presented in Table 4.2.

*Table 4.2: Design systems water properties*

| Item | | $\dot{V}$, m³/s | $T_{avg}$, °C | $C_{p,water}$, kJ/kg • °C | $\rho_{water}$, kg/m³ |
|---|---|---|---|---|---|
| Heating water | | Monitored | 32.2 | 4.174 | 994.9 |
| Chilled water | | Measured | 9.45 | 4.196 | 999.3 |
| Chilled water CSB | | Monitored | 9.45 | 4.196 | 999.3 |
| Condenser water | | Measured | 33.6 | 4.174 | 994.4 |
| HX-1 | Hot side | 0.0955 | 44.6 | 4.174 | 990.2 |
| | Cold side | 0.1073 | 40.6 | 4.174 | 991.8 |
| HX-2 | Cold side | 0.1073 | 43.5 | 4.174 | 990.5 |
| HX-3 | Hot side | 0.1073 | 35.0 | 4.174 | 994.0 |
| | Cold side | 0.1073 | 32.2 | 4.174 | 994.9 |

## 4.2 Data monitored at the CSB central plant

Information about the as-built and as-operated thermal performance of the CSB is obtained from the Monitoring and Data Acquisition System (MDAS) through the collaboration of the Physical Plant of Concordia University. The system uses a leading controls manufacturer's DDC control system. The data points are monitored every fifteen minutes. The complete list of monitored data is presented in Appendix A.

### 4.2.1 Additional measurements

During the first year of operation of the central plant, various changes were made to the systems by the facility management team compared to the design specifications to ensure the systems were operating properly. Changes were made to the chilled water system and heat recovery systems through the heat exchanger HX-3. Therefore, to identify the changes, the water flow rates of all the chilled and condenser water pumps (constant speed pumps) were measured, with the collaboration of CanmetENERGY

Research Centre on September 25th 2008, using an ultrasonic water flow meter, Controlotron system 1010 model 1010EWDPTRE-TIDXGZ (Table 4.3).

*Table 4.3: Controlotron system datasheet*

| Transit-time accuracy | At least 1% to 2% of indicated flow (better than 0.5% possible with calibration) |
|---|---|
| Flow sensitivity | 0.001 fps (0.0003 m/s) – even at zero flow |
| Zero drift-stability | Less than 0.5% |
| Response rate (damping) | Smart Slew[TM] effective from 0.25 second to 5 minutes |
| Flow velocity range | Min ±40 ft/s (±12 m/s), incl. zero flow |
| Linearity | 0.003 ft/s (0.001 m/s) |
| Flow profile compensation | Automatic Reynolds number correction of reported flow rate |

The pumps measurements are presented in Table 4.4. The flow for the condenser water pump is determined using the manufacturer pump curve. The installed pump is a Bell & Gossett VSCS 10x12x11 with a 27 cm (10.75 inches) impeller. The measured pressure is 290 kPa (42 psi), and thus, the flow for the condenser water pump is evaluated at 110 L/s.

*Table 4.4: Cooling pumps water flow measurements*

| Item | Tag | Pipe size, mm | $V_s$, m/s | $\dot{V}_{measured}$, gpm | Flow, L/s | Uncertainty, L/s (Equation (4.1)) |
|---|---|---|---|---|---|---|
| CHW pump | P-1 & P-2 | 150 | 1485 | 1375 | 86.75 | 0.97 |
| COND pump | P-3 & P-4 | 300 | | 1750 | 110.00 | N/A |
| HX-3 (COND) pump | P-5 | 200 | 1495 | 950 | 60.00 | 0.67 |
| HX-3 (HW) pump | P-6 | 200 | 1501 | 1700 | 107.25 | 1.20 |

For the chilled water pumps, P-1 and P-2, the measured water flow rates are about 20% higher than the design specifications (Monfet and Zmeureanu 2009a). Originally, two set of pumps, one for the AD building and one for the CSB, were included in the design. However, the pumps specified for the CSB were sufficient to provide the required flow to both buildings, and therefore, the existing pumps (pumps to AD building) were removed and the flow increased on the CSB pumps to meet the required flow rate of both buildings. The pumps P-3 and P-4 between the condenser and cooling tower were sized based on the cooling tower manufacturer's specification of 4540 kW and 131.5 L/s. The

measurements revealed a water flow rate of only 110.0 L/s. Perhaps the pressure loss in the condenser-cooling tower loop is greater than the design value used in the selection of pumps.

The anticipated heat recovery of the heat exchanger HX-3 was underestimated. In the current operation, in order to meet the building heating demand, only 55% of the water flow rate (pump P-5) from the condenser is needed to be directed to the heat exchanger (HX-3) instead of 80% as it was designed for.

### 4.2.2 Measurement uncertainties

The accuracies on selected measurements are presented in Table 4.5. The uncertainties are estimated using information presented in ASHRAE Guideline 2-2005 (ASHRAE 2005b).

Table 4.5: Accuracy information for selected measurements

| Item | Accuracy | Zero-drift |
|------|----------|------------|
| Constant water flow meter | 1% | 0.5% |
| Chiller power | 5% | - |
| Temperature | ± 1°C | - |

Equation (4.1) defines the uncertainty for fixed measurement in its general form:

$$U_C = \sqrt{(U_a \cdot X)^2 + (U_{zd} \cdot X)^2} \tag{4.1}$$

where $U_a$ is the accuracy uncertainty, $U_{zd}$ is the zero-drift uncertainty, and $X$ is the measurement. The uncertainties for the constant water flow measurements are presented in Table 4.4.

For cases where measured data are used together to calculate a new variable, there is propagation of errors. To illustrate the error propagation, the equation used to calculate the uncertainty for the COP is presented (Equation (4.2)).

$$\frac{U_{COP}}{COP} = \sqrt{\left(\frac{U_V}{V}\right)^2 + \left(\frac{U_{\Delta T}}{\Delta T}\right)^2 + \left(\frac{U_E}{E}\right)^2} \qquad (4.2)$$

where $U_v$ is the accuracy uncertainty of the chilled water volumetric flow rate (Table 4.4), $U_{\Delta T}$ is accuracy uncertainty of the temperature difference between the entering and leaving chilled water at the evaporator, and $U_E$ is the accuracy uncertainty of the electric power input.

## 4.3 Overview of the CSB central plant operation and performance

The monitored data were originally analyzed for the summer 2008, from June 23rd to September 21st 2008 (Monfet and Zmeureanu 2009a).

For the 2008 summer season, the instantaneous electric power input to the chillers was not being monitored; however, the percent relative load amperage (*%RLA*) was continuously being monitored with respect to the maximum amperage. The building operators manually recorded the chiller instantaneous current ($I_{CH}$) and corresponding *%RLA* twice a day. Based on this information, a correlation was developed to estimate the intensity of the electric current, in Amperes (Equation (4.3)), with a $R^2$ value of 0.975:

$$I_{CH} = 5.8334 \cdot (\%RLA) + 0.7978 \qquad (4.3)$$

A correlation was also developed for the chiller power factor (*PF*$_{manufacturer}$) based on manufacturer information (Equation (4.4)), with a $R^2$ value of 0.9865 (Monfet and Zmeureanu 2009a):

$$PF_{manufacturer} = -0.0365 \cdot \left(\frac{Q_E}{Q_{Edesign}}\right)^2 + 0.2483 \cdot \left(\frac{Q_E}{Q_{Edesign}}\right) + 0.4915 \qquad (4.4)$$

where $Q_E$ is the evaporator cooling load, calculated from the water flow rate and temperature difference of the chilled water (Equation(4.5)) and $Q_{Edesign}$ is the evaporator cooling load at design conditions, which is equal to 3165 kW, both in kW:

$$Q_E = C_p \cdot \left( \sum_{i=1}^{2} \dot{m}_{P-i} \right) \cdot (T_{CHWR} - T_{CHWSpt}) \qquad (4.5)$$

where $m_{P-i}$ is the measured water flow rate of pumps *P-1* and/or *P-2* in kg/s; $C_p$ is the water specific heat and has a value of 4.196 kJ/(kg·°C) at the average chilled water temperature of 9.45°C; $T_{CHWR}$ is the monitored chilled water return temperature; and $T_{CHWSpt}$ is the chilled water supply temperature setpoint (6.8˚C). The instantaneous electric power input for each chiller, in kW, is then calculated by assuming that the voltage ($V$) is constant (Equation (4.6)).

$$\dot{E}_{CH} = \sqrt{3} \cdot V \cdot I_{CH} \cdot PF \qquad (4.6)$$

In March 2009, additional monitored data points became available through the MDAS: the voltage, the current, the power factor and electric power input to each chiller. The developed correlations were used to evaluate the electric power input to the chiller and compared with the new 2009 monitored data points, and discrepancies between the data evaluated using the approach taken in 2008 compared with the new measured data were found. Table 4.6 presents the average electric power input and electricity used for the power estimated using Equations (4.3) to (4.6) and the monitored electric power input over the summer 2009. The average electric power inputs and energy consumption for chiller CH-1 and chiller CH-2 are underestimated when the preliminary correlations are used.

*Table 4.6: Electric power input to chillers, summer 2009*

| Item | Calculated (Equations (4.3) to (4.6)) | | Measured | |
|------|----------------|----------|----------------|----------|
| | Power, kW | E, kWh | Power, kW | E, kWh |
| CH-1 | $224 \pm 69$ | 291,365 | $313 \pm 93$ | 406,155 |
| CH-2 | $211 \pm 61$ | 139,995 | $299 \pm 85$ | 198,330 |

## 4.4 Overview of the equipment operation

The analysis is therefore presented for the summer 2009 monitored data: the as-operated performance of the CSB central plant is analyzed in detail for the first week of summer, which starts on Monday June 22$^{nd}$ and ends on Sunday June 28$^{th}$ 2009, followed by a comparison of seasonal and annual monitored data for 2009 and 2010.

Sections 4.4 to 4.7 present monitored and estimated data for the week of June 22$^{nd}$ to 28$^{th}$ 2009, while section 4.8 presents the seasonal and some annual data for 2009 and 2010. For the week of June 22$^{nd}$ to June 28$^{th}$ 2009, the heating water system is always required. The heat exchanger (HX-1) is bypassed and the steam supply valve to the heat exchanger (HX-2) is close when chillers CH-1 or CH-2 are operating. The heating water is warmed up via the heat recovery system (HX-3) installed between the condenser water loop and the heating water loop. The heat recovered reduced the overall central plant energy use. The heat exchanger (HX-3) is always in operation when chillers CH-1 or CH-2 are in operation. During the summer months, steam is provided to hot water tanks, specific lab applications and humidifiers if required.

### 4.4.1 Chillers

For the week of June 22$^{nd}$ to June 28$^{th}$ 2009, chiller CH-2 is in operation every day, except on June 22$^{nd}$ between 4h45 and 7h45. Both chillers, CH-1 and CH-2, are operating simultaneously from 12h30 on June 25$^{th}$ to 00h30 on June 26$^{th}$, and from 11h45 to 21h00 on June 26$^{th}$ 2009.

The electric power input to the chiller is generally higher at start-ups, and varies between 150 kW and 550 kW for chiller CH-2 and between 200 kW and 400 kW for chiller CH-1 (Figure 4.4). The chiller electric power input increases when the outdoor air temperature increases (Figure 4.5). For outdoor air temperatures above 23°C, the two chillers, CH-1 and CH-2, operate simultaneously if required. This occurs when one of the chillers is running at 90% of its capacity. When both chillers are operating simultaneously, they both operate at around 55-65 % of their capacity (Figure 4.4).
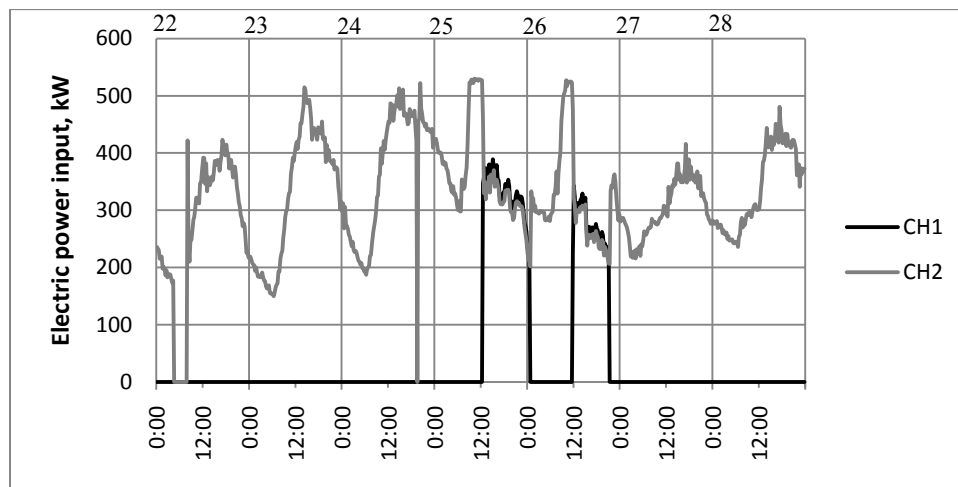


*Figure 4.4: Chiller electric power input variation, June 22$^{nd}$ to 28$^{th}$ 2009*
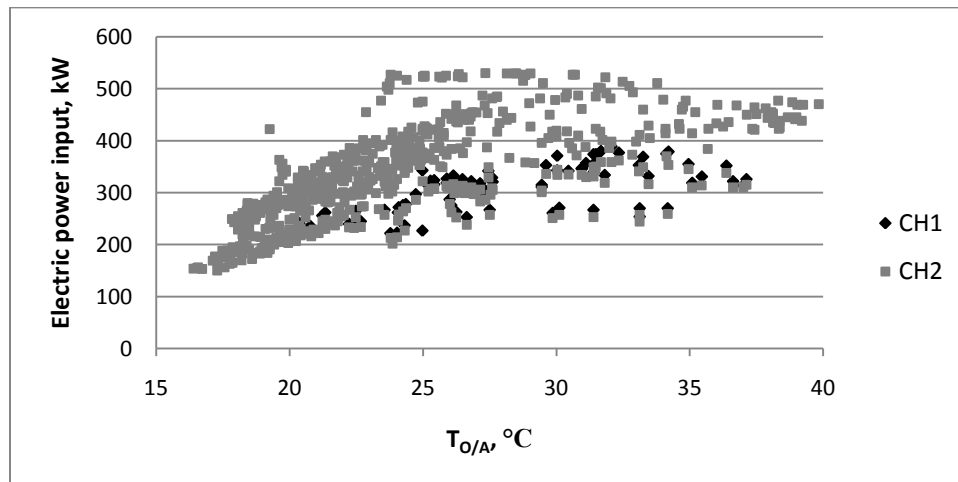


*Figure 4.5: Chiller electric power input variation with outdoor air temperature, June 22$^{nd}$ to 28$^{th}$ 2009*

61

For chiller CH-1, the evaporator water temperature difference can be estimated using the evaporator water temperature difference given by the sensors integrated within chiller itself or by calculating the difference between the entering and leaving chilled temperatures monitored using two thermometers installed on the water pipes. The direct reading of the evaporator water temperature difference at the chiller is only available for chiller CH-1. For the week of June $22^{nd}$ to June $28^{th}$ 2009, when chiller CH-1 is operating on June $25^{th}$ and $26^{th}$, the water temperature difference calculated using the two thermometers is slightly higher than the value recorded by the chiller, especially at start-up (Figure 4.7). The average difference on June $25^{th}$ and $26^{th}$ is 0.6±0.7°C, while being 0.5±0.5°C over the complete summer season. The average difference at start-up only is higher, 1.9±2.7°C over the summer season. The measurement differences are explained by the different location of the thermometers (within the chiller itself and outside the chiller); hence, the interaction with the environment is different. Also, the sensors might be calibrated differently and the accuracy of the internal thermometer is ±0.5°C compared to ±1°C for the thermometers installed on the water pipes (Table 4.5). The analysis of the monitored data is carried out using the water temperature difference calculated using the two thermometers for both chillers.
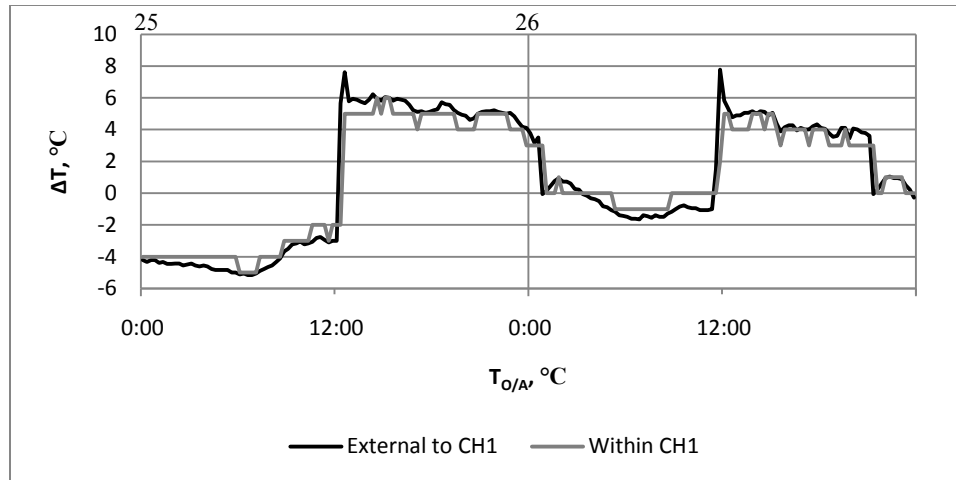
*Figure 4.6: Evaporator water temperature difference comparison for chiller CH-1, June 25$^{th}$ to 26$^{th}$ 2009*

### 4.4.2 Cooling towers

For the cooling towers, the fan variable frequency drive (VFD) level is monitored. The fan VFD level varies between 30 % and 80 % of its full capacity (Figure 4.7). Both cooling towers are in operation when chillers CH-1 and CH-2 are operating simultaneously. Otherwise, the cooling tower CT-1 is in operation when chiller CH-1 is in operation. Similarly, the cooling tower CT-2 is in operation when CH-2 is in operation. The VFD level increases with increase in outdoor air temperature (Figure 4.8), having a similar trend to the electric power input to the chillers.
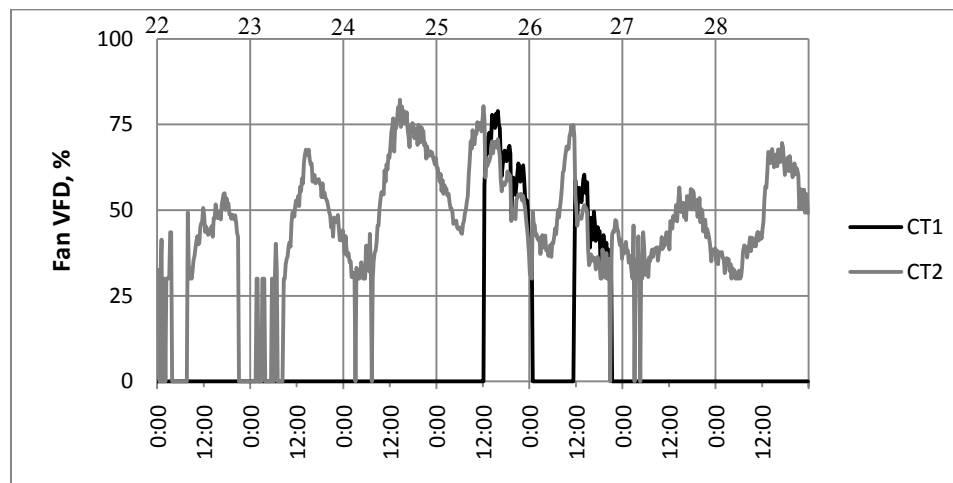


*Figure 4.7: Cooling tower fans VFD variation, June 22$^{nd}$ to 28$^{th}$ 2009*
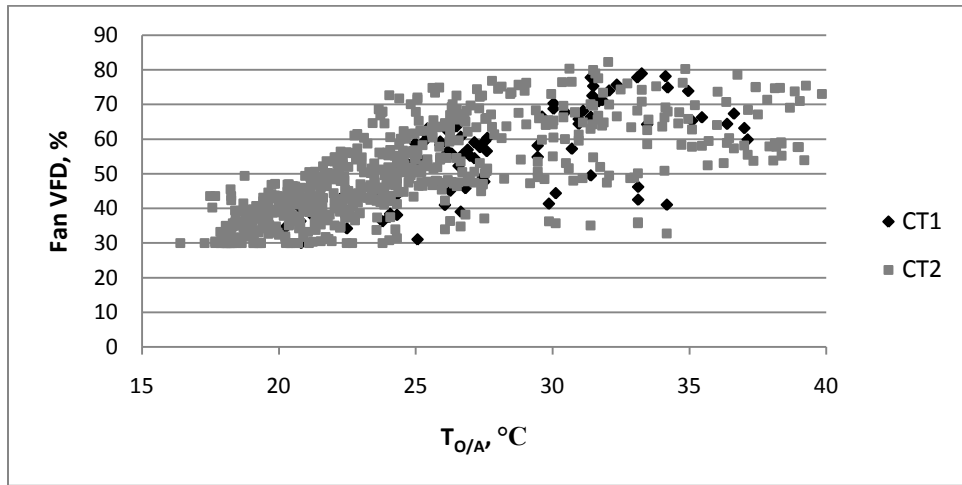
*Figure 4.8: Cooling tower fans VFD variation with outdoor air temperature, June 22$^{nd}$ to 28$^{th}$ 2009*

### 4.4.3 *Heating equipment*

The steam load varies throughout the day (Figure 4.9). The load is lower during the weekend (June 27$^{th}$ and 28$^{th}$). No specific trend can be noticed with changes in outdoor air temperature (Figure 4.10) or outdoor air relative humidity (Figure 4.11).
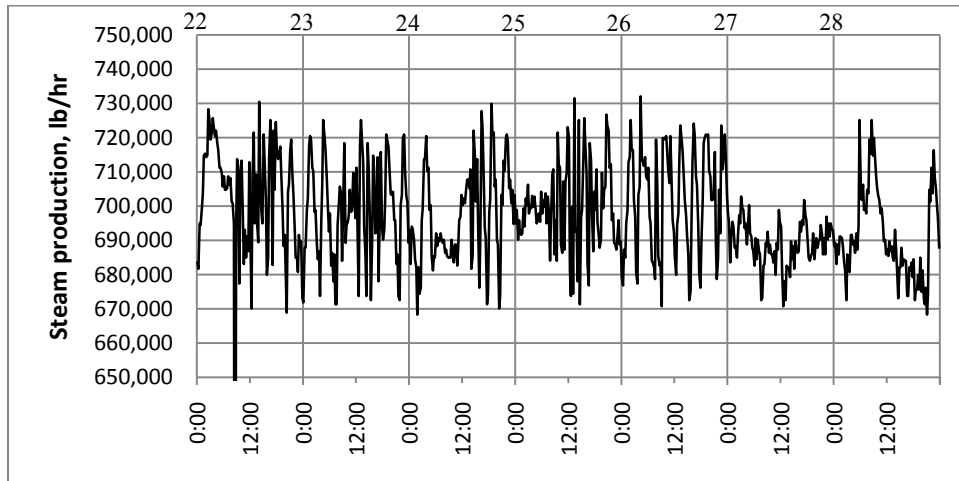


*Figure 4.9: CSB steam production rate, June 22$^{nd}$ to 28$^{th}$ 2009*

64
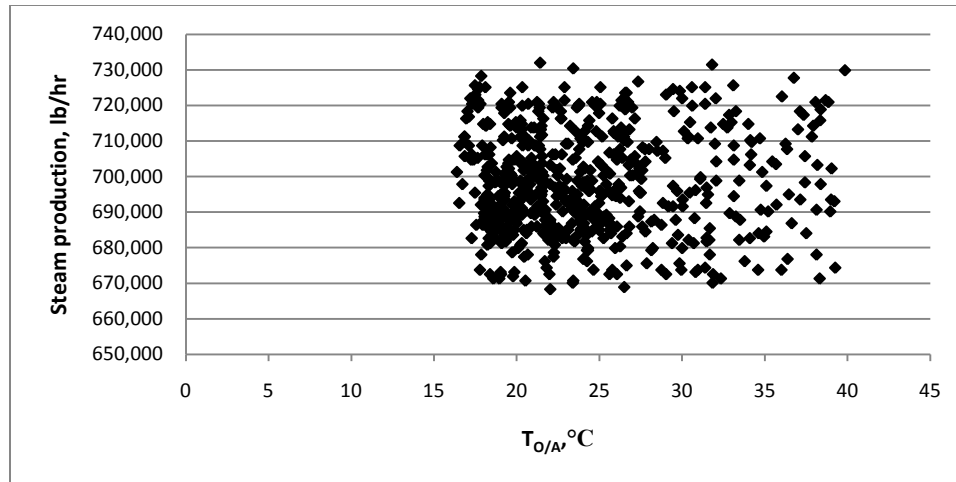
*Figure 4.10: CSB steam production rate, June 22$^{nd}$ to 28$^{th}$ 2009 versus outdoor air temperature*
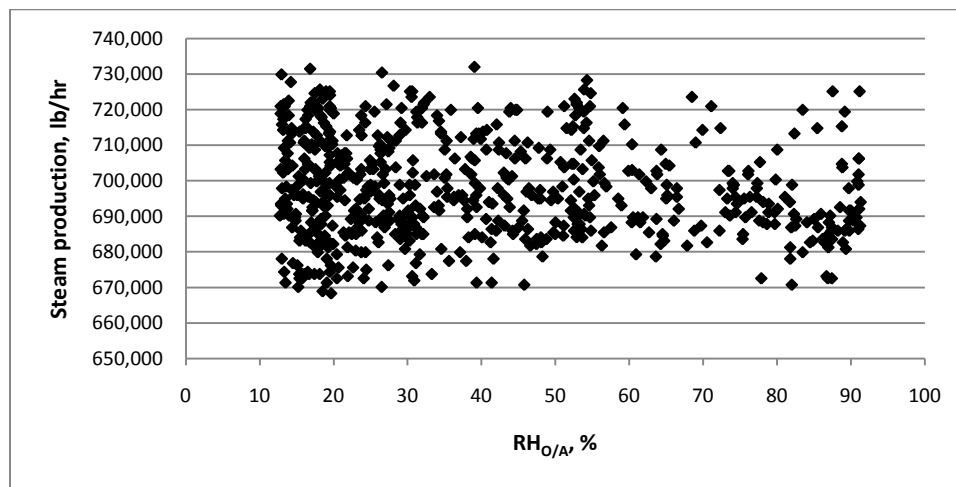


*Figure 4.11: CSB steam production rate, June 22$^{nd}$ to 28$^{th}$ 2009 versus outdoor air relative humidity*

Information about the heating water distribution systems, such as the pumps VFD level is available (Figure 4.12). Three pumps (P-7 to P-9) are available for heating water distribution; however, one pump is operating at a time for the analyzed period (June 22$^{nd}$ to 28$^{th}$ 2009). When in operation, the pump VFD levels vary between 60% and 90%.
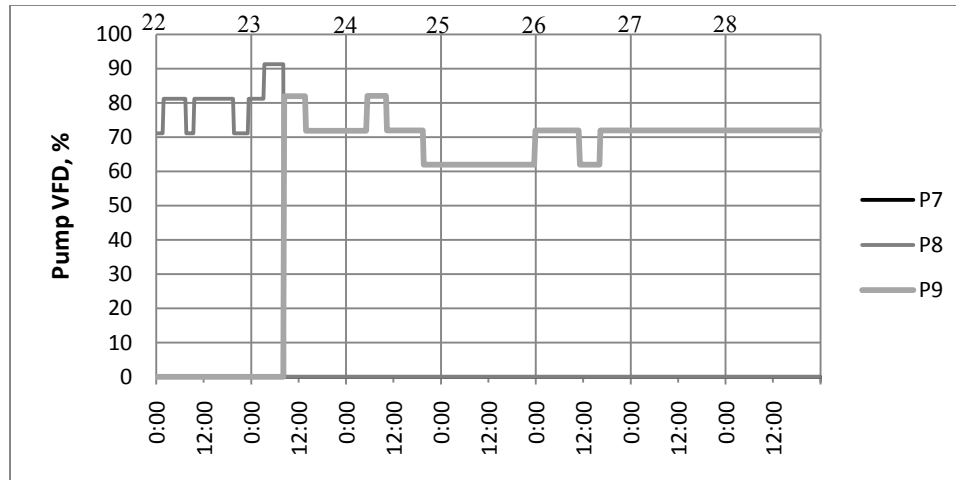
*Figure 4.12: Heating water distribution pumps VFD level, June 22nd to 28th 2009*

### 4.4.4  Heat exchanger

During the week of June $22^{nd}$ to June $28^{th}$ 2009, the heat exchanger HX-3 is the only heat exchanger in operation. It recovers the heat from the condenser water loop to pre-warm the heating water. Figure 4.13 presents the water temperature leaving the heat exchanger HX-3 on the cold side ($T_8^{HX-3}$, see Figure 4.3) and the heating water supply temperature ($T_{HWS}^{CSB}$). For the week of June $22^{nd}$ to June $28^{th}$ 2009, the heat exchanger HX-3 recovered enough heat from the condenser water loop to maintain the heating load demand of the CSB.
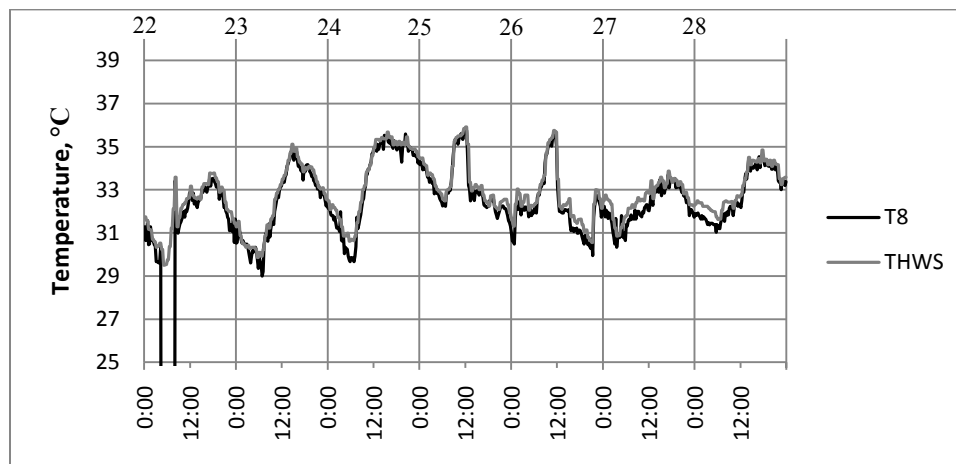


*Figure 4.13: Heating water temperature comparison, June 22nd to 28th 2009*

66

### 4.4.5 Daily average monitored data

The daily average measured data for the week of June 22$^{nd}$ to June 28$^{th}$ 2009 are presented, as an example, in Table 4.7.

*Table 4.7: Daily average measurements, June 22$^{nd}$ to 28$^{th}$ 2009*

| Item | 6/22 | 6/23 | 6/24 | 6/25 | 6/26 | 6/27 | 6/28 |
|---|---|---|---|---|---|---|---|
| $T_{db}$, °C | 22.1 ± 4.5 | 25.2 ± 7.0 | 26.9 ± 6.1 | 26.8 ± 4.7 | 23.6 ± 3.2 | 20.9 ± 2.5 | 23.1 ± 5.7 |
| RH, % | 34.8 ±13.5 | 23.0 ± 9.4 | 20.5 ± 5.1 | 34.3 ±16.7 | 41.1 ±14.3 | 68.5 ±15.6 | 63.1 ±29.0 |
| $\dot{V}_{CHW}^{CSB}$, L/s | 84.9 ± 3.9 | 84.0 ± 5.2 | 86.7 ± 4.8 | 119.6 ±30.9 | 113.3 ±29.1 | 86.7 ± 2.0 | 87.9 ± 2.1 |
| $T_{CHWS}^{CSB}$, °C | 7.2 ± 0.2 | 7.2 ± 0.1 | 7.2 ± 0.1 | 7.2 ± 0.3 | 7.2 ± 0.3 | 7.2 ± 0.1 | 7.2 ± 0.1 |
| $T_{CHWR}^{CSB}$, °C | 11.4 ± 1.2 | 11.6 ± 1.7 | 12.4 ± 1.6 | 12.7 ± 1.0 | 11.9 ± 1.1 | 11.5 ± 0.8 | 12.1 ± 1.1 |
| $\dot{V}_{HW}^{CSB}$, L/s | Missing data | Missing data | Missing data | 35.9 ± 3.0 | 40.8 ± 3.6 | 42.0 ± 1.6 | 41.4 ± 2.6 |
| $T_{HWS}^{CSB}$, °C | 32.0 ± 1.2 | 32.5 ± 1.7 | 33.6 ± 1.8 | 33.4 ± 1.1 | 32.6 ± 1.3 | 32.6 ± 0.7 | 33.1 ± 1.0 |
| $T_{HWR}^{CSB}$, °C | 29.4 ± 0.7 | 29.5 ± 0.9 | 30.8 ± 1.4 | 30.2 ± 0.9 | 29.6 ± 1.0 | 30.0 ± 0.5 | 30.4 ± 0.8 |
| $T_{CHWS}^{CH-1}$, °C | OFF | OFF | OFF | 6.7 ± 0.1 | 6.7 ± 0.1 | OFF | OFF |
| $T_{CHWR}^{CH-1}$, °C | OFF | OFF | OFF | 12.1 ± 0.6 | 11.1 ± 0.8 | OFF | OFF |
| $T_{CNDS}^{CH-1}$, °C | OFF | OFF | OFF | 33.8 ± 0.7 | 32.6 ± 0.8 | OFF | OFF |
| $T_{CDNR}^{CH-1}$, °C | OFF | OFF | OFF | 28.3 ± 0.4 | 28.4 ± 0.3 | OFF | OFF |
| $T_{CHWS}^{CH-2}$, °C | 6.7 ± 0.1 | 6.7 ± 0.1 | 6.7 ± 0.1 | 6.8 ± 0.2 | 6.7 ± 0.1 | 6.7 ± 0.1 | 6.7 ± 0.1 |
| $T_{CHWR}^{CH-2}$, °C | 11.1 ± 1.3 | 11.2 ± 1.8 | 11.9 ± 1.6 | 12.3 ± 1.0 | 11.5 ± 1.1 | 11.0 ± 0.8 | 11.5 ± 1.1 |
| $T_{CNDS}^{CH-2}$, °C | 33.4 ± 1.6 | 33.7 ± 2.2 | 34.6 ± 1.9 | 34.5 ± 1.3 | 33.6 ± 1.5 | 33.3 ± 0.9 | 34.0 ± 1.3 |
| $T_{CNDR}^{CH-2}$, °C | 28.6 ± 0.4 | 28.5 ± 0.5 | 28.6 ± 0.4 | 28.6 ± 0.2 | 28.5 ± 0.3 | 28.5 ± 0.3 | 28.5 ± 0.2 |
| $T_7^{HX-3}$, °C | 30.9 ± 0.9 | 31.2 ± 1.7 | 32.5 ± 1.9 | 32.2 ± 1.1 | 31.3 ± 1.3 | 31.4 ± 0.7 | 31.9 ± 1.1 |
| $T_8^{HX-3}$, °C | 32.0 ± 1.1 | 32.3 ± 1.7 | 33.3 ± 2.0 | 33.2 ± 1.2 | 32.2 ± 1.4 | 32.2 ± 0.8 | 32.8 ± 1.1 |
| $\dot{m}_{steam}$, kg/s | 88.4 ± 3.1 | 88.1 ± 1.8 | 87.8 ± 1.8 | 88.2 ± 1.6 | 88.5 ± 1.9 | 86.8 ± 0.8 | 87.1 ± 1.6 |
| $T_{condensate}$, °C | 101.3 ± 1.5 | 101.4 ± 1.5 | 101.2 ± 1.0 | 101.2 ± 1.2 | 100.9 ± 1.3 | 101.1 ± 1.0 | 101.2 ± 1.2 |

## 4.5 Operating characteristics of the central plant

The operation of the central plant is evaluated using different indices. For the CSB central plant, the cooling and heating loads, the heat recovered and the heat rejected are estimated. In its general form, the load and heat rate are determined using Equation (4.7):

$$\dot{Q} = \dot{V} \cdot C_{p,water} \cdot \rho_{water} \cdot \Delta T \qquad (4.7)$$

where $\dot{Q}$ is the calculated load, kW; $\dot{V}$ is the volumetric flow rate, m$^3$/s; $C_{p,water}$ is the specific heat of water at the average design water temperature, kJ/kg · °C; $\rho_{water}$ is the

water density at the average design water temperature, kg/m$^3$; and $\Delta T$ is the water temperature difference between the supply and return, °C.

The central plant heat rejected is the heat rejected via the condenser of the chillers. The heat rejected is calculated using Equation (4.8):

$$\dot{Q}_{reject.} = C_{p,water} \cdot \rho_{water} \cdot \sum_{i=1}^{2} (\dot{V}_i \cdot \Delta T_i) \tag{4.8}$$

where $\dot{Q}_{reject.}$ is the calculated heat rejected, kW; $\dot{V}_i$ is the water flow rate for each cooling tower (CT-1 & CT-2), m$^3$/s; $C_{p,water}$ is the specific heat of water at the average design water temperature, kJ/kg·°C; $\rho_{water}$ is the water density at the average design water temperature, kg/m$^3$; and $\Delta T_i$ is the water temperature difference between the supply and return monitored at the condensers of the chillers.

The total load is determined using Equation (4.9):

$$Q = \left[ \sum \dot{Q}_j \cdot \Delta t \right] \tag{4.9}$$

where $Q$ is the total load over time, MJ; $\dot{Q}_j$ is the summation of the load over time, kW; and $\Delta t$ is the time interval, h.

The loads of the central plant are estimated to demonstrate the interaction between the various systems installed in the CSB central plant.

### 4.5.1    Central plant thermal loads

Figure 4.14 shows the CSB cooling and heating loads. The chilled water load increases almost linearly when the outdoor air temperature is between 16°C and 26°C (Figure 4.14). At outdoor air temperatures above 26°C, the total chilled water load is around 2500 ± 1000 kW. The heating water load varies slightly throughout the day. For

the studied period, the average heating load is around 500 kW and does not vary significantly with changes in outdoor air temperature. By convention, the heating loads are presented graphically as negative values.
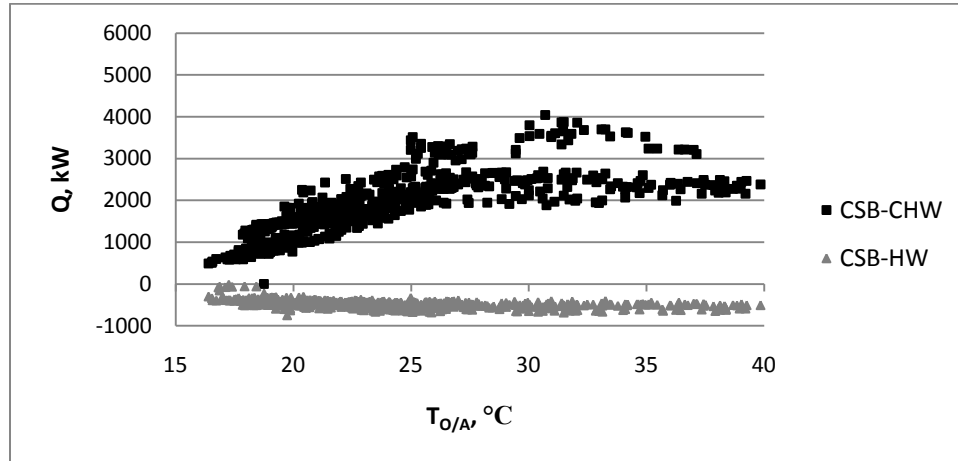


*Figure 4.14: Total heating and chilled water load versus outdoor air temperature, June 22$^{nd}$ to 28$^{th}$ 2009*

### 4.5.2   Central plant heat recovered

During the summer, when either chillers CH-1 or CH-2 are in operation, the boiler economizer heat exchanger (HX-1) is not operational. For the heat exchanger HX-3, the heat recovered is calculated on the cold side (heating water loop). The heat recovered varies during system operation, with a maximum value close to 600 kW (Figure 4.15). The average heat recovered is 400±90 kW. The heat recovered increases with increase in outdoor air temperatures between 15°C and 25°C, while varying between 400 kW and 500 kW for outdoor air temperature higher than 25°C (Figure 4.16).

69
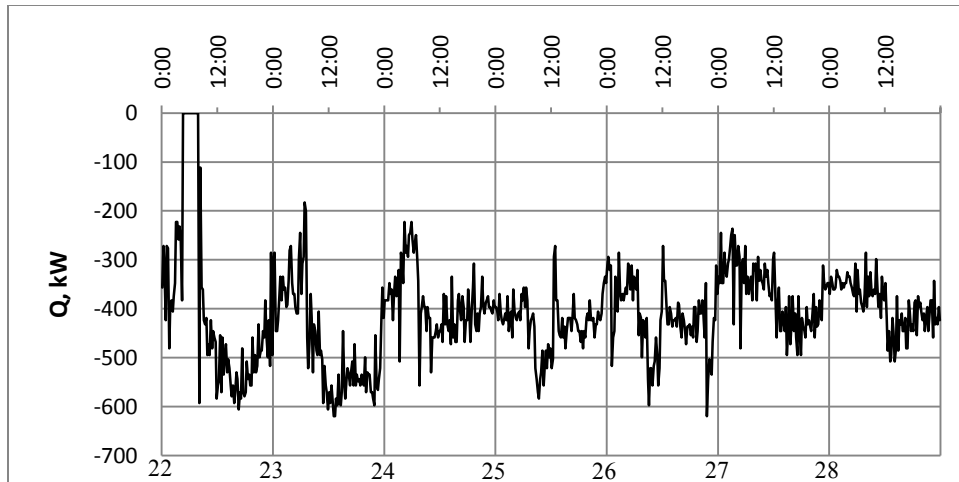
*Figure 4.15: Heat recovered from heat exchanger HX-3, June 22ⁿᵈ to 28ᵗʰ 2009*
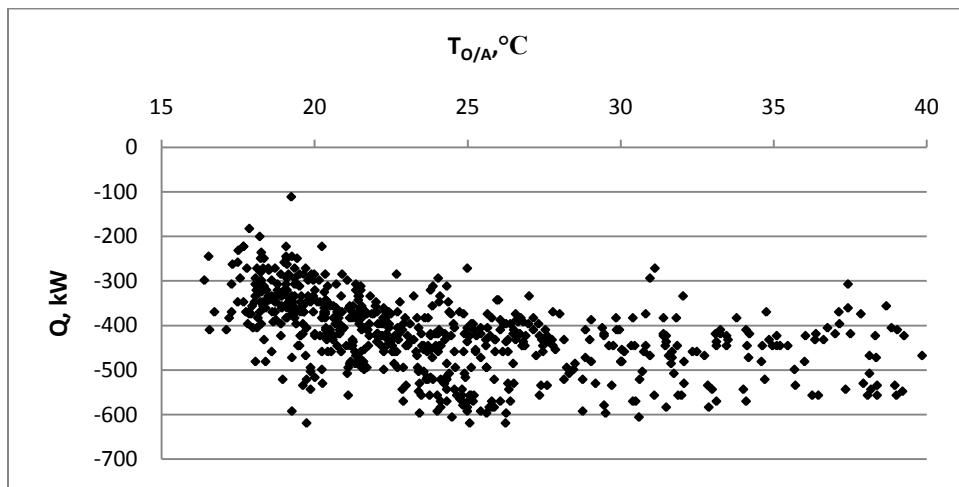


*Figure 4.16: Heat recovered from heat exchanger HX-3 versus outdoor air temperature, June 22ⁿᵈ to 28ᵗʰ 2009*

### 4.5.3   Central plant heat rejected

The central plant heat rejected (Equation (4.8)) varies with the cooling water load, peaking during the afternoon (Figure 4.17). The heat rejected increases with the increase in outdoor air temperatures (Figure 4.18). The load increases almost linearly between 15°C and 28°C, from 1000 kW to close to 4500 kW.
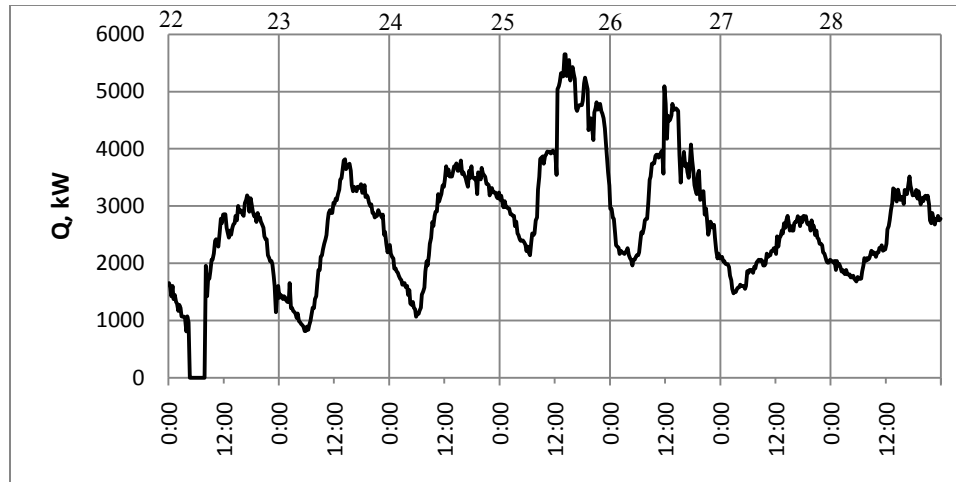
*Figure 4.17: Central plant heat rejected load, June 22$^{nd}$ to 28$^{th}$ 2009*
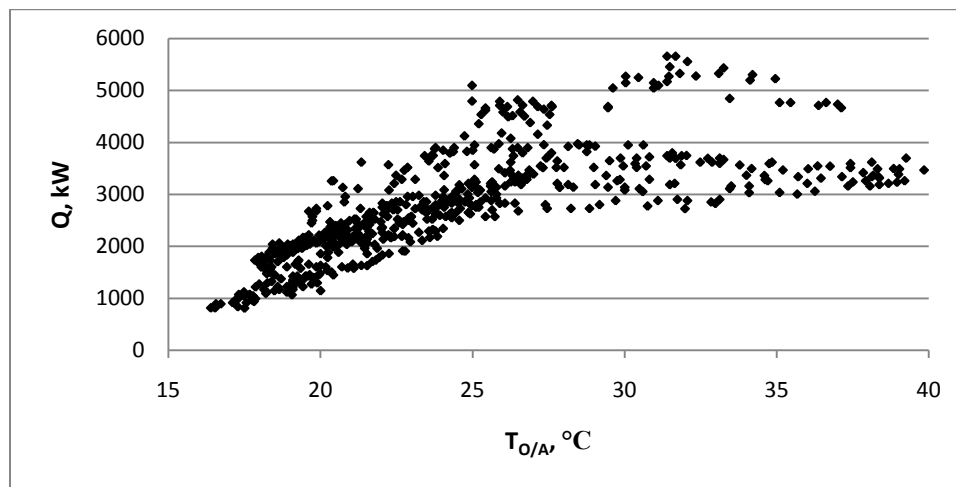


*Figure 4.18: Central plant heat rejected load versus outdoor air temperature, June 22$^{nd}$ to 28$^{th}$ 2009*

### 4.5.4    Daily average load data

Figure 4.19 presents chilled water load, the heat recovered and the heat rejected for the week of June 22$^{nd}$ to 28$^{th}$ 2009, as an example. Daily thermal energy (MJ) and peak load (kW) are presented in Table 4.8. The $Q_{CHW}^{CSB}$ is calculated at the CSB entrance, while the $Q_{CHW}$ is calculated at the chillers. There are discrepancies in the peak chilled water load estimated for the central plant and the CSB, where $Q_{CHW}^{CSB}$ is higher than $Q_{CHW}$. This issue is explained by the accuracy of the water flow meters and thermometers, and

71

the location of the equipment used to monitor the data: the CSB temperature readings are influenced by heat losses/gains along the water pipes installed between the chillers and where the thermometers are installed.
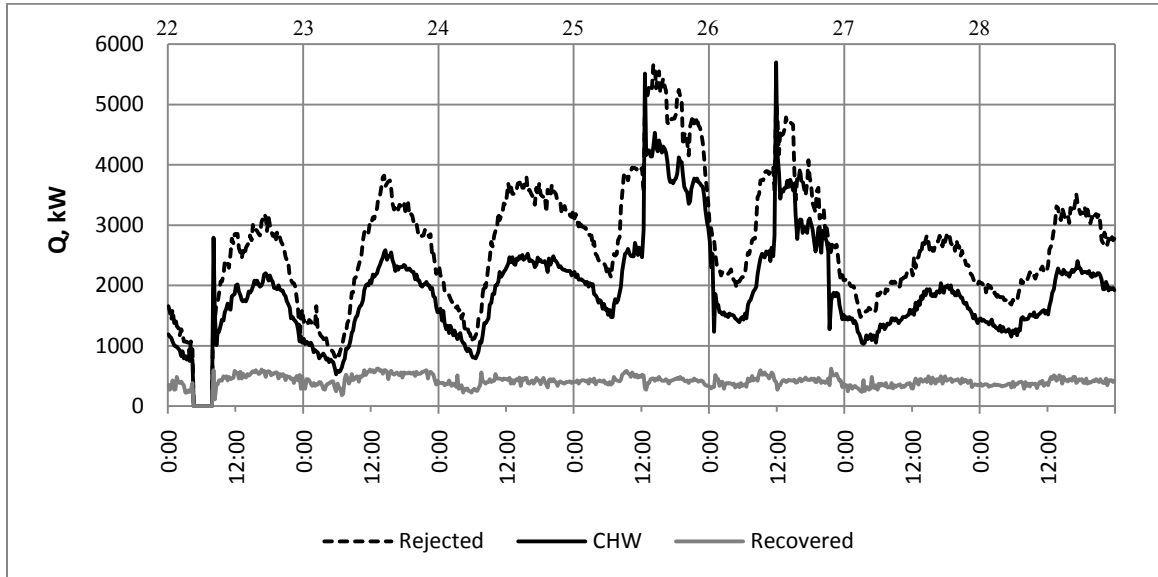


*Figure 4.19: Central plant cooling load analysis, June 22nd to 28th 2009*

*Table 4.8: Daily energy and peak load, June 22nd to 28th 2009*

| Date<br>Item | 06/22 | 06/23 | 06/24 | 06/25 | 06/26 | 06/27 | 06/28 |
|---|---|---|---|---|---|---|---|
| $Q_{HW}^{CSB}$, MJ/day | 40,075 | 44,050 | 39,165 | 41,235 | 43,430 | 39,475 | 40,775 |
| (Peak, kW) | (685) | (680) | (590) | (645) | (745) | (570) | (565) |
| $Q_{CHW}^{CSB}$, MJ/day | 109,770 | 137,140 | 164,285 | 235,365 | 187,635 | 135,800 | 156,220 |
| (Peak, kW) | (2210) | (2570) | (2665) | (4040) | (3515) | (2230) | (2600) |
| $Q_{CHW}$, MJ/day | 116,755 | 141,695 | 161,920 | 254,985 | 207,315 | 134,045 | 151,230 |
| (Peak, kW) | (2790) | (2585) | (2525) | (5515) | (5700) | (2040) | (2405) |
| $Q_{rec.}$, MJ/day | 33,775 | 40,770 | 33,535 | 37,280 | 36,315 | 31,955 | 33,810 |
| (Peak, kW) | (605) | (620) | (555) | (585) | (620) | (495) | (510) |
| $Q_{reject.}$, MJ/day | 163,550 | 203,570 | 236,270 | 337,440 | 273,755 | 191,020 | 217,300 |
| (Peak, kW) | (3185) | (3820) | (3795) | (5655) | (5095) | (2830) | (3515) |

## 4.6 Electric demand and energy use

The operation of the central plant is also evaluated by determining the electricity used for the installed mechanical equipment compared with the chilled and heating water

loads. Equation (4.10) is used to estimate the total electricity use for the mechanical equipment.

$$E = \sum_{t}^{T} (\dot{E}_t \cdot \Delta t)$$

(4.10)

where $E$ is the electric energy use, kWh; $\dot{E}_t$ is the instantaneous electric power, kW; and $\Delta t$ is the time interval, h.

The energy use is evaluated first for the cooling equipment for the week of June 22nd to June 28th 2009 and then for the year 2009 and 2010.

### 4.6.1 Electric power input of chillers

Since March 2009, the electrical power input is directly recorded by the CSB MBAS for both chillers. The uncertainty range of the power measurement readings are ±5%. Figure 4.20 shows the accuracy of the electric power input variations of chiller CH-2 for the week of June 22nd to June 28th 2009.
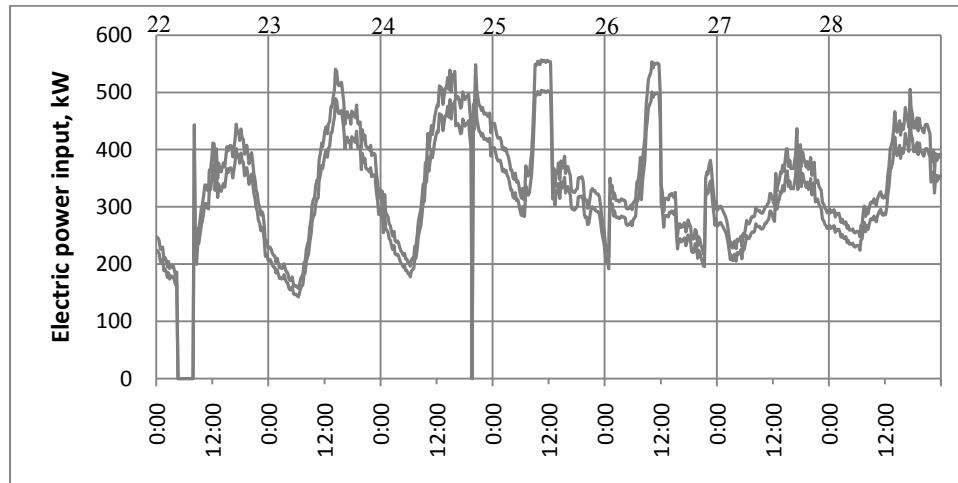


Figure 4.20: Uncertainty range of chiller CH-2 electric power input variation, June 22nd to 28th 2009

### 4.6.2  Electric power input of cooling towers

For the cooling towers, the fan VFD level is monitored. The instantaneous power is evaluated using Equation (4.11):

$$\dot{E}_{CT} = \left[\frac{(\%VFD/100) \cdot RPM}{RPM_{design}}\right]^3 \cdot P_{fan} \tag{4.11}$$

where $\dot{E}_{CT}$ is the instantaneous electric power, kW; *%VFD* is the fan VFD level, %; *RPM* is the rated motor rotation per minute, 1800 RPM; $RPM_{design}$ is the design motor rotation per minute, 1800 RPM; and $P_{fan}$ is the fan full capacity, 30 kW.

The energy use is evaluated for each cooling tower and summed to get the overall cooling towers electricity use.

### 4.6.3  Electric power input of pumps

The electric power input is calculated with Equation (4.12) for pumps with variable speed drive and Equation (4.13) for constant speed pumps. Pumps design information is presented in Table 4.1.

$$\dot{E}_{pump,VFD} = \left[\frac{\%VFD/100 \cdot RPM}{RPM_{design}}\right]^3 \cdot P_{pump} \tag{4.12}$$

where $\dot{E}_{pump,VFD}$ is the variable speed pump instantaneous electric power use, kW; *%VFD* is the pump VFD level, %; *RPM* is the rated motor rotation per minute, RPM; $RPM_{design}$ is the design motor rotation per minute, RPM; and $P_{pump}$ is the pump motor full capacity, kW.

$$\dot{E}_{pump,const.} = P_{pump} \tag{4.13}$$

where $\dot{E}_{pump,const.}$ is the constant speed pump instantaneous electric power use, kW and $P_{pump}$ is the pump motor operating capacity, kW.

### 4.6.4 Central plant electricity use

The central plant electricity use is then determined using Equation (4.14):

$$E_{elec} = E_{chillers} + E_{CT} + E_{pumps} \qquad (4.14)$$

Daily results are presented for the week of June 22$^{nd}$ to June 28$^{th}$ 2009 (Table 4.9). The chillers use the largest amount of electricity, 58% of the total central plant electricity use. The pumps account for 40% of the overall electricity consumption. The cooling pumps (chilled and condenser water) account for 62% of the electricity used by the pumps.

*Table 4.9: Daily central plant electricity consumption, June 22$^{nd}$ to June 28$^{th}$ 2009*

| Item \ Day | 06/22 | 06/23 | 06/24 | 06/25 | 06/26 | 06/27 | 06/28 |
|---|---|---|---|---|---|---|---|
| $E_{chiller}$, kWh/day | 6320 | 7755 | 8780 | 12,680 | 10,370 | 7240 | 8110 |
| $E_{CT}$, kWh/day | 85 | 145 | 330 | 500 | 220 | 120 | 200 |
| $E_{pumps}$, kWh/day | 4625 | 5290 | 5115 | 6455 | 6430 | 5100 | 5100 |
| $E_{elec}$, kWh/day | 11,030 | 13,190 | 14,225 | 19,635 | 17,020 | 12,460 | 13,410 |

## 4.7 Performance characteristics

The performance of various equipment or group of equipment is evaluated using the coefficient of performance (COP) or the effectiveness. The COP is defined as the desired output cooling load divided by the required electric input (Equation (4.15)):

$$COP = \frac{Q_E}{\dot{E}_{input}} \qquad (4.15)$$

where *COP* is the coefficient of performance; $Q_E$ is the evaporator load determined using Equation (4.7), kW; and $\dot{E}_{input}$ is the electric power input, kW.

### 4.7.1 COP of chillers

For comparison purposes, the COP of chillers is presented at design conditions in Table 4.10 and compared with the COP based on monitored data (Table 4.11). The $COP_{chiller}^{design}$ is determined using the rated chiller information (Table 4.1) and the measured flow rate of the pumps. The COP at pumps of 5.10 is based on the operating characteristics of the chillers and is lower than the manufacturer rated value of 5.76.

For the $COP_{CH}$, the evaporator load is determined using monitored water temperature and the measured pump water flow rate. The average uncertainty on the COP for the week of June 22$^{nd}$ to June 28$^{th}$ 2009 is estimated at ±1.26 for CH-1 and ±1.22 for CH-2. The measured COP (Table 4.11) are comparable with the COP calculated using the revised pump water flow rate (Table 4.10).

Table 4.10: Electric power input and COP for chillers based on design conditions

| Item | Design CHW flow rate | |
| --- | --- | --- |
| | At evaporator | At pumps |
| $Q_{CND}$, kW | 3771 | 2568 |
| $Q_E$, kW | 3127 | 2801 |
| $E$, kW | 549 | 549 |
| $COP_{chiller}^{design}$ | 5.76 | 5.10 |

Table 4.11: Daily average chillers performances, June 22$^{nd}$ to 28$^{th}$ 2009

| Item | Day | 06/22 | 06/23 | 06/24 | 06/25 | 06/26 | 06/27 | 06/28 |
| --- | --- | --- | --- | --- | --- | --- | --- | --- |
| **CH-1** | $Q_E$, kW | OFF | OFF | OFF | 1960 ± 220 | 1600 ± 300 | OFF | OFF |
| | $E$, kW | OFF | OFF | OFF | 335 ± 30 | 271 ± 36 | OFF | OFF |
| | $COP_{CH}$ | OFF | OFF | OFF | 5.85 ±0.38 | 5.91 ±1.08 | OFF | OFF |
| | $Q_E/Q_{Edesign}$ | OFF | OFF | OFF | 0.62 ±0.07 | 0.50 ±0.09 | OFF | OFF |
| **CH-2** | $Q_E$, kW | 1580 ± 460 | 1640 ± 655 | 1875 ± 590 | 2015 ± 315 | 1715 ± 390 | 1550 ± 275 | 1750 ± 395 |
| | $E$, kW | 308 ± 77 | 323 ± 117 | 370 ± 111 | 368 ± 77 | 316 ± 86 | 302 ± 49 | 338 ± 72 |
| | $COP_{CH}$ | 5.07 ±0.39 | 4.97 ±0.42 | 5.02 ±0.26 | 5.54 ±0.50 | 5.50 ±0.46 | 5.13 ±0.19 | 5.16 ±0.16 |
| | $Q_E/Q_{Edesign}$ | 0.50 ±0.15 | 0.52 ±0.21 | 0.59 ±0.19 | 0.64 ±0.10 | 0.54 ±0.12 | 0.49 ±0.09 | 0.55 ±0.13 |

### 4.7.2  COP of central cooling plant

Several COP values can be used to assess the overall central plant performance: (1) the chillers COP, (2) the central plant COP (including chillers, cooling towers, and pumps P-3 to P-4), as defined by Hartman (2001), (3) the central plant COP*, which is similar to the central plant COP but also includes the heat exchanger condenser water pumps (P-3 to P-5), and (4) the cooling COP (including chillers, cooling towers, and pumps P-1 to P-5) (Table 4.12). The monitored chillers COP is about 15% lower than the rated COP of 5.76. Overall, the performance of the cooling system indicates that the chillers and pumps have the largest impact on the overall COP.

*Table 4.12: Daily average COP of central cooling plant, June 22$^{nd}$ to 28$^{th}$ 2009*

| Item \ Day | 06/22 | 06/23 | 06/24 | 06/25 | 06/26 | 06/27 | 06/28 |
|---|---|---|---|---|---|---|---|
| $COP_{CH}$ | 5.07±0.39 | 4.97±0.42 | 5.02±0.26 | 5.54±0.50 | 5.13±0.19 | 5.13±0.19 | 5.16±0.16 |
| $COP_{central\ plant}$ | 4.22±0.45 | 4.12±0.54 | 4.19±0.33 | 4.60±0.33 | 4.54±0.37 | 4.26±0.21 | 4.32±0.19 |
| $COP^*_{central\ plant}$ | 3.90±0.47 | 3.80±0.58 | 3.91±0.37 | 4.38±0.36 | 4.27±0.39 | 3.93±0.23 | 4.02±0.23 |
| $COP_{cooling}$ | 3.27±0.49 | 3.21±0.63 | 3.35±0.43 | 3.75±0.29 | 3.58±0.33 | 3.30±0.25 | 3.42±0.27 |

### 4.7.3  Effectiveness of heat exchanger HX-3

The effectiveness is calculated for the heat exchanger HX-3. To calculate the effectiveness of HX-3 (Figure 4.21), the entering hot side water temperature ($T_9^{HX-3}$) is equal to the condenser leaving water temperature that is being redirected to the heat exchanger. The heat exchanger supply and return cold side water temperatures ($T_7^{HX-3}$ and $T_8^{HX-3}$) are being monitored, and assuming the heat exchanged between the cold side and hot side is 100%, the leaving hot side water temperature ($T_{10}^{HX-3}$) is calculated according to Equation (4.16) and using the measured water flow rates presented in Table 4.4.
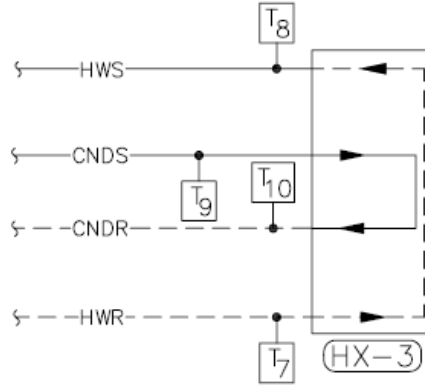
*Figure 4.21: Temperature locations for heat exchanger HX-3*

$$T_{10}^{HX-3} = T_9^{HX-3} - \left( \frac{\dot{V}_{P-6} \cdot C_{p,HW} \cdot \rho_{HW} \cdot (T_8^{HX-3} - T_7^{HX-3})}{\dot{V}_{P-5} \cdot C_{p,CND} \cdot \rho_{CND}} \right) \qquad (4.16)$$

where $\dot{V}$ is the volumetric flow rate, m$^3$/s; $C_p$ is the specific heat of water at the average design water temperature, kJ/kg · °C; $\rho$ is the water density at the average design water temperature, kg/m$^3$; and $T$ are the water temperatures, °C.

Based on NTU method for counterflow heat exchanger, the effectiveness of the heat exchanger HX-3 is given by Equation (4.17) (McQuiston et al. 2005), for the case $\left( \dot{V}_{P-6} \cdot C_{p,HW} \cdot \rho_{HW} \right) > \left( \dot{V}_{P-5} \cdot C_{p,CND} \cdot \rho_{CND} \right)$, where $\dot{V}_{P-6}$ = 0.107 m$^3$/s, $\dot{V}_{P-5}$ = 0.060 m$^3$/s, $C_{p,HW} = C_{p,CND}$, and $\rho_{HW} = \rho_{CND}$:

$$\epsilon_{HX-3} = \frac{T_9^{HX-3} - T_{10}^{HX-3}}{T_9^{HX-3} - T_7^{HX-3}} \qquad (4.17)$$

Table 4.13 presents the average effectiveness of heat exchanger HX-3 for the week of June 22nd to June 28th 2009. For the week analysed, the effectiveness of heat exchanger HX-3 varies between 0.69 and 0.75.

*Table 4.13: Daily average effectiveness for heat exchanger HX-3, June 22nd to 28th 2009*

| Item \ Day | 06/22 | 06/23 | 06/24 | 06/25 | 06/26 | 06/27 | 06/28 |
|---|---|---|---|---|---|---|---|
| $\epsilon_{HX-3}$ | 0.69±0.11 | 0.71±0.13 | 0.71±0.16 | 0.75±0.08 | 0.72±0.14 | 0.74±0.12 | 0.73±0.12 |

**4.8    Overview of the as-operated characteristics of the CSB central plant**

To portray a complete scheme of the CSB central plant operation, seasonal and yearly data for 2009 and 2010 are analyzed. Weekly data for the year 2009 are also presented in Appendix B.

### *4.8.1    Equipment operating characteristics*

Table 4.14 and Table 4.15 present seasonal monitored data for the year 2009 and 2010, respectively. The average outdoor air temperature is about 4°C higher in the winter, 2°C higher in the spring, and about 1°C higher in the summer in 2010 compared to 2009. The relative humidity is also higher in 2010.

The heating water flow rate, which is variable, is higher, while the supply temperatures are similar in 2010 compared to 2009. The average temperatures at the heat exchangers are similar for both years. The steam flow rate is slightly higher in 2010 when compared to 2009.

*Table 4.14: Seasonally average monitored data, 2009*

| Season[1] Item | Winter | Spring | **Summer** | Fall |
|---|---|---|---|---|
| $T_{db}$, °C | -6.5 ± 7.3 | 12.6 ± 7.2 | **21.1 ± 5.2** | 5.1 ± 7.0 |
| $RH$, % | 38.6 ±13.5 | 36.8 ±22.3 | **43.5 ±21.6** | 46.0 ±19.9 |
| $\dot{V}_{CHW}^{CSB}$, L/s | OFF | 82.5 ± 8.4 | **94.2 ±24.6** | 84.3 ± 2.6 |
| $T_{CHWS}^{CSB}$, °C | OFF | 7.7 ± 2.4 | **7.1 ± 0.5** | 7.2 ± 0.8 |
| $T_{CHWR}^{CSB}$, °C | OFF | 11.2 ± 2.2 | **11.7 ± 1.6** | 12.5 ± 1.5 |
| $\dot{V}_{HW}^{CSB}$, L/s | 72.8 ±12.4 | 53.0 ± 9.9 | **46.1 ± 7.2** | 65.1 ±11.8 |
| $T_{HWS}^{CSB}$, °C | 38.3 ± 2.5 | 33.3 ± 3.1 | **31.7 ± 1.7** | 35.7 ± 3.9 |
| $T_{HWR}^{CSB}$, °C | 38.3 ± 2.5 | 31.7 ± 3.0 | **29.5 ± 1.4** | 33.9 ± 3.0 |
| $\dot{m}_{steam}$, kg/s | 52.9 ±12.8 | 71.4 ±17.8 | **87.5 ± 8.5** | 75.9 ±17.0 |
| $T_{condensate}$, °C | 100.3± 7.7 | 101.7 ± 4.0 | **100.6 ± 6.7** | 101.2± 4.4 |
| $T_1^{HX-1}$, °C | 46.8 ± 5.5 | 34.3 ± 3.6 | 31.3 ± 1.6 | 37.8 ± 5.1 |
| $T_2^{HX-1}$, °C | 39.8 ± 2.6 | 32.7 ± 3.0 | 30.2 ± 1.6 | 35.0 ± 3.1 |
| $T_3^{HX-1}$, °C | 38.2 ± 2.4 | 32.1 ± 2.9 | 30.3 ± 1.6 | 34.1 ± 2.8 |
| $T_4^{HX-1}$, °C | 42.0 ± 3.3 | 33.4 ± 3.2 | 30.7 ± 1.5 | 36.1 ± 3.6 |
| $T_7^{HX-3}$, °C | OFF | 30.0 ± 1.5 | 31.0 ± 1.5 | 31.1 ± 1.2 |
| $T_8^{HX-3}$, °C | OFF | 30.8 ± 1.8 | **32.1 ± 1.6** | 32.4 ± 1.4 |

[1] Winter is from 12/22/2008 to 03/22/2009, spring is from 03/23/2009 to 06/21/2009, summer is from 06/22/2009 to 09/20/2009, and fall is from 09/21/2009 to 12/20/2009

*Table 4.15: Seasonally average monitored data, 2010*

| Season[1] \ Item | Winter | Spring | **Summer** | Fall |
|---|---|---|---|---|
| $T_{db}$, °C | -2.5 ± 6.6 | 14.3 ± 8.2 | **22.1 ± 5.5** | 5.5 ± 7.7 |
| $RH$, % | 42.5 ±17.4 | 37.5 ±23.1 | **47.0 ±22.1** | 49.6 ±21.0 |
| $\dot{V}_{CHW}^{CSB}$, L/s | OFF | 88.4 ±12.5 | **105.7 ±28.8** | 83.5 ±17.8 |
| $T_{CHWS}^{CSB}$, °C | OFF | 7.1 ± 0.7 | **7.1 ± 0.6** | 7.3 ± 2.0 |
| $T_{CHWR}^{CSB}$, °C | OFF | 11.0 ± 1.5 | **11.7 ± 1.5** | 10.5 ± 2.0 |
| $\dot{V}_{HW}^{CSB}$, L/s | 69.2 ±11.9 | 58.2 ±13.5 | **55.5 ±10.4** | 64.1 ±12.9 |
| $T_{HWS}^{CSB}$, °C | 40.0 ± 3.7 | 32.6 ± 2.8 | **30.0 ± 2.0** | 36.2 ± 4.2 |
| $T_{HWR}^{CSB}$, °C | 36.7 ± 2.7 | 31.0 ± 2.7 | **28.0 ± 1.6** | 34.3 ± 3.5 |
| $\dot{m}_{steam}$, kg/s | 48.2 ± 9.5 | 80.4 ±13.9 | **87.1 ± 6.3** | 68.1 ±16.7 |
| $T_{condensate}$, °C | 97.8 ±12.4 | 96.6 ±14.0 | **99.7 ± 4.9** | 99.2 ± 6.9 |
| $T_1^{HX-1}$, °C | 42.9 ± 5.1 | 34.6 ± 2.5 | 31.4 ± 1.4 | 38.6 ± 5.2 |
| $T_2^{HX-1}$, °C | 38.2 ± 2.5 | 33.2 ± 2.1 | 30.3 ± 1.3 | 36.0 ± 3.5 |
| $T_3^{HX-1}$, °C | 36.6 ± 2.7 | 32.4 ± 2.0 | 29.9 ± 1.3 | 34.9 ± 3.1 |
| $T_4^{HX-1}$, °C | 39.5 ± 3.8 | 33.4 ± 2.4 | 30.7 ± 1.4 | 36.8 ± 3.9 |
| $T_7^{HX-3}$, °C | OFF | 29.9± 1.3 | **29.4 ± 1.2** | 28.7 ± 1.0 |
| $T_8^{HX-3}$, °C | OFF | 30.8± 1.4 | **30.4 ± 1.2** | 29.5 ± 1.1 |

[1] Winter is from 12/21/2009 to 03/21/2010, spring is from 03/22/2010 to 06/20/2010, summer is from 06/21/2010 to 09/19/2020, and fall is from 09/20/2010 to 12/19/2010

### 4.8.2 *Operating characteristics of the central plant*

The central plant thermal load, such as the chilled and heating water loads, the heat recovered and the heat rejected are evaluated. Seasonal and annual data are presented for the year 2009 and 2010 to demonstrate the energy use and peak variations throughout the year (Table 4.16 and Table 4.17).

The outdoor air conditions are different between 2009 and 2010 (see section 4.8.1), and they influences the central plant thermal loads. The annual chilled water load, the heat recovered, and the heat rejected are 33%, 20% and 10% higher in 2010 compared to 2009, respectively. The heating water load is 15% lower in 2010 compared to 2009.

*Table 4.16: Seasonally and annual energy use and peak loads, 2009*

| Item, GJ/season | Winter | Spring | **Summer** | Fall | Year 2009 |
|---|---|---|---|---|---|
| $Q_{CHW}^{CSB}$ (Peak, kW) | OFF | 2,285 (2700) | **11,070 (4925)** | 235 (2845) | 13,595 (4925) |
| $Q_{CHW}$ (Peak, kW) | OFF | 2,435 (7495) | **11,665 (5700)** | 245 (2705) | 14,345 (7495) |
| $Q_{rec.}$ (Peak, kW) | OFF | 400 (1065) | **2,620 (3735)** | 65 (745) | 3,085 (3735) |
| $Q_{reject.}$ (Peak, kW) | OFF | 3,280 (4025) | **15,930 (7870)** | 350 (4000) | 19,560 (7870) |
| $Q_{HW}^{CSB}$ (Peak, kW) | 10,825 (8630) | 2,620 (2805) | **3,105 (1080)** | 4,345 (3920) | 21,140 (8630) |
| $Q_{BE}$ (Peak, kW) | 8,075 (2560) | 1,435 (1760) | 315 (800) | 2,855 (2080) | 12,660 (2560) |
| $Q_{HX-1}$ (Peak, kW) | 9,795 (4630) | 1,800 (2060) | 175 (560) | 3,855 (3465) | 15,905 (4630) |
| $Q_{HX-2}$ (Peak, kW) | 1,240 (4795) | 520 (1240) | 485 (1035) | 580 (2310) | 2,755 (4795) |

*Table 4.17: Seasonally and annual energy use and peak loads, 2010*

| Item, GJ/season | Winter | Spring | **Summer** | Fall | Year 2010 |
|---|---|---|---|---|---|
| $Q_{CHW}^{CSB}$ (Peak, kW) | OFF | 3,970 (4375) | **13,715 (5330)** | 570 (4580) | 18,255 (5330) |
| $Q_{CHW}$ (Peak, kW) | OFF | 4,045 (4870) | **14, 535 (5840)** | 555 (4485) | 19,135 (5840) |
| $Q_{rec.}$ (Peak, kW) | OFF | 1,020 (965) | **2,500 (1735)** | 160 (655) | 3,680 (1735) |
| $Q_{reject.}$ (Peak, kW) | OFF | 5,030 (7130) | **15,720 (6240)** | 650 (4865) | 21,400 (7130) |
| $Q_{HW}^{CSB}$ (Peak, kW) | 8,995 (4385) | 2,985 (2530) | **3,085 (1715)** | 3,655 (3050) | 17,775 (4385) |
| $Q_{BE}$ (Peak, kW) | 5,875 (2240) | 835 (1120) | 45 (640) | 2,660 (2400) | 9,280 (2560) |
| $Q_{HX-1}$ (Peak, kW) | 7,715 (3930) | 985 (1315) | 50 (730) | 3,065 (2660) | 11,250 (3930) |
| $Q_{HX-2}$ (Peak, kW) | 1,120 (3255) | 1,080 (2510) | **630 (960)** | 645 (2135) | 3,460 (3255) |

### 4.8.3 Electric demand and energy use of the central plant equipment

The electricity used for the installed mechanical equipment in the central plant is estimated. The 2009 and 2010 seasonal and annual monitored information are presented in Table 4.18 and Table 4.19.

The total electricity consumption is 17% higher in 2010 compared to 2009. There is a large increase in electricity consumption in the spring and the summer 2010 compared to 2009, 49% and 18% respectively. In the winter and fall, the electricity consumption is about 10% lower in 2010 compared to 2009. The electricity consumption of the central plant is influenced by the outdoor air conditions: the outdoor air temperatures and relative humidity are higher in 2010 compared to 2009 (see section 4.8.1).

*Table 4.18: Seasonally average central plant electricity consumption, 2009*

| Item / Season | Winter | Spring | **Summer** | Fall | Year 2009 |
|---|---|---|---|---|---|
| $E_{CH}$, kWh/season | OFF | 131,090 | **604,485** | 11,090 | 746,660 |
| $E_{CT}$, kWh/season | OFF | 1,580 | **14,800** | 245 | 16,625 |
| $E_{pumps}$, kWh/season | 170,995 | 167,535 | **415,995** | 140,545 | 899,255 |
| $E_{elec}$, kWh/season | 170,995 | 300,205 | **1,035,280** | 151,880 | 1,662,540 |

*Table 4.19: Seasonally average central plant electricity consumption, 2010*

| Item / Season | Winter | Spring | **Summer** | Fall | Year 2010 |
|---|---|---|---|---|---|
| $E_{CH}$, kWh/season | OFF | 218,545 | **713,175** | 32,300 | 964,020 |
| $E_{CT}$, kWh/season | OFF | 3,960 | **32,245** | 465 | 36,670 |
| $E_{pumps}$, kWh/season | 154,425 | 225,120 | **476,340** | 106,900 | 940,410 |
| $E_{elec}$, kWh/season | 154,425 | 447,625 | **1,221,760** | 139,665 | 1,941,100 |

### 4.8.4 *Performance characteristics*

The performances of various equipment or groups of equipment are evaluated using the coefficient of performance (COP) and the effectiveness for heat exchangers, in a similar way as presented in section 4.7.2. Table 4.20 and Table 4.21 present the 2009 and 2010 seasonal averages.

The average COP over the summer 2010 season is slightly higher than in 2009, which could be explained by the measurements uncertainty (Equation (4.2)). The average COP uncertainty over the summer 2009 is ±1.09, while being ±1.24 for the summer 2010.

*Table 4.20: Seasonally average central plant performance indices, 2009*

| Item / Season | Winter | Spring | **Summer** | Fall |
|---|---|---|---|---|
| $COP_{CH}$(uncertainty) | OFF | 5.05±1.14 | **5.24±1.03** **(±1.20)** | 5.29±0.30 |
| $COP_{central\ plant}$ | OFF | 4.10±0.89 | **4.31±0.71** | 4.49±0.32 |
| $COP^*_{central\ plant}$ | OFF | 3.86±0.89 | **4.04±0.69** | 4.20±0.34 |
| $COP_{cooling}$ | OFF | 3.38±0.83 | **3.38±0.63** | 3.60±0.36 |
| $\epsilon_{HX-1}$ | 0.47±0.12 | 0.59±0.20 | 0.37±0.20 | 0.59±0.18 |
| $\epsilon_{HX-3}$ | OFF | 0.55±0.31 | **0.74±0.12** | 0.71±0.11 |

*Table 4.21: Seasonally average central plant performance indices, 2010*

| Item / Season | Winter | Spring | **Summer** | Fall |
|---|---|---|---|---|
| $COP_{CH}$ (uncertainty) | OFF | 4.99±0.71 | **5.36±0.70** **(±1.42)** | 4.53±0.75 |
| $COP_{central\ plant}$ | OFF | 4.07±0.68 | **4.37±0.61** | 3.61±0.76 |
| $COP^*_{central\ plant}$ | OFF | 3.77±0.69 | **4.12±0.64** | 3.28±0.77 |
| $COP_{cooling}$ | OFF | 3.13±0.68 | **3.45±0.60** | 2.67±0.73 |
| $\epsilon_{HX-1}$ | 0.48±0.20 | 0.48±0.27 | 0.51±0.16 | 0.55±0.14 |
| $\epsilon_{HX-3}$ | OFF | 0.67±0.15 | **0.59±0.11** | 0.59±0.12 |

The central plant and modified central plant COP over the summer 2009 and 2010 are compared with the benchmark scale proposed by Hartman (2001), which considered the electricity consumption of chillers, cooling towers and condenser water pumps to calculate the COP (Figure 4.20). The average central plant COP and central plant COP*, which also includes the heat recovery pump P-5 on the condenser water loop to the heat exchanger HX-3, over the summer 2009 and 2010 are evaluated as "good" when compared to the benchmark scale.
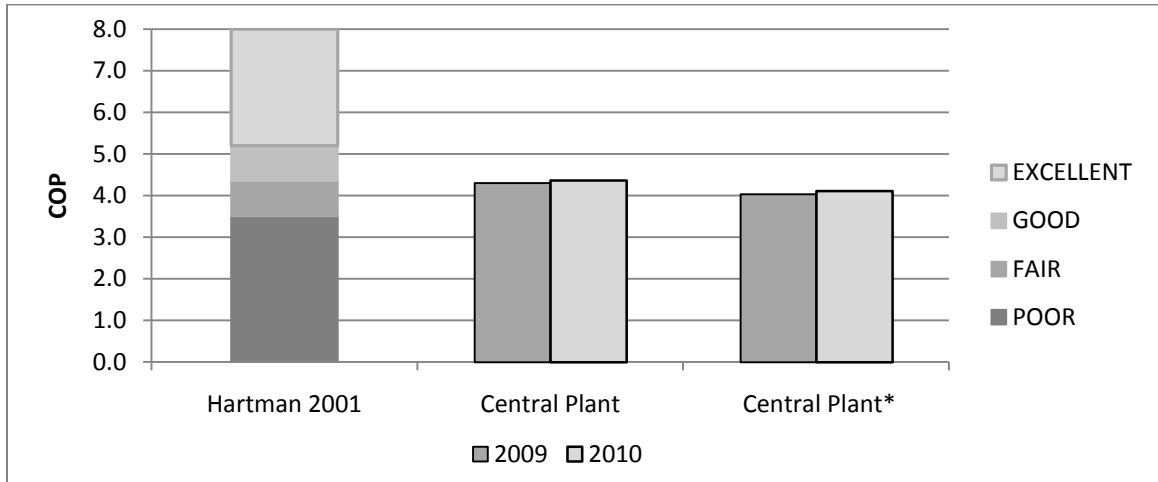


*Figure 4.22: Comparison of central plant and modified central plant COP, summer 2009 and summer 2010*

## 4.9 Conclusions

The analysis of monitored data of the CSB showed changes in operation compared to the design information. The main differences are modified water flow rate to

constant speed pumps and slight variation of the temperature setpoints. The as-operated conditions, thermal loads, electricity used, COP and effectiveness of the main equipments were analyzed in detail for the first week of the summer 2009, from June 22$^{nd}$ to June 28$^{th}$ 2009 (sections 4.4 to 4.7), and presented for seasonal and yearly data of the year 2009 and 2010 (section 4.8).

The comparison between the 2009 and 2010 seasonal and yearly data showed higher outdoor air conditions in 2010 compared to 2009. This has a direct effect on the total heating, cooling loads and heat rejected, and the seasonal and annual electricity use. In terms of heat recovered and COP, the values were similar. The small differences can be explained by the uncertainty of the measurements.

The analyzed information is useful to develop the benchmarking models and to calibrate the model of the central cooling plant in the TRNSYS program.

# 5 BENCHMARKING MODELS AND APPLICATION

The proposed benchmarking approach, presented in Chapter 3, is tested using monitored data from the central plant of the Concordia Sciences Building (CSB), located on the Loyola campus in Montréal, Canada. The data used to establish the models are obtained through the collaboration of the Physical Plant of Concordia University from the Monitoring and Data Acquisition System (MDAS) installed at the CSB. The data monitored over the 2009 summer season, from June 22$^{nd}$ to September 20$^{th}$ 2009, are used to initially evaluate the benchmark models. Additional monitored data, collected over the 2010 summer season, from June 21$^{st}$ to September 19$^{th}$ 2010, are used to further verify the developed models. A total of fifty-eight points are monitored every fifteen minutes and available to establish benchmarking models and evaluate the proposed approach.

## 5.1 Monitored data pre-processing

Prior to establishing the benchmark models, a detailed analysis of the monitored data is performed to identify any data monitoring problems or outliers. The following rules were applied to the data set:

All monitored data

1. There could be a time delay in the data recording between some points at start-up and shut-down of the equipment between the system signal and recording of monitored data points. For example, at start-up, the ON/OFF signal of the chiller could indicate that the equipment is ON, while the monitored data point (sensor) for the electric power input to the chiller would show a value different from zero

only at the next recorded time step, i.e. 15 minutes. If this situation occurs, the set

of data monitored at this time-step is incomplete and removed from the original

data set.

2.    In a few cases, it was noticed that at the pump start-up, the calculation of the

thermal water load, based on temperature difference between the supply and

return flows, gives a negative value or zero since both temperature sensors are at

the same temperature. This situation generates an incomplete set of monitored

data for that time-step and the data are removed from the original data set.

Training and testing sets

To improve the quality of the data used to develop the model, outliers are

removed from the initial data set. The initial data set includes both the training and testing

data sets. For each data set selected to establish the benchmark models (training and

testing sets), outliers are identified for the electric power input, COP, thermal loads and

water supply and return temperatures. Outliers are observations that are numerically

distant from the rest of the data. In most cases, an outlier indicates a measurement error

or an abrupt change in operation that is unusual for normal operation. Outliers removal

can be done by visual inspection or using a mathematical approach. Measurements

satisfying the conditions of Equations (5.1a) and (5.1b) are considered to be outliers and

are automatically eliminated from the data sets used to establish the models.

$$y_i < (\bar{y} - 3 \cdot \sigma) \tag{5.1a}$$
$$y_i > (\bar{y} + 3 \cdot \sigma) \tag{5.1b}$$

where $y_i$ is the measured value, $\bar{y}$ is the mean of the measured values in the data

set, and $\sigma$ is the standard deviation. The standard deviation is a measure of the variability

or dispersion of observations about the mean. According to Chebyshev's theorem, when using three standard deviations, there are at least ~90% (8/9) of the observations of any distribution that fall in that interval (Walpole et al. 2002). The use of a larger data set for training ensures that the observations selected to establish the benchmark models cover a wide range of operating conditions without including observations that could increase the noise level within the data set.

Data set used during ongoing commissioning

The analysis of monitored data revealed that at start-up, the electrical power input to pumps or chillers and positive thermal water loads are often outside the normal operation values of the equipment. For example, for chiller CH-1, the electrical power input (Figure 5.1) and the evaporator thermal load (Figure 5.2) are higher at start-up. The start-up of the chiller creates a spike in electricity demand, while the evaporator load is higher because the time for the return chilled water temperature to reach its normal operating temperature range is longer than for the supply chilled water; therefore, the evaporator load, calculated based on the water temperature difference, is higher. To avoid false warnings being sent to the building operators, the first complete set of monitored data at start-up is ignored.
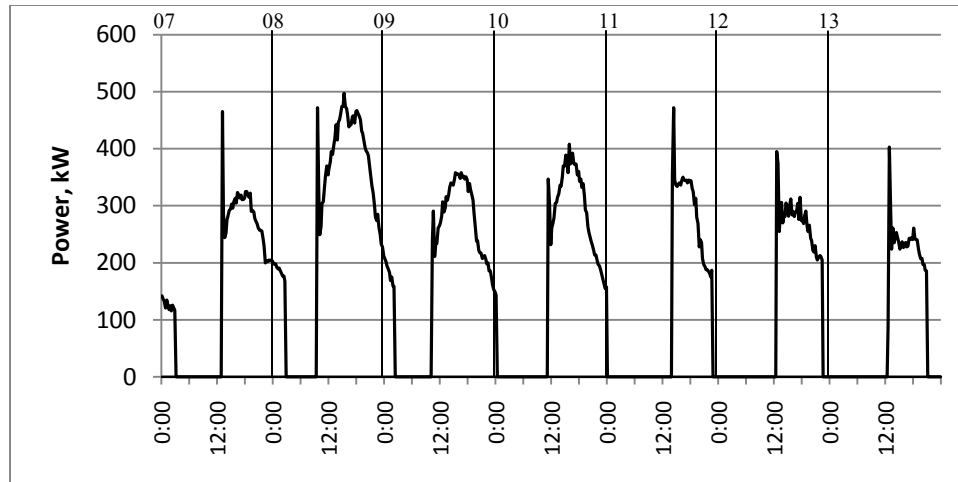
*Figure 5.1: Chiller CH-1 electric power input variation at start-up, September 7ᵗʰ to 13ᵗʰ 2009*
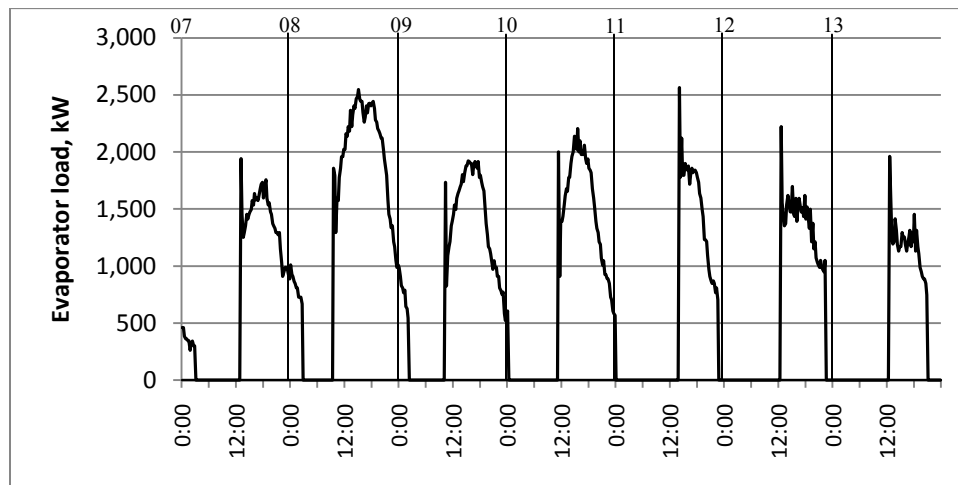


*Figure 5.2: Chiller CH-1 evaporator load variation at start-up, September 7ᵗʰ to 13ᵗʰ 2009*

Verification set

The verification set is used to further evaluate the accuracy of the benchmark models. To avoid false errors in the calculation of the various model criteria, the first complete set of monitored data at start-up is ignored and the outliers are removed from the verification data.

## 5.2 Evaluation criteria

Different criteria are used to evaluate the precision of the proposed models, which are calculated after the data pre-processing tasks are done (Section 5.1). The coefficient of determination ($R^2$), which is the sum of squares of the residual compared with the total sum of squares of the variation (proportional to the sample variance), is used to evaluate the correctness of the identified correlation coefficients of the developed benchmarking model (Equation (5.2)). The $R^2$ value can vary between 0 and 100% and indicates how much the variation of the dependent variable ($y$) is explained by the variation of independent variable ($x_i$). A $R^2$ of zero means none of the variation is explained by the model, while a $R^2$ of 100% means that the model explains the whole variation of the dependent variable ($y$) due to the variation of the independent variables. A $R^2$ greater than 75% is usually considered acceptable for a good relationship amongst the energy and independent variables (IPMVP 2007).

$$R^2 = \left(1 - \frac{\sum_{i=1}^{n}(y_i - \hat{y}_i)^2}{\sum_{i=1}^{n}(y_i - \bar{y})^2}\right) \cdot 100 \qquad (5.2)$$

where $y_i$ is the measured value, $\hat{y}_i$ is the predicted value, $\bar{y}$ is the mean of the measured value sample data, and $n$ is the number of data used to establish the regression equation.

The Coefficient of Variance of the Root-Mean-Squared-Error (CV(RMSE)), the Root-Mean-Squared-Error (RMSE), and the Mean Bias Error (MBE) are used to assess the precision of the models for the different data sets - Equations (5.3) to (5.5) as defined by IPMVP (2007). A CV(RMSE) of 3-5% for prediction of power input at the component level is acceptable (Haberl and Bou-Saada 1998, Kammerud et al. 1999). For models of

whole building energy use, the model is considered acceptable if the CV(RMSE) is less

than 30% when using hourly data, or 5% to 15% for monthly data (ASHRAE 2002).

$$CV(RMSE) = \frac{\sqrt{\frac{\sum_{i=1}^{n}(\hat{y}_i - y_i)^2}{n-1}}}{\bar{y}} \cdot 100 \tag{5.3}$$

$$RMSE = \sqrt{\frac{\sum_{i=1}^{n}(\hat{y}_i - y_i)^2}{n-1}} \tag{5.4}$$

$$MBE = \frac{\sum_{i=1}^{n}(\hat{y}_i - y_i)}{n} \tag{5.5}$$

An additional criterion, the Relative Error (R.E.), is used to compare the estimates

of energy consumption of each equipment or equipment group with the measured values

over the verification set (Equation (5.6)).

$$R.E. = \frac{\sum_{i=1}^{n}(\hat{y}_i \cdot \Delta t) - \sum_{i=1}^{n}(y_i \cdot \Delta t)}{\sum_{i=1}^{n}(y_i \cdot \Delta t)} \cdot 100 \tag{5.6}$$

## 5.3    Model types

New correlations and existing correlations, as well as new ANN models, are

evaluated for the equipment installed in the CSB. Models are developed that characterize

the operation of the systems under normal operating conditions (benchmarking). The

benchmarking models, which are energy baseline models, are obtained and updated using

monitored data.

For each technique, the data set selected from monitored data used to develop the

benchmarking model is divided in two sub-sets: (1) a training data set and (2) a testing

data set. Different methods of dividing the selected data set into training and testing data

sets (e.g., random selection) can be considered. For this project, the training data set uses

the first two-thirds of the benchmarking data set (Kreider and Haberl 1994) to identify the

model coefficients or train the ANN models, and the testing data set uses the balance of

the data set to verify the correctness of the models before it is used for benchmarking. Once the benchmarking model is developed, the actual monitored data, outside the initial data set, are compared with the model results to detect abnormal energy performance. Different training and retraining techniques using static windows or dynamic windows (sliding window or augmented window) are used in this chapter, and the results compared. For the correlation-based models, the model coefficients are identified using least-square regression in STATGRAPHICS (2008), while for the ANN models, the models are trained in MATLAB (2008) with the Bayesian regularization backpropagation.

## 5.4    Training and testing data sets

The techniques used for the development of benchmarking models of the energy performance of the central plant equipment using monitored data are presented in this section. For general presentation and description of the proposed techniques, refer to Chapter 3, section 3.3.1. To facilitate the comparison between the correlation-based and ANN models, the same training and testing data sets are used for both models. Examples of benchmarking models are presented in Section 5.5.

For the correlation-based or ANN models, the models are trained using several techniques. The set names represent the period of time from which the data points are taken from. The data set excludes the data points when the equipment is not in operation. Thus, the data set size indicates the number of time-step (15 minutes) during operation for each data set. The first part of the set name indicates the equipment for which the model is developed. For example, CH1 for chiller CH-1, while the second part is the

91

abbreviation for the period of data set used to establish the models (Table 5.1). The number in front of each abbreviation indicates the period of time used as an initial data set, which includes both the training and testing data sets.

*Table 5.1: Definition of the abbreviations used for the various benchmark models*

| Abbreviation | Signification |
|---|---|
| WW | Number of work week excluding holidays |
| WEH | Number of week end including holidays |
| H | Number of hours used to established the models |
| D | Number of days used to established the models |
| R | Number of days before retraining occurs for the sliding window models |

For the cooling systems, the equipment is divided into three groups: (1) chiller CH-1 and cooling tower CT-1, (2) chiller CH-2 and cooling tower CT-2, and (3) heat exchanger HX-3. From June 22$^{nd}$ to July 6$^{th}$ 2009, the chiller CH-2 and cooling tower CT-2 are the first group of equipment to be start-up, while after July 6$^{th}$ 2009, the chiller CH-1 and the cooling tower CT-1 become the first group of equipment to be started-up, when required. Since the quantity of monitored data during operation is different at the beginning of the summer, the models are established with slightly different training data set. However, once the initial data set is selected, which is composed of 30 hours of operation over the first two weeks of the summer for CH-1 and CT-1 (CH1-30H, CT1-30H) and the first day of summer for CH-2 and CT-2 (CH2-1D, CT2-1D), the general rule to increase the initial training and testing data sets is similar.

### 5.4.1 Training data set by static technique

Static models can be of two different types: (1) a typical static technique that uses a pre-defined training and testing data set that includes both working days, weekends and holidays, and (2) a split static technique, where models are developed for various day types (separate models for working days and weekends & holidays for example).

92

*5.4.1.1  Typical static*

For the typical static technique, the initial data set of 30 hours for chiller CH-1 (CH1-30H) and cooling tower CT-1 (CT1-30H), and of one day for chiller CH-2 (CH2-1D) and cooling tower CT-2 (CT2-1D) are first used to established the models. Additional static models are also evaluated, and the result compared: the data sets, used for training and testing, are presented in Table 5.2 for CH-1 and CT-1 and in Table 5.3 for CH-2 and CT-2.

*Table 5.2: Training and testing data sets for typical static technique, CH-1 and CT-1*

| Set name | Training set | | Testing set | |
|---|---|---|---|---|
| | Date | Data set size | Date | Data set size |
| CH or CT1-30H | 06/22 to 06/26 – 22.5 h | 85 | 06/27 to 07/06 – 8 h | 29 |
| CH or CT1-7D | 06/22 to 07/10 | 331 | 07/11 to 07/12 | 186 |
| CH or CT1-10D | 06/22 to 07/12 | 517 | 07/13 to 07/15 | 94 |
| CH or CT1-14D | 06/22 to 07/15 | 610 | 07/16 to 07/19 | 227 |
| CH or CT1-21D | 06/22 to 07/19 | 822 | 07/20 to 07/26 | 608 |
| CH or CT1-28D | 06/22 to 07/24 | 1271 | 07/25 to 08/02 | 822 |

*Table 5.3: Training and testing data sets for typical static technique, CH-2 and CT-2*

| Set name | Training set | | Testing set | |
|---|---|---|---|---|
| | Date | Data set size | Date | Data set size |
| CH or CT2-1D | 06/22 0:00 to 16:00 | 47 | 06/22 16:00 to 24:00 | 32 |
| CH or CT2-7D | 06/22 to 06/26 | 443 | 06/27 to 06/28 | 192 |
| CH or CT2-10D | 06/22 to 06/27 | 538 | 06/28 to 07/01 | 380 |
| CH or CT2-14D | 06/22 to 06/30 | 833 | 07/01 to 07/05 | 400 |
| CH or CT2-21D | 06/22 to 07/05 | 1233 | 07/06 to07/12 | 91 |
| CH or CT2-28D | 06/22 to 07/10 | 1336 | 07/11 to 07/19 | 49 |

*5.4.1.2  Split static*

Due to low chilled water demand from the buildings, chiller CH-1 and cooling tower CT-1 are only really being operated after July 6th; consequently, the development of split static models for CH-1 and CT-1 at the beginning of the summer season, where different models are used for working days and weekend & holidays, is not possible. Therefore, split static models are only presented for the chiller CH-2 and cooling tower CT-2. The monitored data from the equipment are used to establish different models for

working days (WW) and weekends & holidays (WEH). Table 5.4 specifies the data used to establish the models. For instance, the first selected data set contains the first working weeks of the summer (CH2-1WW), while the second data set contains one holiday and one weekend (CH2-1WEH). The data set size indicates the number of data in the set for each monitored variable.

*Table 5.4: Training and testing data sets for split static technique, CH-2 and CT-2*

| Set name | Training set | | Testing set | |
|---|---|---|---|---|
| | Date | Data set size | Date | Data set size |
| CH or CT2-1WW | 06/22 to 06/23 and 06/25 0:00 to 12:00 | 218 | 06/25 12:00 to 06/26 | 139 |
| CH or CT2-1WEH | 06/24 and 06/27 | 184 | 06/28 | 95 |
| CH or CT2-2WW | 06/22 to 06/23, 06/25 to 06/26 and 06/29 to 06/30 | 538 | 07/02 to 07/03 | 189 |
| CH or CT2-2WEH | 06/24, 06/27, 06/28, 07/01 | 383 | 07/04 to 07/05 | 120 |

### 5.4.2   *Training data set by window technique*

Two different window types, augmented and sliding, are evaluated for both chillers, with different training set size.

### 5.4.2.1   *Augmented window*

In terms of training and testing, the typical static and the augmented window techniques are similar. For example, a 7D typical static model is trained with the same data set as the 7D augmented window model. The difference lies in the retraining of the model. For the typical static, the pre-defined set size is used to establish the model and there is no retraining for the rest of the summer. For the augmented window, the model is established and used until additional data are available; the model is then retrained using the augmented data set (see Section 3.3.1.2).

Between June 22nd and July 6th 2009, chiller CH-1 and cooling tower CT-1 are the second operating group of cooling equipment and are only operating for a total of 30.25

hours. The initial model for the cooling equipment group one uses the first 30 hours of operation collected over the first two weeks of the summer season, plus the first full week of data monitored during which CH-1 and CT-1 are the first group of equipment to be started-up when required. As the monitored data become available, the training set size is increased every seven days. Thus, the models are then developed using 14, 21 and 28 days of monitored data, excluding non-operating hours. Data sets for training and testing the benchmarking models for chiller CH-1 and cooling tower CT-1, using the augmented window technique, are presented in Table 5.5.

Table 5.5: Training and testing data sets for augmented window technique, CH-1 and CT-1

| Set name | Training set | | Testing set | |
|---|---|---|---|---|
| | Date | Data set size | Date | Data set size |
| CH or CT1-7D | 06/22 to 07/10 | 331 | 07/11 to 07/12 | 186 |
| CH or CT1-14D | 06/22 to 07/15 | 610 | 07/16 to 07/19 | 227 |
| CH or CT1-21D | 06/22 to 07/19 | 822 | 07/20 to 07/26 | 608 |
| CH or CT1-28D | 06/22 to 07/24 | 1271 | 07/25 to 08/02 | 822 |

Since chiller CH-2 and cooling tower CT-2 are in operation from the beginning of the summer season, the following augmented windows are proposed to establish the benchmarking models (Table 5.6). It is important to mention that chiller CH-2 and cooling CT-2 operate for 339 hours between June $22^{nd}$ and July $6^{th}$ 2009 and for 330 hours between July $7^{th}$ and September $20^{th}$ 2009.

Table 5.6: Training and testing data sets for augmented window technique, CH-2 and CT-2

| Set name | Training set | | Testing set | |
|---|---|---|---|---|
| | Date | Data set size | Date | Data set size |
| CH or CT2-7D | 06/22 to 06/26 | 443 | 06/27 to 06/28 | 192 |
| CH or CT2-14D | 06/22 to 06/30 | 833 | 07/01 to 07/05 | 400 |
| CH or CT2-21D | 06/22 to 07/05 | 1233 | 07/06 to07/12 | 91 |
| CH or CT2-28D | 06/22 to 07/10 | 1336 | 07/11 to 07/19 | 49 |

5.4.2.2 *Sliding window*

Two different window sizes are used for the cooling equipment: (1) a 14 days (14D) window, where the first ten days of data are used to establish the model and the

95

last four days for testing, and (2) a 21 days (21D) window, where the first fourteen days of data are used to establish the model and the last seven days of data are used for testing. For the first model, the retraining occurs after seven days (R7), while for the second model it occurs after ten days (R10) (Table 5.7).

*Table 5.7: Training and testing data sets for sliding window technique*

| Set name | Training set | Testing set | Retraining |
|----------|--------------|-------------|------------|
| CH, CT or HX-14D-R7 | 10 days | 4 days | After 7 days |
| CH, CT or HX -14D-R7 | | | |
| CH, CT or HX -21D–R10 | 14 days | 7 days | After 10 days |
| CH, CT or HX -21D–R10 | | | |

## 5.5    Development of benchmarking models for chillers

Once pre-processing of the data is completed and the data sets are selected, new correlation-based models and ANN models are developed in this study for different equipment of the central plant and evaluated using the different training techniques. For the chillers, different benchmarking correlation-based and ANN models are proposed and compared with existing models as well as with results available in the literature. The evaluated models are general models, while the identified model coefficients or trained ANN models are case oriented.

### 5.5.1    Proposed correlation-based models

Previous studies of the performance of the Concordia Sciences Building have revealed that the total supply airflow rate does not significantly vary with the variation of outdoor air temperature (Monfet et al. 2009); however, the chilled water load and electric power input to chiller increase when the outdoor air temperature rises (Figure 5.3), while no specific trend was noticed with changes in the outdoor air relative humidity.

96
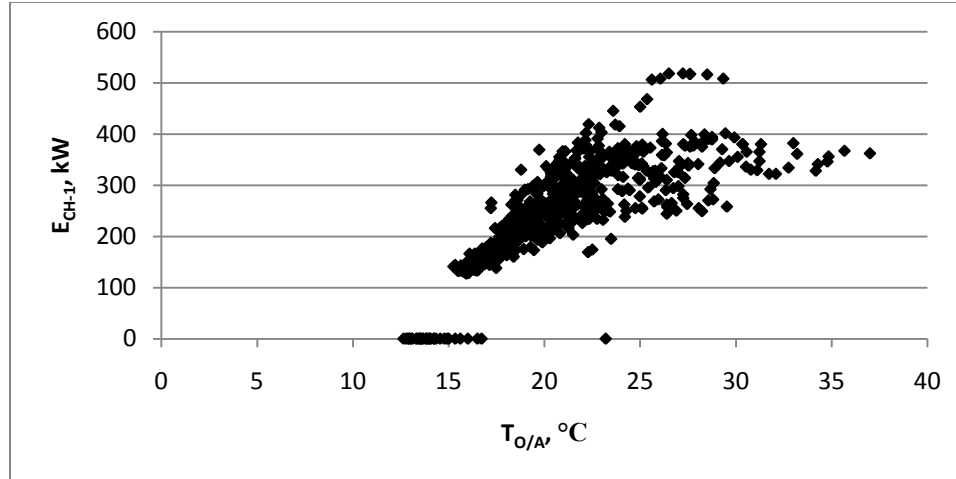
*Figure 5.3: Chiller CH-1 electric power input variation versus outdoor air temperature*

The analysis of monitored data shows that the supply chilled water and return condenser water temperatures are almost constant (Table 5.8), and the electric power input to the chillers increases with outdoor air temperatures. Therefore, the parameters used to characterize the performance of the chiller include the evaporator load ratio ($Q_E/Q_{Edesign}$), the supply condenser water temperature and the outdoor air temperature. Different correlation-based models for the chiller electric power input and COP are proposed: (1) a Multivariable Linear (ML) model for power input defined by Equation (5.7) and a Multivariable non-Linear (ML) model for COP defined by Equation (5.8); and (2) a multivariable polynomial (MP) model, Equation (5.9) for power input and Equation (5.10) for COP.

*Table 5.8: Chillers operating characteristics, summer 2009*

| Item | Chiller CH-1 | Chiller CH-2 |
|------|-------------|-------------|
| $T_{CHWS}$°C | $6.8 \pm 0.7$ | $6.8 \pm 0.6$ |
| $T_{CNDR}$, °C | $28.3 \pm 0.4$ | $28.5 \pm 0.5$ |

$$\dot{E}_{CH} = \alpha_1 \cdot \frac{\dot{Q}_E}{\dot{Q}_{Edesign}} + \alpha_2 \cdot T_{CNDS} + \alpha_3 \cdot T_{O/A} \qquad (5.7)$$

97

$$COP_{CH} = \gamma_1 \cdot \frac{1}{\left(\dfrac{\dot{Q}_E}{\dot{Q}_{Edesign}}\right)} + \gamma_2 \cdot T_{CNDS} + \gamma_3 \cdot T_{O/A} \tag{5.8}$$

$$\dot{E}_{CH} = \beta_0 + \beta_1 \cdot \left(\frac{\dot{Q}_E}{\dot{Q}_{Edesign}}\right)^2 + \beta_2 \cdot \frac{\dot{Q}_E}{\dot{Q}_{Edesign}} + \beta_3 \cdot (T_{CNDS})^2 + \beta_4 \cdot T_{CNDS} + \beta_5 \cdot T_{O/A} \tag{5.9}$$

$$COP_{CH} = \delta_1 \cdot \left(\frac{\dot{Q}_E}{\dot{Q}_{Edesign}}\right)^2 + \delta_2 \cdot \frac{\dot{Q}_E}{\dot{Q}_{Edesign}} + \delta_3 \cdot (T_{CNDS})^2 + \delta_4 \cdot T_{CNDS} + \delta_5 \cdot T_{O/A} \tag{5.10}$$

where $\dot{E}_{CH}$ is the instantaneous electric power input, in kW; $COP_{CH}$ is the calculated instantaneous chiller coefficient of performance; $\dot{Q}_E$ is the instantaneous chilled water load, equal to the evaporator load (Equation (4.5)), in kW; $\dot{Q}_{Edesign}$ is the design evaporator capacity, 3165 kW; $T_{CNDS}$ is the condenser water leaving temperature, in °C; and $T_{O/A}$ is the dry-bulb outdoor air temperature, in °C.

The models described by Equations (5.7) to (5.10) are valid for normal operating conditions of the chillers installed in the central plant, where $T_{CHWS}$ is ~6.8°C and the $T_{CNDR}$ ~28°C.

### 5.5.2  Existing correlation-based models used for comparison purposes

This section presents four models available in the literature which can be used to evaluate the performance of chillers. Their use as benchmarking models is presented in Section 5.5.4.1.

EnergyPlus model

One model used by the EnergyPlus program (DOE 2009) simulates the electric power input ($P_{CH}$) of an electric liquid chiller. The chiller power input is determined using Equation (5.11):

$$P_{CH} = \left(\dot{Q}_{avail}\right) \cdot \left(\frac{1}{COP_{ref}}\right) \cdot (EIRFTemp) \cdot (EIRFPLR) \tag{5.11}$$

98

where $P_{CH}$ is the chiller compressor power, kW and $\dot{Q}_{avail}$ is the available cooling capacity of the chiller in kW, defined by Equation (5.12);

$$\dot{Q}_{avail} = \dot{Q}_{ref} \cdot (CapFTemp) \tag{5.12}$$

where $\dot{Q}_{ref}$ is chiller capacity at reference conditions (reference temperatures and flow rates defined by the user) and *CapFTemp* is the cooling capacity factor for different operating temperatures, given by Equation (5.13); $COP_{ref}$ is the reference coefficient of performance; *EIRFTemp* is the energy input to cooling output ratio at full load, given by Equation (5.14); and *EIRFPLR* is the energy input to cooling output ratio at part load ratio, given by Equation (5.15).

The model, developed by Hydeman et al. (2002) as part of the CoolTools™ project sponsored by Pacific Gas and Electric Company (PG&E), uses Equations (5.13) to (5.15) to determine the various coefficients used in the chiller power equation (5.11).

$$\begin{aligned} CapFTemp = a_0 + (a_1 \cdot T_{CHWS}) + \left(a_2 \cdot T_{CHWS}^2\right) + (a_3 \cdot T_{CNDS}) + \left(a_4 \cdot T_{CNDS}^2\right) \\ + (a_5 \cdot T_{CHWS} \cdot T_{CNDS}) \end{aligned} \tag{5.13}$$

$$\begin{aligned} EIRFTemp = b_0 + (b_1 \cdot T_{CHWS}) + \left(b_2 \cdot T_{CHWS}^2\right) + (b_3 \cdot T_{CNDS}) + \left(b_4 \cdot T_{CNDS}^2\right) \\ + (b_5 \cdot T_{CHWS} \cdot T_{CNDS}) \end{aligned} \tag{5.14}$$

$$\begin{aligned} EIRFPLR = c_0 + (c_1 \cdot T_{CNDS}) + \left(c_2 \cdot T_{CNDS}^2\right) + (c_3 \cdot PLR) + (c_4 \cdot PLR^2) \\ + (c_5 \cdot T_{CDNS} \cdot PLR) + (c_6 \cdot PLR^3) \end{aligned} \tag{5.15}$$

where *PLR* is the part-load and calculated using Equation (5.16).

$$PLR = \frac{Q_E}{Q_{avail}} \tag{5.16}$$

The coefficients of the performance curves (Equations (5.13) to (5.15)) can either be generated using manufacturer's data or measured data. In this study, the Hydeman and

Gillespie (2002) technique, which is based on Hydeman et al. (2002), is used with some modifications for the identification of the coefficients $a_j$, $b_j$, and $c_j$.

*Initial training set*

The training data set contains monitored data at each time-step of the following variables: $P_{CH}$ $Q_E$, $COP$, $T_{CHWS}$, $T_{CHWR}$, $T_{CNDS}$, and $T_{CNDR}$, where $T_{CHWS}$ is the supply chilled water temperature; $T_{CHWR}$ is the return chilled water temperature; $T_{CNDR}$ is the return condenser water temperature from the cooling tower; $T_{CNDS}$ is the condenser water leaving temperature to the cooling tower; $Q_E$ is the instantaneous chilled water load, equal to the evaporator load determined using the formulation presented in ASHRAE 2002; $P_{CH}$ is the instantaneous electric power input; and $COP$ is the coefficient of performance equal to $Q_E/P_{CH}$, dimensionless.

1.  In the training data set, the maximum evaporator load $Q_{E,max}$ is identified. The maximum $Q_{E,max}$ and the corresponding electric power $P_{CH,max}$, and $COP$ are then used as the reference values ($Q_{ref} = Q_{Emax}$, $P_{ref} = P_{CH,max}$, *and* $COP_{ref}$) in the modified approach, which is proposed in this study;

2.  For all data in the training data set, the *CAPFT* is calculated using Equation (5.17), where $Q_{ref} = Q_{E,max}$ and $Q_E$ is the evaporator load at each time-step;

$$CAPFT = \frac{Q_E}{Q_{ref}}$$
(5.17)

3.  The training data set is split into (1) full-load and (2) part-load conditions based on the *CAPFT* values calculated using Equation (5.17). For this study, the full-load conditions data set was selected for *CAPFT* values greater than or equal to

0.85 (*CAPFT≥0.85*), while the part-load conditions for *CAPFT* values lower than 0.85 (*CAPFT<0.85*). A *CAPFT* greater than 0.85 is selected for the full load conditions since the chillers operate around 55-60% of their full design capacity most of the time.

*Full-load conditions data set (CAPFT ≥ 0.85)*

4. For the full-load conditions data set (*CAPFT* ≥ 0.85), the *EIRFT* is calculated at each time-step using Equation (5.18), where *CAPFT* is calculated using Equation (5.17), $P_{ref} = P_{CH,max}$, and $P_{CH}$ is the instantaneous monitored power input to the chiller;

$$EIRFT = \frac{P_{CH}}{P_{ref} \cdot CAPFT} \tag{5.18}$$

5. The full-load conditions data set is used to identify the coefficients $a_j$ of Equation (5.14) where *CapFTemp* is equal to *CAPFT* (Equation (5.17)), and the coefficients $b_j$ of Equation (5.13) where *EIRTemp* is equal to *EIRFT* (Equation (5.18)).

*Full-load and part-load conditions data set*

6. Using the coefficients $a_j$ and $b_j$ identified in (5), the estimates of *CapFTemp\** (Equation (5.13)) and *EIRTemp\** (Equation (5.14)) are calculated for all the data in the training data set, i.e. for the full- and part-load conditions;

7. The *PLR* (Equation (5.16)) and *chillerEIRFLPR* (Equation (5.19)) are calculated for all the data in the training data set, i.e. for the full- and part-load conditions, where *CapFTemp\** is the estimate of *CapFTemp* and *EIRTemp\** is the estimate of *EIRTemp*;

$$chillerEIRFPLR = \frac{P_{CH}}{P_{ref} \cdot CapFTemp^* \cdot EIRTemp^*} \qquad (5.19)$$

8.  All the data in the training data set are used to identify the coefficients $c_j$ of
    Equation (5.15), where *EIRFPLR* is equal to *chillerEIRFLPR* (Equation (5.19));

9.  Using the coefficients $c_i$ identified in (8), *EIRFPLR\** (Equation (5.15)) is
    estimated for all the data in the training data set, i.e. for the full- and part-load
    conditions;

10. The electric power input to the chiller (Equation (5.11)) is calculated for all data
    points with the variables calculated in (6), *CapFTemp\** and *EIRTemp\**, and in (9),
    *EIRFPLR\**.

To illustrate the proposed approach, a sample of data for the CH1-28D data set is
presented in Table 5.9. The results for the calculations performed on the full-load
conditions are presented in Table 5.9 and for the full- and part-load conditions in Table
5.10, while the identified coefficients are presented in Table 5.11. The proposed approach
is used to identify the coefficients of the performance curves for the electric power input
to the chiller.

*Initial training set* (Table 5.9)

1.  The maximum evaporator load $Q_{Emax}$ =2666 kW is identified at 07/21 12:45 (bold
    values in Table 5.9); therefore $Q_{ref} = Q_{Emax} = 2666$ kW, $P_{ref} = 517$ kW, and
    $COP_{ref} = 5.157$.

2.  *CAPFT* is calculated using Equation (5.20). For example, at 12:00 on 07/21:

$$CAPFT = \frac{Q_E}{Q_{ref}} = \frac{2546\ kW}{2666\ kW} = 0.955 \qquad (5.20)$$

3. The training data set is split into (1) full-load conditions (FL), where $CAPFT \geq$ 0.85 and (2) part-load conditions (PL), where $CAPFT < 0.85$.

*Full-load conditions data set* (Table 5.9)

4. For the full-load conditions data set ($CAPFT \geq 0.85$), the $EIRFT$ is calculated at each time-step using Equation (5.21). For example, at 12:00 on 07/21:

$$EIRFT = \frac{P_{CH}}{P_{ref} \cdot CAPFT} = \frac{497}{517 \cdot 0.955} = 1.0066 \tag{5.21}$$

5. The coefficients $a_j$ of Equation (5.13) and the coefficients $b_j$ of Equation (5.14) are identified using the calculated $CAPFT$ and $EIRFT$, respectively, along with measurements of temperatures (Table 5.9). The identified coefficients $a_j$ and $b_j$ for both chillers CH-1 and CH-2 are presented in Table 5.11, and compared with the default values of a TRANE chiller, as presented in the EnergyPlus program (section 5.5.4.1).

*Full-load and part-load conditions data set* (Table 5.10)

6. Using the coefficients $a_j$ and $b_j$, the estimates of *CapFTemp\** (Equation (5.13)) and *EIRTemp\** (Equation (5.14)) are calculated for all the data in the training data set. For example, at 12:00 on 07/21, *CapFTemp\** = 0.9577033 and *EIRTemp\** = 0.9902288.

7. The *PLR* (Equation (5.16)) and *chillerEIRFLPR* (Equation (5.19)) are calculated for all the data in the training data set. For example, at 12:00 on 07/21, the PLR = 0.99716 and:

$$chillerEIRFPLR = \frac{497}{(517 \cdot 0.9577033 \cdot 0.9902288)} = 1.01368 \tag{5.22}$$

8. The coefficients $c_j$ of Equation (5.15) are identified (Table 5.11) by using *EIRFPLR* equal to *chillerEIRFLPR*, along with the calculated *PLR* and measurements of temperatures.

9. Using the coefficients $c_i$ identified in (8), *EIRFPLR** (Equation (5.15)) is estimated for all the data in the training data set. For example, at 12:00 on 07/21, *EIRFPLR** = 0.98197.

10. The electric power input to the chiller (Equation (5.11)) is calculated for all data points with the *CapFTemp**, *EIRTemp**, *EIRFPLR**. For example, at 12:00 on 07/21 :

$$P_{CH} = (2666 * 0.9577033) \cdot (1/5.157) \cdot (0.9902288) \cdot (0.98197) = \ 481 \text{ kW} \qquad (5.23)$$

Table 5.9: Sample of data and calculation of training set for CH1-28D, July 21 2009

| Date | Time | $T_{CHWS}$, °C | $T_{CNDS}$, °C | $Q_E$, kW | $P_{CH}$, kW | COP | CAPFT | FL | PL | EIRFT |
|------|------|------|------|------|------|------|------|------|------|------|
| | | Measurements | | | | | Calculations | | | |
| 7/21 | 12:00 | 6.72 | 36.66 | 2546 | 497 | 5.123 | 0.955 | X | | 1.0066 |
| 7/21 | 12:15 | 6.72 | 36.55 | 2586 | 505 | 5.121 | 0.970 | X | | 1.0070 |
| 7/21 | 12:30 | 6.72 | 37.05 | 2568 | 481 | 5.339 | 0.963 | X | | 0.9659 |
| **7/21** | **12:45** | **6.72** | **36.89** | **2666** | **517** | **5.157** | 1.000 | X | | 1.0000 |
| 7/21 | 13:00 | 6.78 | 36.83 | 2644 | 511 | 5.175 | 0.992 | X | | 0.9965 |
| | ⋮ | | | | | | | | | |
| 7/21 | 20:00 | 6.72 | 35.66 | 2346 | 445 | 5.272 | 0.880 | X | | 0.9781 |
| 7/21 | 20:15 | 6.78 | 35.33 | 2280 | 435 | 5.243 | 0.855 | X | | 0.9836 |
| 7/21 | 20:30 | 6.78 | 34.94 | 2200 | 419 | 5.252 | 0.825 | | X | |
| 7/21 | 20:45 | 6.72 | 35.5 | 2244 | 420 | 5.344 | 0.842 | | X | |

Table 5.10: Sample of calculation for training set of CH1-28D, July 21 2009

| Date | Time | CapFTemp* | EIRTemp* | PLR | chillerEIRFLPR | EIRFPLR* | $P_{CH}$, kW |
|------|------|------|------|------|------|------|------|
| 7/21 | 12:00 | 0.9577033 | 0.9902288 | 0.99716 | 1.01368 | 0.98197 | 481 |
| 7/21 | 12:15 | 0.9487055 | 0.9882193 | 1.02243 | 1.04188 | 1.01906 | 494 |
| 7/21 | 12:30 | 0.9931338 | 0.9959175 | 0.96982 | 0.94064 | 0.93934 | 480 |
| 7/21 | 12:45 | 0.9779322 | 0.9938546 | 1.02257 | 1.02889 | 1.01168 | 508 |
| 7/21 | 13:00 | 0.9755892 | 0.9980719 | 1.01663 | 1.01508 | 1.00464 | 506 |
| | ⋮ | | | | | | |
| 7/21 | 20:00 | 0.8920124 | 0.9654081 | 0.98647 | 0.99951 | 0.98965 | 440 |
| 7/21 | 20:15 | 0.8714134 | 0.9676649 | 0.98161 | 0.99781 | 0.99049 | 431 |
| 7/21 | 20:30 | 0.8576679 | 0.9543319 | 0.96235 | 0.99016 | 0.97481 | 412 |
| 7/21 | 20:45 | 0.8848609 | 0.9600703 | 0.95127 | 0.95627 | 0.95004 | 417 |

104

*Table 5.11: Example of coefficients for the electric power input models for chillers*

| ITEM | CH1-28D | CH2-7D | Trane |
|---|---|---|---|
| $a_0$ | 55.6849 | 11.9917 | -0.2176 |
| $a_1$ | -5.9214 | -7.7791 | -0.0494 |
| $a_2$ | 0.13986 | 0.71449 | 8.70 E-05 |
| $a_3$ | -1.98856 | 0.86498 | 0.09612 |
| $a_4$ | 0.01810 | -0.00760 | -0.00203 |
| $a_5$ | 0.11092 | -0.05142 | 0.00254 |
| $b_0$ | -42.7144 | -51.5804 | -0.0199 |
| $b_1$ | 6.25958 | 22.43780 | -0.07848 |
| $b_2$ | -0.19697 | -2.30418 | 0.00194 |
| $b_3$ | 1.19876 | -1.34114 | 0.07123 |
| $b_4$ | -7.36280 E-03 | -3.78277 E-03 | -9.17380E-04 |
| $b_5$ | -0.09546 | 0.24441 | -0.00058 |
| $c_0$ | 1.94517 | 2.33977 | 0.35161 |
| $c_1$ | -0.01389 | -0.08433 | 0.00921 |
| $c_2$ | -1.49532 E-03 | 6.53170 E-04 | -2.382325E-05 |
| $c_3$ | -1.91033 | -1.91995 | 0.12232 |
| $c_4$ | -1.53332 | -0.10428 | -0.18201 |
| $c_5$ | 0.12419 | 0.07856 | -0.00784 |
| $c_6$ | 0.46424 | 0.03295 | 0.68849 |

## York & Cappiello (Y&C) model

The model proposed by York and Cappiello (1982) estimates the electric power input to chillers based on a triquadratic polynomial (Equation (5.24)). To identify the coefficients $d_j$, the following monitored data points must be available: $E_{CH}$, $Q_E$, $T_{CHWS}$, and $T_{CNDR}$.

$$\dot{E}_{CH} = d_0 + d_1 \cdot Q_E + d_2 \cdot T_{CNDR} + d_3 \cdot T_{CHWS} + d_4 \cdot Q_E{}^2 + d_5 \cdot T_{CNDR}{}^2$$
$$+ d_6 \cdot T_{CHWS}{}^2 + d_7 \cdot Q_E \cdot T_{CNDR} + d_8 \cdot Q_E \cdot T_{CHWS} + d_9 \cdot T_{CNDR} \qquad (5.24)$$
$$\cdot T_{CHWS} + d_{10} \cdot Q_E \cdot T_{CNDR} \cdot T_{CHWS}$$

where the coefficients $d_i$ have no physical meaning and are identified with available data points.

<u>Gordon & Ng (G&Ng) model</u>

Gordon and Ng (2000) proposed a different model that is based on the following monitored data points: $COP$, $Q_E$, $T_{CHWR}$, and $T_{CNDR}$. The three-parameter model is defined by Equation (5.25).

$$\left(\frac{1}{COP}+1\right)\frac{T_{CHWR}^K}{T_{CNDR}^K}-1 = e_1\frac{T_{CHWR}^K}{Q_E} + e_2\frac{(T_{CNDR}^K - T_{CHWR}^K)}{(T_{CNDR}^K \cdot Q_E)} + e_3\frac{(1/COP+1)\cdot Q_E}{T_{CNDR}^K} \tag{5.25}$$

where the coefficients $e_1$ corresponds to the total entropy production in the chiller, $e_2$ corresponds to the heat losses (or gains) from (or into) the chiller, $e_3$ corresponds to the total heat exchanger thermal resistance; the chilled water return and condenser water return temperatures are in Kelvin. The coefficients $e_j$ are identified using Equation (5.25) along with measurements and used in (Equation (5.26)) to evaluate the electricity power input of the chiller.

$$\dot{E}_{CH} = Q_E \cdot \left[\left(\frac{\left(e_1\frac{T_{CHWR}^K}{Q_E}\right) + e_2\frac{(T_{CNDR}^K - T_{CHWR}^K)}{(T_{CNDR}^K \cdot Q_E)} + 1}{\frac{T_{CHWR}^K}{T_{CNDR}^K} - e_3\frac{Q_E}{T_{CNDR}^K}}\right) - 1\right] \tag{5.26}$$

<u>Swider model</u>

Swider (2003) proposed a simple model to estimate the COP of chillers (Equation (5.27)) that is evaluated in this study for benchmarking purposes. Given the $COP$, $T_{CHWR}$, and $T_{CNDR}$, the $f_i$ coefficients are identified.

$$COP = f_1 \cdot Q_E + f_2 \cdot T_{CHWR} + f_3 \cdot T_{CNDR} \tag{5.27}$$

### 5.5.3 *Proposed ANN models*

The proposed benchmark ANN models are developed using MATLAB (2008). The ANN model output is the chiller power ($E_{CH}$) in kW and the coefficient of

performance ($COP_{CH}$). The proposed models are based on the same input variables used in the correlation-based models, presented in Sections 5.5.1 and 5.5.2, for the same training and testing set sizes. The inputs and reference model names are presented in Table 5.12.

*Table 5.12: ANN model inputs*

| ANN inputs | Reference names |
|---|---|
| $Q_E/Q_{Edesign}$, $T_{CNDS}$, $T_{O/A}$ | Proposed |
| $Q_E$, $T_{CNDR}$, $T_{CHWS}$ | Y&C |
| $Q_E$, $T_{CNDR}$, $T_{CHWR}$ | G&Ng and Swider |

### 5.5.4   Discussion of results

This section presents the results over the training and testing set for the developed benchmark models. The coefficients of the correlation-based models, which are identified using the training data set and STATGRAPHICS (2008), are presented in Appendix C. When the correlation-based model estimates the electric power input, rather than directly estimating the COP, the COP is calculated using Equation (5.28).

$$COP = \frac{Q_E \ (from \ measurements)}{E_{CH} \ (from \ regression \ model)}$$

(5.28)

For the sliding window technique, the results are presented in Monfet and Zmeureanu (2011) for the Power-ML model for the electric power input to the chillers. The results demonstrated that the monitored data available to establish the models have a great impact on the prediction made by the model. For chiller CH-1, between July 6th and August 12th 2009 when it is the first chiller to be start-up when required, both sliding window sizes (14 days and 21 days) provide accurate identification of the correlation coefficients, α, β and γ, with $R^2$ of about 98%. Better results are obtained with the 14-day sliding window (CH1-14D-R7): the predictions over the testing data set have CV(RMSE)

values below 9%, and the average MBE below -19.0 kW (Monfet and Zmereuanu 2011). For chiller CH-2, since only a limited amount of monitored data is available to establish the model, the accuracy of the predictions varies throughout the testing data sets, with large CV(RMSE) and MBE values. Therefore, the sliding window technique is not recommended if the chiller is less frequently used (in this case less than 25% of time for most of the summer 2009). The models are more accurate when the operation is over a longer period of time.

Reddy et al. (2003a) compared the sliding window approach and the incremental window approach applied to two different chillers. The incremental window of 100 data points (from hourly data) or 200 data points (from 15-minute data) is an acceptable window period for the initial model identification (larger sliding window improved the model predictions (Reddy et al. 2003a)). The two sliding windows presented larger variability. Reddy et al. (2003b) found, by analyzing the coefficient of variance of the prediction errors, that the incremental window approach is preferable to be used.

Since the operation of both chillers varies throughout the summer, the sliding window technique is not recommended. Therefore, no further testing and evaluation of the sliding window technique is included in this study.

### 5.5.4.1   Training and testing

The models for the chillers are trained using data sets presented in Table 5.2 to Table 5.4 for the static technique and Table 5.5 and Table 5.6 for the augmented window technique. Results are presented for the correlation-based and ANN models. For all

tables, the light grey cells represent the results that are part of both the typical static and augmented window techniques.

Proposed correlation-based models

Four different models are proposed to evaluate the performance of the chillers: (1) multivariable linear and non-linear models (ML), Equation (5.7) for power and Equation (5.8) for COP, and (2) multivariable polynomial (MP) models, Equation (5.9) for power and Equation (5.10) for COP. The identified coefficients, $\alpha_j$, $\beta_j$, $\gamma_j$, and $\delta_j$, are presented in Table 5.13 for the electric power input and in Table 5.14 for the COP.

The coefficients identified for chiller CH-1 and chiller CH-2 are different for both the proposed electric power input and COP models, thus demonstrating the need to develop different models even if the chillers are identical (Table 5.13 and Table 5.14). The difference in the performance characteristics of the chillers are a result of distinct operating patterns. Also, since different data sets are used to develop each model, the identified coefficients vary from one data set to another.

*Table 5.13: Model coefficients for the electric power input for chillers - proposed models*

| Set name | Power-ML | | | Power-MP | | | | | |
|---|---|---|---|---|---|---|---|---|---|
| | $\alpha_1$ | $\alpha_2$ | $\alpha_3$ | $\beta_0$ | $\beta_1$ | $\beta_2$ | $\beta_3$ | $\beta_4$ | $\beta_5$ |
| CH1-30H | 464.60 | 0.70191 | 0.81996 | -5408.81 | 223.720 | 216.50 | -4.9612 | 330.63 | 0.64336 |
| CH1-7D | 510.92 | 1.82066 | -0.99732 | 1055.96 | 132.120 | 271.08 | 1.1741 | -66.57 | -0.73922 |
| CH1-10D | 476.80 | 2.31547 | -0.85339 | 1312.93 | 65.781 | 348.69 | 1.4013 | -82.53 | -0.70090 |
| CH1-14D | 471.72 | 2.36141 | -0.79136 | 1253.31 | 57.131 | 362.42 | 1.3316 | -78.54 | -0.69385 |
| CH1-21D | 507.46 | 2.24646 | -1.28093 | 1742.77 | 44.928 | 373.05 | 1.8171 | -109.32 | -0.85319 |
| CH1-28D | 530.85 | 2.01938 | -1.40941 | 1640.15 | 98.936 | 329.71 | 1.6884 | -101.71 | -0.88002 |
| CH2-1D | 492.94 | 0.75163 | 1.79606 | 1042.26 | 0.021 | 510.90 | 0.9918 | -62.639 | -0.16431 |
| CH2-7D | 602.74 | 1.37629 | -1.83149 | 1936.68 | 140.262 | 256.95 | 2.1452 | -124.95 | -1.08592 |
| CH2-10D | 601.30 | 1.33543 | -1.75639 | 1920.91 | 121.095 | 288.99 | 2.1109 | -123.49 | -1.27857 |
| CH2-14D | 580.98 | 1.37976 | -1.44529 | 2007.90 | 105.695 | 300.35 | 2.1768 | -128.45 | -1.13956 |
| CH2-21D | 574.21 | 1.37861 | -1.21520 | 2056.98 | 67.068 | 350.78 | 2.1870 | -130.80 | -0.97738 |
| CH2-28D | 573.29 | 1.41835 | -1.21357 | 2213.31 | 47.887 | 374.38 | 2.3267 | -140.34 | -0.98673 |
| CH2-1WW | 539.65 | 1.00756 | 0.35866 | 1885.38 | 2.769 | 434.27 | 1.9821 | -120.10 | 0.01066 |
| CH2-1WEH | 582.48 | 0.13299 | 0.65181 | -515.54 | 392.304 | 154.45 | -0.4917 | 36.00 | -0.43687 |
| CH2-2WW | 584.42 | 1.75760 | -2.23004 | 2316.38 | 72.953 | 343.50 | 2.4442 | -146.94 | -1.36038 |
| CH2-2WEH | 545.20 | 0.44678 | 1.02425 | -759.71 | 391.460 | 137.73 | -0.7153 | 50.81 | -0.09463 |

109

*Table 5.14: Model coefficients for the coefficient of performance for chillers - proposed models*

| Set name | COP-ML | | | COP-MP | | | | |
|---|---|---|---|---|---|---|---|---|
| | $\gamma_1$ | $\gamma_2$ | $\gamma_3$ | $\delta_1$ | $\delta_2$ | $\delta_3$ | $\delta_4$ | $\delta_5$ |
| CH1-30H | 0.06274 | 0.18691 | -0.01942 | 1.5025 | 0.5489 | -0.00727 | 0.40527 | -0.01599 |
| CH1-7D | 0.01451 | 0.14956 | 0.01773 | -6.5134 | 10.1854 | -0.00757 | 0.30205 | 0.01215 |
| CH1-10D | -0.21018 | 0.16761 | 0.00985 | -8.5893 | 12.0013 | -0.00591 | 0.23678 | 0.01129 |
| CH1-14D | -0.22241 | 0.16943 | 0.00831 | -8.4305 | 11.7326 | -0.00563 | 0.23020 | 0.01098 |
| CH1-21D | -0.13141 | 0.15578 | 0.01651 | -7.1582 | 10.4771 | -0.00607 | 0.25108 | 0.01292 |
| CH1-28D | -0.03979 | 0.14584 | 0.02017 | -7.0071 | 10.1708 | -0.00587 | 0.24666 | 0.01456 |
| CH2-1D | -0.09780 | 0.16260 | -0.00948 | -5.8075 | 7.8268 | -0.00349 | 0.21420 | -0.02632 |
| CH2-7D | 0.11646 | 0.12850 | 0.02508 | -6.8091 | 10.8512 | -0.01026 | 0.37961 | 0.01736 |
| CH2-10D | 0.11836 | 0.13079 | 0.02237 | -6.3936 | 10.1936 | -0.00995 | 0.37282 | 0.02055 |
| CH2-14D | 0.07874 | 0.13444 | 0.02208 | -6.4561 | 10.3185 | -0.00978 | 0.36660 | 0.02012 |
| CH2-21D | 0.03928 | 0.13959 | 0.01646 | -6.3274 | 9.9876 | -0.00881 | 0.33936 | 0.01719 |
| CH2-28D | 0.01328 | 0.14202 | 0.01460 | -6.3922 | 9.9527 | -0.00850 | 0.32996 | 0.01710 |
| CH2-1WW | -0.06884 | 0.16486 | -0.01610 | -4.9122 | 8.1320 | -0.00739 | 0.31945 | -0.00308 |
| CH2-1WEH | 0.11347 | 0.16023 | -0.02401 | -5.3292 | 6.8202 | -0.00435 | 0.23519 | 0.00503 |
| CH2-2WW | 0.12552 | 0.12000 | 0.04212 | -6.1646 | 9.7600 | -0.00940 | 0.35756 | 0.02486 |
| CH2-2WEH | -0.02247 | 0.17377 | -0.03183 | -5.9575 | 7.8975 | -0.00437 | 0.22793 | 0.00052 |

For the Power-ML model for chiller CH-1, the CH1-30H, the CH1-10D and the CH1-21D data sets provide the best results, with CV(RMSE) below 4.4% and average MBE below ±4.1 kW over the testing set (Table 5.15). For chiller CH-2, over the testing data set for the typical static and augmented window techniques, the maximum CV(RMSE) is 5.0% and the average MBE below ±6.8 kW, with the exception of the CH2-28D, where the CV(RMSE) is 7.0% and the average MBE is -20.6 kW (Table 5.15). For the model developed using the split static technique, the results are accurate over the testing set when the CH2-2WW data set and the CH2-1WEH are used for training, the CV(RMSE) are lower than 4.9% over the testing set.

For the Power-MP, the models developed using the typical static and augmented window techniques provide accurate results over the testing set for all training set size for chillers CH-1 and CH-2, with CV(RMSE) below 4.3% and RMSE below 15.4 kW (Table 5.16). The best results are obtained for the CH1-30H and CH1-10D data sets for chiller CH-1 and the CH2-1D and CH2-28D data set for chiller CH-2. For the split static

technique, the models developed provide accurate results when the CH2-2WW and CH2-1WEH data set are used for training, with CV(RMSE) below 3.4% over the testing set.

Table 5.15: Results for the electric power input models for chillers, static and augmented window techniques - proposed correlation-based ML model

| Set name | Training set | | | Testing set | | |
|----------|-------|-------|----------|-------|----------|---------|
|          | $R^2$, % | CV, % | RMSE, kW | CV, % | RMSE, kW | MBE, kW |
| CH1-30H  | 99.89 | 3.4 | 10.5 | 2.2 | 6.5 | 1.33 |
| CH1-7D   | 99.81 | 4.5 | 14.3 | 5.5 | 13.2 | -8.07 |
| CH1-10D  | 99.82 | 4.5 | 13.0 | 3.9 | 9.5 | -3.31 |
| CH1-14D  | 99.82 | 4.4 | 12.5 | 6.3 | 19.5 | -10.15 |
| CH1-21D  | 99.79 | 4.8 | 13.8 | 4.4 | 14.6 | -4.04 |
| CH1-28D  | 99.81 | 4.6 | 14.2 | 5.4 | 17.1 | 8.77 |
| CH2-1D   | 99.91 | 3.1 | 8.8 | 2.8 | 9.9 | 6.77 |
| CH2-7D   | 99.61 | 6.5 | 21.9 | 3.2 | 10.1 | -0.11 |
| CH2-10D  | 99.65 | 6.1 | 20.2 | 4.5 | 14.8 | 3.85 |
| CH2-14D  | 99.65 | 6.0 | 19.8 | 4.9 | 15.2 | -4.98 |
| CH2-21D  | 99.70 | 5.7 | 18.4 | 5.0 | 11.4 | -6.47 |
| CH2-28D  | 99.69 | 5.8 | 18.5 | 7.0 | 29.5 | -20.57 |
| CH2-1WW  | 99.83 | 4.2 | 14.2 | 12.8 | 41.3 | 31.07 |
| CH2-1WEH | 99.92 | 3.0 | 10.2 | 2.8 | 9.5 | 2.62 |
| CH2-2WW  | 99.65 | 6.0 | 19.7 | 4.9 | 17.7 | -5.57 |
| CH2-2WEH | 99.91 | 3.0 | 10.0 | 6.6 | 15.2 | -1.40 |

Table 5.16: Results for the electric power input models for chillers, static and augmented window techniques - proposed correlation-based MP model

| Set name | Training set | | | Testing set | | |
|----------|-------|-------|----------|-------|----------|---------|
|          | $R^2$, % | CV, % | RMSE, kW | CV, % | RMSE, kW | MBE, kW |
| CH1-30H  | 95.28 | 3.2 | 9.8 | 2.5 | 7.5 | 2.92 |
| CH1-7D   | 96.11 | 3.9 | 12.4 | 3.7 | 8.8 | 0.29 |
| CH1-10D  | 97.89 | 3.8 | 11.1 | 4.0 | 9.7 | -3.24 |
| CH1-14D  | 98.01 | 3.9 | 10.9 | 3.8 | 11.8 | -7.61 |
| CH1-21D  | 98.15 | 3.7 | 10.8 | 2.9 | 9.7 | -1.36 |
| CH1-28D  | 98.55 | 3.4 | 10.5 | 4.2 | 13.4 | 5.75 |
| CH2-1D   | 98.78 | 3.0 | 8.6 | 2.2 | 7.6 | 1.43 |
| CH2-7D   | 97.64 | 4.3 | 14.5 | 3.9 | 12.5 | -5.71 |
| CH2-10D  | 97.53 | 4.2 | 13.9 | 3.7 | 12.1 | 0.68 |
| CH2-14D  | 97.22 | 4.3 | 14.1 | 3.8 | 11.8 | -1.19 |
| CH2-21D  | 97.83 | 4.1 | 13.3 | 4.1 | 9.4 | -1.50 |
| CH2-28D  | 98.04 | 4.1 | 13.1 | 3.7 | 15.4 | -12.13 |
| CH2-1WW  | 99.79 | 3.2 | 10.8 | 8.8 | 28.3 | 20.15 |
| CH2-1WEH | 99.09 | 2.5 | 8.5 | 2.6 | 8.8 | 1.12 |
| CH2-2WW  | 97.03 | 4.3 | 14.2 | 3.4 | 12.1 | -1.05 |
| CH2-2WEH | 99.01 | 2.6 | 8.5 | 6.9 | 15.9 | 4.34 |

For the proposed COP-ML models, the CV(RMSE) are 2.8% and 5.2% for the CH1-30H and CH1-10D data set over the testing set, respectively (Table 5.17). For chiller CH-2, the CH2-1D and CH2-7D provide the best results over the testing set with

111

CV(RMSE) of 3.6% and 4.0%, respectively. The average MBE errors are low for all data set, ±0.36. The split static technique does not provide accurate results over the testing set with CV(RMSE) greater than 5%, except for the model developed using one week-end and holiday (CH2-1WEH).

*Table 5.17: Results for the coefficient of performance for chillers, static and augmented window techniques - proposed correlation-based ML model*

| Set name | Training set | | | Testing set | | |
|---|---|---|---|---|---|---|
| | $R^2$, % | CV, % | RMSE | CV, % | RMSE | MBE |
| CH1-30H | 99.84 | 4.0 | 0.2 | 2.8 | 0.2 | -0.02 |
| CH1-7D | 99.64 | 5.9 | 0.3 | 11.5 | 0.6 | 0.33 |
| CH1-10D | 99.64 | 6.0 | 0.3 | 5.2 | 0.3 | 0.04 |
| CH1-14D | 99.66 | 5.9 | 0.3 | 8.2 | 0.4 | 0.21 |
| CH1-21D | 99.62 | 6.3 | 0.3 | 6.6 | 0.3 | 0.12 |
| CH1-28D | 99.61 | 6.3 | 0.3 | 7.6 | 0.4 | -0.19 |
| CH2-1D | 99.86 | 3.8 | 0.2 | 3.6 | 0.2 | -0.07 |
| CH2-7D | 99.19 | 9.1 | 0.5 | 4.0 | 0.2 | -0.03 |
| CH2-10D | 99.31 | 8.4 | 0.4 | 6.0 | 0.3 | -0.07 |
| CH2-14D | 99.33 | 8.2 | 0.4 | 6.7 | 0.3 | 0.11 |
| CH2-21D | 99.41 | 7.7 | 0.4 | 7.3 | 0.3 | 0.11 |
| CH2-28D | 99.39 | 7.8 | 0.4 | 11.0 | 0.5 | 0.36 |
| CH2-1WW | 99.64 | 6.0 | 0.3 | 15.8 | 0.9 | -0.68 |
| CH2-1WEH | 99.85 | 3.9 | 0.2 | 2.8 | 0.1 | -0.05 |
| CH2-2WW | 99.36 | 8.1 | 0.4 | 6.8 | 0.3 | 0.12 |
| CH2-2WEH | 99.85 | 3.9 | 0.2 | 9.2 | 0.4 | 0.04 |

The proposed COP-MP model performs well for all typical static and augmented window training set sizes, with CV(RMSE) below 5.0% and average MBE below ±0.12 over the testing sets (Table 5.18) for both chillers. The best results are obtained for the CH1-30H and CH1-21D data sets for chiller CH-1 and the CH2-1D and CH2-28D data sets for chiller CH-2. The split static technique performs well for models developed with two work weeks (CH2-2WW) and two weekend and holidays (2WEH), with CV(RMSE) below 5.0% and average MBE below ±0.02.

The statistical criteria calculated for the split static technique show no improvement in the prediction over the testing set compared with the other proposed techniques.

112

*Table 5.18: Results for the coefficient of performance for chillers, typical static and augmented window techniques - proposed MP model*

| Set name | Training set | | | Testing set | | |
|---|---|---|---|---|---|---|
| | $R^2$, % | CV, % | RMSE | CV, % | RMSE | MBE |
| CH1-30H | 99.88 | 3.4 | 0.2 | 2.2 | 0.1 | -0.03 |
| CH1-7D | 99.84 | 4.0 | 0.2 | 4.3 | 0.2 | 0.08 |
| CH1-10D | 99.85 | 3.9 | 0.2 | 4.1 | 0.2 | 0.06 |
| CH1-14D | 99.85 | 3.9 | 0.2 | 3.4 | 0.2 | 0.09 |
| CH1-21D | 99.87 | 3.7 | 0.2 | 2.9 | 0.2 | 0.01 |
| CH1-28D | 99.88 | 3.4 | 0.2 | 5.0 | 0.2 | -0.12 |
| CH2-1D | 99.91 | 3.0 | 0.2 | 3.3 | 0.2 | -0.12 |
| CH2-7D | 99.76 | 4.9 | 0.3 | 3.7 | 0.2 | 0.10 |
| CH2-10D | 99.78 | 4.7 | 0.2 | 4.0 | 0.2 | -0.04 |
| CH2-14D | 99.77 | 4.8 | 0.3 | 4.0 | 0.2 | 0.03 |
| CH2-21D | 99.80 | 4.5 | 0.2 | 4.3 | 0.2 | 0.05 |
| CH2-28D | 99.80 | 4.5 | 0.2 | 3.1 | 0.2 | 0.11 |
| CH2-1WW | 99.87 | 3.7 | 0.2 | 9.8 | 0.6 | -0.41 |
| CH2-1WEH | 99.94 | 2.5 | 0.1 | 2.4 | 0.1 | -0.01 |
| CH2-2WW | 99.75 | 5.0 | 0.3 | 3.3 | 0.2 | 0.01 |
| CH2-2WEH | 99.93 | 2.7 | 0.1 | 5.0 | 0.2 | 0.02 |

Based on the analysis of the proposed models over the testing data sets, the proposed MP-models provide the most accurate results over the testing sets for both chillers when established using the typical static or augmented window techniques. For the MP models, the models developed with CH1-30H, CH1-10D, CH2-1D and CH2-28D provide the best results over the testing set. For chiller CH-1, over the testing set, the CV(RMSE) is below 2.9% for both the Power-MP and COP-MP. The RMSE and MBE are below ±9.7 kW and ±2.9 kW for the Power-MP model and 0.2 and ±0.03 for the COP-MP model, respectively. For chiller CH-2, the CV(RMSE) are below 3.7% for the Power-MP and COP-MP model. The RMSE and MBE are below ±15.4 kW and ±12.1 kW for the Power-MP and 0.2 and ±0.1 for the COP-MP models, respectively.

<u>Existing correlation-based models</u>

For the existing models, the EnergyPlus model (Table 5.19) provides good results over the training sets for models established using 30 hours or 28 days of data for chiller CH-1, and more than 7 days of data for chiller CH-2. Over the testing set, the CV(RMSE)

are below 4.5% for the CH1-30H and CH1-28D data sets. For chiller CH-2, the developed models provide good results over the testing sets, with the exception of the CH2-1D data set: the CV(RMSE) are below 4.2% and the average MBE below -10.8 kW.

*Table 5.19: Results for the electric power input model for chillers, typical static and augmented window techniques - proposed technique for the EnergyPlus model*

| Set name | Training set | | Testing set | | |
|---|---|---|---|---|---|
| | CV, % | RMSE, kW | CV, % | RMSE, kW | MBE, kW |
| CH1-30H | 2.9 | 8.9 | 2.5 | 7.4 | 1.72 |
| CH1-7D | 5.3 | 16.9 | 5.4 | 12.9 | -3.95 |
| CH1-10D | 5.5 | 16.1 | 12.3 | 29.8 | -3.42 |
| CH1-14D | 8.4 | 23.8 | 7.4 | 22.8 | -5.29 |
| CH1-21D | 6.5 | 18.8 | 7.2 | 24.1 | -1.37 |
| CH1-28D | 3.7 | 11.4 | 4.5 | 14.3 | 6.25 |
| CH2-1D | 10.8 | 30.8 | 11.0 | 37.7 | 10.41 |
| CH2-7D | 4.9 | 16.4 | 4.0 | 12.9 | -5.56 |
| CH2-10D | 4.8 | 15.8 | 4.2 | 13.9 | -1.73 |
| CH2-14D | 4.2 | 13.9 | 3.9 | 12.1 | -2.21 |
| CH2-21D | 4.0 | 12.9 | 4.0 | 9.0 | -1.34 |
| CH2-28D | 4.1 | 13.2 | 3.5 | 14.5 | -10.82 |

Pre-determined coefficients are available in the EnergyPlus program. The chillers installed at the Concordia Sciences Building are Trane CVHF0910 models with COP of 5.76 at design conditions. This model is not available as a default in EnergyPlus. Therefore, the Trane chiller model that has the closest capacity, which is the Trane CVHF0796 with COP of 6.4, is used for comparison purposes. The coefficients defined in EnergyPlus are presented in Table 5.11. Figure 5.4 presents the measured electric power input variations compared to the EnergyPlus model developed using the proposed technique for the CH1-28D for chiller CH-1 and the default EnergyPlus model. The prediction made by the proposed technique over part of the testing set (July 29th to July 31st 2009), shows agreement with the measured data, especially when the electric power input is high, while the prediction made using the default Trane coefficients available in EnergyPlus underestimates the electric power input. The CV(RMSE) over the testing set

for the CH1-28D using the proposed approach is 4.5%, while being 12.3% when the Trane coefficients available in EnergyPlus are used.
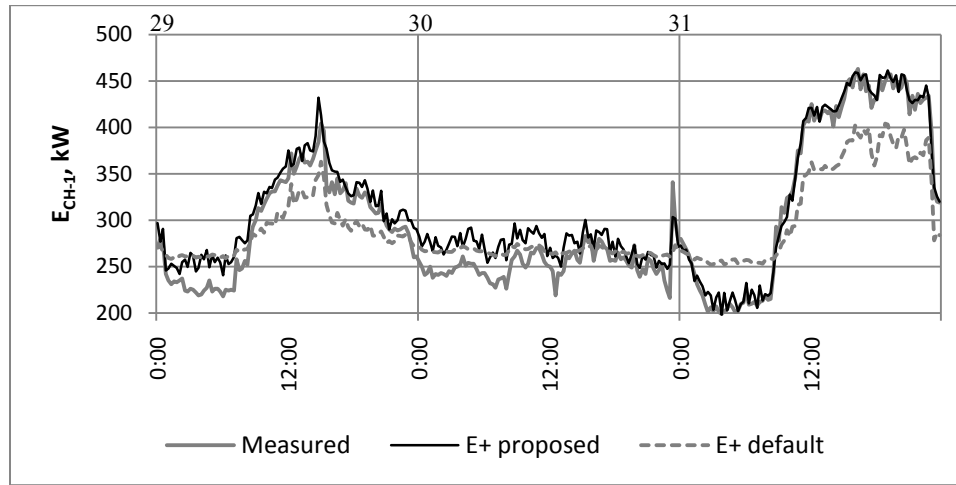


*Figure 5.4: Chiller CH-1 power electric input variation for EnergyPlus model, July 29th to July 31st 2009*

For the Y&C model, the CV(RMSE) are below 5.1% over the testing set except for models developed using the split static technique for chillers CH-1 and CH-2 (Table 5.20). The model developed with the CH1-30H, CH1-21D, CH2-1D and CH2-21D provide the most accurate results.

*Table 5.20: Results for the electric power input model for chillers, static and augmented window techniques - York & Cappiello model*

| Set name | Training set | | | Testing set | | |
|---|---|---|---|---|---|---|
| | $R^2$, % | CV, % | RMSE, kW | CV, % | RMSE, kW | MBE, kW |
| CH1-30H | 96.42 | 2.8 | 0.2 | 2.1 | 0.1 | 0.28 |
| CH1-7D | 95.57 | 4.1 | 13.2 | 4.9 | 11.7 | 1.96 |
| CH1-10D | 97.79 | 4.0 | 11.6 | 4.1 | 9.9 | -3.49 |
| CH1-14D | 97.91 | 4.0 | 11.3 | 5.1 | 15.8 | -11.38 |
| CH1-21D | 97.74 | 4.1 | 12.0 | 3.2 | 10.8 | -3.51 |
| CH1-28D | 98.27 | 3.7 | 11.5 | 4.7 | 14.9 | 6.93 |
| CH2-1D | 98.92 | 2.8 | 8.1 | 2.4 | 8.4 | 2.13 |
| CH2-7D | 95.38 | 6.0 | 20.2 | 4.3 | 13.7 | -10.12 |
| CH2-10D | 95.36 | 5.8 | 19.1 | 4.5 | 14.6 | -1.63 |
| CH2-14D | 94.86 | 5.8 | 19.1 | 4.1 | 12.7 | -4.60 |
| CH2-21D | 96.36 | 5.3 | 17.1 | 3.9 | 8.9 | -0.49 |
| CH2-28D | 96.75 | 5.3 | 16.7 | 4.7 | 19.6 | -15.92 |
| CH2-1WW | 98.32 | 3.8 | 12.7 | 12.4 | 39.8 | 29.89 |
| CH2-1WEH | 99.17 | 2.4 | 8.1 | 2.4 | 8.1 | 1.69 |
| CH2-2WW | 93.80 | 6.3 | 20.5 | 4.0 | 14.5 | -9.05 |
| CH2-2WEH | 99.04 | 2.5 | 8.3 | 7.0 | 16.2 | 3.63 |

For the Gordon & Ng model, the CV(RMSE) are below 5.0% over the testing set for chiller CH-1 and CH-2, except for the models developed for chiller CH-2 with 28 days of data and the split static technique (Table 5.21). For the split static technique, the models developed using two working weeks (CH2-2WW) provide accurate results with CV(RMSE) below 4.3% and average MBE of ±9.7 kW over the testing set.

Table 5.21: Results for the electric power input model for chillers, static and augmented window techniques - Gordon & Ng model

| Set name | Training set | | | Testing set | | |
|---|---|---|---|---|---|---|
| | $R^2$, % | CV, % | RMSE, kW | CV, % | RMSE, kW | MBE, kW |
| CH1-30H | 99.73 | 3.7 | 11.1 | 2.5 | 7.3 | -2.20 |
| CH1-7D | 99.60 | 4.5 | 14.3 | 3.5 | 8.5 | -1.72 |
| CH1-10D | 99.69 | 4.3 | 12.4 | 4.3 | 10.5 | -4.61 |
| CH1-14D | 99.69 | 4.3 | 12.1 | 4.8 | 14.9 | -11.14 |
| CH1-21D | 99.68 | 4.4 | 12.6 | 3.4 | 11.4 | -3.49 |
| CH1-28D | 99.72 | 4.0 | 12.4 | 5.0 | 15.8 | 7.29 |
| CH2-1D | 99.84 | 3.2 | 9.2 | 2.6 | 8.8 | 3.90 |
| CH2-7D | 99.34 | 6.2 | 20.8 | 3.9 | 12.5 | -8.18 |
| CH2-10D | 99.41 | 5.9 | 19.5 | 4.6 | 14.9 | -1.85 |
| CH2-14D | 99.42 | 5.9 | 19.5 | 4.2 | 13.1 | -4.49 |
| CH2-21D | 99.53 | 5.4 | 17.6 | 3.4 | 7.6 | -1.47 |
| CH2-28D | 99.54 | 5.5 | 17.4 | 5.2 | 21.7 | -18.02 |
| CH2-1WW | 99.74 | 4.2 | 14.2 | 11.9 | 38.1 | 27.06 |
| CH2-1WEH | 99.88 | 2.6 | 8.8 | 2.7 | 9.2 | 2.22 |
| CH2-2WW | 99.28 | 6.4 | 21.1 | 4.3 | 15.5 | -9.72 |
| CH2-2WEH | 99.85 | 2.7 | 9.1 | 6.4 | 14.8 | 3.90 |

If the York and Cappiello and the Gordon-Ng models are used to evaluate the COP (Equation (5.28)), the CV(RMSE) are below 4.6% and the average MBE below ± 0.2 for chiller CH-1 over the testing set (Table 5.22). For chiller CH-2, the CV(RMSE) varies between 2.6% and 6.5% over the testing set, with the exception of the model developed using one work week of data (CH2-1WW).

For the existing COP model (Swider 2003) for chiller CH-1, the CV(RMSE) vary between 3.8% and 8.1% over the training set; the CH1-30H and the CH1-21D data sets provide the best results over the testing set, with CV(RMSE) below 6.2% and average MBE below ±0.12 with variations within ±0.9 (Table 5.23). For chiller CH-2, the split

static models have CV(RMSE) greater than 5% over the testing set, except for the CH1-1WEH model. The CH2-1D and the CH2-7D data sets provide the best results over the testing set, with CV(RMSE) below 3.6% and average MBE below ±0.05 with variations within ±0.8.

*Table 5.22: Results for the coefficient of performance for chillers, static and augmented window techniques - calculated from the existing electric power input models*

| Set name | COP – Power Y&C | | | | | COP - Power G&Ng | | | | |
| | Training set | | Testing set | | | Training set | | Testing set | | |
| | CV, % | RMSE | CV, % | RMSE | MBE | CV, % | RMSE | CV, % | RMSE | MBE |
|---|---|---|---|---|---|---|---|---|---|---|
| CH1-30H | 2.8 | 0.2 | 1.9 | 0.1 | -0.003 | 3.6 | 0.2 | 2.4 | 0.1 | 0.04 |
| CH1-7D | 4.2 | 0.2 | 5.0 | 0.2 | -0.06 | 4.6 | 0.3 | 3.3 | 0.2 | 0.02 |
| CH1-10D | 3.9 | 0.2 | 3.8 | 0.2 | 0.06 | 4.3 | 0.2 | 4.1 | 0.2 | 0.09 |
| CH1-14D | 3.9 | 0.2 | 4.6 | 0.2 | 0.18 | 4.2 | 0.2 | 4.5 | 0.2 | 0.18 |
| CH1-21D | 4.0 | 0.2 | 3.2 | 0.2 | 0.05 | 4.3 | 0.2 | 3.4 | 0.2 | 0.05 |
| CH1-28D | 3.8 | 0.2 | 5.2 | 0.3 | -0.13 | 4.0 | 0.2 | 5.6 | 0.3 | -0.14 |
| CH2-1D | 2.5 | 0.1 | 2.4 | 0.1 | -0.04 | 2.9 | 0.1 | 2.4 | 0.1 | -0.06 |
| CH2-7D | 6.3 | 0.3 | 4.6 | 0.2 | 0.18 | 6.5 | 0.3 | 4.0 | 0.2 | 0.14 |
| CH2-10D | 6.0 | 0.3 | 4.7 | 0.2 | 0.02 | 6.2 | 0.3 | 4.8 | 0.3 | 0.03 |
| CH2-14D | 6.0 | 0.3 | 3.9 | 0.2 | 0.07 | 6.2 | 0.3 | 3.9 | 0.2 | 0.06 |
| CH2-21D | 5.4 | 0.3 | 4.1 | 0.2 | -0.003 | 5.6 | 0.3 | 3.3 | 0.2 | 0.02 |
| CH2-28D | 5.3 | 0.3 | 4.6 | 0.2 | 0.19 | 5.5 | 0.3 | 5.0 | 0.2 | 0.21 |
| CH2-1WW | 3.8 | 0.2 | 11.9 | 0.7 | -0.52 | 4.1 | 0.2 | 11.3 | 0.6 | -0.47 |
| CH2-1WEH | 2.4 | 0.1 | 2.2 | 0.1 | -0.02 | 2.6 | 0.1 | 2.4 | 0.1 | -0.02 |
| CH2-2WW | 6.5 | 0.3 | 4.0 | 0.2 | 0.14 | 6.7 | 0.4 | 4.1 | 0.2 | 0.14 |
| CH2-2WEH | 2.4 | 0.1 | 5.3 | 0.3 | -0.08 | 2.7 | 0.1 | 5.0 | 0.2 | -0.09 |

*Table 5.23: Results for the coefficient of performance for chillers, static and augmented window techniques - existing Swider model*

| Set name | Training set | | | Testing set | | |
| | $R^2$, % | CV, % | RMSE, kW | CV, % | RMSE, kW | MBE, kW |
|---|---|---|---|---|---|---|
| CH1-30H | 99.85 | 3.8 | 0.2 | 2.6 | 0.2 | 0.02 |
| CH1-7D | 99.70 | 5.5 | 0.3 | 11.9 | 0.6 | 0.37 |
| CH1-10D | 99.58 | 6.5 | 0.3 | 6.4 | 0.3 | 0.08 |
| CH1-14D | 99.69 | 6.4 | 0.3 | 7.9 | 0.4 | 0.14 |
| CH1-21D | 99.63 | 6.1 | 0.3 | 6.2 | 0.3 | 0.12 |
| CH1-28D | 99.65 | 5.9 | 0.3 | 7.0 | 0.4 | -0.17 |
| CH2-1D | 99.87 | 3.6 | 0.2 | 3.6 | 0.2 | -0.01 |
| CH2-7D | 99.36 | 8.1 | 0.4 | 3.2 | 0.2 | 0.05 |
| CH2-10D | 99.45 | 7.4 | 0.4 | 5.3 | 0.3 | -0.01 |
| CH2-14D | 99.47 | 7.3 | 0.4 | 5.9 | 0.3 | 0.14 |
| CH2-21D | 99.54 | 6.8 | 0.4 | 7.9 | 0.4 | 0.18 |
| CH2-28D | 99.52 | 6.9 | 0.4 | 8.7 | 0.4 | 0.32 |
| CH2-1WW | 99.71 | 5.5 | 0.3 | 13.3 | 0.8 | -0.59 |
| CH2-1WEH | 99.88 | 3.6 | 0.2 | 2.8 | 0.1 | -0.06 |
| CH2-2WW | 99.41 | 7.7 | 0.4 | 5.9 | 0.3 | 0.20 |
| CH2-2WEH | 99.85 | 3.9 | 0.2 | 9.6 | 0.5 | 0.16 |

The statistical results calculated over the training and testing sets for the proposed models are comparable to the one calculated for the existing models. Figure 5.5 and Figure 5.6 present a comparison of the models providing the lowest CV(RMSE) over the training and testing set for the proposed and existing correlation-based models for the electric power input and COP of chillers, respectively. Based on the training and testing set analysis, the proposed multivariate polynomial (MP) models for the electric power input and COP, followed by the G&Ng and the Y&C models provide the most accurate predictions for the chillers used in this case study.
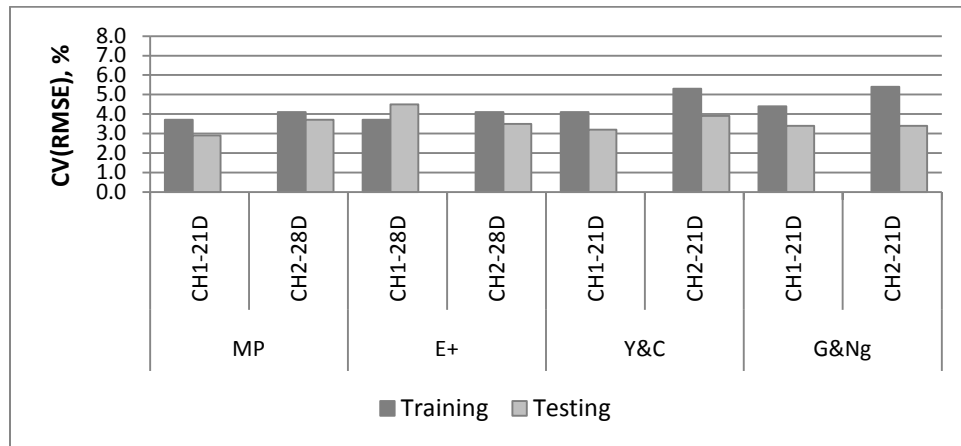


Figure 5.5: Comparison of the proposed and existing correlation-based model for the chillers power electric input over the training and testing sets
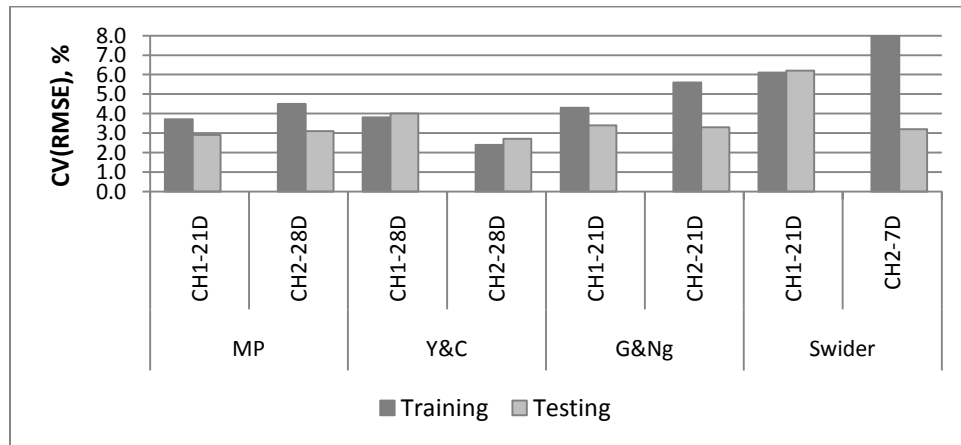


Figure 5.6: Comparison of the proposed and existing correlation-based model for the chillers COP over the training and testing sets

ANN models

For each proposed models (Table 5.12), the ANN model architecture is composed of three inputs, one hidden layer with 5 neurons for example and two outputs (Figure 5.7).
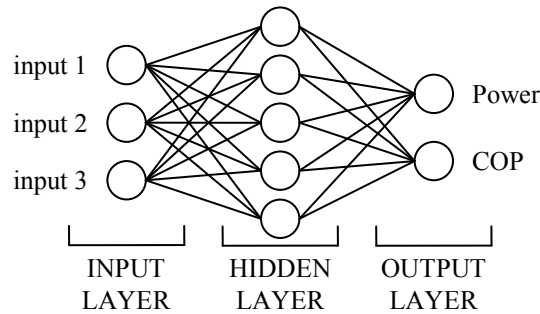


*Figure 5.7: General feedforward ANN model*

For the chiller models, since the number of inputs and outputs are low, only one hidden layers is used. Also, since the number of input is fewer than 5, approximately twice as many hidden neurons are used in the proposed network (Priddy and Keller 2005). Therefore, the models are trained with various training set size (30H, 7D, 10D, 14D, 21D and 28D) for different number of neurons per hidden layer (one hidden layer (1H) with 3 to 12 neurons – 1H3N to 1H12N). For each ANN models, different combinations of neurons per layers are tested and the number of neurons that provides the best results in terms of CV(RMSE) and MBE over the testing set, are selected. The results obtained for each training set sizes and number of neurons are presented in Appendix D.

For the models developed using the inputs to the new proposed model, the models developed using the typical or augmented window techniques provide accurate results with CV(RMSE) below 5.8% for both the electric power input and COP over the testing

119

set (Table 5.24). For chiller CH-1, the MBE and the RMSE are the lowest for the model developed for the CH1-21D-1H9N. For chiller CH-2, the split static models, the results are only within the 5% acceptable CV(RMSE) range for the one weekend & holidays and two work weeks, where the average MBE are below ±1.0 kW for the electric power input to the chiller and ±0.01 for the COP. For the typical static and augmented window techniques, the chiller CH-2 models are trained with nine neurons per hidden layer and provide accurate results over the testing set, with CV(RMSE) below 4.1% for both the chiller electric power input and COP. The best results for chiller CH-2 are obtained with the CH2-28D-1H9N data set.

*Table 5.24: Results for chillers, static and augmented window techniques - proposed ANN models*

| Set name | Power - $Q_E/Q_{Edesign}$, $T_{CNDS}$, $T_{O/A}$ | | | | | COP - $Q_E/Q_{Edesign}$, $T_{CNDS}$, $T_{O/A}$ | | | | |
| | Training set | | Testing set | | | Training set | | Testing set | | |
| | CV, % | RMSE, kw | CV, % | RMSE, kw | MBE, kW | CV, % | RMSE | CV, % | RMSE | MBE |
| CH1-30H-1H3N | 3.2 | 9.6 | 2.4 | 7.0 | 0.75 | 3.2 | 0.2 | 2.3 | 0.1 | -0.03 |
| CH1-7D-1H3N | 3.9 | 12.3 | 4.1 | 9.8 | 0.33 | 3.9 | 0.2 | 5.8 | 0.3 | 0.12 |
| CH1-10D-1H3N | 3.8 | 11.2 | 4.2 | 10.1 | -3.53 | 3.8 | 0.2 | 4.0 | 0.2 | 0.07 |
| CH1-14D-1H3N | 3.8 | 10.7 | 4.0 | 12.3 | -7.49 | 3.7 | 0.2 | 3.5 | 0.2 | 0.11 |
| CH1-21D-1H9N | 3.4 | 9.7 | 3.0 | 9.9 | -1.88 | 3.4 | 0.2 | 3.0 | 0.2 | 0.04 |
| CH1-28D-1H9N | 3.1 | 9.5 | 4.1 | 12.9 | 5.56 | 3.1 | 0.2 | 4.6 | 0.2 | -0.11 |
| CH2-1D -1H9N | 2.8 | 8.0 | 3.0 | 10.3 | -1.24 | 2.5 | 0.1 | 4.0 | 0.2 | 0.08 |
| CH2-7D-1H9N | 2.8 | 9.5 | 3.7 | 11.8 | 2.74 | 3.1 | 0.2 | 3.6 | 0.2 | -0.02 |
| CH2-10D-1H9N | 2.9 | 9.6 | 3.0 | 9.9 | -1.70 | 3.1 | 0.2 | 3.4 | 0.2 | 0.03 |
| CH2-14D-1H9N | 2.9 | 9.5 | 3.7 | 11.6 | 0.38 | 3.1 | 0.2 | 3.9 | 0.2 | 0.01 |
| CH2-21D-1H9N | 3.0 | 9.8 | 4.1 | 9.3 | -0.76 | 3.2 | 0.2 | 4.0 | 0.2 | 0.02 |
| CH2-28D-1H9N | 3.1 | 9.9 | 2.5 | 10.3 | -7.52 | 3.2 | 0.2 | 2.5 | 0.1 | 0.08 |
| CH2-1WW-1H3N | 3.2 | 10.7 | 8.6 | 27.6 | 18.89 | 3.0 | 0.2 | 8.9 | 0.5 | -0.36 |
| CH2-1WEH-1H3N | 2.5 | 8.4 | 2.6 | 8.7 | 0.58 | 2.4 | 0.1 | 2.2 | 0.1 | -0.004 |
| CH2-2WW -1H8N | 2.8 | 9.1 | 3.0 | 10.8 | 0.95 | 3.0 | 0.2 | 3.0 | 0.2 | -0.01 |
| CH2-2WEH -1H8N | 2.3 | 7.7 | 6.1 | 14.1 | 6.88 | 2.4 | 0.1 | 4.9 | 0.2 | -0.12 |

For the model developed based on the inputs to the Y&C model, the models giving the most accurate results over the testing sets are developed using eight neurons per hidden layer (Table 5.25). Except for the split static technique, the CV(RMSE) over the testing sets are below 5.2% for both chillers. The best results are obtained over the

testing set when the CH1-21D-1H8N and CH2-28D-1H8N data set and ANN architecture are used.

*Table 5.25: Results for chillers, static and augmented window techniques - Y&C ANN models*

| Set name | Power - $Q_E, T_{CNDR}, T_{CHWS}$ | | | | | COP - $Q_E, T_{CNDR}, T_{CHWS}$ | | | | |
|---|---|---|---|---|---|---|---|---|---|---|
| | Training set | | Testing set | | | Training set | | Testing set | | |
| | CV, % | RMSE, kw | CV, % | RMSE, kw | MBE, kW | CV, % | RMSE | CV, % | RMSE | MBE |
| CH1-30H-1H8N | 2.4 | 7.2 | 2.3 | 6.7 | -0.42 | 2.3 | 0.1 | 2.0 | 0.1 | -0.003 |
| CH1-7D-1H8N | 3.4 | 10.7 | 5.2 | 12.4 | 3.33 | 3.4 | 0.2 | 4.6 | 0.2 | 0.06 |
| CH1-10D-1H8N | 3.3 | 9.5 | 3.4 | 8.3 | -2.64 | 3.3 | 0.2 | 3.4 | 0.2 | 0.06 |
| CH1-14D-1H8N | 3.3 | 9.3 | 4.5 | 13.9 | -8.38 | 3.2 | 0.2 | 3.9 | 0.2 | 0.13 |
| CH1-21D-1H8N | 3.3 | 9.5 | 3.3 | 11.0 | -1.12 | 3.2 | 0.2 | 3.2 | 0.2 | 0.02 |
| CH1-28D-1H8N | 3.1 | 9.5 | 4.2 | 13.2 | 5.61 | 3.1 | 0.2 | 4.7 | 0.3 | -0.11 |
| CH2-1D -1H8N | 2.7 | 7.6 | 3.3 | 11.2 | -1.05 | 2.2 | 0.1 | 2.7 | 0.1 | -0.01 |
| CH2-7D-1H8N | 4.4 | 14.8 | 4.4 | 14.0 | -3.23 | 4.7 | 0.2 | 4.7 | 0.2 | 0.09 |
| CH2-10D-1H8N | 4.2 | 14.0 | 4.2 | 13.6 | -0.42 | 4.5 | 0.2 | 4.5 | 0.2 | 0.01 |
| CH2-14D-1H8N | 4.2 | 14.0 | 4.2 | 13.2 | -1.37 | 4.6 | 0.2 | 4.3 | 0.2 | 0.04 |
| CH2-21D-1H8N | 4.2 | 13.6 | 4.2 | 9.4 | 0.09 | 4.5 | 0.2 | 4.1 | 0.2 | -0.002 |
| CH2-28D-1H8N | 4.2 | 13.2 | 2.5 | 10.4 | -5.48 | 4.5 | 0.2 | 3.4 | 0.2 | 0.09 |
| CH2-1WW -1H8N | 2.2 | 7.5 | 15.7 | 50.4 | 23.41 | 2.3 | 0.1 | 15.7 | 0.9 | -0.40 |
| CH2-1WEH -1H8N | 2.4 | 8.1 | 2.4 | 8.0 | 1.72 | 2.3 | 0.1 | 2.0 | 0.1 | -0.02 |
| CH2-2WW -1H8N | 3.3 | 10.8 | 3.1 | 11.3 | -1.30 | 3.6 | 0.2 | 3.4 | 0.2 | 0.04 |
| CH2-2WEH -1H8N | 2.3 | 7.8 | 7.8 | 18.0 | 5.56 | 2.3 | 0.1 | 5.3 | 0.3 | -0.04 |

The inputs to the Gordon-Ng and Swider models are the same: evaporator load, chilled water return water temperature and condenser water return temperature. For all data set sizes, the models trained with one hidden layers with eight neurons (1H8N) provides accurate results over the testing sets (Table 5.26). The CV(RMSE) over the testing sets varies between 2.4% and 6.8% for the electric power input and COP, except for the models developed using the split static technique. For chiller CH-2, the split static model for one week-end & holidays and the two work weeks gives CV(RMSE) below 4.7% over the testing set. The best results are obtained over the testing set when the CH1-21D-1H8N and CH2-28D-1H8N data set and ANN architecture are used.

For all the tested ANN models, the models established with the typical static or augmented window techniques provide accurate results over the testing data set with

CV(RMSE) below 6.8% for all training set sizes. The models developed with 21-days of data for chiller CH-1 (CH1-21D) and 28-days of data for chiller CH-2 (CH2-28) provide the most accurate results (Figure 5.8). Over the testing set, the CV(RMSE) are often lower for the ANN models compared with the proposed and existing correlation-based models.

*Table 5.26: Results for chillers, static and augmented window techniques - G&Ng and Swider ANN models*

| Set name | Power - $Q_E$, $T_{CNDR}$, $T_{CHWR}$ | | | | | COP - $Q_E$, $T_{CNDR}$, $T_{CHWR}$ | | | | |
| | Training set | | Testing set | | | Training set | | Testing set | | |
| | CV, % | RMSE, kw | CV, % | RMSE, kw | MBE, kW | CV, % | RMSE | CV, % | RMSE | MBE |
|---|---|---|---|---|---|---|---|---|---|---|
| CH1-30H -1H8N | 2.3 | 6.9 | 2.7 | 7.8 | -1.18 | 2.3 | 0.1 | 2.4 | 0.1 | 0.02 |
| CH1-7D-1H8N | 3.3 | 10.5 | 3.5 | 8.4 | -1.15 | 3.4 | 0.2 | 6.8 | 0.3 | 0.12 |
| CH1-10D-1H8N | 3.2 | 0.4 | 4.5 | 10.9 | -1.74 | 3.2 | 0.2 | 4.0 | 0.2 | 0.03 |
| CH1-14D-1H8N | 3.3 | 9.3 | 4.2 | 13.0 | -7.65 | 3.2 | 0.2 | 4.2 | 0.2 | 0.13 |
| CH1-21D-1H8N | 3.3 | 9.7 | 3.0 | 10.2 | -1.36 | 3.3 | 0.2 | 2.9 | 0.2 | 0.03 |
| CH1-28D-1H8N | 3.1 | 9.6 | 4.1 | 13.1 | 5.78 | 3.1 | 0.2 | 4.7 | 0.3 | -0.11 |
| CH2-1D -1H8N | 2.8 | 7.9 | 2.8 | 9.6 | 0.05 | 2.4 | 0.1 | 2.9 | 0.1 | -0.01 |
| CH2-7D-1H8N | 4.3 | 14.4 | 4.3 | 13.7 | -3.42 | 4.5 | 0.2 | 4.3 | 0.2 | 0.09 |
| CH2-10D-1H8N | 4.2 | 14.0 | 4.0 | 13.1 | -0.30 | 4.5 | 0.2 | 4.4 | 0.2 | 0.02 |
| CH2-14D-1H8N | 4.3 | 14.1 | 4.2 | 13.1 | -1.28 | 4.7 | 0.2 | 4.2 | 0.2 | 0.04 |
| CH2-21D-1H8N | 4.1 | 13.3 | 5.0 | 11.3 | -1.1 | 4.4 | 0.2 | 4.3 | 0.2 | 0.02 |
| CH2-28D-1H8N | 4.2 | 13.4 | 2.7 | 11.3 | -6.72 | 4.5 | 0.2 | 3.5 | 0.2 | 0.10 |
| CH2-1WW -1H8N | 2.3 | 7.6 | 13.9 | 44.6 | 22.25 | 2.3 | 0.1 | 12.7 | 0.7 | -0.38 |
| CH2-1WEH -1H8N | 2.4 | 7.9 | 2.2 | 7.6 | 1.62 | 2.2 | 0.1 | 2.0 | 0.1 | -0.01 |
| CH2-2WW -1H8N | 4.4 | 14.3 | 3.6 | 13.0 | -1.22 | 4.7 | 0.2 | 4.1 | 0.2 | 0.04 |
| CH2-2WEH -1H8N | 2.3 | 7.8 | 7.7 | 17.8 | 5.10 | 2.2 | 0.1 | 5.8 | 0.3 | -0.01 |
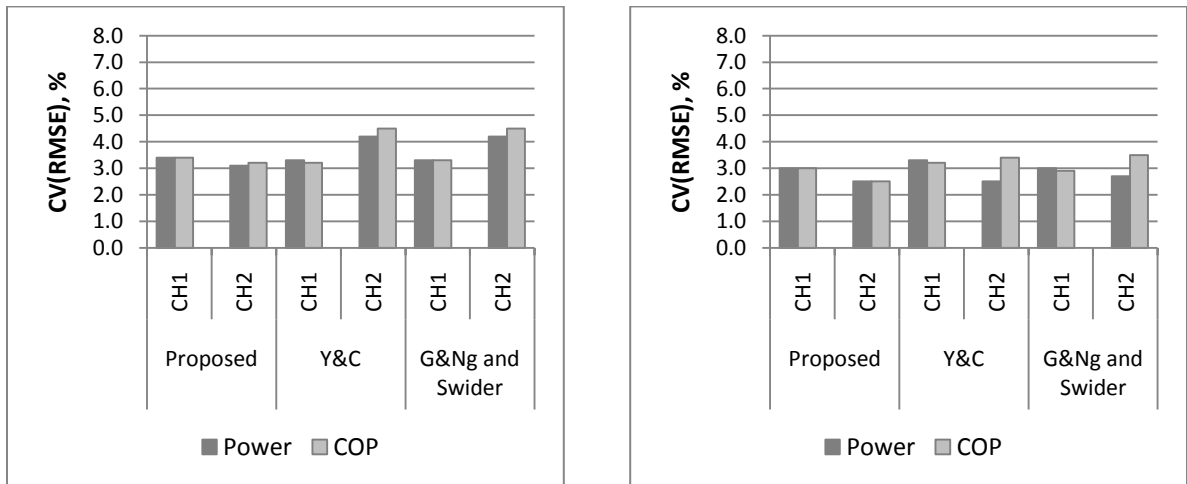


*Figure 5.8: Comparison of the ANN – a) over the training set, b) over the testing set*

*5.5.4.2 Benchmarking predictions versus monitored data*

Once the benchmarking models are tested, the developed models are used to predict the expected performance of the equipment under normal operation without known problems; the monitored performance is then compared with the expected performance to detect abnormal performance of the equipment. For the correlation-based models, the analysis carried over the training and testing sets has demonstrated that the proposed multivariate polynomial (MP) models for the electric power input and COP and the Gordon & Ng model provide the most accurate predictions for the chillers used in this case study. Therefore, the MP models for the electric power input (Equation (5.9)) and the coefficient of performance (Equation (5.10)) developed using the 21 days data set for CH-1 (CH1-21D) are used to illustrate the ongoing commissioning approach using benchmark models.

Figure 5.9 and Figure 5.10 present the interval of confidence for the model predictions, defined in Chapter 3 section 3.3.2 Equations (3.5) and (3.6), as well as the measured or currently being monitored data on July $31^{st}$ 2009 for the electric power input and COP of chiller CH-1, respectively. If the measured data are outside the model boundaries for more than one hour, a warning is sent to the building operators. Since the water distribution system is large, a one hour delay is necessary for the system to adjust to any changes made to the operating conditions. On July $31^{st}$ 2009, the performance of chiller CH-1 is within the prediction limits. However, if an operating problem was detected, warnings would be sent to the building operating team, and eventually other application software for diagnostics or automatic action to be undertaken on some of the equipment would be activated.
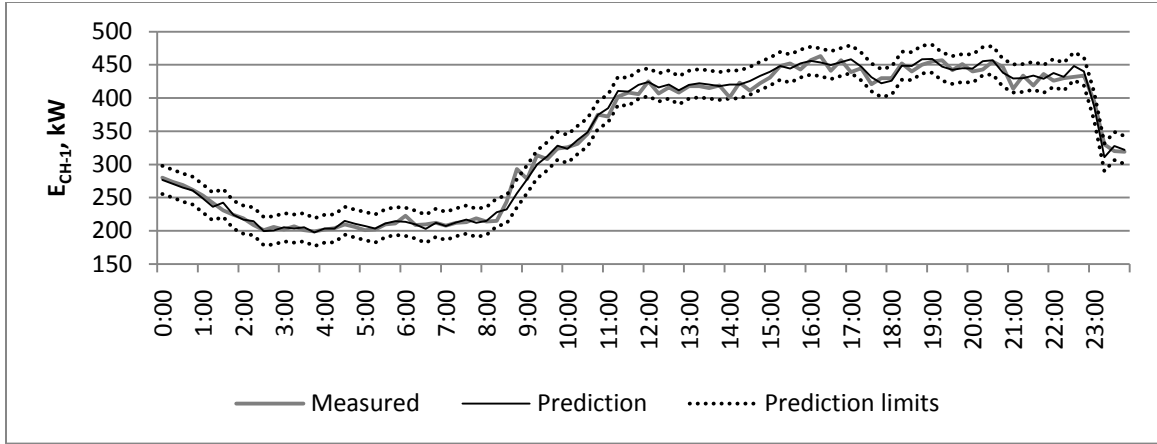
*Figure 5.9: Ongoing commissioning of chiller CH-1 power electric input – CH1-21D Power-MP model, July 31ˢᵗ 2009*
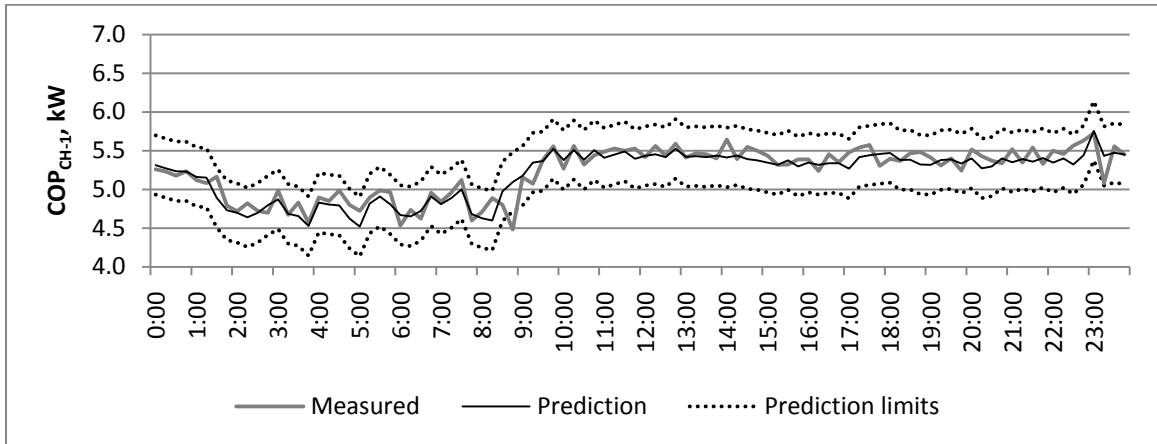


*Figure 5.10: Ongoing commissioning of chiller CH-1 coefficient of performance – CH1-21D COP-MP model, July 31ˢᵗ 2009*

For chiller CH-2, the ANN models provide more accurate results over the testing set; therefore, the proposed ANN model trained with 7 days of data (CH2-7D-1H9N) is selected to illustrate the ongoing commissioning approach. Figure 5.11 and Figure 5.12 present the interval of confidence for the model predictions as well as the measured or currently being monitored data on June 30ᵗʰ 2009 from 8:00 to 18:00 for the electric power input and COP of chiller CH-2, respectively. The electric power input is outside the predictions boundaries from 11h45 to 12h30, while the COP is outside the boundary conditions at 13h15, which is around when chiller CH-1 is started-up (12h45). Once the

second chiller is started, the electric power input and COP of chiller CH-2 are back to be within the model limits.
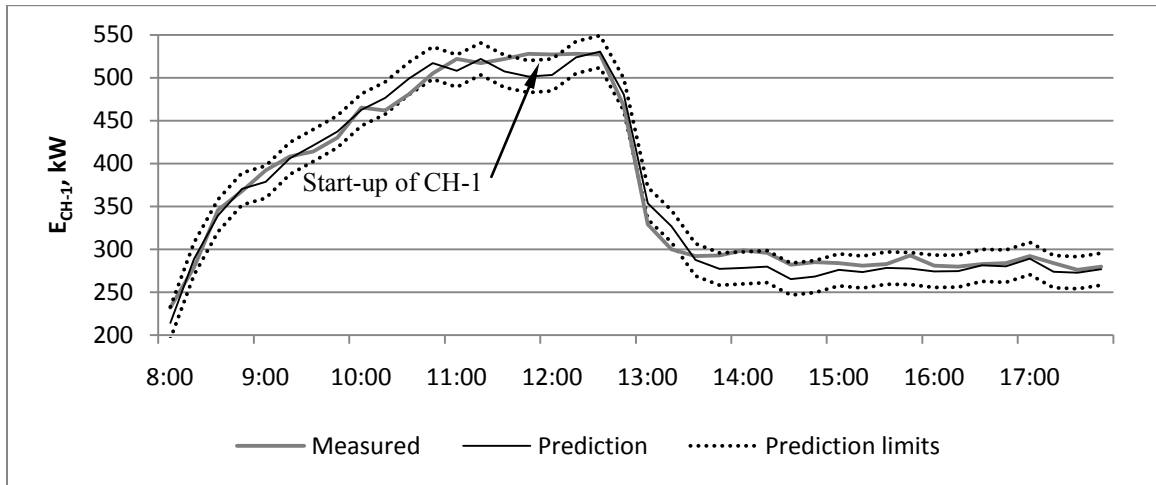


*Figure 5.11: Ongoing commissioning of chiller CH-2 power electric input – CH2-7D-1H9N proposed ANN, June 30th 2009*
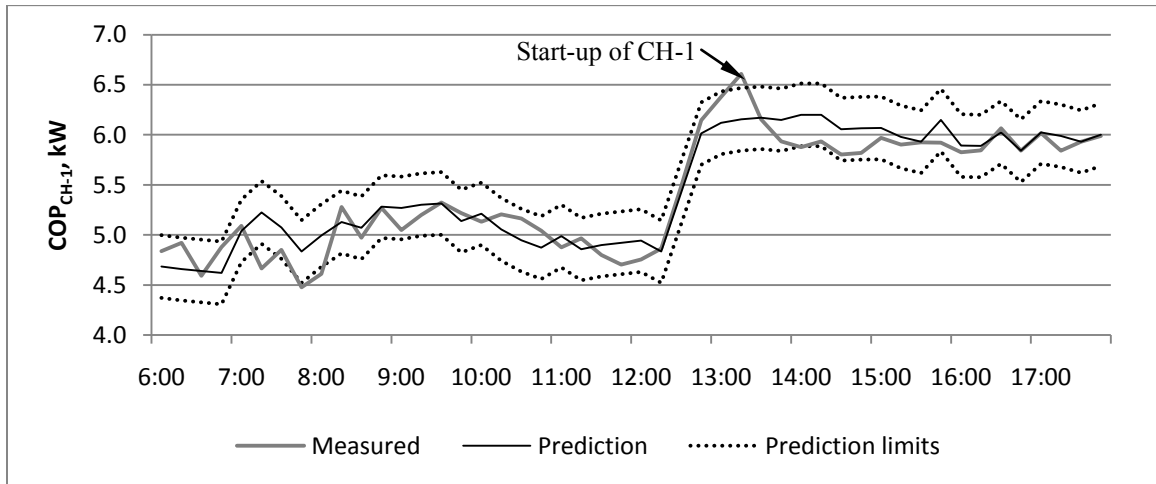


*Figure 5.12: Ongoing commissioning of chiller CH-2 coefficient of performance – CH2-7D-1H9N proposed ANN, June 30th 2009*

### 5.5.5 *Additional models verification*

An additional monitored data set, the verification set, is used to further assess the performance of the developed benchmarking models. Data over the remaining of the 2009 summer season are used to evaluate the predictions made by the developed benchmark models for normal operating conditions without known problems. The

125

evaluation criteria calculated over the training, testing and verification sets are compared also with information available in the literature.

### 5.5.5.1 *Proposed correlation-based models*

For the verification set, it is assumed that the monitored data represent normal operating conditions that prevailed during the training and testing periods. The verification set is used to further assess the performance of the models for a longer period of time. For example, the CV(RMSE) for the Power-ML model for chillers CH1-30H and CH2-1D are 3.4% and 3.1% over the training set and 2.2% and 2.8% over the testing set respectively (Table 5.15); however, over the verification set, the CV(RMSE) are 10.7% and 12.0%, respectively. By increasing the window size to seven days (Power ML-CH1-7D and Power ML-CH2-7D), the CV(RMSE) drops to 6.7% for chiller CH-1 and 10.1% for chiller CH-2, over the verification period (Table 5.27).

*Table 5.27: Results for the electric power input for chillers from the proposed models – verification set*

| Verification set | Power ML (5.7) | | | | Power MP (5.9) | | | |
|---|---|---|---|---|---|---|---|---|
| | CV, % | RMSE, kW | MBE, kW | R.E. % | CV, % | RMSE, kW | MBE, kW | R.E. % |
| CH1-30H, 07/06 to 09/22 | 10.7 | 33.4 | -25.7 | -9.8 | 13.9 | 43.6 | -31.4 | -11.6 |
| CH1-7D, 07/13 to 09/22 | 6.7 | 21.0 | -6.0 | -3.5 | 5.4 | 17.0 | -1.1 | -1.9 |
| CH1-10D, 07/16 to 09/22 | 6.8 | 21.5 | -4.3 | -2.9 | 5.4 | 17.2 | -1.5 | -2.0 |
| CH1-14D, 07/20 to 09/22 | 6.8 | 21.7 | -3.7 | -2.9 | 5.5 | 17.5 | -0.8 | -1.8 |
| CH1-21D, 07/27 to 09/22 | 6.8 | 21.3 | 0.8 | -1.3 | 5.8 | 18.4 | 2.5 | -0.8 |
| CH1-28D, 08/03 to 09/22 | 7.1 | 22.1 | 0.9 | -1.3 | 6.2 | 19.4 | 2.5 | -0.8 |
| CH2-1D, 06/23 to 09/20 | 12.0 | 35.9 | 20.9 | 3.7 | 9.6 | 28.7 | 16.9 | 2.4 |
| CH2-7D, 06/29 to 09/20 | 10.1 | 29.0 | 14.6 | 1.5 | 6.4 | 18.5 | 7.3 | -0.9 |
| CH2-10D, 07/02 to 09/20 | 10.8 | 30.6 | 16.1 | 0.1 | 7.1 | 20.1 | 10.1 | -2.0 |
| CH2-14D, 07/06 to 09/20 | 11.4 | 31.5 | 19.6 | 1.2 | 7.7 | 21.2 | 12.2 | -1.4 |
| CH2-21D, 07/13 to 09/20 | 12.1 | 34.0 | 24.6 | 2.0 | 8.4 | 23.4 | 15.3 | -1.1 |
| CH2-28D, 07/20 to 09/20 | 12.6 | 34.6 | 26.6 | 5.8 | 8.5 | 23.3 | 16.4 | 2.3 |
| CH2-1WW | 12.3 | 9.5 | 23.9 | 4.2 | 8.7 | 25.9 | 16.1 | 2.1 |
| CH2-1WEH | 11.2 | 29.0 | 12.7 | | 8.8 | 22.6 | 11.8 | |
| CH2-2WW | 9.9 | 15.2 | 14.5 | 0.6 | 7.0 | 19.7 | 10.0 | -1.2 |
| CH2-2WEH | 16.2 | 40.2 | 35.0 | | 12.6 | 30.7 | 25.7 | |

Figure 5.13 and Figure 5.14 show the variation of the CV(RMSE) over the verification set for the different training and testing set sizes for chillers CH-1 and CH-2, respectively. For both chillers, it is clearly shown that the proposed Power-MP models perform slightly better than the Power-ML model for all training and testing set sizes over the verification set.
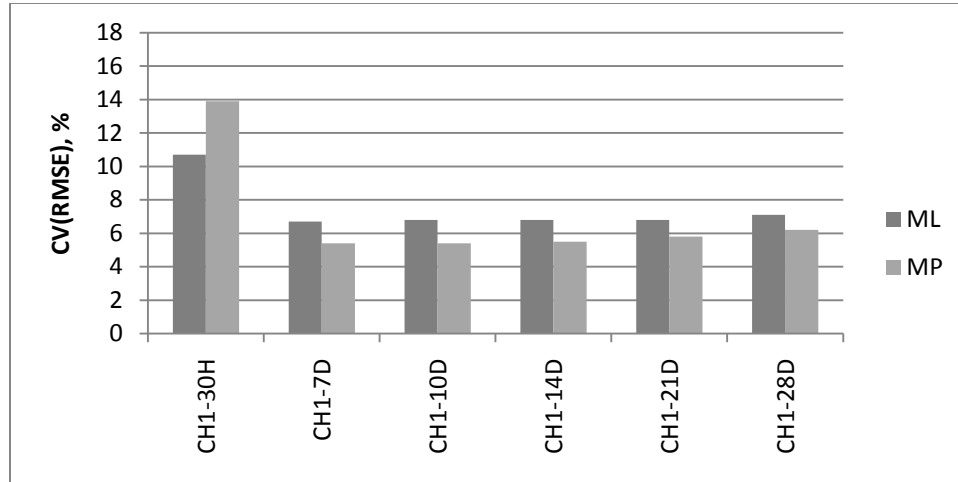


*Figure 5.13: Comparison of the electrical power input from the proposed correlation-based models over the verification set for different training set size, chiller CH-1*
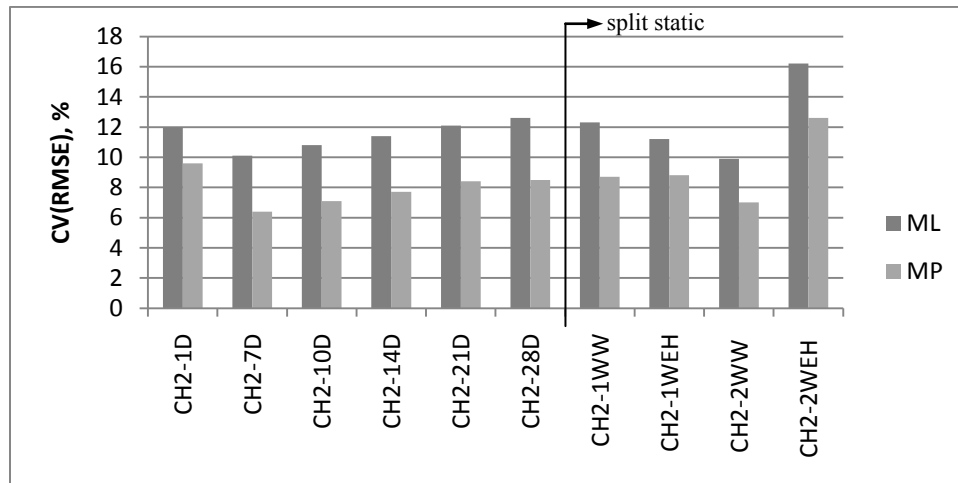


*Figure 5.14: Comparison of the electrical power input from the proposed correlation-based models over the verification set for different training set size, chiller CH-2*

For the chiller CH-1 of this case study, increasing the size of the window when using the augmented window technique or using a typical static window larger than seven

days does not significantly improve the prediction accuracy over the verification set. Hence, the minimum training and testing data set for the Power ML-CH1 and Power MP-CH1 model should be seven days (CH1-7D).

For the chiller CH-2 of the case study, the split static technique does not improve the CV(RMSE) over the verification set compared to the typical static or augmented window techniques (Figure 5.14). The use of the augmented window technique after seven days does not improve the prediction accuracy of the verification set. Thus, for chiller CH-2, the minimum training and testing data set for the Power ML-CH2 and Power MP-CH2 models should be seven days (CH2-7D).

For the proposed COP-ML and COP-MP models, the results over the verification set are presented in Table 5.28. For both chillers, the results clearly show that the propose COP-MP model performs better than the COP-ML model for all training and testing set sizes over the verification set (Figure 5.15 and Figure 5.16).

For chiller CH-1, increasing the augmented window or using a typical static window larger than seven days does not significantly improve the prediction accuracy over the verification set (Figure 5.15). Hence, the minimum training and testing data set for the COP-ML-CH1 and COP-MP-CH1 model should be seven days (CH1-7D).

For chiller CH-2, for the proposed models for the COP, the CV(RMSE) are higher for the COP-ML models and vary between 13.2% and 18.3% (Table 5.28). For the MP models, the CV(RMSE) are lower than 8.3% for model established with more than seven days of data over the verification set. The typical static or augmented window techniques provide better results than the split static technique over the verification set (Figure 5.16). The use of the augmented window technique after seven days does not improve the

prediction accuracy of the verification set. Thus, for chiller CH-2, the minimum training and testing data set for the COP-ML-CH2 and COP-MP-CH2 models should be seven days (CH2-7D).

*Table 5.28: Results for the COP for chillers from the proposed models – verification data set*

| Verification set | COP ML (5.8) | | | COP MP (5.10) | | |
|---|---|---|---|---|---|---|
| | CV, % | RMSE | MBE | CV, % | RMSE | MBE |
| CH1-30H, 07/06 to 09/22 | 16.2 | 0.9 | 0.67 | 13.7 | 0.7 | 0.54 |
| CH1-7D, 07/13 to 09/22 | 9.6 | 0.5 | 0.17 | 5.9 | 0.3 | 0.02 |
| CH1-10D, 07/16 to 09/22 | 8.7 | 0.5 | 0.10 | 5.8 | 0.3 | -0.01 |
| CH1-14D, 07/20 to 09/22 | 8.8 | 0.5 | 0.09 | 5.9 | 0.3 | -0.03 |
| CH1-21D, 07/27 to 09/22 | 8.7 | 0.5 | 0.01 | 6.3 | 0.3 | -0.05 |
| CH1-28D, 08/03 to 09/22 | 9.4 | 0.5 | 0.01 | 6.6 | 0.4 | -0.04 |
| CH2-1D, 06/23 to 09/20 | 13.3 | 0.7 | -0.42 | 11.7 | 0.6 | -0.40 |
| CH2-7D, 06/29 to 09/20 | 13.2 | 0.7 | -0.33 | 6.8 | 0.4 | -0.14 |
| CH2-10D, 07/02 to 09/20 | 13.9 | 0.8 | -0.36 | 7.5 | 0.4 | -0.18 |
| CH2-14D, 07/06 to 09/20 | 13.9 | 0.8 | -0.44 | 7.7 | 0.4 | -0.22 |
| CH2-21D, 07/13 to 09/20 | 14.1 | 0.8 | -0.58 | 8.2 | 0.5 | -0.30 |
| CH2-28D, 07/20 to 09/20 | 14.3 | 0.8 | -0.62 | 8.3 | 0.5 | -0.33 |
| CH2-1WW | 14.8 | 0.8 | -0.53 | 9.5 | 0.5 | -0.32 |
| CH2-1WEH | 14.5 | 0.8 | -0.32 | 9.6 | 0.5 | -0.24 |
| CH2-2WW | 13.0 | 0.7 | -0.29 | 7.4 | 0.4 | -0.17 |
| CH2-2WEH | 18.3 | 1.0 | -0.93 | 12.5 | 0.7 | -0.60 |
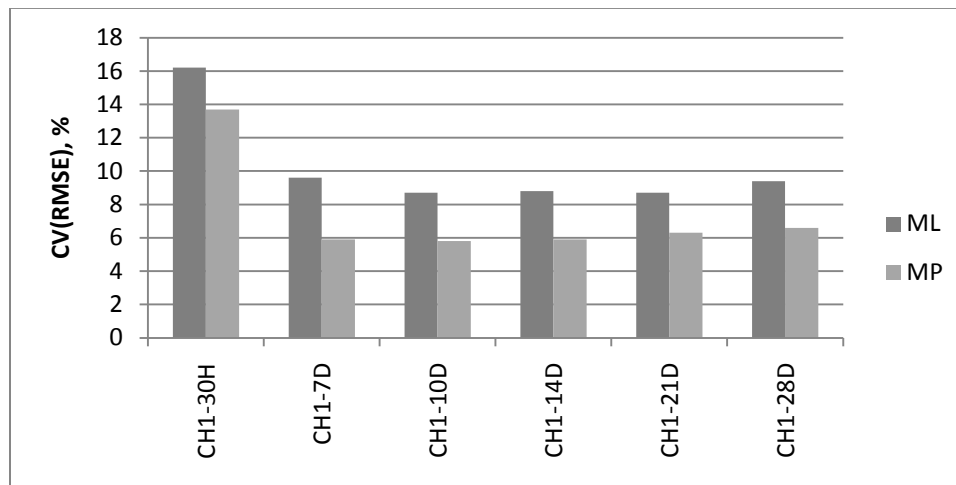


*Figure 5.15: Comparison of COP from the proposed correlation-based models over the verification set for different training set size, chiller CH-1*

129
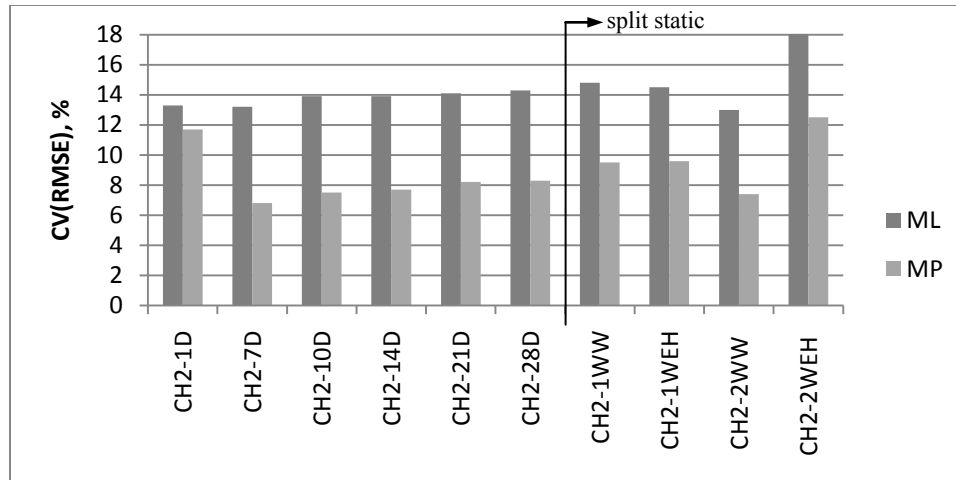
*Figure 5.16: Comparison of the COP from the proposed correlation-based models over the verification set for different training set size, chiller CH-2*

### 5.5.5.2 Existing correlation-based models

For the EnergyPlus model, for all training data sets, the CV(RMSE) over the testing set are lower than 7.4% (Table 5.19), with one exception for chillers CH-1 and CH-2 (CH1-10D and CH2-1D). However, the CV(RMSE) over the verification set vary between 6.0-12.3% and 7.4-9.6%, respectively for chiller CH-1 and CH-2 (Table 5.29).

*Table 5.29: Results for the electric power input for chillers from the EnergyPlus model – verification set*

| Verification set | CV, % | RMSE, kW | MBE, kW | R.E., % |
|---|---|---|---|---|
| CH1-30H, 07/06 to 09/22 | 12.3 | 38.5 | -25.4 | -9.6 |
| CH1-7D, 07/13 to 09/22 | 11.7 | 36.9 | -2.3 | -2.3 |
| CH1-10D, 07/16 to 09/22 | 11.9 | 37.7 | -2.2 | -2.2 |
| CH1-14D, 07/20 to 09/22 | 16.0 | 50.9 | 0.2 | -1.4 |
| CH1-21D, 07/27 to 09/22 | 8.1 | 25.5 | 3.3 | -0.5 |
| CH1-28D, 08/03 to 09/22 | 6.0 | 18.8 | 3.0 | -0.6 |
| CH2-1D, 06/23 to 09/20 | 44.7 | 133.5 | 91.7 | 17.1 |
| CH2-7D, 06/29 to 09/20 | 7.4 | 21.2 | 7.9 | -0.7 |
| CH2-10D, 07/02 to 09/20 | 8.1 | 22.9 | 10.9 | -1.5 |
| CH2-14D, 07/06 to 09/20 | 8.5 | 23.4 | 15.2 | -0.2 |
| CH2-21D, 07/13 to 09/20 | 9.4 | 26.2 | 19.2 | 0.3 |
| CH2-28D, 07/20 to 09/20 | 9.6 | 26.4 | 20.3 | 3.7 |

For chiller CH-1, it is important to mention that for the models develop with the CH1-7D, CH1-10D and CH1-14D data sets, the predictions made with the identified curve coefficients are negative for $T_{CHWS}$ greater or equal to 7.28°C. For the complete

summer, from June 22$^{nd}$ to September 20$^{th}$ 2009, the average $T_{CHWS}$ when the chiller is operating, excluding start-up, is 6.72±0.20°C. For that same period, the minimum $T_{CHWS}$ is 6.44°C, which is within one standard deviation. A $T_{CHWS}$ of 7.28°C is almost an outlier since it is close to three standard deviations from the average (Equation (5.1)) and could indicate the limit of the developed model. Therefore, the augmented window technique is not recommended. The used of a typical static window of 28-days provides good prediction accuracy over the verification set, with CV(RMSE) below 6.0%.

For chiller CH-2, the CV(RMSE) are below 9.6%, except for the model trained with one day of data (CH2-1D). The use of the augmented window technique after seven days does not improve the prediction accuracy of the verification set. Thus, for chiller CH-2, the minimum training and testing data set for the EnergyPlus model should be seven days (CH2-7D).

For the York & Cappiello models and the Gordon & Ng models, the CV(RMSE) over the testing set for the typical and augmented window techniques are below 5.1% (Table 5.20) and 5.2% (Table 5.21), respectively. However, the CV(RMSE) are higher, between 5.9% and 13.9% over the verification set (Table 5.30).

For chiller CH-1, for both models, the accuracy of the prediction does not improved over the verification set when the augmented window technique is used. For that reason, it is preferable to use a typical static window rather than using the augmented window technique. For chiller CH-2, the CV(RMSE) are comparable for the static techniques and the augmented window technique. However, increasing the training and testing set to more than seven days does not significantly improved the accuracy of the prediction over the verification set. Hence, the minimum training and testing data set for

131

the York & Cappiello and the Gordon & Ng models is seven days for both chillers (CH1-

7D and CH2-7D).

*Table 5.30: Results for the electric power input for chillers from existing models – verification data set*

| Verification set | Power Y&C | | | | Power Gordon & Ng | | | |
|---|---|---|---|---|---|---|---|---|
| | CV, % | RMSE, kW | MBE, kW | R.E. % | CV, % | RMSE, kW | MBE, kW | R.E. % |
| CH1-30H, 07/06 to 09/22 | 9.8 | 30.8 | -22.2 | -8.6 | 8.5 | 26.6 | -19.4 | -7.7 |
| CH1-7D, 07/13 to 09/22 | 5.7 | 17.8 | -2.7 | -2.4 | 6.1 | 19.1 | -4.5 | -3.0 |
| CH1-10D, 07/16 to 09/22 | 5.6 | 17.8 | -3.4 | -2.6 | 5.9 | 18.6 | -3.3 | -2.5 |
| CH1-14D, 07/20 to 09/22 | 5.8 | 18.3 | -2.7 | -2.3 | 5.9 | 18.6 | -2.2 | -2.2 |
| CH1-21D, 07/27 to 09/22 | 5.9 | 18.5 | 2.5 | -0.7 | 6.2 | 19.3 | 2.3 | -0.8 |
| CH1-28D, 08/03 to 09/22 | 6.1 | 19.2 | 3.5 | -0.4 | 6.4 | 20.2 | 3.0 | -0.6 |
| CH2-1D, 06/23 to 09/20 | 10.6 | 31.7 | 17.8 | 2.8 | 10.4 | 31.1 | 19.8 | 3.4 |
| CH2-7D, 06/29 to 09/20 | 8.9 | 25.7 | 12.0 | 0.7 | 9.2 | 26.6 | 12.7 | 1.0 |
| CH2-10D, 07/02 to 09/20 | 10.2 | 28.8 | 17.9 | 0.8 | 10.3 | 29.0 | 17.4 | 0.7 |
| CH2-14D, 07/06 to 09/20 | 11.2 | 30.8 | 22.7 | 2.4 | 11.4 | 31.4 | 22.6 | 2.4 |
| CH2-21D, 07/13 to 09/20 | 12.0 | 33.5 | 26.2 | 2.7 | 12.1 | 33.9 | 25.9 | 2.6 |
| CH2-28D, 07/20 to 09/20 | 12.3 | 33.7 | 27.2 | 6.2 | 12.6 | 34.4 | 27.4 | 6.2 |
| CH2-1WW | 11.2 | 33.2 | 22.6 | 4.0 | 10.9 | 32.3 | 20.9 | 3.5 |
| CH2-1WEH | 9.7 | 25.0 | 14.1 | | 9.8 | 25.2 | 13.9 | |
| CH2-2WW | 10.3 | 28.9 | 19.9 | 1.8 | 10.5 | 29.4 | 19.7 | 1.7 |
| CH2-2WEH | 13.9 | 34.0 | 29.1 | | 13.9 | 34.0 | 29.3 | |

For the existing COP model, the CV(RMSE) are below 5.2% over the testing set

for the York & Cappiello and Gordon & Ng model, except for the split static technique,

where it varies between 2.2% and 11.9% (Table 5.22). Over the verification set, the

CV(RMSE) are below 11.3%, except for the CH1-30H and the split static technique

(Table 5.31). For the Swider model, the CV(RMSE) are below 13.3% over the testing set

(Table 5.23), while varying between 9.1% and 14.2% over the verification set (Table

5.31). Increasing the training and testing set beyond seven days or using split models

does significantly improve the prediction over the verification set. Hence, the minimum

training and testing data set for the existing COP models is seven days for both chillers

(CH1-7D and CH2-7D).

For the proposed and existing correlation-based models, the use of a split static

technique, versus typical static or augmented window techniques, to develop the

benchmark models does not improve the model predictions. For most models, increasing the training and testing set size beyond seven days, using either the typical static of augmented window techniques, does not significantly improve the prediction over the verification set. Hence, the minimum training and testing data set for the proposed and existing correlation-based models is seven days for both chillers (CH1-7D and CH2-7D).

Table 5.31: Results for the COP for chillers from the existing models – verification data set

| Verification set | COP – Power Y&C | | | COP – Power G&Ng | | | COP – Swider | | |
|---|---|---|---|---|---|---|---|---|---|
| | CV, % | RMSE | MBE | CV, % | RMSE | MBE | CV, % | RMSE | MBE |
| CH1-30H, 07/06 to 09/22 | 196.8 | 10.4 | 0.56 | 8.7 | 0.5 | 0.34 | 12.8 | 0.7 | 0.48 |
| CH1-7D, 07/13 to 09/22 | 5.9 | 0.3 | 0.02 | 6.1 | 0.3 | 0.05 | 9.3 | 0.5 | 0.19 |
| CH1-10D, 07/16 to 09/22 | 5.8 | 0.3 | 0.04 | 6.0 | 0.3 | 0.04 | 9.3 | 0.5 | 0.10 |
| CH1-14D, 07/20 to 09/22 | 5.9 | 0.3 | 0.02 | 6.1 | 0.3 | 0.02 | 9.5 | 0.5 | 0.09 |
| CH1-21D, 07/27 to 09/22 | 6.2 | 0.3 | -0.06 | 6.4 | 0.3 | -0.06 | 9.1 | 0.5 | 0.02 |
| CH1-28D, 08/03 to 09/22 | 6.4 | 0.3 | -0.07 | 6.7 | 0.4 | -0.07 | 9.5 | 0.5 | 0.02 |
| CH2-1D, 06/23 to 09/20 | 10.7 | 0.6 | -0.34 | 10.3 | 0.6 | -0.36 | 11.8 | 0.6 | -0.33 |
| CH2-7D, 06/29 to 09/20 | 8.7 | 0.6 | -0.23 | 9.0 | 0.5 | -0.25 | 11.8 | 0.6 | -0.26 |
| CH2-10D, 07/02 to 09/20 | 9.7 | 0.6 | -0.34 | 9.8 | 0.5 | -0.33 | 12.5 | 0.7 | -031 |
| CH2-14D, 07/06 to 09/20 | 10.4 | 0.5 | -0.43 | 10.6 | 0.6 | -0.43 | 13.0 | 0.7 | -0.41 |
| CH2-21D, 07/13 to 09/20 | 11.1 | 0.5 | -0.50 | 11.2 | 0.6 | -0.49 | 13.3 | 0.8 | -0.53 |
| CH2-28D, 07/20 to 09/20 | 11.1 | 0.6 | -0.51 | 11.3 | 0.6 | -0.51 | 13.5 | 0.8 | -0.57 |
| CH2-1WW | 10.9 | 0.6 | -0.41 | 10.4 | 0.6 | -0.38 | 13.3 | 0.7 | -0.45 |
| CH2-1WEH | 9.7 | 0.5 | -0.30 | 9.7 | 0.5 | -0.30 | 12.1 | 0.6 | -0.21 |
| CH2-2WW | 9.6 | 0.5 | -0.37 | 9.8 | 0.5 | -0.37 | 12.4 | 0.7 | -0.32 |
| CH2-2WEH | 12.7 | 0.7 | -0.62 | 12.7 | 0.7 | -0.62 | 14.2 | 0.8 | -0.70 |

### 5.5.5.3  ANN models

For all evaluated ANN models, the CV(RMSE) are below 5.2% over the testing set, except for the split static technique (Table 5.24 to Table 5.26). Over the verification sets, the CV(RMSE) varies between 5.5% and 15.4% for the model based on the proposed input (Table 5.32), between 5.6% and 14.6% for the model based on the York & Cappiello input (Table 5.33), and between 5.5% and 14.4% for the model based on the Gordon & Ng and Swider input (Table 5.34).

For all ANN models, increasing the training and testing set beyond seven days or using split models does significantly improve the prediction over the verification set.

Hence, the minimum training and testing data set for all the proposed ANN models is seven days for both chillers (CH1-7D and CH2-7D).

*Table 5.32: Results for chillers from the proposed ANN models – verification data set*

| Verification set | Power, $Q_E/Q_{Edesign}$, $T_{CNDS}$, $T_{O/A}$ | | | | COP, $Q_E/Q_{Edesign}$, $T_{CNDS}$, $T_{O/A}$ | | |
|---|---|---|---|---|---|---|---|
| | CV, % | RMSE, kW | MBE, kW | R.E., % | CV, % | RMSE | MBE |
| CH1-30H-1H3N | 12.5 | 39.2 | -24.91 | -9.5 | 15.4 | 0.8 | 0.59 |
| CH1-7D-1H3N | 6.1 | 19.3 | -4.13 | -2.9 | 6.3 | -0.3 | 0.05 |
| CH1-10D-1H3N | 5.5 | 17.4 | -1.73 | -2.1 | 5.7 | 0.3 | 0.02 |
| CH1-14D-1H3N | 5.5 | 17.5 | -0.96 | -1.8 | 5.7 | 0.3 | -0.01 |
| CH1-21D-1H9N | 5.7 | 17.9 | 1.35 | -1.2 | 6.0 | 0.3 | -0.03 |
| CH1-28D-1H9N | 6.2 | 19.4 | 2.29 | -0.8 | 6.5 | 0.3 | -0.04 |
| CH2-1D -1H9N | 12.4 | 37.1 | 17.70 | 2.6 | 12.0 | 0.6 | -0.33 |
| CH2-7D-1H9N | 6.3 | 18.2 | 4.72 | -1.8 | 6.3 | 0.3 | -0.06 |
| CH2-10D-1H9N | 7.2 | 20.2 | 6.42 | -3.2 | 6.6 | 0.4 | -0.09 |
| CH2-14D-1H9N | 7.1 | 19.5 | 6.61 | -3.3 | 6.6 | 0.4 | -0.10 |
| CH2-21D-1H9N | 7.8 | 21.9 | 10.59 | -2.7 | 7.1 | 0.4 | -0.20 |
| CH2-28D-1H9N | 8.8 | 24.1 | 13.52 | 1.3 | 7.6 | 0.4 | -0.24 |
| CH2-1WW-1H3N | 8.7 | 25.8 | 15.54 | 2.0 | 9.1 | 0.5 | -0.30 |
| CH2-1WEH-1H3N | 9.6 | 24.7 | 14.10 | | 9.6 | 0.5 | -0.24 |
| CH2-2WW -1H8N | 6.7 | 19.0 | 5.60 | -2.6 | 6.7 | 0.4 | -0.07 |
| CH2-2WEH -1H8N | 11.7 | 28.5 | 23.48 | | 11.9 | 0.7 | -0.57 |

*Table 5.33: Results for chillers from the Y&C ANN models – verification data set*

| Verification set | Power – $Q_E$, $T_{CNDR}$, $T_{CHWS}$ | | | | COP – $Q_E$, $T_{CNDR}$, $T_{CHWS}$ | | |
|---|---|---|---|---|---|---|---|
| | CV, % | RMSE, kW | MBE, kW | R.E., % | CV, % | RMSE | MBE |
| CH1-30H-1H8N | 10.0 | 31.3 | -20.08 | -8.0 | 14.3 | 0.8 | 0.50 |
| CH1-7D-1H8N | 6.1 | 19.2 | -2.53 | -2.3 | 5.9 | 0.3 | 0.04 |
| CH1-10D-1H8N | 5.6 | 17.9 | -2.30 | -2.2 | 5.9 | 0.3 | 0.03 |
| CH1-14D-1H8N | 6.2 | 19.8 | -2.22 | -2.2 | 6.1 | 0.3 | 0.01 |
| CH1-21D-1H8N | 6.0 | 19.0 | 2.15 | -0.9 | 6.3 | 0.3 | -0.05 |
| CH1-28D-1H8N | 5.9 | 18.4 | 1.91 | -0.9 | 6.2 | 0.3 | -0.03 |
| CH2-1D -1H8N | 11.7 | 35.0 | 14.87 | 1.8 | 10.8 | 0.6 | -0.30 |
| CH2-7D-1H8N | 9.6 | 27.7 | 10.86 | 0.4 | 8.0 | 0.4 | -0.16 |
| CH2-10D-1H8N | 8.8 | 24.7 | 10.04 | -1.8 | 8.6 | 0.5 | -0.17 |
| CH2-14D-1H8N | 9.7 | 26.8 | 15.31 | -0.2 | 8.5 | 0.5 | -0.26 |
| CH2-21D-1H8N | 10.5 | 29.4 | 20.31 | 0.7 | 9.7 | 0.6 | -0.38 |
| CH2-28D-1H8N | 10.5 | 28.9 | 20.43 | 3.8 | 9.6 | 0.5 | -0.38 |
| CH2-1WW -1H8N | 13.0 | 38.5 | 23.58 | 4.2 | 12.9 | 0.7 | -0.40 |
| CH2-1WEH -1H8N | 9.8 | 25.2 | 13.55 | | 10.6 | 0.6 | -0.23 |
| CH2-2WW -1H8N | 7.2 | 20.2 | 9.04 | -1.4 | 7.7 | 0.4 | -0.13 |
| CH2-2WEH -1H8N | 14.6 | 35.7 | 30.67 | | 13.2 | 0.8 | -0.64 |

*Table 5.34: Results for chillers from the G&Ng and Swider ANN models – verification data set*

| Verification set | Power – $Q_E$, $T_{CNDR}$, $T_{CHWR}$ | | | | COP – $Q_E$, $T_{CNDR}$, $T_{CHWR}$ | | |
|---|---|---|---|---|---|---|---|
| | CV, % | RMSE, kW | MBE, kW | R.E., % | CV, % | RMSE | MBE |
| CH1-30H -1H8N | 15.3 | 47.9 | -22.50 | -8.7 | 13.4 | 0.7 | 0.52 |
| CH1-7D-1H8N | 5.5 | 17.3 | -2.05 | -2.2 | 6.6 | 0.3 | 0.04 |
| CH1-10D-1H8N | 5.5 | 17.4 | -2.41 | -2.3 | 5.6 | 0.3 | 0.01 |
| CH1-14D-1H8N | 5.8 | 18.4 | -1.64 | -2.0 | 5.9 | 0.3 | 0.02 |
| CH1-21D-1H8N | 5.8 | 18.2 | 2.36 | -0.8 | 6.0 | 0.3 | -0.05 |
| CH1-28D-1H8N | 6.0 | 18.9 | 1.68 | -1.0 | 6.3 | 0.3 | -0.03 |
| CH2-1D -1H8N | 11.1 | 33.2 | 16.43 | 2.3 | 10.9 | 0.6 | -0.32 |
| CH2-7D-1H8N | 8.4 | 24.1 | 5.46 | -1.5 | 8.0 | 0.4 | -0.10 |
| CH2-10D-1H8N | 8.5 | 24.0 | 9.99 | -1.9 | 5.3 | 0.5 | -0.18 |
| CH2-14D-1H8N | 9.4 | 26.0 | 13.31 | -0.9 | 9.0 | 0.5 | -0.24 |
| CH2-21D-1H8N | 9.7 | 27.1 | 17.22 | -0.3 | 9.2 | 0.5 | -0.33 |
| CH2-28D-1H8N | 10.8 | 29.6 | 21.5 | 4.1 | 9.8 | 0.6 | -0.40 |
| CH2-1WW -1H8N | 11.4 | 33.9 | 21.57 | 3.8 | 10.7 | 0.6 | -0.37 |
| CH2-1WEH -1H8N | 10.4 | 26.8 | 15.31 | | 10.3 | 0.6 | -0.27 |
| CH2-2WW -1H8N | 9.0 | 25.4 | 11.85 | -0.6 | 8.0 | 0.4 | -0.17 |
| CH2-2WEH -1H8N | 14.4 | 35.3 | 30.19 | | 13.0 | 0.7 | -0.63 |

### *5.5.5.4 Other studies of correlation-based and ANN models for chillers*

Several studies have previously compared the accuracy of correlation-based models and ANN models. In most cases, manufacturer's data or laboratory test data are used to identify the coefficients (Hydeman et al. 2002, Jiang & Reddy 2003, Lee and Lu 2010). The models are developed using steady-state conditions and the evaluation criteria are usually calculated over the training data set rather than a testing set or verification set as presented in this study.

Correlation-based models

Hydeman et al. 2002 compared the modified DOE2 model, which is one of the models used in EnergyPlus program, and the Gordon & Ng model using the same two manufacturer's data set for training and testing. For the modified DOE2 model, the CV(RMSE) were below 2.7%, while for the same data set, the Gordon & Ng model gave CV(RMSE) of 2.9% and 9.2%

The Gordon & Ng model was also evaluated using manufacturer's data for centrifugal chillers having a capacity between 386 to 400 tons. For this data set, the CV(RMSE) varies between 1.6% and 7.3% (Jiang and Reddy 2003).

Swider (2003) and Lee and Lu (2010) compared the accuracy of different empirically based models for chillers using different manufacturing or measured data sets. Swider used a training set to identify the COP model coefficients for a single circuited centrifugal chiller. The training set contained about 90% of the monitored data. The relative root-mean-squared-error (R-RMSE), which is calculated similarly to the CV(RMSE) used in this study, varies between 2.3% and 4.9% for the model similar to the York and Cappiello model. For the Gordon & Ng model, the CV(RMSE) varies between 5.1% and 5.6%, while it varies between 3.1% and 5.2% for the Swider model.

Lee and Lu (2010) tested different models for different classes of data set. For constant condenser and chilled water flow rates, ten laboratory test data sets were used to develop the models to predict the COP. The CV(RMSE) are calculated for the training data sets. For the model similar to the York and Cappiello model, the CV(RMSE) varies between 0.05% and 1.24%. For the Gordon & Ng model, the CV(RMSE) varies between 1.0% and 3.8%, while it varies between 2.3% and 9.2% for the Swider model.

Table 5.35 presents an overview of the data available in the literature on model accuracy for correlation-based models, while Figure 5.17 and Figure 5.18 present the CV(RMSE) from the models developed in this study over the testing and verification sets using the seven days data set (CH1-7D and CH2-7D), except for the EnergyPlus model for chiller CH-1 where the 28 days data set is used (CH1-28D). The accuracy of the

136

models available in the literature is represented by the CV(RMSE) range and the average value.

Over the testing set, the CV(RMSE) are slightly higher or lower than the range available in the literature (Figure 5.17) for all models, including the proposed models. Over the verification set, the proposed MP models perform as well as the existing models, with CV(RMSE) close to the value available in the literature.

*Table 5.35: Accuracy of correlation-based models available in the literature*

| Authors | Data type | EnergyPlus CV(RMSE), % | Y&C CV(RMSE)[3], % | Gordon & Ng CV(RMSE)[3], % | Swider CV(RMSE)[3], % |
|---|---|---|---|---|---|
| Hydeman et al. (2002) | 1 | 0.7 – 2.7 | | 2.9 – 9.2 | |
| Jiang & Reddy (2003) | 1 | | | 1.6 – 7.3 | |
| Swider (2003) | 2 | | 2.3 – 4.9 | 5.1 – 5.6 | 3.1 – 5.2 |
| Lee & Lu (2010) | 1 | | 0.05 – 1.24 | 1.0 – 3.8 | 2.3 – 9.2 |

1. Based on manufacturer data
2. Used of a training set to identify the coefficient of the COP models, which contained about 90% of the monitored data, while the testing set included an additional 50 monitored data points.
3. The information presented is for either the CV(RMSE) or the relative root-mean-squared-error (R-RMSE), which is calculated similarly to the CV(RMSE).
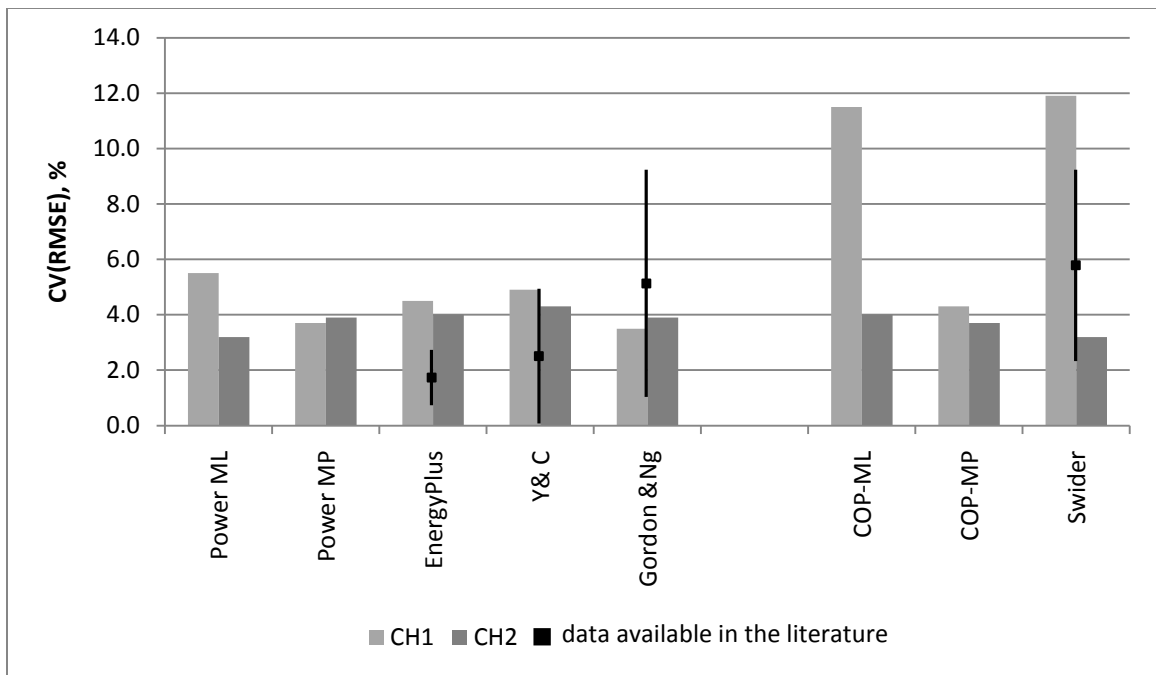


*Figure 5.17: Comparison of the correlation-based models over the testing set for different training set size*
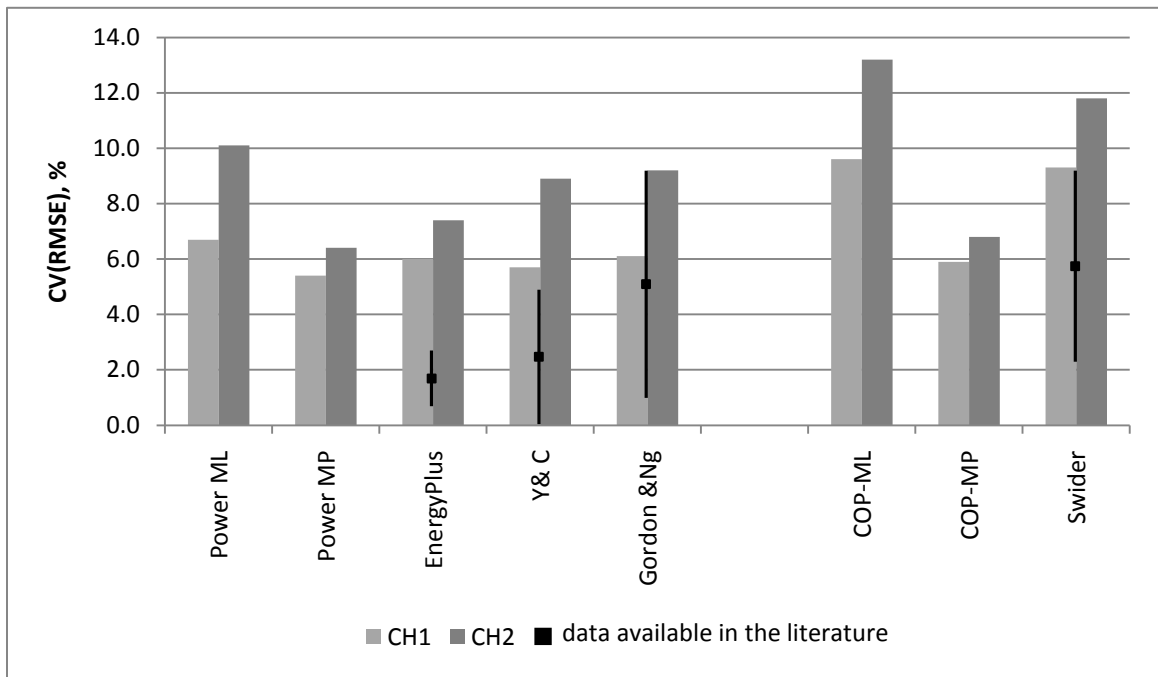
*Figure 5.18: Comparison of the correlation-based models over the verification set for different training set size*

ANN models

For the ANN models, most models are developed using the generalized radial basis function network. Swider and al. (2001) tested this approach for screw chillers. Two different data sets were used to train and test the model: the first one contained 450 data points, while the second one included 342 data points. An additional 50 data points set was used for validation. For the power and COP, the CV(RMSE) calculated on the model set, are below 2.3% and 3.9%, respectively. Over the validation set, the CV(RMSE) are below 2.7% for the electric power and below 3.9% for the COP.

Swider (2003) also tested the generalized radial basis function network and the multilayer perceptron model to estimate the COP of a single circuited centrifugal chiller. The training set contained about 90% of the monitored data, while the testing set included 50 monitored data points. The relative root-mean-squared-error (R-RMSE), which is

138

calculated similarly to the CV(RMSE) defined in this study, varied between 1.7% and 2.1% for the radial basis function network and is around 1.7% for the multilayer perceptron model, over the testing set.

Figure 5.19 presents the CV(RMSE) over the verification set for the three proposed ANN models for the electric power input and the COP of chillers CH-1 and CH-2 as well as the accuracy range found in the literature. The results are shown for the models developed using seven days of data (CH1-7D and CH2-7D). Over the verification set, the CV(RMSE) are slightly higher than the one available in the literature. However, over the testing set, the results are within the accuracy range found in the literature.
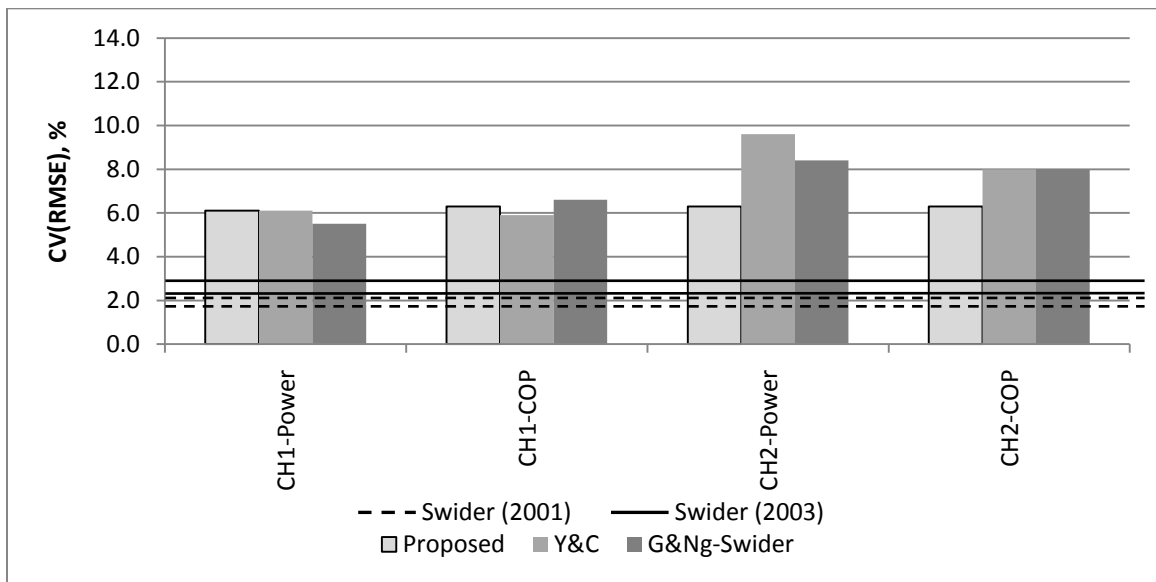


*Figure 5.19: Comparison of the ANN models over the verification set for different training set size*

Initial training set size

In terms of initial training data set size, Reddy et al. (2003a) concluded that an incremental window with 100 points (for hourly data) or 200 points (for 15-minute data) can provide accurate estimates to evaluate the performance of chillers. Reddy et al

(2003b) also found that about 320 to 400 points (from hourly data) are required for the incremental window approach.

The study presented in this thesis concluded that seven days of data monitored at 15-minute interval at the beginning of the summer season for both chillers, which corresponds to a training data set of 331 and 443 of data points during operation for chiller CH-1 and chiller CH-2 respectively, provides accurate model predictions over the remaining of the summer season.

### 5.5.5.5 Summer 2010

Data monitored over the summer 2010, from June 21$^{st}$ to September 19$^{th}$ 2010, are also available. Table 5.36 presents an overview of the operating characteristics for both chillers over the summer 2009 and 2010. For both chillers, the condenser supply water temperature is one degree lower in 2010 compared to 2009. For chiller CH-1 the average electric power input is 10 kW lower in 2010 and consequently, the COP is higher compared to 2009. For chiller CH-2, the average operating characteristics are similar; however, chiller CH-2 was in operation more often in 2010.

*Table 5.36: Comparison of chillers operating characteristics, summer 2009 and 2010*

| Item | CH-1 | | CH-2 | |
|---|---|---|---|---|
| | **2009** | **2010** | **2009** | **2010** |
| $T_{CHWS}$, °C | 6.8 ± 0.4 | 6.8 ± 0.6 | 6.7 ± 0.2 | 6.7 ± 0.5 |
| $T_{CHWR}$, °C | 11.3 ± 1.5 | 11.4 ± 1.5 | 11.2 ± 1.3 | 11.4 ± 1.3 |
| $T_{CNDR}$, °C | 28.3 ± 0.4 | 28.4 ± 0.3 | 28.5 ± 0.4 | 28.5 ± 0.3 |
| $T_{CNDS}$, °C | 33.3 ± 1.8 | 32.4 ± 1.4 | 33.3 ± 1.6 | 32.4 ± 1.2 |
| $Q_E$, kW | 1671 ± 549 | 1682 ± 510 | 1615 ± 477 | 1681 ± 456 |
| $Q_E/Q_{Edesign}$ | 0.53 ± 0.2 | 0.53 ± 0.2 | 0.51 ± 0.2 | 0.53 ± 0.1 |
| Power, kW | 313 ± 92 | 301 ± 78 | 299 ± 77 | 300 ± 73 |
| COP | 5.29 ± 1.0 | 5.50 ± 0.7 | 5.39 ± 1.3 | 5.57 ± 0.7 |
| No. operating hours | 1299 | 1183 | 663 | 1190 |
| Electricity use, kWh | 406,155 | 355,950 | 198,330 | 357,225 |

The models that were developed with seven days of data for both chillers, except for the EnergyPlus model for chiller CH-1 where the CH1-28D data set was used, are verified over the summer 2010 (Table 5.37).

*Table 5.37: Results for chillers from the developed benchmark models – summer 2010 data set*

| Models | | CH1-7D | | | CH2-7D | | |
|---|---|---|---|---|---|---|---|
| | | P, kW | | COP | P, kW | | COP |
| | | CV, % | R.E.,% | CV, % | CV, % | R.E.,% | CV, % |
| Proposed correlation-based models | Power-ML | 7.6 | 1.9 | 8.2 | 12.8 | 6.9 | 12.8 |
| | **Power-MP** | **5.7** | **-0.04** | **5.8** | **7.9** | **-1.2** | **7.9** |
| | COP-ML | | | 11.0 | | | 16.0 |
| | COP-MP | | | 6.1 | | | 7.9 |
| Existing correlation-based models | EnergyPlus | 6.1[1] | 0.3[1] | 7.9[1] | 9.2 | -3.6 | 10.6 |
| | Y&C | 7.7 | 3.1 | 7.5 | 12.5 | 6.3 | 11.9 |
| | Gordon&Ng | 7.4 | 3.1 | 7.6 | 12.6 | 6.4 | 12.1 |
| | Swider | | | 9.6 | | | 13.4 |
| ANN models | Proposed | 5.8[2] | 2.2[2] | 6.3[2] | 8.8[3] | 1.3[3] | 20.9[3] |
| | Y&C[4] | 13.5 | -3.2 | 14.8 | 18.1 | 12.4 | 14.8 |
| | G&Ng and Swider[4] | 43.5 | -33.9 | 46.5 | 10.6 | 1.1 | 14.8 |

1. Based on the EnergyPlus model developed with 28 days of data (CH1-28D)
2. Based on CH1-7D-1H3N model
3. Based on CH2-7D-1H9N model
4. Based on CH-7D-1H8N models

The results shows that the proposed Power-MP correlation-based model gives accurate prediction with CV(RMSE) below 5.7% and 7.9% for the electric power input and 5.8% and 7.9% for the COP for chillers CH-1 and CH-2, respectively.

### 5.5.6  Concluding remarks

Several studies have previously compared the accuracy of correlation-based models and ANN models (see Section 5.5.5.4). Measured data are rarely used to establish benchmark models. Furthermore, the evaluation criteria, such as the CV(RMSE), are calculated over the training set rather than over a testing or verification set for steady-state conditions. In this study, a different technique is proposed to establish and evaluate the accuracy of different benchmark models. Measured data were used to develop several

correlation-based and ANN benchmark models to evaluate different training techniques. The initial data set was divided into training and testing sets, where the training set is used to develop the model and the testing set to verify its accuracy.

For the proposed correlation-based models, the results showed that the MP models provide accurate results over the testing set. The MP models were also compared with existing models developed using the same training and testing data sets, and the proposed MP models (power and COP) provide CV(RMSE) below 5.0%, which is close to or better than the CV(RMSE) determined for the existing correlation-based models. The ANN models also gave accurate prediction over the testing set, with CV(RMSE) below 6.8%.

After the models coefficients are identified or the model is trained using the training data set and the accuracy of the prediction verified over the testing set, the ongoing commissioning process can begin. Section 5.5.4.2 presented how the models are used to perform ongoing commissioning.

To complete the analysis, an additional data set, the verification data set was used to evaluate the accuracy of the prediction over a larger period, outside the initial training and testing sets. A model can show CV(RMSE) below 5% over the training and testing sets, but the results can be quite different over the verification set. Studies found in the literature used the training and testing set to evaluate the accuracy of their models; in this study, the verification set, which represents different periods in the summer, is used to evaluate the accuracy of the prediction.

For the various models, the performance of the model varies with the sizes of the training data set. When the static window techniques are compared, the results over the

testing and verification sets demonstrate that the accuracy of the predictions is not improved with the use of separate models for week days and weekend & holidays. This remark applies to all correlation-based and ANN models evaluated in this study.

For chiller CH-1, all the models developed with the 30 hours (CH1-30H) provide accurate results over the testing set with CV(RMSE) varying between 1.9% and 2.9%, while over the verification set the CV(RMSE) are greater than 10.0%. The CV(RMSE) calculated in this study over the verification set are higher than data calculated over training and testing sets published in previous studies. Increasing the training and testing sets to more than seven days does not significantly improve the accuracy of the prediction over the verification set, except for the EnergyPlus model. Therefore, for chiller CH-1, training and testing data sets of seven days for all models are recommended to establish the benchmark model (CH1-7D), except for the EnergyPlus model.

For chiller CH-2, all the models developed with one day of data (CH2-1D) provide accurate results over the testing set, with CV(RMSE) varying between 2.2% and 11.0%, while over the verification set, the CV(RMSE) are greater than 10.4%. Over the testing set, the CV(RMSE) are comparable to data published in previous studies; however, over the verification set, the CV(RMSE) are higher. The use of the augmented window technique does not improve the prediction over the verification set. For chiller CH-2, the models developed with seven days of data give accurate results over the testing and verification sets, with CV(RMSE) below 4.6% over the testing set and 10.8% over the verification set for the electric power input, and below 6.0% over the testing set and 13.9% over the verification set for the COP. Therefore, for chiller CH-2, training and

testing data sets of seven days for all models is recommended to establish the benchmark model (CH2-7D).

The models developed using seven days of data (CH-7D-2009) were verified using data monitored over the summer 2010 season. For both chillers, the results showed that the proposed Power-MP model, which is valid for normal operating conditions of the chillers installed in the central plant, where $T_{CHWS}$ is ~6.8°C and the $T_{CNDR}$ ~28°C, provide accurate prediction over the summer 2010 season with CV(RMSE) below 7.9% for both the electric power input and COP.

# 6   DEVELOPMENT OF THE CALIBRATED COMPUTER MODEL USING

# TRNSYS

The use of simulation is becoming more common to assess the operating energy performance of the systems, identify issues and propose retrofits in buildings as part of the ongoing commissioning process. Several studies have demonstrated the use of calibrated simulation models to identify opportunities to improve the whole building energy performance (e.g. Lawrence and Braun. 2007, Lee et al. 2007, and Pan et al. 2007), and different procedures have been proposed to calibrate computer models (e.g. Pedrini et al. 2002, Yoon et al. 2003, and Lui and Lui 2011).

The complexity of the calibration method differs from one author to another. Claridge (1998) introduced different methods to analyze measured energy data from commercial buildings. The review included a simplified approach to calibrate energy model using the energy signature and energy characteristics of systems and buildings that was later on evaluated (Lui and Claridge 1998; Lui et al. 2004) and described in more detail in Lui et al. 2003 and Lui et al. 2006.

Reddy (2006) also carried out a literature review on calibration of building energy simulations programs. Based on the review, an approach based on a general stochastic methodology for calibrating detailed building energy simulation programs with utility bills and audit information was recommended and tested (Reddy et al. 2007a, 2007b). The proposed methodology leads to a small set of solutions rather than a single calibrated solution, where a sensitivity analysis is performed to identify influential input parameters. The influential parameters are then varied to improve the calibration results, leading to parameter vector solutions used to evaluate uncertainty of retrofit savings.

In this study, a different approach is proposed where manufacturer and as-operated equipment data are used to extract data for the simulation of power input and energy use of the mechanical components and systems, and finally to calibrate the simulation results.

Prior to this study, the calibration of a model developed using the EnergyPlus program (DOE 2009) for the CSB air-side systems was carried out using data obtained from the Monitoring and Data Acquisition System (MDAS) through the collaboration of the Physical Plant of Concordia University (Monfet et al. 2009). Input parameters, such as night time setback temperature set points, minimum outdoor air flow rate and economizer setting were modified based on visual comparison between the simulation results and measured data. In the end, the calibration exercise indicated that the computer model developed gave good estimations of the whole-building cooling loads, supply airflow rate and supply and return air temperatures.

In this study, the computer model of the CSB central cooling plant is developed using TRaNsient SYstem Simulation (TRNSYS) program version 16 (TRNSYS 2006). A flow chart of the model developed in TRNSYS is presented in Figure 6.1. The simulation is run with a time-step of 15 minutes that is equal to the monitoring time step. Some selected measured data or data calculated from measurements are input to the model at each time step (Table 6.1). The interaction between the heating water loop and the chilled water loop is modeled via the heat recovery heat exchanger HX-3. The information of Table 6.1 is directly input into the "TRNSYS load", "TRNSYS psychometric", and "TRNSYS HX-3" components. The TRNSYS components are then used to model the performance of the equipment shown in Figure 6.1, where the darker links show the

146

physical connections between each piece of equipment. The output boxes represent the simulation outputs that could be used to simulate the whole building and the central plant heating components to complete the simulation at a later stage. OUTPUT 1 gives the supply chilled water temperature ($T_{CHWS}$) calculated by TRNSYS rather than the temperature setpoint defined by the user and used to calculate the cooling load as presented in Table 6.1, and OUTPUT 2 the supply heating water temperature ($T_{HWS}$ or $T_8$) leaving the cold-side of heat exchanger HX-3. Additional outputs are also available for each TRNSYS components, such as water temperatures and more importantly the electric power input that are used to perform the calibration. The approach undertaken to calibrate the TRNSYS CSB central cooling plant model is presented in the following sections.
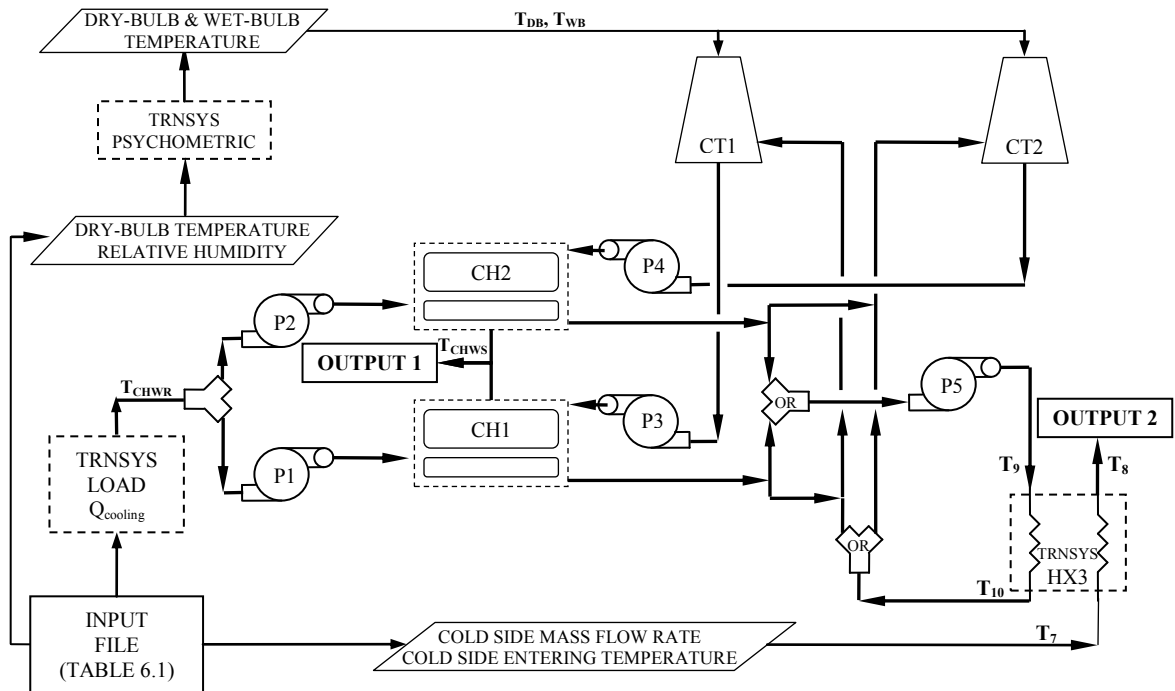


*Figure 6.1: TRNSYS model flow chart*

| Item | Unit |
|---|---|
| Outdoor air dry-bulb temperature ($T_{DB}$) | ˚C |
| Outdoor relative humidity (RH) | % |
| Chiller CH-1 chilled water supply temperature ($T_{CHWS}$) setpoint | ˚C |
| Chiller CH-1 chilled water return temperature ($T_{CHWR}$) | ˚C |
| Chiller CH-1 chilled water flow rate | kg/hr |
| Chiller CH-2 chilled water supply temperature ($T_{CHWS}$) setpoint | ˚C |
| Chiller CH-2 chilled water return temperature ($T_{CHWR}$) | ˚C |
| Chiller CH-2 chilled water flow rate | kg/hr |
| Chiller CH-1 or CH-2 to HX-3 | (1,2) |
| Cold side mass flow rate to HX-3 | kg/hr |
| Cold side entering temperature (heating water return temperature), $T_7$ | ˚C |

## 6.1 2008 TRNSYS model of the CSB central cooling plant

A computer model of the CSB central cooling plant was initially modeled in TRNSYS and calibrated with monitored data of June 23rd to June 29th, 2008, and then tested with data over the summer season, from June 23rd to September 21st, 2008 (Monfet and Zmeureanu 2009b). The summer 2008 TRNSYS model was calibrated using correlations, developed from monitored data, that characterized the performance of the chillers and showed good agreement between the simulated and monitored/correlations results: the simulated chilled and heating water temperatures, compared at key locations, were in good agreement with the monitored data with a CV(RMSE) value below 8%; the cooling electricity used was also within the acceptable range, the maximum relative error (R.E.) was less than 5% and the CV(RMSE) about 7.5%.

In March 2009, additional monitored data points became available through the MDAS: the voltage, the current, the power factor and the electric power input to each chiller. The correlations characterising the performance of the chillers were evaluated using the 2009 data and compared with the actual measured electric power input to the chillers (section 4.3). Differences between the results evaluated using the approach taken in 2008 compared with the new 2009 monitored data points were found: for chiller CH-1,

the average electric power input and energy consumption are underestimated by 30% and 40%, respectively, while for chiller CH-2 the average electric power input and energy consumption are underestimated by 40% when the preliminary correlations are used. Hence, to reflect the actual measured electric power input to the chillers and provide more accurate prediction of the total power and energy use of the central cooling plant, the model is recalibrated using the summer 2009 monitored data.

## 6.2    Description of the calibration approach

The calibration approach proposed in this study is based (1) the modification of input data and parameters to minimize the difference between the TRNSYS predictions and the measurements using a sub-set of monitored data, and (2) the comparison between the predictions and the measurements for all data monitored over the summer 2009. The various inputs and parameters used in the TRNSYS program are defined using manufacturer data and a sub-set of monitored data over the summer 2009 that are already available from the MDAS, without modifying some variables by trial-and-error or using stochastic approaches. The comparison between the predictions made by TRNSYS and the measurements is performed for the complete summer season and carried out for water temperatures at key locations, the electric power input and the electricity use.

The proposed calibration approach, in its general form, is based on identifying and modifying the inputs, parameters and external files used by the TRNSYS types for the main piece of equipment. The TRNSYS types are modified using the available manufacturer data from the operation and maintenance manual or using seven days (7D) of measured operating data at the beginning of the summer season, as defined in this

thesis, already available from the MDAS. The proposed approach is later on used to calibrate the TRNSYS model of the CSB central cooling plant.

In this study, the use of measured data is preferred to identify inputs and parameters to the TRNSYS types compared to manufacturer catalogue data or TRNSYS default files when possible. As a guideline, the identification and modification of the following inputs, parameters and/or default TRNSYS files are recommended for the following major equipment:

**vi.** Water-cooled chiller (Type666)

    a. Initial step: compare the external default TRNSYS files for the chiller performance curves with manufacturer and measured data; if the measured chiller performance is different than the default files at the operating water temperatures, modify the TRNSYS performance files.

    b. File modification: if a three by three matrix of manufacturer data points, which is the minimum of data points required in TRNSYS, is available, modify the files with the manufacturer data points only. If only a limited number of performance data points are available, use curve shifting to modify the original TRNSYS files to identify new performance coefficients with measured data (Section 6.3.1).

    c. Results comparison: the chilled water and condenser water leaving temperatures, the electric power input and the COP are used to verify if the model is calibrated (Section 6.4.1.1).

**vii.** Cooling Tower: user-supplied performance coefficients (Type51b)

   a. Inputs: the cooling tower performance is characterized by the mass transfer constant (L/G), which is equal to the inlet water mass flow rate (kg/s) over the air mass flow rate (kg/s) and the mass transfer exponent (n). Evaluate the mass transfer constant (L/G) using the pump flow rate and the manufacturer air mass flow rate. For the mass transfer exponent, isolate the cooling tower from the rest of the simulation and select the exponent that provide the most accurate prediction of cooling tower leaving water temperature.

   b. Control: the cooling tower electric power input varies with the percentage of the variable frequency drive required to maintain a constant cooling tower leaving water temperature. A correlation-based model developed using seven days (7D) of data is proposed (Section 6.3.2).

   c. Results comparison: the cooling tower leaving water temperature and the electric power input are used to verify if the model is calibrated.

**viii.** Counter flow heat exchanger (Type5b): identify the average UA-value based on measurements of heat flow and temperature difference on both water streams, and compare the heat exchanger leaving water temperature.

Once the main components are calibrated, the simulation results are compared with the measured data for the total central electric power input, electricity energy use and COP over the complete summer season. The approach undertaken to modify the TRNSYS default information is presented in Section 6.3 for the case study used in this project.

## 6.3 Model input data

This section presents the inputs to the model, and the TRNSYS types used to simulate the major equipment. TRNSYS types are divided into main categories such as heat exchangers, HVAC, hydronics, loads and structures, output and weather data reading and processing, just to name a few. Each type includes a list of inputs, outputs and parameters that characterize the mathematical model used to simulate the component (TRNSYS 2006). The TRNSYS types are used to create the model that replicates the equipment arrangement of the central plant to be modeled. The complete list of types selected to simulate the energy use of the CSB central plant is presented in Table 6.2.

For each major component, the main input and output variables and parameters are presented in the following sub-sections. Also, additional monitored data or manufacturer data are used to determine additional parameters, where required.

*Table 6.2: TRNSYS types used in the cooling central plant model*

| Name | TRNSYS type |
|------|-------------|
| Counter flow heat exchanger (HX-3) | Type5b |
| Data reader for generic data files (Input:Table 6.1) | Type9a |
| Flow mixer | Type11d |
| Controlled flow diverter | Type11f |
| Pipe/duct (to and from CT-1 & CT-2) | Type31 |
| Psychometrics: dry-bulb and relative humidity known | Type33e |
| Cooling tower: user-supplied performance coefficients (CT-1 & CT-2) | Type51b |
| Online plotter with file | Type65a |
| Single speed pump (P-1 to P-5) | Type654 |
| Water cooled chiller (CH-1 & CH-2) | Type666 |
| Heating and cooling loads imposed on a flow stream | Type682 |
| Equation | N/A |

Four main groups of equipment are present in the CSB central cooling plant: (1) chillers, (2) cooling towers, (3) heat exchanger, and (4) pumps. The pumps are constant flow and required little effort for calibration since the design and manufacturer information are easily entered as inputs and parameters in the TRNSYS types.

152

For the chillers, cooling towers and heat exchanger, manufacturer and monitored data are used to define the inputs and parameters to the TRNSYS types. For identifications and modifications of the TRNSYS types parameters or inputs using monitored data, the training monitored data sets recommended for benchmarking are selected (see Section 5.5.6): for both chillers, the training data set of seven days at the beginning of the summer season were recommended to establish the benchmark model (Table 6.3).

*Table 6.3: Recommended training data sets*

| Set name | | | Training set | |
|---|---|---|---|---|
| | | | Date | Data set size |
| CH-7D | CT1-7D | | 06/22 to 07/10 | 331 |
| CH2-7D | CT2-7D | HX3-7D | 06/22 to 06/26 | 443 |

### 6.3.1 Chillers (Type666)

The input variables to the chillers are presented in Table 6.4. At this stage of development, the chiller is turned ON whenever the cooling load calculated for each chiller based on measurements is greater than zero (Equation (6.1)). When the first chiller is turned on, the first chiller water pumps and cooling tower are started. Similarly, when the second chiller is turn on, the second chiller water pumps and cooling tower are started. The following output variables are calculated by TRNSYS: the supply chilled water temperature ($T_{CHWS}$), the condenser supply water temperature ($T_{CNDS}$), the electric input to the chiller, and the chiller COP.

$$Q_E = C_p \cdot (m_{P-1 \, or \, P-2}) \cdot (T_{CHWR} - T_{CHWSst}) \qquad (6.1)$$

where $Q_E$ is the calculated chiller evaporator load, kW; $m_{P-1 \, or \, P-2}$ is the measured water flow rate of pumps *P-1* or *P-2,* kg/s; $C_p$ is the water specific heat at the average chilled water temperature of 9.45°C, 4.196 kJ/(kg·°C); $T_{CHWR}$ is the monitored chilled

153

water return temperature, °C; and $T_{CHWSst}$ is the chilled water supply temperature setpoint, °C.

Table 6.4: Type666 - Input variables for chillers

| Item | Input |
|---|---|
| Chilled water inlet temperature ($T_{CHWR}$), ˚C | From measurements |
| Chilled water flow rate, kg/hr | From measurements |
| Condenser entering water temperature ($T_{CNDR}$), ˚C | From simulation |
| Cooling water flow rate, kg/hr | From measurements |
| Set point temperature for chilled water supply ($T_{CHWS}$), ˚C | Average monitored data |
| Control signal | ON/OFF, monitored |

Two external files are also used to define: (1) the chiller performance data, which defines (i) the capacity ratio in kW/kW as the ratio between the chiller evaporator load for leaving chilled water and entering condenser water temperatures different than the design conditions and the load at design conditions of 3165 kW; and (ii) the COP ratio as the COP at operating conditions divided by the design COP of 5.76, and (2) the electric input part-load ratio (PWR) in terms of cooling part-load ratio (PLR).

The calibration process includes modifying the chillers default files in TRNSYS (Appendix E: Table E.1) using manufacturer data or measured data to obtain accurate prediction of the electric power input.

The condenser water temperature entering the chiller is almost constant (28.3±0.4°C for chiller CH-1 and 28.5±0.4°C for CH-2 over the summer 2009). Therefore, the value is kept constant at the average value during the initial simulation.

Two sets of data have been provided by the manufacturer. The first one as part of the CSB operation and maintenance manual (Table 6.5), while the second one was generated using the manufacturer selection software for specific chilled and condenser water temperatures (Table 6.6).

*Table 6.5: Manufacturer information for chiller available in the operation and maintenance manual*

| PLR, % | Capacity, kW | CHWS, °C | CHWR, °C | CNDR, °C | CNDS, °C | Electric power input, kW | PWR |
|---|---|---|---|---|---|---|---|
| 100 | 3165 | 5.6 | 13.3 | 29.4 | 35.0 | 548.5 | 1.0000 |
| 90 | 2850 | 5.6 | 12.6 | 27.2 | 32.2 | 454.0 | 0.8276 |
| 80 | 2530 | 5.6 | 11.8 | 25.0 | 29.4 | 377.5 | 0.6882 |
| 70 | 2215 | 5.6 | 11.0 | 22.8 | 26.6 | 314.0 | 0.5724 |
| 60 | 1900 | 5.6 | 10.2 | 20.6 | 23.8 | 259.8 | 0.4737 |
| 50 | 1580 | 5.6 | 9.4 | 18.3 | 21.0 | 211.0 | 0.3847 |
| 40 | 1265 | 5.6 | 8.7 | 18.3 | 20.5 | 178.6 | 0.3257 |
| 30 | 950 | 5.6 | 7.9 | 18.3 | 20.0 | 145.9 | 0.2659 |
| 20 | 630 | 5.6 | 7.1 | 18.3 | 19.5 | 112.3 | 0.2047 |
| 10 | 315 | 5.6 | 6.3 | 18.3 | 18.9 | 75.7 | 0.1380 |

*Table 6.6: Additional information for chiller from manufacturer's selection software*

| CHWS, °C | CHWR, °C | CNDR, °C | CNDS, °C | Flow, L/s | Electric power input, kW | Capacity ratio, kW/kW | COP ratio |
|---|---|---|---|---|---|---|---|
| 5 | 13.3 | 16 | 29.4 | 80.35 | 434.5 | 0.8942 | 1.1508 |
| **6** | 13.3 | **20** | 25.5 | 91.32 | 393.7 | **0.8938** | **1.2738** |
| **7** | 13.3 | **25** | 29.4 | 118.98 | 531.3 | **1.0050** | **1.0624** |
| 8 | 15.6 | 30 | 37.7 | 99.80 | 557.8 | 1.0169 | 1.0069 |
| 9 | 15.6 | 35 | 40.6 | 115.04 | 592.5 | 1.0180 | 0.9497 |

The TRNSYS default file that contains the capacity ratio and COP ratio for a combination of leaving chilled water and entering condenser water temperatures (Appendix E: Table E.1) requires at least two chilled water temperature and condenser water temperature points to characterise the performance of the chillers. Since the information available from the operation and maintenance manual only includes one supply chilled water temperature ($T_{CHWS}$ = 5.6°C), the TRNSYS default file is modified using the additional manufacturer data (Table 6.6) for leaving chilled water temperature between 5°C and 9°C and condenser entering temperature between 16°C and 35°C.

Figure 6.2 and Figure 6.3 presents the TRNSYS default data and the manufacturer data. It is important to note a change in performance for the manufacturer data between the 6°C/20°C and the 7°C/25°C data points (Table 6.6). The manufacturer only provided five capacity ratio and COP ratio points, which is insufficient to develop surface curves that characterise the performance of the chiller. Therefore, using the difference between

155

the TRNSYS default value compared to the manufacturer data, the TRNSYS default points are shifted to pass through the capacity ratio and COP ratio provided by the manufacturer. The shift is carried out for the chilled water and condenser water temperatures separately first. For example, for all the data points at $T_{CHWS}$ = 5 °C, the default curve is shifted to fit through the 5°C/16°C manufacturer data point. Similarly, for the $T_{CNDS}$ = 30 °C, for example, the five default data points are shifted to pass through the 7°C/30°C manufacturer data point. The average between the shift carried out for the chilled water and condenser water temperatures is used as the final value in the new TRNSYS data files (Appendix E: Table E.1). Figure 6.4 and Figure 6.5 presents, as examples, the new coefficients used in TRNSYS for the capacity ratio, which are developed by shifting the TRNSYS default data to fit through the provided manufacturer data.
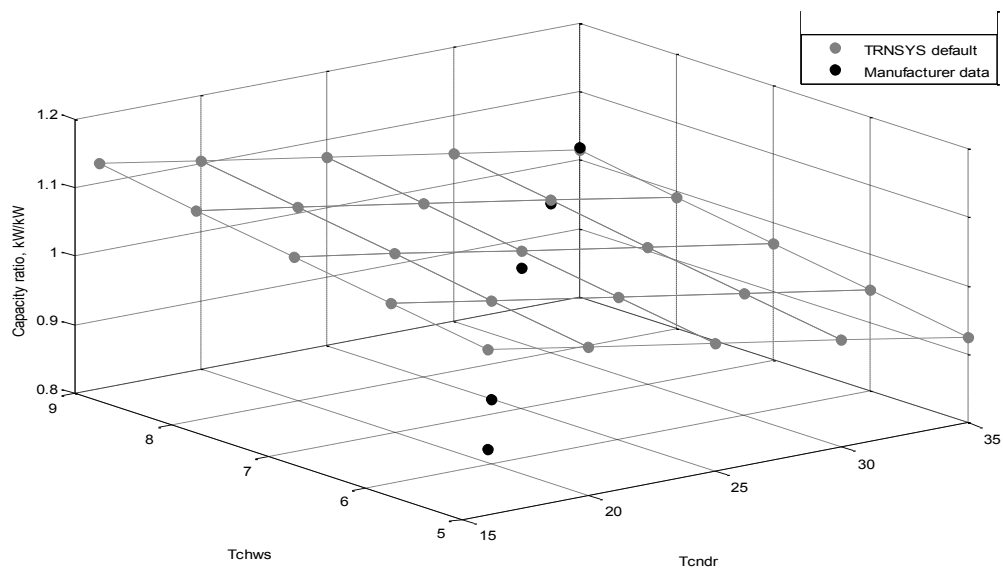


*Figure 6.2: Comparison between TRNSYS default and manufacturer data of chiller cooling capacity to cooling capacity at design conditions*
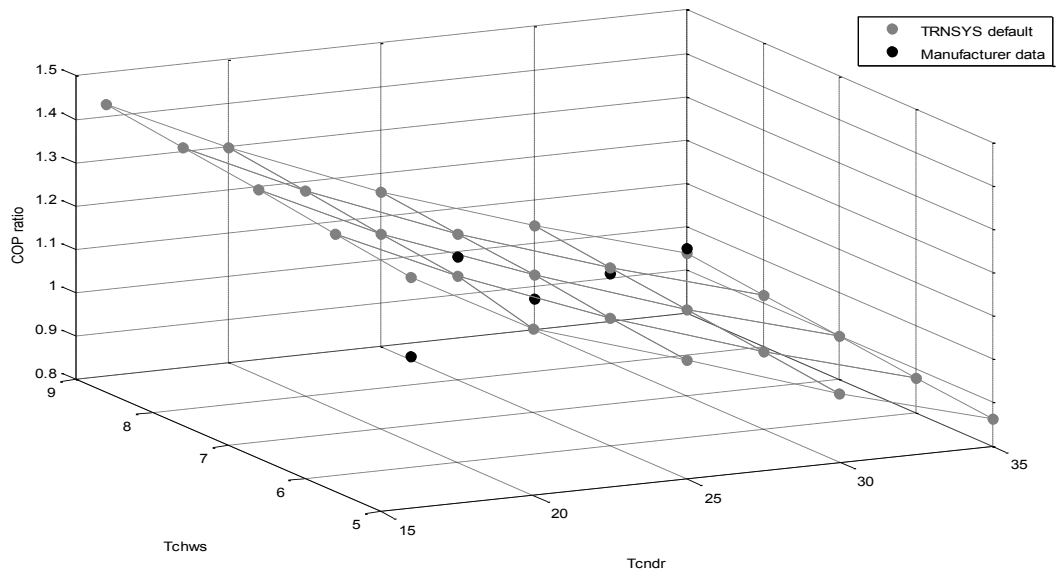
*Figure 6.3: Comparison between TRNSYS default and manufacturer data of chiller COP to COP at design conditions*
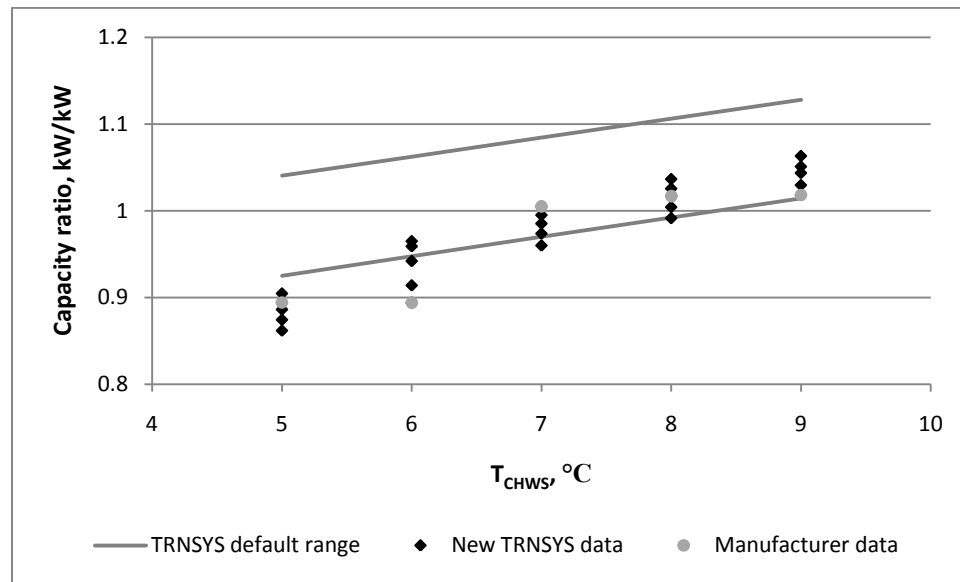


*Figure 6.4: Chiller cooling capacity to cooling capacity at design conditions performance curves versus chiller water temperatures*
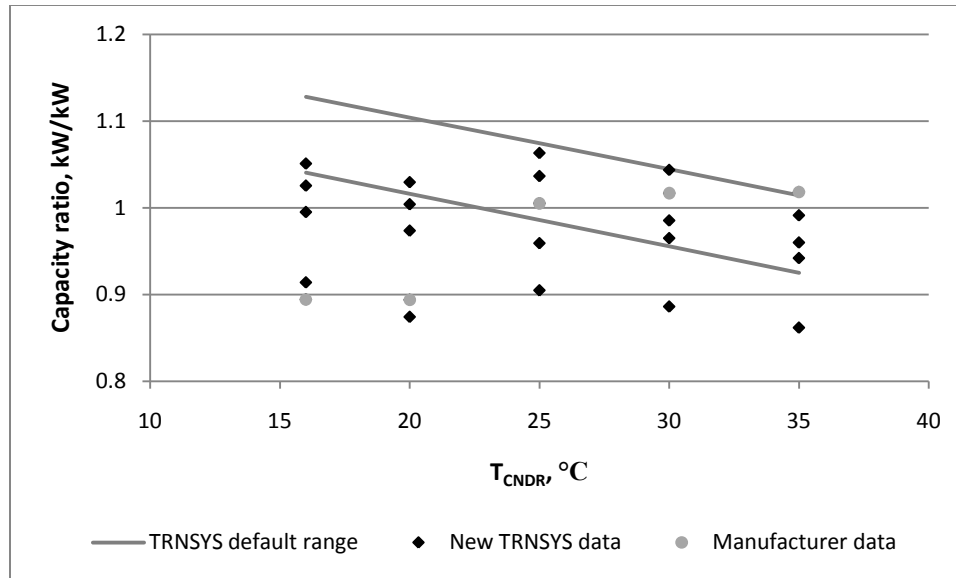
*Figure 6.5: Chiller cooling capacity to cooling capacity at design conditions performance curves versus condenser water temperature*

The second external file defines the chiller power input ratio (PWR) in terms of the part-load cooling load ratio (PLR) at the evaporator (Appendix E: Table E.2). This file is also modified based on manufacturer data (Table 6.5) or using measured data (Table 6.7).

*Table 6.7: Electric PWR versus part-load cooling load PLR based on measurements*

| PLR | PWR | |
|-----|-----|-----|
| | CH-1 | CH-2 |
| 0.1 | 0.1572 | 0.1404 |
| 0.2 | 0.2853 | 0.2583 |
| 0.3 | 0.3912 | 0.3601 |
| 0.4 | 0.4820 | 0.4522 |
| 0.5 | 0.5644 | 0.5412 |
| 0.6 | 0.6455 | 0.6333 |
| 0.7 | 0.7321 | 0.7352 |
| 0.8 | 0.8312 | 0.8532 |
| 0.9 | 0.9496 | 0.9937 |
| 1.0 | 1.0944 | 1.1633 |

When the manufacturer data is used, the data presented in Table 6.5 replace the original data of the TRNSYS default file. When the measured data is used, a simple cubic model correlating the PWR in function of PLR is developed based on the recommended

seven day training data set, CH1-7D and CH2-7D (Table 6.3), and the tabulated results are presented in Table 6.7. The values presented in Table 6.7 replace the original data of the TRNSYS default file. Figure 6.6 presents the different PWR versus PLR curves.
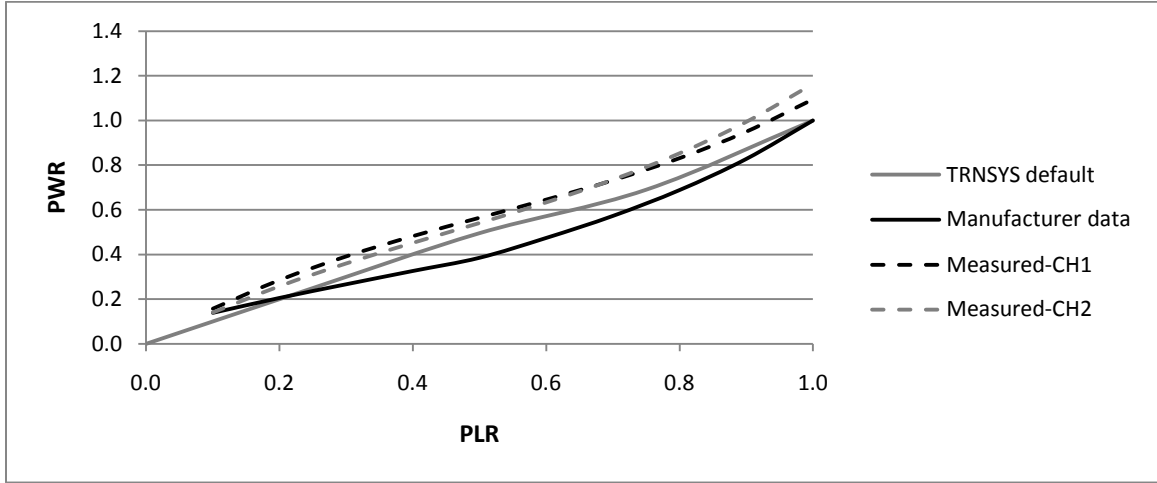


*Figure 6.6: TRNSYS input file, PWR versus PLR*

The CV(RMSE) (Equation (5.3)) and the NMBE (Equation (6.2)) are calculated between the measured electric power input and the predicted electric power input by TRNSYS (Figure 6.7) for different cases to see if modifying the external chiller input files improve the prediction made by TRNSYS.

$$NMBE = \frac{\sum_{i=1}^{n}(y_i - \hat{y}_i)}{(n-1)\cdot\bar{y}} \cdot 100 \qquad (6.2)$$

where $y_i$ is the measured value, $\hat{y}_i$ is the predicted value, $\bar{y}$ is the mean of the measured value sample data, and $n$ is the number of data.

The modification to the external files for the chillers to improve the predictions made by TRNSYS program is carried out as follows:

i.   TRNSYS default: run the simulation using the TRNSYS default, where the data for the external files for the capacity ratio and COP ratio and the PWR versus PLR are presented in Appendix E: Table E.1 and Table E.2, respectively.

159

**ii.** New TRNSYS data based on manufacturer data: run the simulation using the manufacturer data to generate the new TRNSYS external files.

  a. External file for the capacity ratio and COP ratio is generated by shifting the TRNSYS defaults data to pass through the manufacturer data points (Appendix E: Table E.1, Figure 6.4 and Figure 6.5)

  b. External file for the PWR versus PLR is modified using the data presented in Table 6.5.

**iii.** New TRNSYS data based on manufacturer and measured data: run the simulation using the new TRNSYS external files generated using manufacturer data for the capacity ratio and COP ratio (same file as **ii.a**), and by modifying the external file for the PWR versus PLR using measured data (Table 6.7).

The first set of modifications made to the two external files (**ii**) does not improve the CV(RMSE) and NMBE for the electric power input to the chillers. However, modifying the PWR versus PLR files using measured data significantly improve the CV(RMSE) and NMBE for the electric power input prediction of chiller CH-1, while the CV(RMSE) and NMBE are slightly higher for chiller CH-2 (Figure 6.7). The measured data used to modifying the PWR versus PLR files covers a wider range of operating water temperatures and conditions, thus providing more accurate predictions of the electric power input to the chillers compared to the prediction made using the manufacturer data. The difference in the performance characteristics of the chillers is explained by distinct operating patterns: chiller CH-1 has a more constant operation, while chiller CH-2 cycle ON and OFF throughout most of the summer.
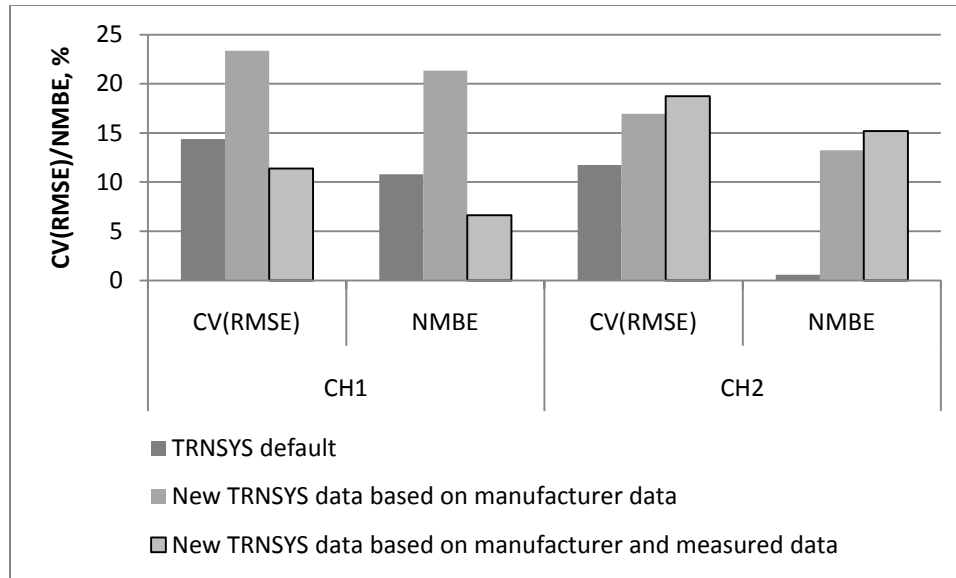
*Figure 6.7: Impact of modifying the chiller external files on the prediction of electric power input*

### 6.3.2 *Cooling towers (Type51b)*

For the cooling towers, two coefficients are user-defined: the mass transfer constant (L/G), which is equal to the inlet water mass flow rate (kg/s) over the air mass flow rate (kg/s) and the mass transfer exponent (n). Based on the measured water flow rate of 110 L/s (Table 4.4) and the manufacturer air mass flow rate (Table 6.8), the mass transfer constant (L/G) is evaluated at 0.6. For the mass transfer exponent, ASHRAE (2004) recommends a value between -0.55 and -0.65. Simulations for mass transfer exponents varying between -0.55 and -0.65 at 0.05 intervals are performed and a value of -0.65 is selected.

*Table 6.8: Manufacturer information for cooling towers*

| Item | Data |
|---|---|
| Number of cells | 2 |
| Motor size, kW/per cell | 30 |
| Cell airflow, $m^3$/s | 78.75 |
| Water flow rate, L/s | 131.5 |

The control of the cooling towers is performed by varying the fan speed to maintain a constant cooling tower leaving water temperature ($T_{CNDR}$). Since the cooling

161

tower outlet temperature is relatively constant at about 28-29 °C, emphasis is put on properly simulating the cooling tower electricity demand.

Preliminary correlations that estimate the variable frequency drive (*VFD*) level for CT-1 (Equation (6.3)) and CT-2 (Equation (6.4)) were developed using measured data, dry-bulb temperature ($T_{DB}$) and relative humidity (*RH*), and the condenser load at the chiller calculated based on measurements of water flow rate and leaving and entering water temperatures (Equation (6.5)) of the week of June 23rd to 29th 2008, where for the training data set the correlation gives a $R^2$ value of 95.7% for CT-1 (Monfet and Zmeureanu 2009b).

$$VFD_{CT-1} = -28.4302 + 0.0186 \cdot Q_{CH1-CT1} + 1.1813 \cdot T_{DB} + 0.2061 \cdot RH \qquad (6.3)$$

$$VFD_{CT-2} = 21.9880 + 0.0197 \cdot Q_{CH2-CT2} - 0.1800 \cdot T_{DB} - 0.0376 \cdot RH \qquad (6.4)$$

$$Q_{CH-CT} = C_p \cdot m_{P-3 \, or \, P-4} \cdot (T_{CNDS} - 29) \qquad (6.5)$$

where $Q_{CH-CT}$ is the calculated thermal condenser load at the chiller, kW; $C_p$ is the water specific heat at the average design water temperature, kJ/(kg·°C); $m_{P-3 \, or \, P-4}$ is the water flow rate of the condenser water pumps P-3 or P-4, 0.110 kg/s; $T_{CNDS}$ is the water temperature of the condenser water leaving the chiller, °C.

Revised correlations (Equations (6.6) and (6.7)) were developed using the summer 2009 monitored data, using the cooling tower load (Equation (6.8)) and the cooling tower approach temperature (Equation (6.9)) as independent variables to predict the VFD level.

$$VFD_{CT-1} = 0.0223266 \cdot Q_{CT1} + 0.290014 \cdot T_{approach,CT1} \qquad (6.6)$$

$$VFD_{CT-2} = 0.0205638 \cdot Q_{CT2} + 0.493558 \cdot T_{approach,CT2} \qquad (6.7)$$

$$Q_{CT-i} = C_p \cdot m_{P-3 \, or \, P-4} \cdot \left( T_{CT-i,in} - T_{CNDS,CT-i_{st}} \right), i = 1,2 \qquad (6.8)$$

$$T_{approach} = T_{CT-i,in} - T_{wb} \tag{6.9}$$

where $Q_{CT-i}$ is the calculated load of the cooling tower $i$, kW; $C_p$ is the water specific heat at the average water temperature, kJ/(kg·°C); $m_{P-3\ or\ P-4}$ is the water flow rate of the condenser water pumps P-3 or P-4, 0.110 kg/s; $T_{CT-i,in}$ is the entering cooling tower water temperature (mix of the water temperature leaving the chiller and of the water leaving the heat exchanger HX-3 if applicable) of cooling tower $i$, °C; $T_{CNDS,CT-i,st}$ is the cooling tower leaving temperature setpoint of cooling tower $i$, °C; and $T_{wb}$ is the outdoor air wet-bulb temperature, °C.

The evaluation of the techniques to establish the benchmark models for the chillers showed that increasing the training and testing data sets to more than seven days does not significantly improve the accuracy of predictions over the verification set (Section 5.5.6). Since the cooling tower operation follows the chillers operation, the coefficients of the new correlations are identified using the CT1-7D and the CT2-7D training data set (Table 6.3): Equations (6.6) and (6.7) for CT-1 and CT-2, respectively. The $R^2$ on the training set is 97.13% for CT-1 and 97.99% for CT-2. The estimated VFD speed is entered as an input to the cooling tower.

An overview of the inputs to the TRNSYS Type51b is presented in Table 6.9. The cooling tower leaving water temperature and electric power input is calculated by TRNSYS.

*Table 6.9: Type51b - Input variables for cooling towers*

| Item | Input |
|---|---|
| Water inlet temperature ($T_{CNDS}$), ˚C | From simulation |
| Inlet water flow rate, kg/hr | For measurements |
| Dry-bulb temperature $T_{DB}$, ˚C | From measurements, directly input to Type51b (Table 6.1) |
| Wet-bulb temperature, ˚C | From measurements, directly input to Type33e (Table 6.1) and output from Type33e connected to Type51b |
| Sump make-up temperature, ˚C | 25 |
| Relative fan speed for cell-1 | Calculated (Equations (6.6) or (6.7)) |
| Relative fan speed for cell-2 | Calculated (Equations (6.6) or (6.7)) |
| Mass transfer constant | 0.6 |
| Mass transfer exponent | -0.65 |

### 6.3.3   Heat exchanger HX-3 (Type5b)

For the heat exchanger, the overall heat transfer coefficient (UA) is user-defined. The overall heat transfer coefficient is first evaluated based on the heat exchanger manufacturer information (Table 6.10) and Equation (6.10). The overall heat transfer coefficient is determined to be 880 kW/K (3,175,430 kJ/hr·K – TRNSYS Type5b input) from manufacturer data (Alfa Laval 2002).

$$\dot{q} = UA \cdot \Delta T_m \tag{6.10}$$

where $\dot{q}$ is the rate of heat transfer, kW; $UA$ is the overall heat-transfer coefficient associated with the heat exchanger surface area, kW/K; and $\Delta T_m$ is the natural logarithmic mean temperature difference between the fluid streams, K.

*Table 6.10: Information for heat exchanger HX-3*

| Item | Manufacturer data | Measured data |
|---|---|---|
| Heat exchanged, kW | 2469 | 463 |
| $\Delta T_m$, K | 2.8 | 1.1 |
| Relative directions of fluids | Countercurrent | Countercurrent |
| Number of passes | 1 | 1 |

For comparison purposes (Section 6.4.1.3), the overall heat transfer coefficient (UA) is also evaluated based on the monitored data (Table 6.10) for the HX3-7D data set (Table 6.3). The average UA-value is 463 kW/K (1,667,235 kJ/hr·K), which is input to

164

the TRNSYS Type5b (Table 6.11). The heat exchanger cold-side outlet temperature $T_8$ is calculated by TRNSYS.

Table 6.11: Type5b - Input variables for the heat exchanger

| Item | Input |
|---|---|
| Hot side inlet temperature $T_9$, ˚C | From simulation |
| Hot side water flow rate, kg/hr | From measurements |
| Cold side inlet temperature ($T_7$), ˚C | From measurements, directly input to Type5b (Table 6.1) |
| Cold side mass flow rate to HX-3, kg/hr | From measurements, directly input to Type5b (Table 6.1) |
| Overall heat transfer coefficient, kJ/hr·K | 1,667,235 (from average measurements for HX-7D) |

### 6.3.4   Cooling and heat recovery pumps (Type 654)

The TRNSYS input information of the pumps (Table 6.12) is based on design (D) conditions, measured (M) pump data (Table 4.4) and manufacturer catalogue (MC) data.

Table 6.12: Input pumps information for the TRNSYS model

| Pump | Description | Flow, L/s (M) | Flow, kg/hr (Type 654 input) | Power, kW (D) | Pump efficiency, % (MC) | Motor efficiency (D) |
|---|---|---|---|---|---|---|
| P-1 | CHW | 86.75 | 312,065 | 75 | 82 | 0.9 |
| P-2 | CHW | 86.75 | 312,065 | 75 | 82 | 0.9 |
| P-3 | CNDW | 110.00 | 395,440 | 56 | 70 | 0.9 |
| P-4 | CNDW | 110.00 | 395,440 | 56 | 70 | 0.9 |
| P-5 | CND-HR | 60.00 | 214,900 | 30 | 75 | 0.9 |
| P-6 | HW-HR | 107.25 | 384,140 | 30 | 84 | 0.9 |

## 6.4   Simulation results

Kaplan and Canner (1992) recommended that the maximum allowable difference between predicted and monitored data be of 15-25% (monthly) and 25-35% (daily) for the simulation of HVAC systems. The annual simulated energy use should be within 10% of collected information, while a difference less than 25% is acceptable on a seasonal basis. For the coefficient of variance (CV (RMSE)) and the normalized mean bias error (NMBE), the value should be within ±30% and ±10% when using hourly data, respectively, or 5% to 15% for monthly data (ASHRAE 2002).

165

The coefficient of variance (CV (RMSE)), the normalized mean bias error (NMBE), and the relative error (R.E.) are used to evaluate the accuracy of the simulation results. The CV(RMSE) and the R.E. are calculated using Equations (5.3) and (5.6), respectively, while the NMBE is calculated using Equation (6.2).

The calibration is carried out for temperatures at key locations and electric power input and energy consumption of the central cooling plant.

### 6.4.1 Overview of the simulated results versus the measured data

Visual and statistical assessments are performed first for the week of July 27$^{th}$ to August 2$^{nd}$ 2009, followed by statistical assessment over the complete summer season, from June 22$^{nd}$ to September 20$^{th}$ 2009.

### 6.4.1.1 Chiller CH-1: simulated results versus measured data

The external files modified using manufacturer data (Table 6.6) for the capacity ratio and COP ratio (Appendix E: Table E.1) and measured data for the electric PWR versus PLR (Table 6.7) are used for the final simulation.

The following output variables are calculated by TRNSYS and compared with measured data: the supply chilled water temperature ($T_{CHWS}$) (Figure 6.8), the condenser supply water temperature ($T_{CNDS}$) (Figure 6.9), the electric input to the chiller (Figure 6.10), and the chiller COP (Figure 6.11).

For the electric power input and the COP, the measurements uncertainty range is shown for the measured value. The predictions made by TRNSYS compare well with monitored data (Table 6.13). The electric power input is slightly overestimated by TRNSYS, while the COP is within the measured uncertainty range.
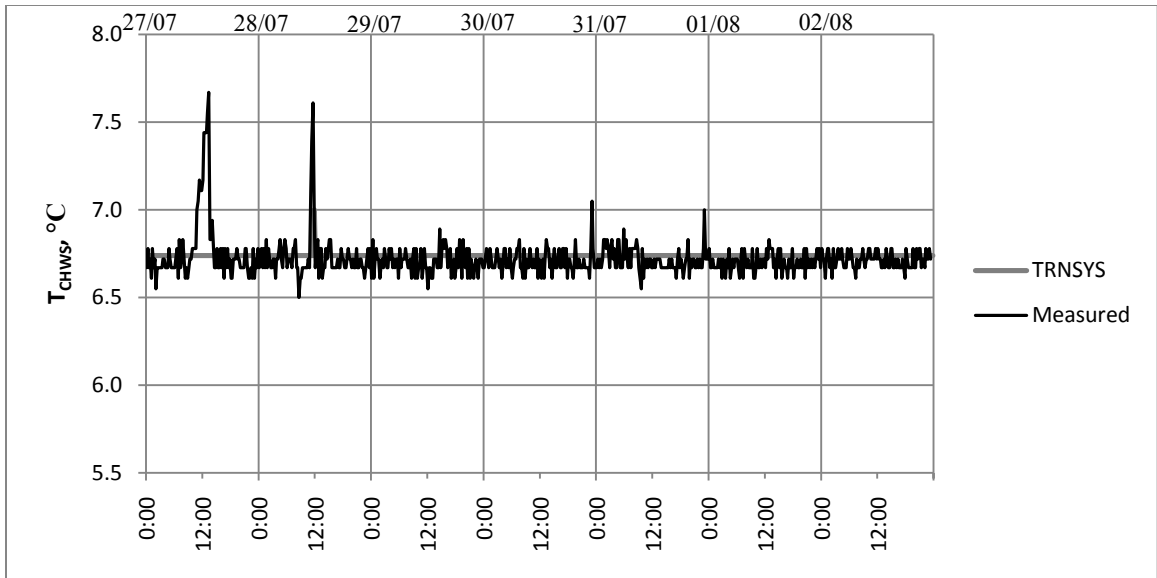
*Figure 6.8: Simulated versus monitored chilled water supply temperature ($T_{CHWS}$) for CH-1, July 27th to August 2nd 2009*
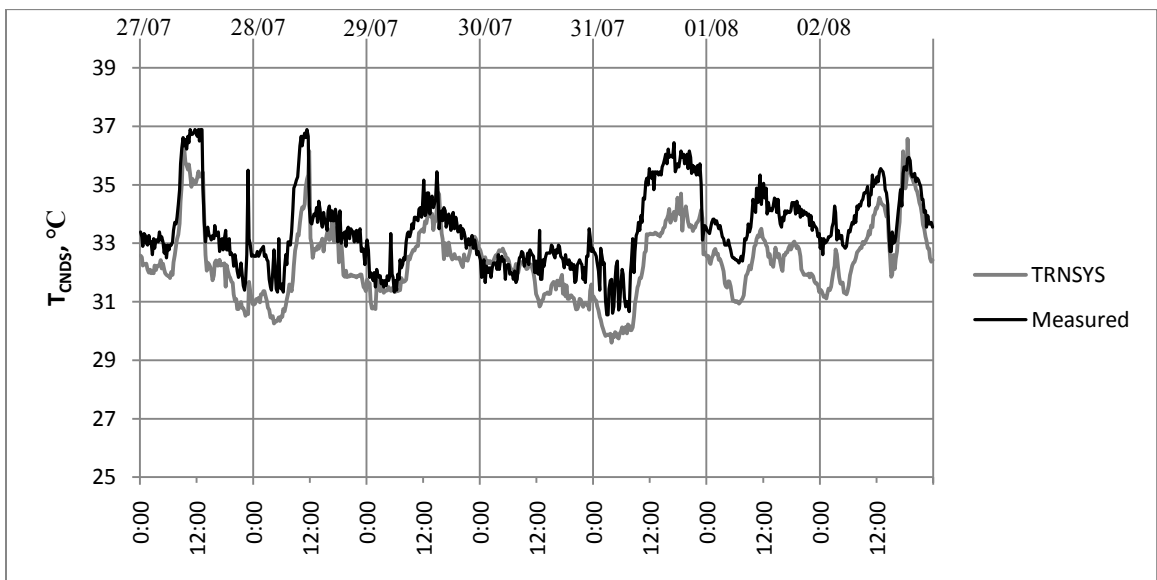


*Figure 6.9: Simulated versus monitored condenser supply water temperature ($T_{CNDS}$) for CH-1, July 27th to August 2nd 2009*

167
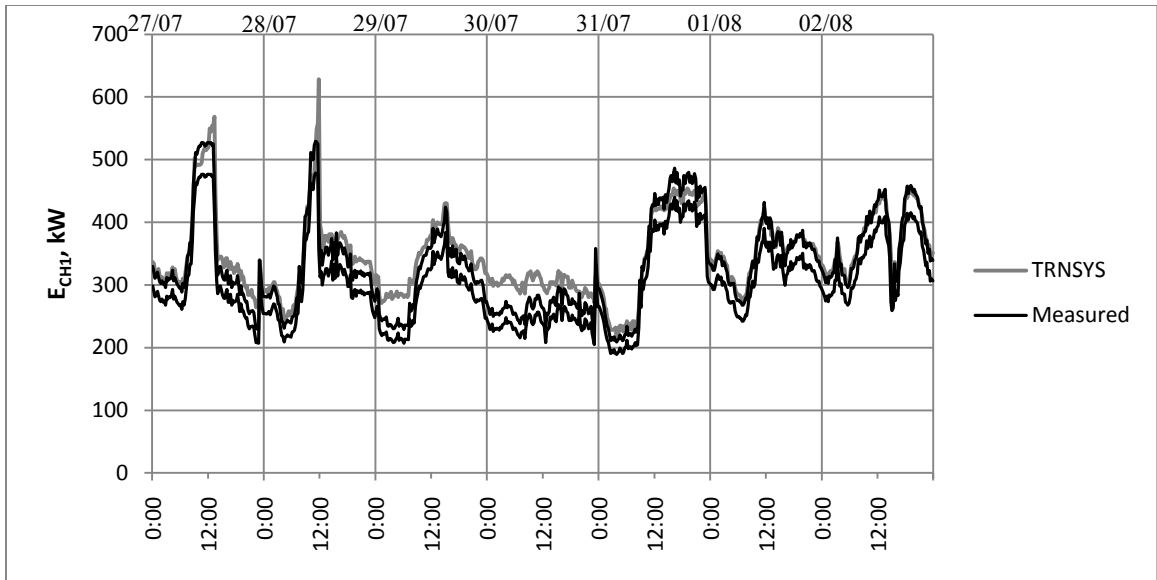
*Figure 6.10: Simulated versus monitored electric power input for CH-1, July 27$^{th}$ to August 2$^{nd}$ 2009*
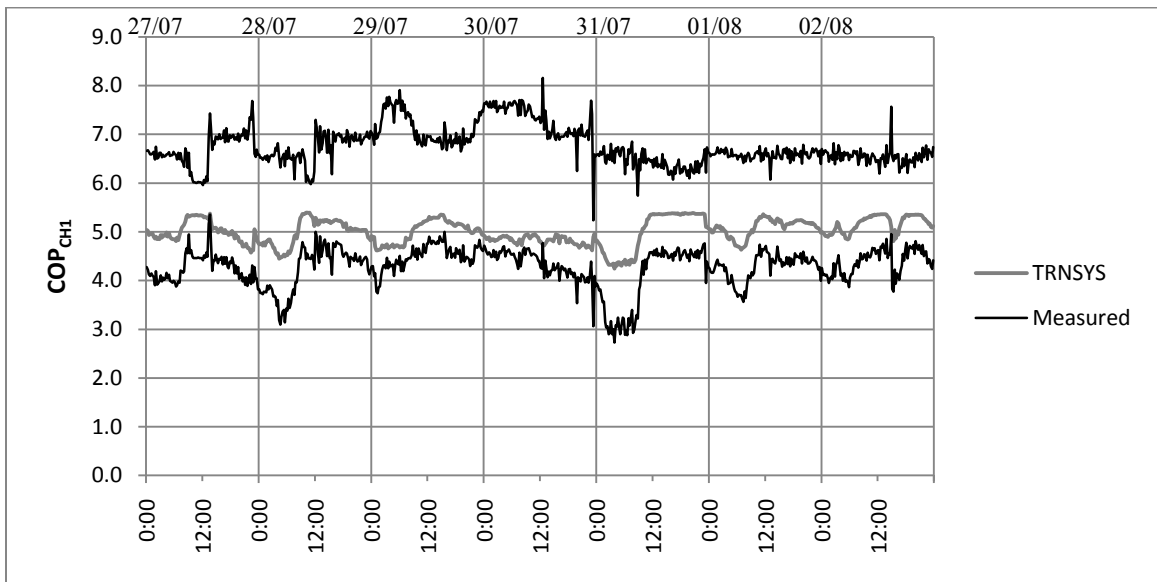


*Figure 6.11: Simulated versus monitored COP for CH-1, July 27$^{th}$ to August 2$^{nd}$ 2009*

*Table 6.13: Simulated versus measured data for chiller CH-1, July 27$^{th}$ to August 2$^{nd}$ 2009*

| ITEM | CV(RMSE), % | NMBE, % | RMSE |
|---|---|---|---|
| $T_{CHWS}$, °C | 2.6 | -0.2 | 0.2 |
| $T_{CNDS}$, °C | 4.0 | 4.2 | 1.3 |
| $E_{CH1}$, kW | 11.1 | -6.5 | 35.0 |
| $COP_{CH1}$ | 11.3 | 6.9 | 1.0 |

168

*6.4.1.2   Cooling tower: simulated results versus measured data*

For the cooling towers, the following output variables are calculated by TRNSYS: the leaving cooling water temperature ($T_{CNDR}$) and the electric input to the cooling tower. The predicted cooling tower leaving water temperature compares well with measured data of July 27th to August 2nd 2009, the CV(RMSE) is 4.5%, the NMBE 4.7% and the RMSE 1.3°C (Figure 6.12).
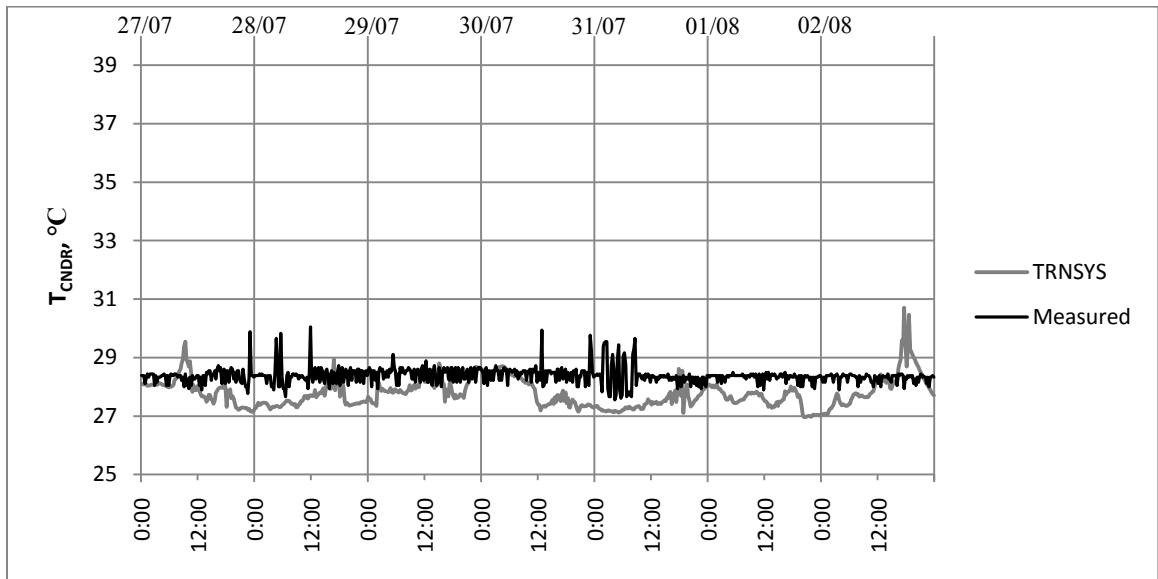


*Figure 6.12: Simulated versus monitored leaving cooling tower water temperature ($T_{CNDR}$) for CT-1, July 27th to August 2nd 2009*

The estimated electricity power input follows the same trend as the measured value; however, the peak value is sometimes underestimated (Figure 6.13). This often occurs when the outdoor air temperature is higher than 30°C, the relative humidity lower than 25% and both cooling tower are operating simultaneously. The training data set does not contain a large sample of monitored data for the outdoor air conditions previously described and when both cooling towers operate simultaneously; hence, the proposed approach to estimate the required cooling tower VFD level (Equation (6.6)) does not

169

grasp such operating conditions. For the week of July 27th to August 2nd 2009, the CV(RMSE) is 39.6%, the NMBE 30.9% and the RMSE 2.8 kW.
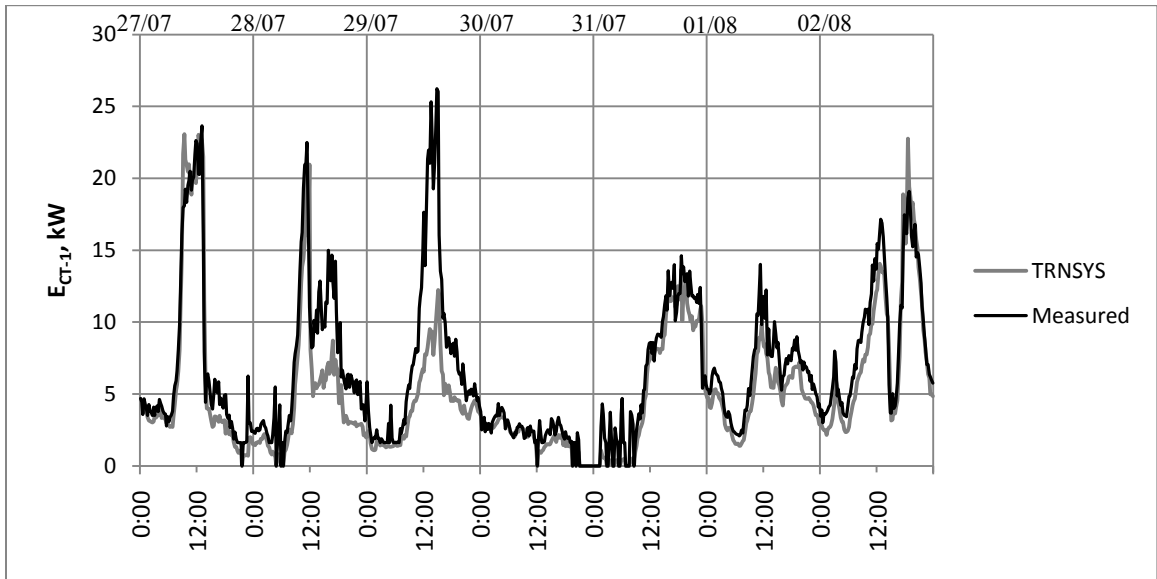


*Figure 6.13: Simulated versus monitored electric input for CT-1, July 27th to August 2nd 2009*

### 6.4.1.3   Heat exchanger HX-3: simulated results versus measured data

For the heat exchanger HX-3, the CV(RMSE), NMBE and RMSE calculated for the cold-side leaving water temperature ($T_8$) are presented for the manufacturer and identified from measurements UA values (Table 6.14). The difference in the cold-side leaving water temperature between the results obtained using the manufacturer UA value and the one based on the modified UA value using measured data is negligible. The predicted cold side leaving water temperature $T_8$, based on the identified UA value from measurements for the heat exchanger, compares well with measured data of July 27th to August 2nd 2009 (Figure 6.14). Hence, average measured data calculated over seven days of monitored data offer a good alternative to characterise the operating characteristic of the heat exchanger if no manufacturer data are available.

170

*Table 6.14: Simulated versus measured data for heat exchanger HX-3, July 27th to August 2nd 2009*

| ITEM | Based on manufacturer UA value (880 kW/K) | Based on identify from measurements UA value (463 kW/K) |
|---|---|---|
| CV(RMSE), % | 1.6 | 1.8 |
| NMBE, % | 1.1 | 1.5 |
| RMSE, °C | 0.5 | 0.6 |
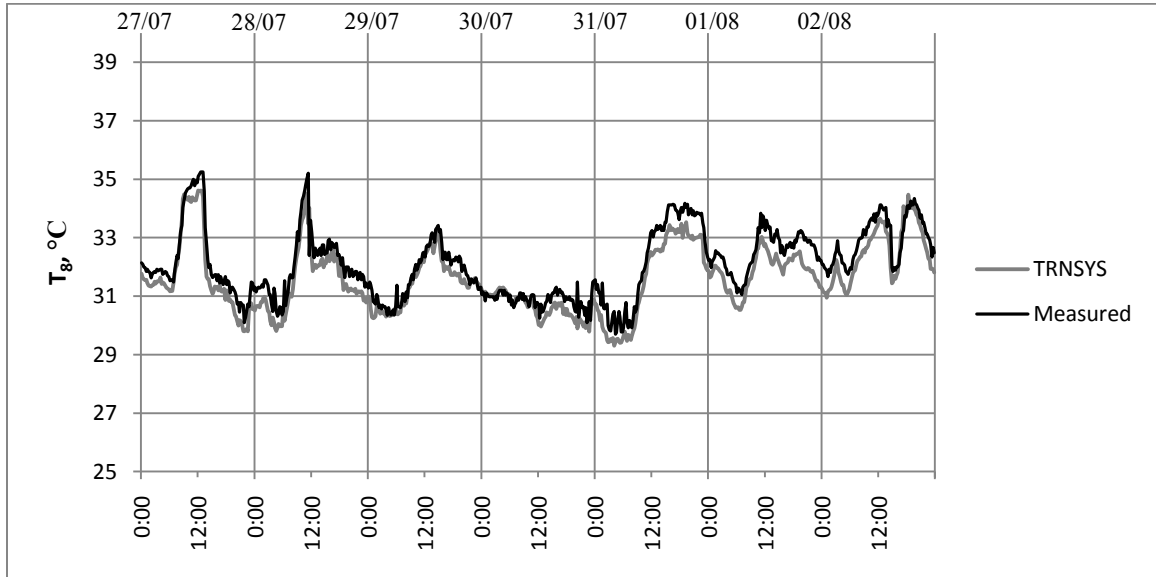


*Figure 6.14: Simulated versus monitored cold-side leaving water temperature ($T_8$) of HX-3, July 27th to August 2nd 2009*

### 6.4.1.4  Summer 2009: simulated results versus measured data

To complete the water temperature analysis at key locations, the temperatures are compared over the complete summer season. The CV(RMSE), the NMBE and the RMSE presented in Table 6.15 show that the simulated chilled and heating water temperatures are in good agreement with the monitored data over the entire summer, from June 22nd to September 20th 2009: the CV(RMSE) is below 5.5%, the NMBE below ±5.0%, and the maximum RMSE is 1.6°C.

*Table 6.15: Simulated versus monitored average water temperature during the system operation, June 22nd to September 20th 2009*

| ITEM | TRNSYS | Measured | CV(RMSE), % | NMBE, % | RMSE, °C |
|---|---|---|---|---|---|
| $T_{HWS,HX-3}$ ($T_8$) | 31.6±1.6 | 32.0±1.6 | 2.3 | 1.5 | 0.73 |
| $T_{CNDR, CT-1}$ | 27.5±0.6 | 28.3±0.4 | 5.4 | 4.7 | 1.58 |
| $T_{CNDR, CT-2}$ | 27.7±0.8 | 28.5±0.4 | 5.2 | 3.7 | 1.52 |
| $T_{CHWS,CH-1}$ | 6.7±0.0 | 6.7±0.4 | 3.8 | -0.2 | 0.25 |
| $T_{CNDS,CH-1}$ | 31.9±1.7 | 33.3±1.8 | 4.9 | 4.2 | 1.62 |
| $T_{CHWS,CH-2}$ | 6.7±0.0 | 6.7±0.2 | 3.4 | 0.1 | 0.23 |
| $T_{CNDS,CH-2}$ | 34.1±1.2 | 33.3±1.6 | 3.0 | -2.4 | 1.00 |

### 6.4.2   Cooling electricity use: simulated results versus measured data

The electricity use of the central plant for cooling purposes, which includes cooling towers, pumps and chillers, is evaluated and compared to the monitored data for the entire summer.

#### 6.4.2.1   Total electric power input

The estimated and measured total electric power inputs are compared. Figure 6.15 presents the total electric power input of the week of July 27th to August 2nd 2009 as an example. During weekends (August 1st and 2nd), the estimated electric power input is close to the measured value. During week days, the variations show similar trends: the TRNSYS simulation results are slightly higher than the measured value.

The CV(RMSE) and NMBE are calculated for the electric power input of the central plant equipment over the summer 2009, from June 22nd to September 20th 2009 for a fifteen minutes time step and a one hour time step, which is based on the average electric power input over an hour. Table 6.16 presents the results for the cooling equipment. The CV(RMSE) and NMBE are similar for both the fifteen minutes and one hour time steps. The CV(RMSE) are below 20% and the NMBE below 16%, except for the cooling towers. For the cooling central plant over the complete summer season, the

172

CV(RMSE) is below 12.2% and the NMBE below ±5.9%, which is below the recommended value by ASHRAE (2002) of ±30% for CV(RMSE) and ±10% for NMBE when using hourly data.
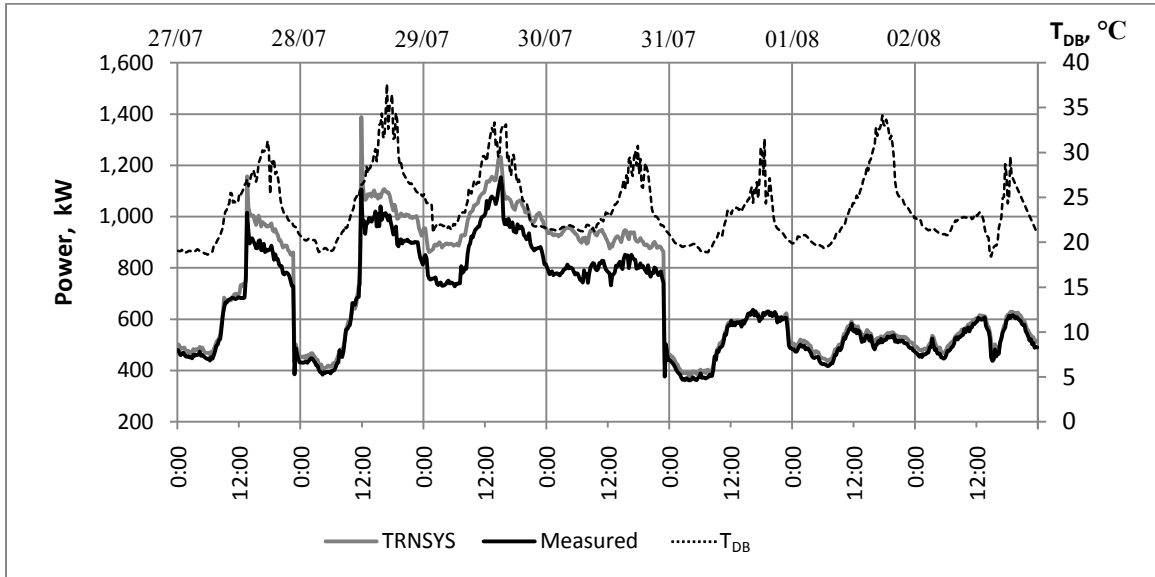


*Figure 6.15: Simulated versus monitored total electric input, July 27th to August 2nd 2009*

*Table 6.16: Simulated versus measured equipment electricity power input, June 22nd to September 20th 2009*

| ITEM | 15 minutes | | Hourly | |
|------|------------|---------|------------|---------|
|      | CV(RMSE), % | NMBE, % | CV(RMSE), % | NMBE, % |
| CH-1 | 11.4 | -6.6 | 9.1 | -6.6 |
| CH-2 | 19.1 | -15.6 | 17.6 | -15.6 |
| CT-1 | 59.8 | 26.3 | 57.3 | 26.3 |
| CT-2 | 58.6 | -17.5 | 61.3 | -18.6 |
| P-1 to P-5 | 0.0 | 0.0 | 4.0 | 0.7 |
| **Total** | **12.2** | **-5.9** | **9.3** | **-5.9** |

### 6.4.2.2 Electric energy use

The daily electricity use for the week of July 27th to August 2nd 2009 is presented in Figure 6.16 as an example. The daily electricity use increases with increase in outdoor temperature, except during weekends (August 1st and 2nd) where the daily electricity use is around 12,000 kWh.

173
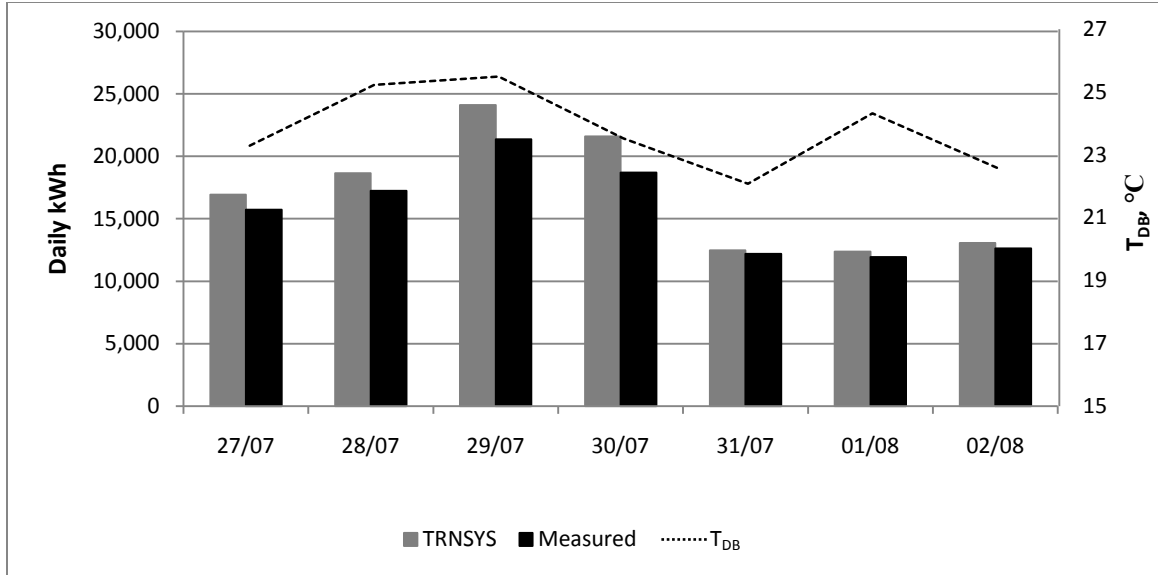
*Figure 6.16: Daily simulated and monitored electric use, July 27$^{th}$ to August 2$^{nd}$ 2009*

Figure 6.17 and Figure 6.18 show the daily Relative Error (R.E.) for the electricity use for the month of July and August 2009, respectively. As a reminder, the R.E. is calculated according to Equation (6.11):

$$R.E. = \frac{\sum_{i=1}^{n}(\hat{y}_i \cdot \Delta t) - \sum_{i=1}^{n}(y_i \cdot \Delta t)}{\sum_{i=1}^{n}(y_i \cdot \Delta t)} \cdot 100 \tag{6.11}$$

where $\hat{y}_i$ is the predicted value, $y_i$ is the measured value, and $n$ is the number of data.

TRNSYS slightly overestimates the daily electricity use. The discrepancies are larger when the outdoor air temperature is higher both in July and August. During July and August, the R.E. does not exceed 10%, except on July 29$^{th}$ and 30$^{th}$ and August 22$^{nd}$ when both chillers and cooling towers are working simultaneously for 24-hours. Over the complete summer season, the R.E. calculated on a daily basis varies between -15.5% and 8.6%.

174
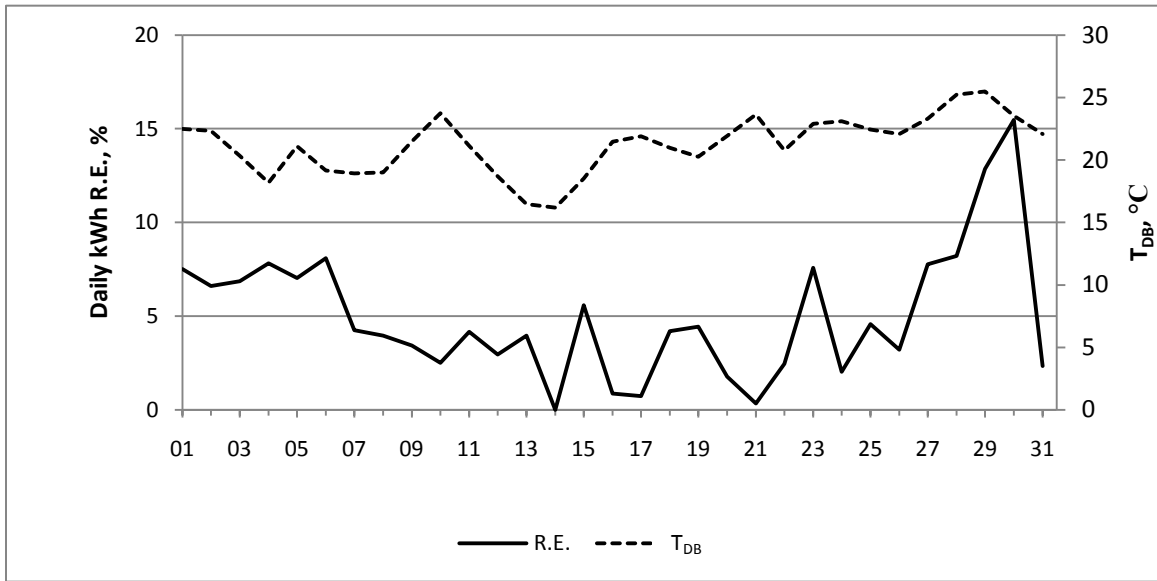
*Figure 6.17: Daily relative error (R.E) between the monitored and simulated electric use, July 2009*
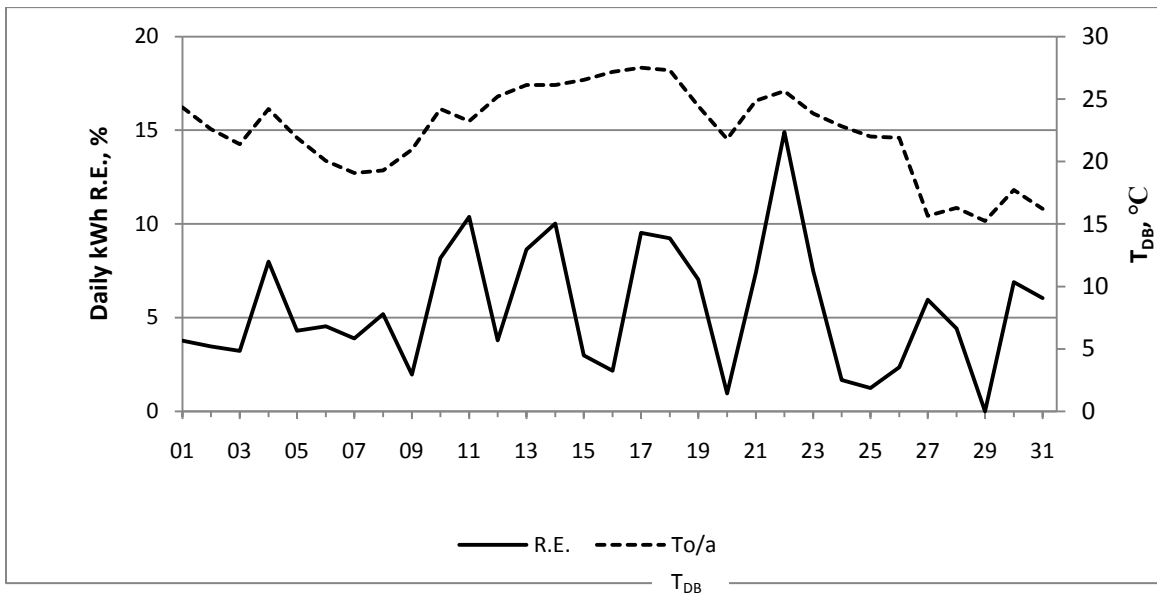


*Figure 6.18: Daily relative error (R.E.) between the monitored and simulated electric use, August 2009*

The electricity use over the summer is also compared (Table 6.17), where CH refers to chillers only, CT to cooling towers, and P to pumps. The daily and seasonal R.E. are calculated for the central plant equipment. For the chillers and pumps, the R.E. is close or better than the recommended value of 25-35% (daily) by Kaplan and Canner

(1992). For the daily total electricity use, the maximum daily R.E. is ±15.4%, while being below 6% on a seasonal basis, which is within the recommended values.

Table 6.17: Simulated versus measured cooling electricity use in kWh, June 22$^{nd}$ to September 20$^{th}$ 2009

| ITEM | TRNSYS | Measured | Seasonal R.E., % |
|---|---|---|---|
| CH-1 | 432,960 | 406,155 | 6.6 |
| CH-2 | 229,130 | 198,270 | 15.6 |
| CH | 662,090 | 604,425 | 9.5 |
| CT | 13,587 | 14,885 | -8.7 |
| P-1 to P-5 | 303,820 | 306,080 | -0.7 |
| **Total** | **979,500** | **925,390** | **5.8** |

### 6.4.3  Coefficient of Performance: simulated results versus measured data

The Coefficient of Performance (COP) is calculated for five cases: (1) for each individual chiller, (2) for both chillers, (3) for the central plant (including chillers, cooling towers, and pumps P-3 to P-4), as defined by Hartman (2001), (4) for the central plant*, including the heat exchanger condenser water pumps (P-3 to P-5), and (5) for the cooling central plant (including chillers, cooling towers, and pumps P-1 to P-5) as defined in Section 4.7.

The estimated COP by TRNSYS and the calculated COP based on measurements are compared for the week of July 27$^{th}$ to August 2$^{nd}$ 2009, which was previously presented for chiller CH-1 in Figure 6.11 and is presented in Figure 6.19 for chiller CH-2. The simulated COP lies within the uncertainty range based on measurements. Both simulated and estimated COP for chillers CH-1 and CH-2 follow similar trend.

The COP values are slightly underestimated by TRNSYS over the summer season (Table 6.18); however, within the uncertainty range. The RMSE is lower than 1.00 which is within the average uncertainty calculated for the COP over the summer season, while the CV(RMSE) are below 18.5% and the NMBE below 7.2%, which is also within the values recommended by ASHRAE (2002).

176
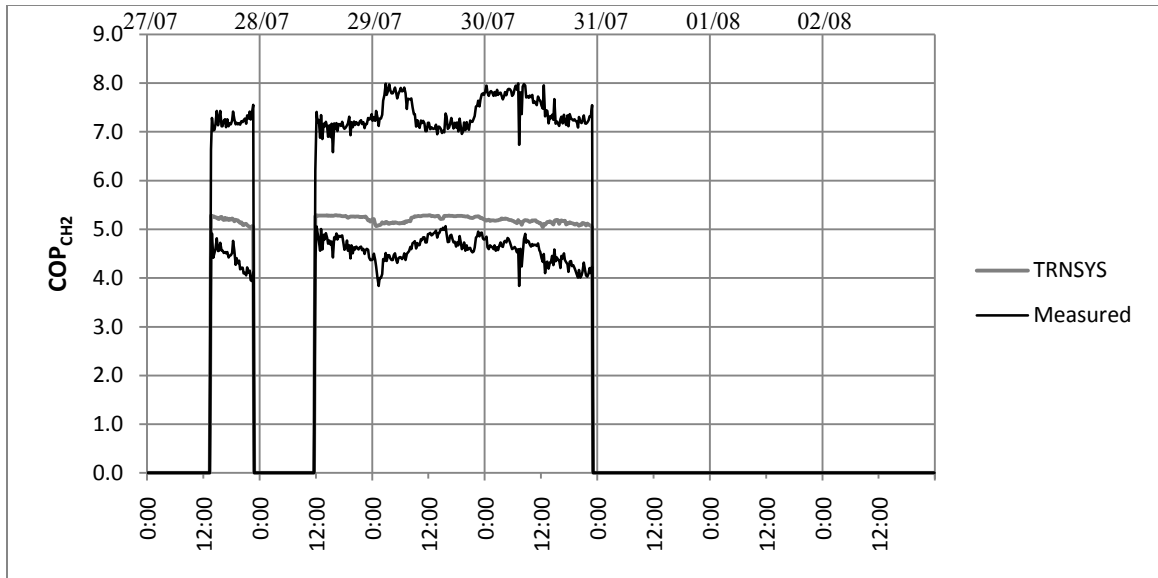
*Figure 6.19: Simulated versus monitored COP of CH-2, July 27$^{th}$ to August 2$^{nd}$ 2009*

*Table 6.18: Simulated versus measured average COP of cooling system, June 22$^{nd}$ to September 20$^{th}$ 2009*

| ITEM | TRNSYS | Measured | CV (RMSE), % | NMBE, % | RMSE |
|---|---|---|---|---|---|
| $COP_{CH-1}$ | 4.91±0.42 | 5.29±1.00 | 18.5 | 7.2 | 0.98 |
| $COP_{CH-2}$ | 5.12±0.20 | 5.39±1.32 | 18.3 | 5.1 | 0.99 |
| $COP_{CH}$ | 4.96±0.39 | 5.24±1.03 | 18.6 | 5.3 | 0.97 |
| $COP_{central\ plant}$ | 4.15±0.48 | 4.31±0.71 | 12.3 | 3.7 | 0.53 |
| $COP^*_{central\ plant}$ | 3.90±0.50 | 4.04±0.69 | 11.4 | 3.2 | 0.46 |
| $COP_{cooling}$ | 3.31±053 | 3.38±0.63 | 9.3 | 2.1 | 0.31 |

## 6.5 Calibration remarks

The analysis of the monitored data combined with the manufacturer's information was used to develop the TRNSYS model. User input files were modified to reflect the operating characteristics of the equipment installed in the central plant and a control equation was proposed for the cooling towers. The model was calibrated and tested with data over the summer season, from June 22$^{nd}$ to September 20$^{th}$ 2009. The comparison between water temperatures and instantaneous electricity demand at key locations ensures that the model developed with TRNSYS accurately mimics the operation of the central plant; not only at the central plant level, but also at the component level.

The simulated chilled and heating water temperatures, compared at key locations, were in good agreement with the monitored data with maximum RMSE of 1.6°C and CV(RMSE) values below 5.5%. For the electric power input for the cooling equipment, the CV(RMSE) is below 12.5%, while the NMBE is below ±6%. For the cooling electricity used, the simulation results are also within the acceptable range recommended by Kaplan and Carner (1992): the maximum daily R.E. is below ±15.5%, while being below 6% on a seasonal basis. At the equipment level, the R.E. calculated over the summer are below ±15.6%.

The COP of chillers and various group of equipment showed good agreement with the measured information: the RMSE are lower than 1.0, the CV(RMSE) below 18.6% and the NMBE below 7.2%. Overall the calibration exercise showed good agreement between the simulated and monitored data.

The proposed calibration approach used in this study is based on using manufacturer data and measured data to modify the inputs, parameters and external files of the TRNSYS types used in the computer model. Therefore, the manufacturer data and measured data available have an influence on the success of the proposed approach to calibrate the CSB central cooling plant. For example, only a limited number of points were provided by the chillers manufacturer to modify the TRNSYS default curves that characterise the performance of the chillers. Additional points from the manufacturer selection software may improve the simulation results. For the cooling tower, the proposed control strategies provides relatively precise leaving cooling tower water temperature, while it does not allow precise predictions of the electric power input. The cubic relationship between the VFD levels, which is input to the cooling tower type in

TRNSYS, to the estimate electric power input to the cooling tower, may amplify the imprecision of the results predicted by TRNSYS. A more complex control strategy, such as the use of a PID controller, would probably improve the simulation results. However, the use of such a strategy requires considerable effort and knowledge of the systems to tune the parameters of the controller. Nevertheless, the approach undertaken to calibrate the CSB central cooling plant shows that it is possible to develop a calibrated model using measurements already available from the MDAS and manufacturer data, without modifying by trial-and-error some variables or using stochastic approaches.

# 7 CONCLUSIONS

This research project proposed a new methodology and tool to perform ongoing commissioning of central plants. The proposed methodology includes a new approach for the development and use of benchmarking models in the context of ongoing commissioning, while the tool is based on establishing benchmark models to perform comparisons between the benchmark and the current performances of the systems.

In this study, a different technique was proposed to establish and evaluate the accuracy of different benchmark models. Measured data were used to develop several correlation-based and ANN benchmark models to evaluate different training techniques. The evaluated models were general models, while the identified model coefficients or trained ANN models were case oriented. Furthermore, the evaluation criteria, such as the CV(RMSE), were calculated over the training set rather than over a testing or verification set for steady-state conditions

The Concordia Sciences Building (CSB) was used as a case study to evaluate the proposed ongoing commissioning methodology. In order to select and establish models that are representative of the operating characteristics of the central plant, a detailed analysis of the central plant systems was performed at the equipment and system levels. The benchmarking methodology was then evaluated for the two chillers installed in the CSB.

For the case under study and for the various models, the performance of the model varies with the size of the training data set. When the static window techniques are compared, the results over the testing and verification sets demonstrate that the accuracy of the predictions is not improved with the use of separate models for week days and

weekend & holidays. This remark applies to all correlation-based and ANN models evaluated in this study. Furthermore, for chiller CH-1, increasing the training and testing sets to more than seven days does not significantly improve the accuracy of the prediction over the verification set, except for the EnergyPlus model. Therefore, for chiller CH-1, training and testing data sets of seven days for all models are recommended to establish the benchmark model (CH1-7D), except for the EnergyPlus model. For chiller CH-2, the use of the augmented window technique does not improve the prediction over the verification set. For chiller CH-2, the models developed with seven days of data give accurate results over the testing and verification sets, with CV(RMSE) below 4.6% over the testing set and 10.8% over the verification set for the electric power input, and below 6.0% over the testing set and 13.9% over the verification set for the COP. Therefore, for chiller CH-2, training and testing data sets of seven days for all models is recommended to establish the benchmark model (CH2-7D).

For the proposed correlation-based models, the results showed that the MP models provide accurate results over the testing set. The MP models were also compared with existing models developed using the same training and testing data sets, and the proposed MP models (power and COP) provide CV(RMSE) below 5.0%, which is close to or better than the CV(RMSE) determined for the existing correlation-based models and within the recommended range of 3-5% for prediction of power input at the component level (Haberl and Bou-Saada 1998, Kammerud et al. 1999). The ANN models also gave accurate prediction over the testing set, with CV(RMSE) below 6.8%.

The evaluation of the proposed methodology using a case study led to various recommendations regarding the development of benchmarking models at the component

level to perform ongoing commissioning. The monitored data available limits the model to be selected to establish the benchmark models. Also, the frequency and quality of the data monitored have a direct impact on the goodness of the developed benchmark models. Therefore, caution is required when adjusting the threshold to identify change in the performance of the equipment.

As part of the ongoing commissioning approach, a calibration approach was proposed in this study which is based on (1) the modification of input data and parameters to minimize the difference between the TRNSYS predictions and the measurements using a sub-set of monitored data, and (2) the comparison between the predictions and the measurements for all summer 2009 monitored data. The simulation results were in good agreement with the monitored data, with CV(RMSE) that do not exceed 5.5% for water temperature at key locations, 12.5% for the electric power input of the cooling equipment, and 18.6% for the COP of chillers and various groups of equipment, which is below the recommended value by ASHRAE (2002) of ±30% for CV(RMSE) and ±10% for NMBE. The Relative Error (R.E.) calculated over the summer season for the cooling electricity used is within ±15.6%, which is also within the recommended value in the literature (Kaplan and Canner 1992; ASHRAE 2002). The approach undertaken to calibrate the CSB central cooling plant showed that it was possible to develop a calibrated model using measurements already available from the Monitoring and Data Acquisition System (MDAS) and manufacturer data, without modifying by trial-and-error some variables or using stochastic approaches.

182

**7.1 Contributions**

The research work undertaken to complete this thesis lead to the following contributions:

1. Development of a new ongoing commissioning concept for the energy performance of central heating and cooling plants in cold climates, which includes:

    a. The proposed general ongoing commissioning methodology and tool,

    b. The approach to establish the benchmark models using monitored data;

2. Development of new benchmarking ANN and correlation-based models from the monitored data and assessment of their performance for ongoing commissioning:

    a. Four new correlation-based models and three new ANN models were evaluated and compared with existing correlation-based models and data available in the literature to evaluate the performance of water-cooled electric chillers,

    b. Different training techniques and training data sets were used to evaluate proposed and existing benchmark models for the chillers of the case study. The results demonstrated that seven days of data monitored at the beginning of the summer season were sufficient to establish accurate models to predict the energy performance of the chillers used in the case study

3. Development and testing of a new calibration approach in TRNSYS using a sub-set of monitored data and manufacturer catalogue data.

## 7.2    Recommendation for future work

The methodology presented in this thesis showed great potential to assist the ongoing commissioning process. However, to complete the evaluation of the proposed ongoing commissioning methodology and tool, the following items are recommended for future work:

- Propose statistical criteria to evaluate the "richness" of monitored data to identify more appropriate inverse models;

- Evaluate different model identification and prediction band techniques to improve the robustness of the developed benchmark models;

- Develop benchmark models for the other main cooling and heating equipment present in the central plant, including cooling tower, heat exchanger, and boilers;

- Develop models for groups of equipment such as the cooling equipment, heating equipment and heat recovery equipment as well as for the complete central plant;

- Evaluate the benchmarking methodology for different ongoing commissioning starting points, such as the first day of the cooling season or anytime during the year;

- Test the approach for other central plants;

- Complete the central plant simulation;

- Evaluate the calibration approach for the other seasons and on an annual basis;

- Optimize the operation of the central plant using the calibrated computer model to establish an "optimal" benchmark target.

# REFERENCES

Abouzelof, Y. 2001. Re-commissioning: an energy management tool. Journal of Energy Engineering 98 (4): 24-39.

ACRx Palm Pilot. http://www.acrx.com/ (latest access 22/07/2008).

Ahmed, A., J. Ploennigs, K. Menzel, and B. Cahill. 2010. Multi-dimensional building performance data management for continuous commissioning. Advanced Engineering Informatics 24: 466-475.

Air Conditioning and Refrigeration, Technology Institute (ARTI). 2003. Methods for automated and continuous commissioning of building systems. Portland Energy Conservation, Inc., Battelle Northwest Division, http://www.osti.gov/bridge/servlets/purl/810800-vomrED/native/810800.PDF (latest access 06/04/2008).

Alfa Laval, 2002. Plate heat exchanger specification, model M20-MFG. University of Concordia.

ASHRAE. 2001. Handbook - Fundamentals. American Society of Heating, Refrigeration and Air Conditioning Engineers Inc., Atlanta, GA.

ASHRAE. 2002. Measurement of energy and demand savings. ASHRAE Guideline 14, American Society of Heating, Refrigeration and Air Conditioning Engineers Inc., Atlanta, GA.

ASHRAE. 2004. HVAC systems and equipment. American Society of Heating, Refrigeration and Air-Conditioning Engineers, Inc., Atlanta, GA.

ASHRAE. 2005a. The Commissioning Process. ASHRAE Guideline 0-2005, American Society of Heating, Refrigeration and Air-Conditioning Engineers, Inc., Atlanta, GA.

ASHRAE. 2005b. ASHRAE Guideline 2-2005: Engineering analysis of experimental data. American Society of Heating, Refrigeration and Air Conditioning Engineers Inc., Atlanta, GA.

ASHRAE. 2007. ASHRAE Guideline 1.1-2007: HVAC&R Technical Requirements for the Commissioning Process. American Society of Heating, Refrigeration and Air Conditioning Engineers Inc., Atlanta, GA.

Baumann, O. 2004. Operation diagnostics - use of operation patterns to verify and optimize building and system operation. http://txspace.tamu.edu/bitstream/handle/1969.1/5087/ESL-IC-04-10-58.pdf?sequence=1, ICEBO - Operation Diagnostics, France: 1-10.

Beasley, R., J.S. Haberl, D.E. Claridge, and W. Dan Turner. 2002. Development of a methodology for baselining the energy use of large multi-building central plants. ASHRAE Transactions 108 (1), American Society of Heating, Refrigeration and Air-Conditioning Engineers, Inc.: 251-259.

Bechtler, H., M.W. Brown, P.K. Bansal, and V. Kecman. 2001. New approach to dynamic modelling of vapour-compression liquid chillers: artificial neural networks. Applied Thermal Engineering 21: 941-953.

Beck, J.V. and K.A. Woodbury. 1998. Inverse problems and parameter estimation: integration of measurements and analysis. Measurement Science & Technology 9 (6): 839-847.

Ben-Nakhi, A.E., and M.A. Mahmoud. 2004. Cooling load prediction for buildings using general regression neural networks. Energy Conversion and Management 45: 2127–2141.

Brandemuehi, M.J., S. Gabel, and I. Andresen. 1993. HVAC 2 toolkit: algorithms and subroutines for secondary HVAC systems energy calculations. ASHRAE.

Braun, J.E. 1988. Methodologies for design and control of central cooling plants. PhD. Dissertation, Department of Mechanical Engineering, University of Wisconsin-Madison.

CANMET Energy Technology Centre, Varennes. 2007. DABO$^{TM}$ User Guide: Fault detection, diagnosis and commissioning. Natural Resources Canada, Canada.

Chen, H., S. Deng, and H. Bruner. 2003. Achieving better building performance and savings using optimal control strategies. http://txspace.tamu.edu/bitstream/1969.1/5200/1/ESL-IC-03-10-08.pdf, Energy Systems Laboratory & Texas A&M University: 1-11.

Chen, Q., C. Xu, J. Zhou, M. Verdict, W.D. Turner, S. Deng, and B. Birch. 2006. Continuous commissioning® of a modern central utility plant. Energy Systems Laboratory & Texas A&M University, http://txspace.tamu.edu/bitstream/1969.1/4645/1/ESL-HH-06-07-08.pdf: 1-8.

Choinière, D. and M. Corsi. 2003. A BEMS-assisted commissioning tool to improve the energy performance of HVAC systems. http://txspace.tamu.edu/bitstream/handle/1969.1/5201/ESL-IC-03-10-09.pdf?sequence=1 (latest access 22/07/2008).

Choinière, D. 2004. Four years of on-going commissioning in CECT-Varennes building with a BEMS assisted Cx tool. http://txspace.tamu.edu/bitstream/handle/1969.1/5043/ESL-IC-04-10-18.pdf?sequence=1, Taxas A&M Librairies, Texas.

Chung, W. 2011. Review of building energy-use performance benchmarking methodologies. Applied Energy 88 (5): 1470-1479.

Claridge, D.E., W.D. Turner, M. Liu, S. Deng, G. Wei, C. Culp, H. Chen, and S.Y. Cho. 2004. Is commissioning once enough? Journal of Energy Engineering 100 (4): 7-19.

Claridge, D.E. 1998. A perspective on methods for analysis of measured energy data from commercial buildings. Journal of solar energy engineering 120: 150-155.

Colker, R.M. 2009. Q&A: Why we need a labeling program. ASHRAE Journal 51 (12): 18-19,21.

Deng, S., W.D. Turner, D.E. Claridge, H. Bruner, H. Chen, and G. Wei. 2001. Lessons and measures learned from continuous commissioning[(SM)] of central chilled/hot

water systems. Energy Systems Laboratory & Texas A&M University, http://txspace.tamu.edu/bitstream/1969.1/5141/1/ESL-IC-01-07-19.pdf: 1-11.

Deng, S., D. Turner, J. Hood, M. Gleen, J. Jones, and B. Lund. 2005. Continuous commissioning of Salt Lake community college South City Campus. Journal of Energy Engineering 102 (6): 26-38.

Department of Energy (DOE). Lawrence Berkeley National Laboratory. 2009. EnergyPlus Engineering Reference.

Djuric, N. and V. Novakovic. 2010. Correlation between standards and the lifetime commissioning. Energy and Buildings 42: 510-521.

Dodier, R. H. and G.P. Henze. 2004. Statistical analysis of neural networks as applied to building energy prediction. Journal of Solar  Energy Engineering 126: 592-600.

ENFORMA. 2009. ENFORMA Building Diagnostics (EBD). Architectural Energy Corporation, http://www.enformadiagnostics.com.

Fausett, L. 1994. Fundamentals of neural networks: architecture, algorithms, and applications. , Prentice-Hall, Inc., New Jersey.

Fels, M.F., C.L. Reynolds, and D.O. Stram. 1986. Documentation for heating-only or cooling-only estimation program: version 4.0. The center for energy and environmental studies, Princeton University, New Jersey.

Fernández-Polanco, D., A. Eastwood, and N. Knight. 2005. Real-time utility system optimization. Journal of Energy Engineering 102 (3): 63-78.

Feuston, B.P. and J.H. Thurtell. 1994. Generalized nonlinear regression with ensemble of neural nets: the great energy predictor shootout. ASHRAE Transactions 100 (2): 1075-1080.

Ginestet, S. and D. Marchio. Retro and on-going commissioning tool applied to an existing building: Operability and results of IPMVP. Energy 35 (4): 1717-1723.

Gordon, J.M. and K.C. Ng. 1994. Thermodynamic modeling of reciprocating chillers. Journal of applied physics 75 (6): 2769-2774.

188

Gordon, J.M., K.C. Ng, and H.T. Chua. 1995. Centrifugal chillers: thermodynamic modelling and a diagnostic case study. International journal of refrigeration 18 (4): 253-257.

Gordon, J.M. and K.C. Ng. 1995. Predictive and diagnostic aspects of a universal thermodynamic model for chillers. Journal of heat mass transfer 38 (5): 807-818.

Gordon, J.M. and K.C. Ng. 2000. Cool thermodynamics. Cambridge press.

Haberl, J.S. and D.E. Claridge. 1987. An expert system for building energy consumption analysis: prototype results. ASHRAE Transactions 93 (1): 979-998.

Haberl, J.S., D.E. Claridge, and J.K. Kissock. 2003. Inverse model toolkit: Application and testing. ASHRAE Transactions 109 (2): 435-448.

Haberl, J.S. and S. Thamilseran. 1996. The great energy predictor shootout II: measuring retrofit savings - overview and discussions of results. ASHRAE Transactions 102 (2): 419-435.

Haberl, J.S., and T.E. Bou-Saada. 1998. Procedures for calibrating hourly simulation models to measured building energy and environmental data. Journal of Solar Energy Engineering 120: 193-204.

Haberl, J.S., and S. Thamilseran. 1998. The great energy predictor shootout II: measuring retrofit savings. ASHRAE Journal 40 (1): 49-56.

Hartman, T. 2001. All-variable speed centrifugal chiller plant. ASHRAE Journal 23 (9): 43-53.

Haves, P., T. Salsbury, D. Claridge, and M, Liu. 2001. Use of whole building simulation in on-line performance assessment: modeling and implementation issues. Seventh International IBPSA Conference, Rio de Janeiro, Brazil: 335-342.

Hydeman, M. and K.L.jr. Gillespie. 2002. Tools and techniques to calibrate electric chiller component models. ASHRAE Transactions 108 (1): 733-741.

Hydeman, M., N, Webb, P. Sreedharan, and S. Blanc. 2002. Development and testing of a reformulated regression-based electric chiller model. ASHRAE Transactions 108 (2): 1118-1127.

International, Performance, Measurement and Verification Protocol (IPMVP). 2007. Concepts and options for determining energy and water savings 1. Efficiency valuation organization.

Jacob, D., S. Dietz, S. Komhard, C. Neumann, and S. Herkel. 2010. Black-box models for fault detection and performance monitoring in buildings. Journal of Building Performance Simulation 3 (1): 53-62.

Jarnagin, R.E. 2009. ASHRAE Building EQ. ASHRAE Journal 51 (12): 18-19.

Jiang, W. and T.A. Reddy. 2003. Reevaluation of the Gordon-Ng performance models for water-cooled chillers. ASHRAE Transactions 109 (2): 272-287.

Kammerud, R., K.L.Jr. Gillespie, and M. Hydeman. 1999. Economic uncertainties in chilled water system design. ASHRAE Transactions 105 (2): 1075-1085.

Kaplan, M. and P. Canner. 1992. Guidelines for energy simulation of commercial buildings. Portland: Bonneville Power Administration.

Katipamula, S., M.R. Brambley, N.N. Bauman, and R.G. Pratt. 2003. Enhancing building operations through automated diagnostics: field test results. http://www.buildingsystemsprogram.pnl.gov/fdd/publications/PNNL-39693.pdf (latest access 05/05/2008).

Kissock, J. K., J.S. Haberl, and D.E. Claridge. 2003. Inverse modeling toolkit: Numerical algorithms. ASHRAE Transactions 9 (2): 425-434.

Krarti, M., J.F. Kreider, D. Cohen, and P. Curtis. 1998. Estimation of energy savings for building retrofits using neural networks. Journal of Solar Energy Engineering 120: 211-216.

Kreider, J.F. and J.S. Haberl. 1994. Predicting hourly building energy use: The great energy shootout - overview and discussion of results. ASHRAE Transactions 100 (2): 1104-1118.

Kreider, J.F., and D.E. Claridge, P. Curtis, R. Dodier, J.S. Haberl, and M. Krarti. 1995. Building energy use prediction and system identification using recurrent neural networks. Journal of Solar Engineering 117: 161-166.

Lash, T. 2005. Tapping into remote building intelligence. ASHRAE Journal 47 (3): 62-69.

Lawrence, T. M. and J. E. Braun. 2007. Calibrated simulation for retrofit evaluation of demand-controlled ventilation in small commercial buildings. ASHRAE Transactions 113 (2): 227-240.

Lebrun, J., J.-P. Bourdouxhe, and J. Grodent. 1994. HVAC 1 Toolkit: a toolkit for primary HVAC system energy calculation. ASHRAE, American Society of Heating, Refrigeration and Air-Conditioning Engineers, Inc.

Lee, S.U, F.L. Painter, and D.E. Claridge. 2007. Whole-building commercial HVAC system simulation for use in energy consumption fault detection. ASHRAE Transactions 113 (2): 52-61.

Lee, T.-S., W.-C. Lu. 2010. An evaluation of empirically-based models for predicting energy performance of vapor-compression water chillers. Applied Energy 87: 3486-3493.

Liu, M. and D.E. Claridge. 1998. Use of calibrated HVAC system models to optimize system operation. Journal of solar energy engineering 120: 131-138.

Liu, M., D.E. Claridge, J.S. Haberl, and W.D. Turner. 1997. Improving building energy system performance by continuous commissioning. Proceedings of the Thirty-Second Intersociety Energy Conversion Engineering Conference (Cat. No.97CH36203) 3, IECEC-97: 1606-1612.

Liu, M., D.E. Claridge, and W.D. Turner. 2002. Continuous Commissioning[SM] Guidebook: Maximizing building energy efficiency and comfort. Federal Energy Management Program, U.S. Department of Energy.

Liu, M., D.E. Claridge, and W.D. Turner. 2003a. Continuous Commissioning of building energy systems. Journal of Solar Energy Engineering 25 (3): 275-281.

Lui, M., D. E. Claridge, N. Bensouda, K. Heinemeier, S. Uk Lee, and G. Wei. 2003b. High performance commercial building systems: manual of procedures for calibrating simulations of building systems. Lawrence Berkeley National Laboratory.

Liu, M., L. Song, G. Wei, and D.E. Claridge. 2004. Simplified building and air-handling unit model calibration and application. Journal of solar energy engineering 126, Transactions of the ASME: 601-609.

Liu, M., G. Liu, D.E. Claridge, and J.S. Haberl. 2006. ASHRAE 1092-RP Final Report: Development of procedures to determine in- situ performance of commonly used HVAC systems, ASHRAE.

Liu, G. and M. Liu. 2011. A rapid calibration procedure and case study for simplified simulation models of commonly used HVAC systems. Building and Environment 46: 409-420.

MacArthur, J.W., A. Mathur, and J. Zhao. 1989. On-line recursive estimation for load profile prediction. ASHRAE Transactions 95 (1): 621-628.

Matlab R2008b. 2008. The MathWorks, Inc.

McFarlane, D. 2010. Technical RCx for office. ASHRAE journal 52 (12): 125-128.

McQuiston, F.C., J.D. Parker, and J.D. Spitler. 2005. Heating, ventilation, and air conditioning: analysis and design. 6th ed., John Wiley & Sons, Inc., Hoboken, N.J.

Mills, E. 2011. Building commissioning: a golden opportunity for reducing energy costs and greenhouse gas emissions in the United States. Energy Efficiency 4: 145-173.

Monfet, D. and R. Zmeureanu. 2009a. Évaluation de la performance d'une centrale thermique d'un campus universitaire à Montréal, Proceedings of CIFQ, Lille, France.

Monfet, D. and R. Zmeureanu. 2009b. Simulation of a large central cooling and heating plant using TRNSYS and calibration with monitored data. IBPSA Conference, Glascow, Scottland.

Monfet, D. and Zmeureanu. 2011. Ongoing commissioning approach for a central cooling and heating plant. ASHRAE Transactions 117 (1).

Monfet, D., R. Zmeureanu, R. Charneux, and N. Lemire. 2009. Calibration of a building energy model using measured data. ASHRAE Transactions 115(1): 348-359.

Nall, D. 2009. How Building EQ works. ASHRAE Journal 51 (12): 20.

Natural Resources Canada. 2008. Energy Efficiency Trends in Canada: 1990 to 2005. Office of Energy Efficiency, http://www.oee.nrcan.gc.ca/Publications/statistics/trends07/pdf/trends07.pdf.

Ohlsson, M.B.O., C.O. Peterson, H. Pi, T.S. Rognvaldsson, and B.P.W. Soderberg. 1994. Predicting system loads with artificial networks - Methods and results from "The great energy predictor shootout". ASHRAE Transactions 100 (2): 1063-1074.

PACRAT. 2009. Introduction to PACRAT. Facility Dynamics, http://www.facilitydynamics.com (latest access 05/05/2008).

Pan, Y., Z. Huang, and G. Wu. 2007. Calibrated building energy simulation and its application in a high-rise commercial building in Shanghai. Energy and Buildings 29: 651-657.

Paris B., T. Talbert, J. Eynard, S. Grieu, A. Traoré, and M. Polit. 2009. On-line monitoring station for energy diagnosis in buildings. Proceedings of Building Simulation 2009, IBPSA: 2013-2019.

Pedrini, A., F.S. Westphal, and R. Lamberts. 2002. A methodology for building energy modelling and calibration in warm climates. Building and Environment 37: 903-912.

Priddy, K.L. and P.E. Keller. 2005. Artificial neural networks: an introduction. The International Society for Optical Engineering, Washington.

Reddy, T.A., K.K Andersen, and D. Niebur. 2003a. Information content of incoming data during field monitoring: application to chiller modeling (RP-1139). HVAC&R Research 9 (4): 365-384.

Reddy, T.A., D. Niebur, K.K Andersen, P.P. Pericolo, and G. Cabrera. 2003b. Evaluation of the suitability of different chiller performance models for on-line training applied to automated fault detection and diagnosis (RP-1139). HVAC&R Research 9 (4): 385-414.

Reddy, T.A. 2006. Literature review on calibration of building energy simulations programs: uses, problems, procedures, uncertainty, and tools. ASHRAE Transactions 112 (1): 226-240.

Reddy, T.A., I. Maor, and C. Panjapornpon. 2007a. Calibrating detailed building energy simulation programs with measured data -Part I: General methodology (RP-1051). HVAC&R Research 13 (2): 221-241.

Reddy, T.A., I. Maor, and C. Panjapornpon. 2007b. Calibrating detailed building energy simulation programs with measured data - Part II: Application to three case study office buildings (RP-1051). HVAC&R Research 13 (2): 243-265.

Roth, K., D. Westophalen, J. Brodrick. 2008. Ongoing Commissioning. ASHRAE Journal 50 (3): 66-71.

Roy, A. 2008. Bilan de la consommation d'énergie et des émissions de gaz à effet de serre dans les cégeps et les universités au Québec : 1990 à 2006. Ministère de l'Éducation, du Loisir et du Sport, Gouvernement du Québec.

Santamouris, M., G. Mihalakakou, P. Patargias, N. Gaitani, K. Sfakianaki, M. Papaglastra, C. Pavlou, P. Doukas, E. Primikiri, and V. Geros. 2007. Using intelligent clustering techniques to classify the energy performance of school buildings. Energy and Buildings 39: 45-51.

Santos, J. J., E.L. Brightbill, and L. Lister. Automated diagnostics from DDC data - PACRAT. http://www.facilitydynamics.com/AutomatedDiag.pdf (latest access 05/05/2008).

Saththasivam, J. and K.C. Ng. 2008. Predictive and diagnostic methods for centrifugal chillers. ASHRAE Transactions 114 (1): 282-287.

Seem, J.E. 2005. Pattern recognition algorithm for determining days of the week with similar energy consumption profiles. Energy and Buildings 37: 127-139.

Seem, J.E. 2007. Using intelligent data analysis to detect abnormal energy consumption in buildings. Energy and Buildings 39: 52-58.

Seidl, R. 2006. Trend analysis for commissioning. ASHRAE Journal 48 (1): 34-43.

Seidl, R. 2007. Universal translator. ASHRAE Journal 49 (7): 12-22.

Solati, B., R. Zmeureanu, and F. Haghighat. 2003. Correlation based models for the simulation of energy performance of screw chillers. Energy conversion and management 44: 1903-1920.

Spielvogel, L. G., J.A. Orlando, and P. Hayes. 1977. Feasibility of an energy index for office building. ASHRAE Transactions: 310-321.

StatPoint Technologies, Inc. 2008. STATGRAHICS. Statgraphics centurion XV.

Sud, I. and R.W.Jr. Wiggins. 1983. Development of a simplified graphical procedure for estimating the energy usage in nonresidential buildings. ASHRAE Transactions 89 (2A): 29-48.

Sullivan, R, S. Nozari, R. Johson, and S. Selkowitz. 1985. Commercial building energy performance analysis using multiple regression. ASHRAE Transactions 91 (2): 337-353.

Swider, D.J. 2003. A comparison of empirically based steady-state models for vapor-compression liquid chillers. Applied Thermal Engineering 23: 539-556.

Swider, D.J., M.W. Browne, P.K. Bansal, and V. Kecman. 2001. Modelling of vapour-compression liquid chillers with neural networks. Applied Thermal Engineering 21: 311-329.

Torrens, J.I., K. Marcus, A. Costa, and J. O'Donnell,.2011. Multi-criteria optimisation using part, real time and predictive performance benchmarks. Simulation Modelling Practice and Theory 19: 1258-1265.

TRNSYS. 2006. TRaNsient SYstem Simulation program. Solar Energy Laboratory of the Univ. of Wisconsin-Madison, TRANSSOLAR Energietechnik GmbH,CSTB – Centre Scientifique et Technique du Bâtiment,, TESS – Thermal Energy Systems Specialists.

Walpole, R.E., R.H. MyersS.L. Myser, and K. Ye. 2002. Probability & Statistics for Engineers & Scientists. 7th ed., Prentice Hall, Upper Saddle River, NJ: 730.

Whole-Building Diagnostician (WBD).
http://www.buildingsystemsprogram.pnl.gov/fdd/wbd/index.stm (latest access 22/07/2008).

Wiggins, S. R. 2005. Retrocommissioning. ASHRAE Journal 47 (3): 76-78.

Wulfinghoff, D. R. 1984. Common sense about building energy consumption analysis. ASHRAE Transactions 90 (3): 437-447.

Yan, C. and J. Yao, 2010. Application of ANN for the prediction of building energy consumption at different climate zones with HDD   and CDD. Proceedings of the 2nd International Conference on Future Computer and Communication 3: 286-289.

Yang, J., H. Rivard, and R. Zmeureanu. 2005. On-line building energy prediction using adaptive artificial neural networks. Energy and Buildings 37: 1250-1259.

Yoon, J., E.J. Lee, and D.E. Claridge. 2003. Calibration procedure for energy performance simulation of a commercial building. Journal of Solar Energy Engineering 125: 251-257.

York, D.A., C.C. Cappiello. 1982. DOE-2 Engineers manual. Lawrence Berkley laboratory, National technical services.

# APPENDIX A: Description of monitored data

*Table A.1: Central plant monitored data, general information and cooling*

| Description of Measured Variable | Acronym |
|---|---|
| Outdoor air temperature | $T_{db}$, °C |
| Outdoor air relative humidity | $RH$,% |
| Chilled water flow rate to CSB | $\dot{V}_{CHW}^{CSB}$, gpm |
| CSB chilled water supply temperature | $T_{CHWS}^{CSB}$, °C |
| CSB chilled water return temperature | $T_{CHWR}^{CSB}$, °C |
| CSB chilled water pressure differential | $\Delta P_{CHW}^{CSB}$, psi |
| Chilled water pump P-1, ON/OFF | $P$-$1$ |
| Chilled water pump P-2, ON/OFF | $P$-$2$ |
| Chilled water valve to AD building, ON/OFF | |
| Chiller CH-1 chilled water supply temperature | $T_{CHWS}^{CH-1}$, °C |
| Chiller CH-1 chiller water return temperature | $T_{CHWR}^{CH-1}$, °C |
| Chiller CH-1 condenser water supply temperature | $T_{CNDS}^{CH-1}$, °C |
| Chiller CH-1 condenser water return temperature | $T_{CNDR}^{CH-1}$, °C |
| Chiller CH-1, ON/OFF | $CH$-$1$ |
| Chiller CH-1 percent RLA | $RLA^{CH-1}$, % |
| Chiller CH-1 condenser water pump, ON/OFF | $P$-$3$ |
| Chiller CH-2 chilled water supply temperature | $T_{CHWS}^{CH-2}$, °C |
| Chiller CH-2 chiller water return temperature | $T_{CHWR}^{CH-2}$, °C |
| Chiller CH-2 condenser water supply temperature | $T_{CNDS}^{CH-2}$, °C |
| Chiller CH-2 condenser water return temperature | $T_{CNDRS}^{CH-2}$, °C |
| Chiller CH-2, ON/OFF | $CH$-$2$ |
| Chiller CH-2 percent RLA | $RLA^{CH-2}$, % |
| Chiller CH-2 condenser water pump, ON/OFF | $P$-$4$ |
| Cooling tower CT-1 supply water temperature | $T_{CNDR}^{CT-1}$, °C |
| Cooling tower CT-1 fan ON/OFF | $CT$-$1$ |
| Cooling tower CT-1 fan VFD level | $VFD^{CT-1}$, % |
| Cooling tower CT-2 supply water temperature | $T_{CNDR}^{CT-2}$, °C |
| Cooling tower CT-2 fan ON/OFF | $CT$-$2$ |
| Cooling tower CT-2 fan VFD level | $VFD^{CT-2}$, % |

*Table A.2: Central plant monitored data, heating and heat exchangers*

| Description of Measured Variable | Acronym |
|---|---|
| CSB steam production | $\dot{m}_{steam}$, lb/hr |
| CSB steam pressure | $P_{steam}$, psi |
| CSB condensate temperature | $T_{condensate}$, °C |
| CSB condensate flow | $\dot{V}_{condensate}$, gpm |
| Heating water flow rate to CSB | $\dot{V}_{HW}^{CSB}$, gpm |
| CSB heating water supply temperature | $T_{HWS}^{CSB}$, °C |
| CSB heating water return temperature | $T_{HWR}^{CSB}$, °C |
| CSB heating water pressure differential | $\Delta P_{HW}^{CSB}$, psi |
| CSB heating water return pressure | $P_{HWR}^{CSB}$, psi |
| CSB heating water pump P-7, ON/OFF | *P-7* |
| CSB heating water pump P-7 VFD level | $VFD^{P\text{-}7}$,% |
| CSB heating water pump P-8, ON/OFF | *P-8* |
| CSB heating water pump P-8 VFD level | $VFD^{P\text{-}8}$,% |
| CSB heating water pump P-9, ON/OFF | *P-9* |
| CSB heating water pump P-9 VFD level | $VFD^{P\text{-}9}$,% |
| SOFAM fan VFD level | $VFD^{BE}$,% |
| Heat exchanger HX-1 hot side entering water temperature | $T_1^{HX\text{-}1}$, °C |
| Heat exchanger HX-1 hot side leaving water temperature | $T_2^{HX\text{-}1}$, °C |
| Heat exchanger HX-1 cold side entering water temperature | $T_3^{HX\text{-}1}$, °C |
| Heat exchanger HX-1 cold side entering water temperature | $T_4^{HX\text{-}1}$, °C |
| Heat exchanger HX-1 bypass valve, ON/OFF | |
| Heat exchanger HX-2 steam valve, ON/OFF | |
| Chiller CH-1 valve to heat exchanger HX-3, ON/OFF | |
| Chiller CH-2 valve to heat exchanger HX-3, ON/OFF | |
| Heat exchanger HX-3 hot side pump P-5, ON/OFF | *P-5* |
| Heat exchanger HX-3 cold side pump P-6, ON/OFF | *P-6* |
| Heat exchanger HX-3 cold side entering water temperature | $T_7^{HX\text{-}3}$, °C |
| Heat exchanger HX-3 cold side entering water temperature | $T_8^{HX\text{-}3}$, °C |

# Appendix B: CSB Weekly average operating information for 2009

*Table B.1: Weekly average weather and CSB chilled and heating water monitored data, 2009*

| Item<br>Week | $T_{db}$, °C | RH, % | $\dot{V}_{CHW}^{CSB}$, L/s | $T_{CHWS}^{CSB}$, °C | $T_{CHWR}^{CSB}$, °C | $\dot{V}_{HW}^{CSB}$, L/s | $T_{HWS}^{CSB}$, °C | $T_{HWR}^{CSB}$, °C |
|---|---|---|---|---|---|---|---|---|
| 12/22 – 12/28 | -5.4±6.7 | 49.2±20.2 | OFF | OFF | OFF | 67.0± 7.2 | 42.0±3.2 | 38.0±2.1 |
| 12/29 – 01/04 | -10.0±5.9 | 36.8±11.1 | OFF | OFF | OFF | 81.0± 5.7 | 44.4±3.0 | 39.8±2.1 |
| 01/05 – 01/11 | -9.4±3.9 | 39.6±10.1 | OFF | OFF | OFF | 80.6± 6.7 | 44.5±2.2 | 39.8±2.0 |
| 01/12 – 01/18 | -14.7±7.2 | 41.0± 7.2 | OFF | OFF | OFF | 88.7± 8.1 | 44.9±2.2 | 39.3±1.8 |
| 01/19 – 01/25 | -10.7±4.8 | 43.0± 9.8 | OFF | OFF | OFF | 78.1± 11.7 | 44.8±2.1 | 39.8±1.9 |
| 01/26 – 02/01 | -10.1±4.5 | 44.4±10.5 | OFF | OFF | OFF | 75.1±11.6 | 44.6±2.0 | 39.8±1.9 |
| 02/02 – 02/08 | -7.6±6.7 | 32.6± 7.0 | OFF | OFF | OFF | 74.6±10.2 | 43.4±3.0 | 38.9±2.0 |
| 02/09 – 02/15 | NO DATA | | | | | | | |
| 02/16 – 02/22 | -4.1±3.6 | 43.3±18.0 | OFF | OFF | OFF | 71.1± 9.7 | 40.8±2.0 | 37.2±1.7 |
| 02/23 – 03/01 | -4.8±6.2 | 38.5±13.0 | OFF | OFF | OFF | 69.8±11.6 | 41.5±3.3 | 37.8±2.5 |
| 03/02 – 03/08 | -2.9±7.3 | 36.8±14.0 | OFF | OFF | OFF | 62.0± 8.6 | 40.4±3.9 | 36.9±2.7 |
| 03/09 – 03/15 | -1.2±5.4 | 31.9±10.2 | OFF | OFF | OFF | 66.2±10.5 | 39.9±2.6 | 36.8±1.9 |
| 03/16 – 03/22 | 2.4±5.0 | 26.9± 8.3 | OFF | OFF | OFF | 59.6±10.9 | 38.6±2.3 | 36.1±1.9 |
| 03/23 – 03/29 | 3.8±6.7 | 33.6±18.9 | OFF | OFF | OFF | 55.7±10.3 | 37.3±3.0 | 35.1±2.1 |
| 03/30 – 04/05 | 6.7±4.1 | 50.7±22.1 | OFF | OFF | OFF | 58.6±11.8 | 35.6±2.1 | 33.9±1.8 |
| 04/06 – 04/12 | 3.5±3.1 | 40.3±20.2 | OFF | OFF | OFF | 60.8± 8.6 | 37.6±1.3 | 35.6±1.3 |
| 04/13 – 04/19 | 9.3±5.4 | 22.6± 3.7 | OFF | OFF | OFF | 48.2±12.4 | 35.4±2.1 | 34.0±1.9 |
| 04/20 – 04/26 | 12.1±6.2 | 33.8±18.7 | 81.4± 8.8 | 7.1±0.9 | 10.6±1.5 | 55.4± 7.9 | 33.1±2.3 | 31.7±2.3 |
| 04/27 – 05/03 | 14.5±6.2 | 28.4±16.8 | 81.8± 6.1 | 7.1±0.4 | 11.4±1.5 | 50.4±11.5 | 32.7±3.3 | 31.3±3.6 |
| 05/04 – 05/10 | 14.1±3.9 | 45.1±25.5 | 77.0±12.4 | 7.2±0.8 | 10.3±1.4 | 57.9± 7.6 | 31.3±2.0 | 30.0±2.2 |
| 05/11 – 05/17 | 14.3±4.9 | 28.2±17.6 | 80.5± 8.8 | 7.3±1.1 | 11.0±1.6 | 52.3±10.1 | 32.0±2.6 | 31.0±2.8 |
| 05/18 – 05/24 | 16.6±6.4 | 24.7± 9.3 | 81.9± 4.5 | 7.2±0.7 | 11.1±1.5 | 48.0± 6.2 | 32.5±1.6 | 30.9±1.9 |
| 05/25 – 05/31 | 13.8±3.4 | 47.2±27.3 | 83.3± 5.4 | 7.5±1.5 | 10.4±1.3 | 54.8± 7.2 | 32.0±2.1 | 31.0±2.1 |
| 06/01 – 06/07 | 16.1±5.6 | 29.3±16.7 | 80.1± 6.4 | 8.7±4.3 | 11.6±3.6 | 48.2± 7.1 | 31.6±1.6 | 30.0±1.8 |
| 06/08 – 06/14 | 18.0±4.6 | 46.1±25.9 | 84.7± 8.7 | 8.2±3.2 | 11.8±2.4 | 51.3± 5.8 | 30.8±1.5 | 29.3±2.2 |
| 06/15 – 06/21 | 20.2±4.7 | 49.9±24.8 | 85.8± 7.8 | 7.3±0.6 | 11.3±1.3 | 47.2± 6.3 | 31.1±2.2 | 29.4±.27 |
| **06/22 – 06/28** | **24.1±5.4** | **40.1±23.2** | **94.9±21.6** | **7.2±0.2** | **12.0±1.3** | **40.3± 3.6** | **32.8±1.4** | **30.0±1.0** |
| **06/29 – 07/05** | **20.8±4.1** | **58.3±24.7** | **89.0±15.0** | **7.3±0.5** | **11.6±1.4** | **48.1± 6.9** | **32.1±1.6** | **29.6±1.0** |
| **07/06 – 07/12** | **20.4±4.3** | **46.2±21.5** | **80.9± 4.4** | **7.2±0.4** | **11.1±1.6** | **48.2± 5.1** | **31.1±1.3** | **29.1±1.0** |
| **07/13 – 07/19** | **19.3±4.0** | **43.8±17.9** | **83.7± 5.4** | **7.1±0.5** | **11.5±1.6** | **46.1± 6.4** | **30.9±1.5** | **29.4±1.6** |
| **07/20 – 07/26** | **22.3±4.0** | **45.7±19.1** | **88.2±17.2** | **7.1±0.6** | **12.0±1.5** | **43.3± 6.0** | **32.5±2.1** | **29.9±2.2** |
| **07/27 – 08/02** | **23.8±3.9** | **49.2±22.5** | **109.0±30.3** | **7.1±0.2** | **12.0±1.1** | **44.3± 4.2** | **32.2±1.2** | **29.4±0.9** |
| **08/03 – 08/09** | **21.0±4.1** | **38.5±17.8** | **84.6±17.2** | **7.1±0.2** | **10.9±1.4** | **52.1± 6.5** | **31.0±1.7** | **28.6±1.2** |
| **08/10 – 08/16** | **25.4±4.5** | **47.3±23.2** | **113.5±31.1** | **7.1±0.4** | **12.7±1.3** | **39.6± 4.5** | **33.0±1.5** | **30.0±1.3** |
| **08/17 – 08/23** | **25.1±3.6** | **49.1±19.2** | **119.7±31.7** | **7.1±0.4** | **12.4±1.3** | **39.9± 3.6** | **32.7±1.4** | **29.8±1.0** |
| **08/24 – 08/30** | **18.9±4.5** | **42.7±24.7** | **82.8± 4.7** | **7.2±0.6** | **11.5±1.7** | **50.0± 7.1** | **31.5±1.7** | **29.6±1.6** |
| **08/31 – 09/06** | **19.0±4.8** | **34.1±16.8** | **81.3± 4.5** | **7.2±0.8** | **11.0±1.8** | **49.1± 7.1** | **30.9±1.2** | **29.2±1.1** |
| **09/07 – 09/13** | **19.3±5.0** | **32.3±15.2** | **81.2± 4.3** | **7.1±0.9** | **11.2±1.6** | **46.6± 7.1** | **30.8±1.3** | **29.3±1.2** |
| **09/14 – 09/20** | **14.9±4.0** | **37.8±18.0** | **78.8± 3.9** | **7.3±1.3** | **10.3±1.7** | **52.1± 6.8** | **30.8±1.4** | **29.9±1.7** |
| 09/21 – 09/27 | 18.9±4.7 | 51.1±25.3 | 84.5± 2.5 | 7.1±0.4 | 12.7±1.4 | Data loss | 30.9±1.5 | 29.5±0.9 |
| 09/28 – 10/04 | 11.2±3.7 | 60.4±20.8 | 83.3± 3.4 | 7.5±1.8 | 11.3±1.7 | 60.2± 8.4 | 31.9±2.1 | 31.4±1.8 |
| 10/05 – 10/11 | 11.1±2.2 | 53.5±21.7 | OFF | OFF | OFF | 64.2± 8.9 | 32.0±1.5 | 31.2±1.3 |
| 10/12 – 10/18 | 4.5±3.4 | 34.5±13.3 | OFF | OFF | OFF | 66.5±15.0 | 35.5±3.2 | 33.5±2.7 |
| 10/19 – 10/25 | 7.2±4.2 | 45.8±21.7 | OFF | OFF | OFF | 60.1± 5.8 | 34.9±2.6 | 33.4±2.3 |
| 10/26 – 11/01 | 8.3±3.1 | 43.5±15.0 | OFF | OFF | OFF | 59.0± 8.4 | 34.1±1.9 | 32.6±1.5 |
| 11/02 – 11/08 | 5.1±3.8 | 35.9±12.2 | OFF | OFF | OFF | 60.3± 9.2 | 35.8±2.1 | 33.8±1.5 |
| 11/09 – 11/15 | 7.8±4.2 | 41.7±24.7 | OFF | OFF | OFF | 60.7±11.5 | 34.8±2.6 | 33.2±2.4 |
| 11/16 – 11/22 | 5.6±2.9 | 44.6±16.6 | OFF | OFF | OFF | 63.3± 8.6 | 35.7±1.9 | 33.6±1.6 |
| 11/23 – 11/29 | 5.7±2.4 | 56.8±17.6 | OFF | OFF | OFF | 63.6± 7.4 | 35.7±1.5 | 33.9±1.4 |
| 11/30 – 12/06 | 2.5±2.7 | 49.5±18.0 | OFF | OFF | OFF | 65.0±10.7 | 37.4±1.8 | 35.2±1.6 |
| 12/07 – 12/13 | -3.6±2.6 | 43.7±17.8 | OFF | OFF | OFF | 73.3± 8.0 | 40.3±2.5 | 37.0±2.2 |
| 12/14 – 12/20 | -9.1±6.1 | 43.6±17.3 | OFF | OFF | OFF | 85.3± 7.9 | 43.3±3.3 | 39.1±2.5 |
| 12/21 – 12/27 | -4.7±5.1 | 52.2±16.2 | OFF | OFF | OFF | 68.1± 4.0 | 41.2±3.1 | 37.6±2.2 |
| 12/28 – 01/03 | -6.7±5.3 | 53.3±12.7 | OFF | OFF | OFF | 73.3± 6.9 | 42.1±2.9 | 38.2±2.1 |

Table B.2: Weekly average monitored data for steam system and heat exchangers, 2009

| Item / Week | $\dot{m}_{steam}$, kg/s | $T_{condensate}$, °C | $T_1^{HX-1}$, °C | $T_2^{HX-1}$, °C | $T_3^{HX-1}$, °C | $T_4^{HX-1}$, °C | $T_7^{HX-3}$, °C | $T_8^{HX-3}$, °C |
|---|---|---|---|---|---|---|---|---|
| 12/22 – 12/28 | 56.6±15.5 | 98.5±13.1 | 45.7±5.0 | 39.3±2.4 | 37.9±2.1 | 41.3±3.0 | OFF | OFF |
| 12/29 – 01/04 | 48.6± 9.1 | 101.6± 4.6 | 50.2±4.4 | 41.4±2.2 | 39.7±2.0 | 44.0±2.7 | OFF | OFF |
| 01/05 – 01/11 | 54.3± 8.3 | 101.2± 5.0 | 49.7±3.3 | 41.4±1.9 | 39.7±2.0 | 44.1±2.1 | OFF | OFF |
| 01/12 – 01/18 | 44.2±12.7 | 93.0±14.5 | 51.3±3.7 | 40.9±1.7 | 39.1±1.8 | 44.0±1.9 | OFF | OFF |
| 01/19 – 01/25 | 48.3±12.2 | 101.3± 4.2 | 50.5±3.5 | 41.4±1.9 | 39.6±1.9 | 44.4±2.0 | OFF | OFF |
| 01/26 – 02/01 | 56.8±10.6 | 101.3± 4.6 | 49.9±3.3 | 41.4±1.8 | 39.7±1.9 | 44.1±1.9 | OFF | OFF |
| 02/02 – 02/08 | 53.4±11.6 | 101.3± 4.8 | 48.4±4.8 | 40.5±2.2 | 38.8±2.0 | 43.0±2.9 | OFF | OFF |
| 02/09 – 02/15 | NO DATA | | | | | | | |
| 02/16 – 02/22 | 55.1±11.2 | 101.3± 5.0 | 44.0±3.5 | 38.6±1.7 | 37.1±1.7 | 40.5±1.9 | OFF | OFF |
| 02/23 – 03/01 | 54.6±11.5 | 101.0± 6.4 | 45.1±5.1 | 39.1±2.7 | 37.7±2.5 | 41.1±3.2 | OFF | OFF |
| 03/02 – 03/08 | 59.1±16.3 | 100.7± 6.3 | 43.8±5.9 | 38.2±2.9 | 36.8±2.6 | 40.1±3.7 | OFF | OFF |
| 03/09 – 03/15 | 51.8±11.7 | 100.5± 7.1 | 42.4±3.9 | 37.9±2.0 | 36.6±1.8 | 39.5±2.5 | OFF | OFF |
| 03/16 – 03/22 | 52.5±12.7 | 101.8± 3.0 | 40.2±2.8 | 37.2±1.8 | 35.9±1.8 | 38.4±2.2 | OFF | OFF |
| 03/23 – 03/29 | 60.1±15.3 | 101.5± 4.2 | 39.0±4.0 | 36.2±2.3 | 35.1±2.1 | 37.3±2.8 | OFF | OFF |
| 03/30 – 04/05 | 68.6±13.4 | 101.8± 2.4 | 36.4±2.3 | 34.8±1.9 | 34.0±1.7 | 35.5±2.0 | OFF | OFF |
| 04/06 – 04/12 | 52.1±12.5 | 101.9± 2.6 | 38.6±1.6 | 36.3±1.2 | 35.5±1.3 | 37.4±1.3 | OFF | OFF |
| 04/13 – 04/19 | 55.1±14.6 | 102.1± 2.4 | 36.3±2.3 | 34.5±1.8 | 33.9±1.8 | 35.3±2.0 | OFF | OFF |
| 04/20 – 04/26 | 70.6±16.5 | 102.1± 3.3 | 34.4±2.2 | 33.0±2.2 | 32.2±2.2 | 33.6±2.3 | 30.0±1.5 | 30.8±1.8 |
| 04/27 – 05/03 | 72.4±15.9 | 102.2± 2.2 | 33.3±2.3 | 32.0±2.1 | 31.5±2.1 | 32.5±2.2 | 30.6±1.3 | 31.7±1.4 |
| 05/04 – 05/10 | 80.2±13.9 | 101.8± 3.4 | 31.8±1.7 | 30.7±1.6 | 30.3±1.5 | 31.1±1.6 | 29.5±0.9 | 30.4±1.1 |
| 05/11 – 05/17 | 68.1±18.0 | 102.0± 2.6 | 32.7±2.3 | 31.3±2.0 | 31.0±1.9 | 31.9±2.1 | 29.9±1.5 | 30.9±1.5 |
| 05/18 – 05/24 | 75.3±15.9 | 102.0± 3.0 | 32.9±1.8 | 31.7±1.6 | 31.5±1.5 | 32.3±1.8 | 30.6±1.1 | 31.5±1.2 |
| 05/25 – 05/31 | 69.1±21.7 | 99.3±10.5 | 32.4±1.9 | 31.2±1.8 | 30.8±1.7 | 31.7±1.9 | 30.1±1.0 | 30.9±1.2 |
| 06/01 – 06/07 | 79.9±11.4 | 102.0± 2.6 | 32.0±1.8 | 30.8±1.7 | 30.2±1.8 | 31.4±1.7 | 30.5±1.0 | 31.0±1.1 |
| 06/08 – 06/14 | 86.2± 6.2 | 102.0± 2.1 | 30.8±1.1 | 29.4±1.3 | 28.6±1.6 | 30.1±1.1 | 27.7±0.3 | 27.8±0.4 |
| 06/15 – 06/21 | 87.9± 2.5 | 101.4± 1.5 | 31.0±1.4 | 29.3±1.8 | 28.8±2.2 | 30.1±1.6 | 30.8±1.7 | 31.5±1.9 |
| **06/22 – 06/28** | **87.8± 2.0** | **101.2± 1.3** | **33.2±1.3** | **32.2±1.3** | **32.2±1.4** | **32.5±1.3** | **31.6±1.4** | **32.6±1.5** |
| **06/29 – 07/05** | **84.4± 2.4** | **101.2± 1.5** | **31.9±2.0** | **30.9±2.0** | **31.0±2.0** | **31.2±1.9** | **31.2±1.3** | **32.2±1.5** |
| **07/06 – 07/12** | **84.4± 2.8** | **101.4± 1.6** | **30.8±0.9** | **29.7±0.9** | **29.9±1.0** | **30.2±0.9** | **30.4±1.2** | **31.4±1.4** |
| **07/13 – 07/19** | **84.7± 2.4** | **101.2± 1.3** | **30.3±0.6** | **29.2±0.7** | **29.1±0.8** | **29.7±0.6** | **30.2±1.7** | **31.6±1.3** |
| **07/20 – 07/26** | **88.3± 4.2** | **101.3± 1.4** | **32.5±2.5** | **31.5±2.5** | **31.6±2.5** | **31.8±2.4** | **31.2±1.3** | **32.3±1.5** |
| **07/27 – 08/02** | **89.5± 1.9** | **101.3± 0.9** | **32.9±0.9** | **31.9±0.9** | **32.1±0.9** | **32.2±0.9** | **31.1±1.1** | **32.1±1.2** |
| **08/03 – 08/09** | **89.5± 3.6** | **101.2± 2.6** | **30.7±1.5** | **29.7±1.5** | **29.7±1.6** | **30.0±1.5** | **29.9±1.6** | **31.1±1.3** |
| **08/10 – 08/16** | **89.6± 2.9** | **101.4± 1.0** | **33.6±1.5** | **32.6±1.5** | **32.6±1.5** | **32.8±1.4** | **31.9±1.5** | **32.9±1.6** |
| **08/17 – 08/23** | **89.6± 2.6** | **101.3± 0.9** | **32.8±1.2** | **31.8±1. 2** | **32.1±1.2** | **32.2±1.2** | **31.7±1.4** | **32.7±1.4** |
| **08/24 – 08/30** | **89.3± 3.6** | **101.5± 0.9** | **30.7±1.0** | **29.7±1.0** | **29.8±1.0** | **30.2±1.0** | **30.9±1.6** | **31.9±1.7** |
| **08/31 – 09/06** | **89.3± 3.9** | **101.6± 1.0** | **30.6±0.8** | **29.5±0.7** | **29.5±0.7** | **30.1±0.8** | **30.4±1.2** | **31.5±1.5** |
| **09/07 – 09/13** | **82.8±20.5** | **97.1±14.9** | **30.4±0.8** | **29.4±0.7** | **29.4±0.7** | **29.9±0.7** | **30.1±1.1** | **31.1±1.2** |
| **09/14 – 09/20** | **87.7±18.4** | **96.7±17.4** | **31.4±1.6** | **30.2±1.3** | **30.3±1.4** | **30.9±1.6** | **29.5±1.2** | **30.4±1.3** |
| 09/21 – 09/27 | 97.6± 3.6 | 101.5± 0.9 | 31.2±1.1 | 30.0±1.1 | 30.2±1.2 | 30.8±1.4 | 31.1±1.2 | 32. 4±1.4 |
| 09/28 – 10/04 | 91.8±16.5 | 100.6± 3.6 | 33.4±2.3 | 31.9±1.9 | 31.6±1.8 | 32.5±2.3 | OFF | OFF |
| 10/05 – 10/11 | 87.1±14.3 | 101.3± 1.7 | 32.7±1.8 | 31.5±1.5 | 31.1±1.4 | 32.0±1.6 | OFF | OFF |
| 10/12 – 10/18 | 79.6±10.6 | 101.7± 1.8 | 37.3±3.4 | 34.6±2.6 | 33.7±2.4 | 35.6±2.8 | OFF | OFF |
| 10/19 – 10/25 | 82.4± 6.7 | 101.5± 2.1 | 35.7±3.0 | 34.1±2.5 | 33.4±2.4 | 34.8±2.7 | OFF | OFF |
| 10/26 – 11/01 | 84.3± 8.3 | 101.5± 1.7 | 34.8±2.0 | 33.4±1.7 | 32.7±1.5 | 34.1±1.8 | OFF | OFF |
| 11/02 – 11/08 | 80.4± 8.0 | 101.6± 2.1 | 37.2±2.6 | 34.8±1.6 | 33.9±1.4 | 35.9±1.8 | OFF | OFF |
| 11/09 – 11/15 | 82.1± 6.8 | 101.8± 1.5 | 36.0±2.8 | 33.8±1.8 | 33.0±1.7 | 34.7±2.1 | OFF | OFF |
| 11/16 – 11/22 | 75.8±11.5 | 101.7± 3.3 | 36.6±2.3 | 34.5±1.6 | 33.5±1.5 | 35.5±1.9 | OFF | OFF |
| 11/23 – 11/29 | 74.9±12.7 | 101.8± 2.0 | 36.5±1.8 | 34.8±1.3 | 33.8±1.4 | 35.6±1.5 | OFF | OFF |
| 11/30 – 12/06 | 60.2±16.2 | 101.0± 4.6 | 38.5±2.0 | 36.2±1.5 | 35.1±1.5 | 37.2±1.7 | OFF | OFF |
| 12/07 – 12/13 | 58.4±13.3 | 98.9±11.2 | 43.0±3.4 | 38.2±2.3 | 36.9±2.2 | 39.8±2.6 | OFF | OFF |
| 12/14 – 12/20 | 49.8±11.0 | 101.0± 5.8 | 48.1±5.5 | 40.6±2.6 | 39.0±2.5 | 42.9±3.1 | OFF | OFF |
| 12/21 – 12/27 | 50.6± 8.9 | 101.2± 5.5 | 44.4±5.1 | 38.9±2.4 | 37.5±2.2 | 40.8±3.0 | OFF | OFF |
| 12/28 – 01/03 | 47.2± 5.6 | 100.9± 5.6 | 45.9±4.9 | 39.5±2.2 | 38.1±2.1 | 41.7±2.8 | OFF | OFF |

Table B.3: Weekly average monitored data for chillers, 2009

| Item / Week | $T_{CHWS}^{CH-1}$, °C | $T_{CHWR}^{CH-1}$, °C | $T_{CNDS}^{CH-1}$, °C | $T_{CNDR}^{CH-1}$, °C | $T_{CHWS}^{CH-2}$, °C | $T_{CHWR}^{CH-2}$, °C | $T_{CNDS}^{CH-2}$, °C | $T_{CNDR}^{CH-2}$, °C |
|---|---|---|---|---|---|---|---|---|
| 12/22 – 04/19 | OFF | OFF | OFF | OFF | OFF | OFF | OFF | OFF |
| 04/20 – 04/26 | 6.8±0.6 | 10.3±1.5 | 32.1±2.0 | 28.2±1.3 | OFF | OFF | OFF | OFF |
| 04/27 – 05/03 | 6.9±1.2 | 11.1±1.6 | 32.7±2.3 | 28.1±1.2 | OFF | OFF | OFF | OFF |
| 05/04 – 05/10 | 6.8±0.9 | 10.0±1.5 | 31.6±1.7 | 28.3±0.7 | OFF | OFF | OFF | OFF |
| 05/11 – 05/17 | 7.0±1.1 | 10.7±1.5 | 32.1±2.2 | 28.1±1.1 | OFF | OFF | OFF | OFF |
| 05/18 – 05/24 | 6.8±0.8 | 10.7±1.4 | 32.4±1.8 | 28.2±0.8 | OFF | OFF | OFF | OFF |
| 05/25 – 05/31 | OFF | OFF | OFF | OFF | 6.9±1.0 | 10.1±1.3 | 31.7±2.6 | 28.2±1.8 |
| 06/01 – 06/07 | 6.7±0.1 | 10.3±1.7 | 32.0±1.8 | 28.3±0.6 | 6.7±0.1 | 9.8±1.6 | 31.6±1.5 | 28.4±0.8 |
| 06/08 – 06/14 | 6.7±0.3 | 11.4±1.7 | 33.3±1.9 | 28.2±0.4 | 6.7±0.1 | 10.4±1.3 | 32.4±1.4 | 28.4±0.5 |
| 06/15 – 06/21 | 7.9±2.0 | 10.4±1.5 | 29.7±1.4 | 28.1±0.6 | 6.7±0.1 | 10.8±1.3 | 33.1±1.5 | 28.6±0.4 |
| **06/22 – 06/28** | **6.7±0.1** | **11.6±0.9** | **33.2±0.9** | **28.4±0.4** | **6.7±0.1** | **11.5±1.3** | **33.9±1.6** | **28.6±0.3** |
| **06/29 – 07/05** | **6.7±0.1** | **11.4±0.7** | **33.1±0.6** | **28.4±0.3** | **6.7±0.1** | **11.2±1.5** | **33.5±1.8** | **28.5±0.4** |
| **07/06 – 07/12** | **6.8±0.6** | **10.9±1.6** | **32.8±1.8** | **28.3±0.5** | **6.7±0.1** | **9.7±1.0** | **31.8±1.3** | **28.5±0.7** |
| **07/13 – 07/19** | **6.8±0.5** | **10.8±1.5** | **32.9±1.7** | **28.3±0.4** | **7.0±0.9** | **12.7±1.6** | **35.2±1.8** | **28.6±0.2** |
| **07/20 – 07/26** | **6.7±0.5** | **11.6±1.5** | **33.7±1.8** | **28.3±0.4** | **6.8±0.3** | **11.4±0.5** | **33.0±0.5** | **28.5±0.1** |
| **07/27 – 08/02** | **6.7±0.2** | **11.5±1.1** | **33.5±1.3** | **28.4±0.3** | **6.7±0.2** | **11.2±0.7** | **32.8±0.8** | **28.5±0.1** |
| **08/03 – 08/09** | **6.7±0.2** | **10.5±1.4** | **32.5±1.7** | **28.3±0.5** | **6.9±1.2** | **11.8±0.9** | **33.4±0.9** | **28.5±0.2** |
| **08/10 – 08/16** | **6.8±0.4** | **12.3±1.3** | **34.3±1.7** | **28.4±0.2** | **6.7±0.1** | **11.3±0.8** | **33.1±0.9** | **28.5±0.1** |
| **08/17 – 08/23** | **6.7±0.4** | **11.9±1.3** | **34.0±1.6** | **28.4±0.2** | **6.7±0.1** | **11.5±1.0** | **33.3±1.2** | **28.5±0.1** |
| **08/24 – 08/30** | **6.7±0.1** | **11.9±1.6** | **34.2±1.8** | **28.4±0.3** | **6.7±0.1** | **9.7±1.0** | **32.1±1.4** | **28.6±0.7** |
| **08/31 – 09/06** | **6.7±0.1** | **10.8±1.6** | **32.8±1.9** | **28.3±0.5** | **6.7±0.1** | **9.0±1.2** | **31.0±1.6** | **28.4±0.7** |
| **09/07 – 09/13** | **6.7±0.1** | **10.7±1.4** | **32.7±1.7** | **28.3±0.6** | **OFF** | **OFF** | **OFF** | **OFF** |
| **09/14 – 09/20** | **6.8±0.2** | **9.7±1.2** | **31.4±1.4** | **28.2±0.7** | **OFF** | **OFF** | **OFF** | **OFF** |
| 09/21 – 09/27 | 6.7±0.1 | 12.1±0.1 | 34.3±1.6 | 28.3±0.4 | OFF | OFF | OFF | OFF |
| 09/28 – 10/04 | 7.2±1.6 | 7.2±1.6 | 32.2±2.1 | 28.1±1.6 | OFF | OFF | OFF | OFF |
| 10/05 – 01/03 | OFF | OFF | OFF | OFF | OFF | OFF | OFF | OFF |

Table B.4: Weekly average energy use and peak loads for cooling systems, 2009

| Item / Week | $Q_{HW}^{CSB}$, MJ/week (Peak, kW) | $Q_{CHW}^{CSB}$, MJ/week (Peak, kW) | $Q_{CHW}$, MJ/week (Peak, kW) | $Q_{rec.}$, MJ/week (Peak, kW) | $Q_{reject.}$, MJ/week (Peak, kW) |
|---|---|---|---|---|---|
| 12/22 – 04/19 | Table B.5 | OFF | OFF | OFF | OFF |
| 04/20 – 04/26 | 200,730 (1225) | 147,580 (2210) | 142,935 (2145) | 33,710 (875) | 198,385 (3110) |
| 04/27 – 05/03 | 193,630 (1250) | 224,145 (2590) | 229,335 (2650) | 70,460 (960) | 311,545 (4025) |
| 05/04 – 05/10 | 170,910 (960) | 176,410 (2290) | 188,565 (2305) | 66,905 (715) | 255,450 (3640) |
| 05/11 – 05/17 | 156,685 (910) | 126,805 (2640) | 128,560 (2545) | 35,000 (1065) | 171,750 (3670) |
| 05/18 – 05/24 | 206,090 (895) | 327,300 (2450) | 334,065 (2445) | 87,510 (655) | 456,655 (3510) |
| 05/25 – 05/31 | 127,210 (1350) | 55,155 (2380) | 58,675 (2570) | 17,615 (640) | 80,785 (3670) |
| 06/01 – 06/07 | 210,020 (890) | 299,745 (2700) | 318,940 (4930) | 18,810 (655) | 424,700 (3895) |
| 06/08 – 06/14 | 170,280 (690) | 473,430 (3095) | 414,100 (7495) | 2,775 (620) | 566,510 (3640) |
| 06/15 – 06/21 | 217,460 (890) | 596,310 (2565) | 617,970 (5115) | 68,075 (695) | 813,880 (3745) |
| **06/22 – 06/28** | **288,205 (745)** | **1,128,045 (4040)** | **1,167,940 (5700)** | **247,440 (620)** | **1,622,905 (5655)** |
| **06/29 – 07/05** | **265,760 (700)** | **904,645 (3825)** | **931,660 (5680)** | **238,305 (720)** | **1,310,205 (5195)** |
| **07/06 – 07/12** | **255,065 (1080)** | **618,710 (2495)** | **642,840 (3695)** | **167,875 (835)** | **887,130 (3925)** |
| **07/13 – 07/19** | **201,420 (885)** | **540,615 (2795)** | **530,860 (2650)** | **183,180 (3130)** | **752,940 (4405)** |
| **07/20 – 07/26** | **271,800 (720)** | **1,015,630 (3770)** | **1,033,670 (4285)** | **255,910 (695)** | **1,442,815 (4740)** |
| **07/27 – 08/02** | **295,250 (775)** | **1,334,140 (4150)** | **1,456,150 (4640)** | **277,075 (680)** | **1,907,415 (6270)** |
| **08/03 – 08/09** | **276,530 (840)** | **807,425 (3850)** | **853,890 (4320)** | **291,115 (3735)** | **1,163,270 (5830)** |
| **08/10 – 08/16** | **291,315 (735)** | **1,552,375 (4290)** | **1,644,365 (4610)** | **282,215 (830)** | **2,207,210 (6290)** |
| **08/17 – 08/23** | **277,600 (620)** | **1,585,695 (4925)** | **1,743,140 (5575)** | **261,555 (815)** | **2,287,830 (7870)** |
| **08/24 – 08/30** | **197,965 (685)** | **567,030 (2701)** | **583,875 (2710)** | **170,815 (730)** | **835,030 (4025)** |
| **08/31 – 09/06** | **199,090 (655)** | **488,290 (2515)** | **490,055 (2585)** | **124,120 (915)** | **691,485 (4000)** |
| **09/07 – 09/13** | **171,160 (745)** | **448,060 (2590)** | **451,155 (2565)** | **88,170 (680)** | **633,500 (3920)** |
| **09/14 – 09/20** | **112,250 (770)** | **137,160 (2345)** | **138,080 (2570)** | **32,920 (710)** | **187,495 (3875)** |
| 09/21 – 09/27 | 61,140 (630) | 217,720 (2845) | 222,710 (2705) | 64,660 (745) | 314,095 (4000) |
| 09/28 – 10/04 | 105,665 (730) | 23,530 (2405) | 23,410 (2345) | OFF | 34,020 (3695) |
| 10/05 – 01/03 | Table B.5 | OFF | OFF | OFF | OFF |

202

*Table B.5: Weekly average energy use and peak loads for heating systems, 2009*

| Item / Week | $Q_{HW}^{CSB}$, MJ/week (Peak, kW) | $Q_{BE}$, MJ/week (Peak, kW) | $Q_{HX-1}$, MJ/week (Peak, kW) | $Q_{HX-2}$, MJ/week (Peak, kW) |
|---|---|---|---|---|
| 12/22 – 12/28 | 843,480 (3325) | 619,455 (2240) | 701,970 (2365) | 168,495 (3015) |
| 12/29 – 01/04 | 1,161,245 (4135) | 852,555 (2080) | 1,067,820 (3570) | 114,925 (1260) |
| 01/05 – 01/11 | 1,067,430 (3785) | 801,475 (1920) | 985,795 (3120) | 94,885 (1790) |
| 01/12 – 01/18 | 1,474,165 (8630) | 1,005,945 (2560) | 1,245,745 (3835) | 242,405 (4795) |
| 01/19 – 01/25 | 959,250 (5315) | 877,165 (2560) | 891,090 (4630) | 84,050 (2700) |
| 01/26 – 02/01 | 1,220,740 (4450) | 820,180 (2080) | 1,116,205 (3880) | 122,000 (2090) |
| 02/02 – 02/08 | 1,026,600 (4100) | 763,630 (2240) | 946,965 (3980) | 103,940 (2030) |
| 02/09 – 02/15 | NO DATA | | | |
| 02/16 – 02/22 | 726,040 (3305) | 525,780 (1920) | 677,055 (3330) | 69,380 (1835) |
| 02/23 – 03/01 | 825,515 (3790) | 577,295 (2080) | 753,725 (3450) | 84,500 (1890) |
| 03/02 – 03/08 | 665,580 (2985) | 520,455 (1920) | 613,170 (2530) | 65,320 (1200) |
| 03/09 – 03/15 | 494,950 (3160) | 422,320 (1920) | 457,895 (2100) | 53,510 (1255) |
| 03/16 – 03/22 | 359,495 (1595) | 287,495 (1280) | 335,860 (1915) | 37,845 (655) |
| 03/23 – 03/29 | 305,950 (2805) | 250,515 (1760) | 277,835 (2060) | 38,620 (1240) |
| 03/30 – 04/05 | 237,775 (2085) | 150,800 (1280) | 220,000 (1600) | 29,880 (1200) |
| 04/06 – 04/12 | 242,680 (1340) | 167,200 (1120) | 222,705 (1380) | 29,250 (995) |
| 04/13 – 04/19 | 182,740 (1170) | 149,645 (960) | 165,015 (1075) | 28,930 (455) |
| 04/20 – 04/26 | 200,730 (1225) | 99,285 (800) | 146,235 (980) | 31,880 (765) |
| 04/27 – 05/03 | 193,630 (1250) | 61,300 (800) | 82,405 (1185) | 49,625 (915) |
| 05/04 – 05/10 | 170,910 (960) | 62,734 (800) | 73,605 (950) | 38,690 (650) |
| 05/11 – 05/17 | 156,685 (910) | 67,340 (800) | 79,345 (850) | 47,280 (815) |
| 05/18 – 05/24 | 206,090 (895) | 63,455 (800) | 74,255 (785) | 48,200 (700) |
| 05/25 – 05/31 | 127,210 (1350) | 75,255 (960) | 82,570 (1215) | 33,180 (660) |
| 06/01 – 06/07 | 210,020 (890) | 89,500 (960) | 121,755 (745) | 74,015 (695) |
| 06/08 – 06/14 | 170,280 (690) | 88,495 (800) | 139,755 (630) | 31,325 (565) |
| 06/15 – 06/21 | 217,460 (890) | 108,350 (800) | 113,940 (905) | 37,795 (605) |
| **06/22 – 06/28** | **288,205 (745)** | 28,490 (160) | 8,685 (160) | 34,810 (360) |
| **06/29 – 07/05** | **265,760 (700)** | 20,435 (160) | 6,810 (250) | 26,275 (460) |
| **07/06 – 07/12** | **255,065 (1080)** | 26,620 (320) | 10,840 (490) | 81,460 (1035) |
| **07/13 – 07/19** | **201,420 (885)** | 36,115 (480) | 29,345 (550) | 44,540 (885) |
| **07/20 – 07/26** | **271,800 (720)** | 9,640 (160) | 2,460 (215) | 21,825 (395) |
| **07/27 – 08/02** | **295,250 (775)** | 8,635 (160) | 810 (60) | 22,245 (435) |
| **08/03 – 08/09** | **276,530 (840)** | 17,700 (480) | 8,025 (420) | 28,185 (410) |
| **08/10 – 08/16** | **291,315 (735)** | 5,610 (160) | 1,045 (365) | 15,365 (510) |
| **08/17 – 08/23** | **277,600 (620)** | 5,180 (160) | 375 (50) | 20,004 (245) |
| **08/24 – 08/30** | **197,965 (685)** | 28,345 (480) | 16,420 (465) | 20,150 (400) |
| **08/31 – 09/06** | **199,090 (655)** | 35,685 (800) | 26,215 (560) | 57,550 (565) |
| **09/07 – 09/13** | **171,160 (745)** | 34,390 (480) | 19,675 (535) | 68,545 (745) |
| **09/14 – 09/20** | **112,250 (770)** | 60,145 (800) | 46,005 (560) | 42,235 (530) |
| 09/21 – 09/27 | 61,140 (630) | 4,460 (800) | 3,260 (440) | 3,945 (350) |
| 09/28 – 10/04 | 105,665 (730) | 91,085 (800) | 91,410 (1595) | 22,445 (685) |
| 10/05 – 10/11 | 153,805 (860) | 99,860 (800) | 127,040 (870) | 36,525 (585) |
| 10/12 – 10/18 | 354,190 (1665) | 237,710 (1280) | 321,275 (1450) | 46,680 (1145) |
| 10/19 – 10/25 | 231,820 (2525) | 131,375 (1440) | 200,805 (2390) | 42,395 (620) |
| 10/26 – 11/01 | 207,485 (1070) | 122,020 (800) | 182,795 (985) | 32,355 (700) |
| 11/02 – 11/08 | 306,735 (1430) | 214,830 (1280) | 286,465 (1395) | 36,220 (1210) |
| 11/09 – 11/15 | 257,555 (1585) | 171,665 (1440) | 232,770 (2170) | 39,985 (960) |
| 11/16 – 11/22 | 316,625 (1880) | 202,745 (1760) | 295,665 (1660) | 35,115 (1225) |
| 11/23 – 11/29 | 288,515 (1450) | 168,930 (960) | 267,395 (1195) | 31,220 (635) |
| 11/30 – 12/06 | 326,665 (1830) | 221,735 (1920) | 305,170 (1785) | 33,650 (1000) |
| 12/07 – 12/13 | 744,545 (3335) | 461,030 (1600) | 640,285 (3175) | 118,680 (1860) |
| 12/14 – 12/20 | 989,565 (3920) | 730,250 (2080) | 902,460 (3465) | 99,930 (2310) |
| 12/21 – 12/27 | 931,805 (4320) | 537,580 (2080) | 849,500 (3620) | 93,310 (2185) |
| 12/28 – 01/03 | 992,415 (4260) | 618,735 (1920) | 905,300 (3470) | 98,820 (1655) |

*Table B.6: Weekly average central plant electricity consumption, 2009*

| Item / Week | $E_{CH}$, kWh/week | $E_{CT}$, kWh/week | $E_{pumps}$, kWh/week | $E_{elec}$, kWh/week |
|---|---|---|---|---|
| 12/22 – 12/28 | 0 | 0 | 12,090 | 12,090 |
| 12/29 – 01/04 | 0 | 0 | 19,390 | 19,390 |
| 01/05 – 01/11 | 0 | 0 | 16,575 | 16,575 |
| 01/12 – 01/18 | 0 | 0 | 19,060 | 19,060 |
| 01/19 – 01/25 | 0 | 0 | 13,865 | 13,865 |
| 01/26 – 02/01 | 0 | 0 | 17,555 | 17,555 |
| 02/02 – 02/08 | 0 | 0 | 16,065 | 16,065 |
| 02/09 – 02/15 | 0 | 0 | NO DATA | NO DATA |
| 02/16 – 02/22 | 0 | 0 | 13,060 | 13,060 |
| 02/23 – 03/01 | 0 | 0 | 14,630 | 14,630 |
| 03/02 – 03/08 | 0 | 0 | 11,265 | 11,265 |
| 03/09 – 03/15 | 0 | 0 | 9,230 | 9,230 |
| 03/16 – 03/22 | 0 | 0 | 7,955 | 7,955 |
| 03/23 – 03/29 | 0 | 0 | 7,605 | 7,605 |
| 03/30 – 04/05 | 0 | 0 | 8,075 | 8,075 |
| 04/06 – 04/12 | 0 | 0 | 8,210 | 8,210 |
| 04/13 – 04/19 | 0 | 0 | 6,415 | 6,415 |
| 04/20 – 04/26 | 8,045 | 60 | 13,635 | 21,740 |
| 04/27 – 05/03 | 12,115 | 100 | 11,485 | 23,700 |
| 05/04 – 05/10 | 10,240 | 50 | 13,000 | 23,290 |
| 05/11 – 05/17 | 6,855 | 40 | 9,950 | 16,845 |
| 05/18 – 05/24 | 17,760 | 130 | 15,220 | 33,110 |
| 05/25 – 05/31 | 3,290 | 25 | 8,820 | 12,135 |
| 06/01 – 06/07 | 17,450 | 125 | 18,735 | 36,310 |
| 06/08 – 06/14 | 21,925 | 430 | 21,810 | 44,165 |
| 06/15 – 06/21 | 33,410 | 625 | 24,555 | 58,590 |
| **06/22 – 06/28** | **61,255** | **1,595** | **38,120** | **100,970** |
| **06/29 – 07/05** | **49,895** | **930** | **34,645** | **85,470** |
| **07/06 – 07/12** | **34,505** | **390** | **28,915** | **63,810** |
| **07/13 – 07/19** | **28,980** | **565** | **23,125** | **52,670** |
| **07/20 – 07/26** | **53,930** | **1,090** | **34,835** | **89,855** |
| **07/27 – 08/02** | **71,835** | **1,810** | **45,495** | **119,140** |
| **08/03 – 08/09** | **45,500** | **420** | **37,370** | **83,290** |
| **08/10 – 08/16** | **81,710** | **3,040** | **45,195** | **129,945** |
| **08/17 – 08/23** | **85,095** | **3,815** | **47,465** | **136,375** |
| **08/24 – 08/30** | **31,645** | **535** | **24,730** | **56,910** |
| **08/31 – 09/06** | **27,270** | **295** | **23,135** | **50,700** |
| **09/07 – 09/13** | **24,780** | **250** | **20,420** | **45,450** |
| **09/14 – 09/20** | **8,075** | **50** | **12,555** | **20,680** |
| 09/21 – 09/27 | 11,090 | 230 | 18,050 | 29,370 |
| 09/28 – 10/04 | 0 | 15 | 9,020 | 9,035 |
| 10/05 – 10/11 | 0 | 0 | 9,980 | 9,980 |
| 10/12 – 10/18 | 0 | 0 | 10,975 | 10,975 |
| 10/19 – 10/25 | 0 | 0 | 8,610 | 8,610 |
| 10/26 – 11/01 | 0 | 0 | 7,855 | 7,855 |
| 11/02 – 11/08 | 0 | 0 | 8,525 | 8,525 |
| 11/09 – 11/15 | 0 | 0 | 8,660 | 8,660 |
| 11/16 – 11/22 | 0 | 0 | 9,495 | 9,495 |
| 11/23 – 11/29 | 0 | 0 | 8,625 | 8,625 |
| 11/30 – 12/06 | 0 | 0 | 9,045 | 9,045 |
| 12/07 – 12/13 | 0 | 0 | 14,550 | 14,550 |
| 12/14 – 12/20 | 0 | 0 | 17,155 | 17,155 |
| 12/21 – 12/27 | 0 | 0 | 14,210 | 14,210 |
| 12/28 – 01/03 | 0 | 0 | 15,555 | 15,555 |

*Table B.7: Weekly average performance indices of the central plant*

| Week | $COP_{CH}$ | $COP_{central\ plant}$ | $COP_{central\ plant}^{modified}$ | $COP_{cooling}$ | $\epsilon_{HX-1}$ | $\epsilon_{HX-3}$ |
|---|---|---|---|---|---|---|
| 12/22 – 12/28 | OFF | OFF | | OFF | 0.45±0.11 | OFF |
| 12/29 – 01/04 | OFF | OFF | | OFF | 0.41±0.06 | OFF |
| 01/05 – 01/11 | OFF | OFF | | OFF | 0.44±0.07 | OFF |
| 01/12 – 01/18 | OFF | OFF | | OFF | 0.41±0.08 | OFF |
| 01/19 – 01/25 | OFF | OFF | | OFF | 0.44±0.06 | OFF |
| 01/26 – 02/01 | OFF | OFF | | OFF | 0.43±0.07 | OFF |
| 02/02 – 02/08 | OFF | OFF | | OFF | 0.43±0.07 | OFF |
| 02/09 – 02/15 | OFF | OFF | | OFF | NO DATA | OFF |
| 02/16 – 02/22 | OFF | OFF | | OFF | 0.53±0.15 | OFF |
| 02/23 – 03/01 | OFF | OFF | | OFF | 0.50±0.14 | OFF |
| 03/02 – 03/08 | OFF | OFF | | OFF | 0.52±0.15 | OFF |
| 03/09 – 03/15 | OFF | OFF | | OFF | 0.53±0.14 | OFF |
| 03/16 – 03/22 | OFF | OFF | | OFF | 0.57±0.15 | OFF |
| 03/23 – 03/29 | OFF | OFF | | OFF | 0.59±0.17 | OFF |
| 03/30 – 04/05 | OFF | OFF | | OFF | 0.66±0.17 | OFF |
| 04/06 – 04/12 | OFF | OFF | | OFF | 0.61±0.15 | OFF |
| 04/13 – 04/19 | OFF | OFF | | OFF | 0.58±0.20 | OFF |
| 04/20 – 04/26 | 4.72±1.10 | 4.69±1.08 | | 2.89±0.88 | 0.62±0.20 | 0.58±0.35 |
| 04/27 – 05/03 | 5.18±0.46 | 5.14±0.45 | | 3.96±0.55 | 0.56±0.23 | 0.74±0.15 |
| 05/04 – 05/10 | 4.94±0.91 | 4.92±0.90 | | 3.54±0.85 | 0.54±0.19 | 0.62±0.21 |
| 05/11 – 05/17 | 5.11±0.57 | 5.09±0.56 | | 3.83±0.69 | 0.52±0.23 | 0.61±0.19 |
| 05/18 – 05/24 | 5.14±0.60 | 5.11±0.59 | | 3.65±0.67 | 0.53±0.25 | 0.66±0.18 |
| 05/25 – 05/31 | 5.02±2.79 | 4.97±2.69 | | 2.87±1.13 | 0.58±0.20 | 0.59±0.20 |
| 06/01 – 06/07 | 4.94±2.06 | 4.90±1.95 | | 3.05±1.14 | 0.64±0.18 | 0.64±0.24 |
| 06/08 – 06/14 | 5.15±0.90 | 5.08±0.86 | | 3.30±0.73 | 0.68±0.18 | 0.02±0.07 |
| 06/15 – 06/21 | 5.08±0.52 | 4.99±0.50 | | 3.30±0.51 | 0.53±0.23 | 0.61±0.27 |
| **06/22 – 06/28** | **5.19±0.41** | **5.08±0.39** | | **3.41±0.44** | 0.28±0.18 | **0.72±0.12** |
| **06/29 – 07/05** | **5.12±0.58** | **5.04±0.57** | | **3.30±0.50** | 0.25±0.15 | **0.72±0.12** |
| **07/06 – 07/12** | **5.03±0.57** | **4.98±0.55** | | **3.17±0.65** | 0.30±0.16 | **0.72±0.13** |
| **07/13 – 07/19** | **5.04±0.41** | **4.96±0.40** | | **3.24±0.46** | 0.45±0.16 | **0.73±0.10** |
| **07/20 – 07/26** | **5.24±0.37** | **5.15±0.35** | | **3.46±0.48** | 0.26±0.22 | **0.73±0.11** |
| **07/27 – 08/02** | **5.56±0.35** | **5.43±0.32** | | **3.63±0.32** | 0.11±0.09 | **0.75±0.10** |
| **08/03 – 08/09** | **5.03±0.68** | **4.99±0.66** | | **3.11±0.70** | 0.31±0.16 | **0.73±0.12** |
| **08/10 – 08/16** | **5.59±0.56** | **5.40±0.54** | | **3.76±0.30** | 0.13±0.13 | **0.76±0.10** |
| **08/17 – 08/23** | **5.70±1.29** | **5.46±0.74** | | **3.76±0.41** | 0.10±0.10 | **0.78±0.09** |
| **08/24 – 08/30** | **5.05±1.34** | **4.98±1.27** | | **3.21±0.74** | 0.37±0.17 | **0.72±0.14** |
| **08/31 – 09/06** | **4.86±1.56** | **4.81±1.53** | | **3.05±0.88** | 0.48±0.19 | **0.71±0.15** |
| **09/07 – 09/13** | **4.98±1.15** | **4.94±1.14** | | **3.19±0.71** | 0.42±0.18 | **0.70±0.15** |
| **09/14 – 09/20** | **5.01±3.82** | **4.94±3.52** | | **2.83±1.30** | 0.49±0.20 | **0.70±0.21** |
| 09/21 – 09/27 | 5.29±0.30 | 5.19±0.29 | | 3.60±0.36 | 0.40±0.17 | 0.71±0.11 |
| 09/28 – 10/04 | OFF | OFF | | OFF | 0.54±0.21 | OFF |
| 10/05 – 10/11 | OFF | OFF | | OFF | 0.57±0.18 | OFF |
| 10/12 – 10/18 | OFF | OFF | | OFF | 0.56±0.19 | OFF |
| 10/19 – 10/25 | OFF | OFF | | OFF | 0.63±0.19 | OFF |
| 10/26 – 11/01 | OFF | OFF | | OFF | 0.66±0.16 | OFF |
| 11/02 – 11/08 | OFF | OFF | | OFF | 0.63±0.18 | OFF |
| 11/09 – 11/15 | OFF | OFF | | OFF | 0.60±0.19 | OFF |
| 11/16 – 11/22 | OFF | OFF | | OFF | 0.64±0.17 | OFF |
| 11/23 – 11/29 | OFF | OFF | | OFF | 0.66±0.16 | OFF |
| 11/30 – 12/06 | OFF | OFF | | OFF | 0.63±015 | OFF |
| 12/07 – 12/13 | OFF | OFF | | OFF | 0.50±0.14 | OFF |
| 12/14 – 12/20 | OFF | OFF | | OFF | 0.46±0.13 | OFF |
| 12/21 – 12/27 | OFF | OFF | | OFF | 0.52±0.13 | OFF |
| 12/28 – 01/03 | OFF | OFF | | OFF | 0.49±0.12 | OFF |

# Appendix C: Correlation-based model coefficients

*Table C.1: Coefficients for the electric power input models for chillers, Equation 5.19 – existing EnergyPlus model*

| Set name | $\dot{Q}_{ref}$ | $P_{ref}$ | $COP_{ref}$ | $a_0$ | $a_1$ | $a_2$ | $a_3$ | $a_4$ | $a_5$ |
|---|---|---|---|---|---|---|---|---|---|
| Trane CVHF 2799 | 2799 | | 6.40 | -0.2176 | -0.0494 | 8.70 E-05 | 0.09612 | -0.00203 | 0.00254 |
| CH1-30H | 2266 | 339 | 6.69 | 108.1450 | -19.2207 | 0.80636 | -2.51884 | 0.01341 | 0.24362 |
| CH1-7D | 2546 | 434 | 5.87 | 60.2946 | -0.9378 | 0.23199 | -3.25442 | 0.05275 | -0.06083 |
| CH1-10D | 2546 | 434 | 5.87 | 66.5676 | -2.1152 | 0.29755 | -3.38759 | 0.05384 | -0.05230 |
| CH1-14D | 2546 | 434 | 5.87 | 75.2669 | 10.6880 | -1.68116 | -6.29507 | 0.05826 | 0.33444 |
| CH1-21D | 2648 | 495 | 5.35 | 5.9293 | 8.8859 | -0.89437 | -2.00399 | 0.02037 | 0.08848 |
| CH1-28D | 2666 | 517 | 5.16 | 55.6849 | -5.9214 | 0.13986 | -1.98856 | 0.01810 | 0.11092 |
| CH2-1D | 2081 | 387 | 5.43 | 255.5610 | -27.6964 | 0.39433 | -9.47780 | 0.07495 | 0.65188 |
| CH2-7D | 2928 | 527 | 5.56 | 11.9917 | -7.7791 | 0.71449 | 0.86498 | -0.00760 | -0.05142 |
| CH2-10D | 2928 | 527 | 5.56 | 11.9917 | -7.7791 | 0.71449 | 0.86498 | -0.00760 | -0.05142 |
| CH2-14D | 2928 | 527 | 5.56 | -8.5273 | 0.2242 | -0.06358 | 0.51072 | -0.00940 | 0.01878 |
| CH2-21D | 2928 | 527 | 5.56 | -0.5696 | -0.7353 | -0.01311 | 0.23578 | -0.00631 | 0.02741 |
| CH2-28D | 2928 | 527 | 5.56 | -8.6454 | 1.8560 | -0.20341 | 0.19041 | -0.00567 | 0.02757 |

*Table C.2: Coefficients for the electric power input models for chillers, Equation 5.20 – existing EnergyPlus model*

| Set name | $b_0$ | $b_1$ | $b_2$ | $b_3$ | $b_4$ | $b_5$ |
|---|---|---|---|---|---|---|
| Trane CVHF 2799 | -0.0199 | -0.07848 | 0.00194 | 0.07123 | -9.17380E-04 | -0.00058 |
| CH1-30H | -56.6583 | 10.49900 | -0.96952 | 1.28252 | -2.69995 E-02 | 0.08165 |
| CH1-7D | -201.5340 | 58.43500 | -4.23824 | 0.28796 | 6.05000 E-06 | -0.03730 |
| CH1-10D | -214.9250 | 59.05250 | -4.11478 | 0.92367 | -2.90940 E-03 | -0.10114 |
| CH1-14D | -219.7120 | 52.00780 | -3.02603 | 2.52346 | -5.34559 E-03 | -0.31393 |
| CH1-21D | -114.9490 | 26.09400 | -1.47054 | 1.48837 | -4.33813 E-03 | -0.16923 |
| CH1-28D | -42.7144 | 6.25958 | -0.19697 | 1.19876 | -7.36280 E-03 | -0.09546 |
| CH2-1D | -473.2240 | 159.48600 | -8.48478 | -3.32317 | 1.74600 E-01 | -1.32621 |
| CH2-7D | -51.5804 | 22.43780 | -2.30418 | -1.34114 | -3.78277 E-03 | 0.24441 |
| CH2-10D | -51.5804 | 22.43780 | -2.30418 | -1.34114 | -3.78277 E-03 | 0.24441 |
| CH2-14D | -42.3250 | 13.03990 | -1.11650 | -0.11793 | -3.16450 E-03 | 0.06007 |
| CH2-21D | -30.8199 | 7.36389 | -0.57089 | 0.31733 | -4.79260 E-03 | 0.01228 |
| CH2-28D | -5.8344 | -0.29780 | -0.02285 | 0.386481 | -6.25419 E-03 | 0.01708 |

*Table C.3: Coefficients for the electric power input models for chillers, Equation 5.21 – existing EnergyPlus model*

| Set name | $c_0$ | $c_1$ | $c_2$ | $c_3$ | $c_4$ | $c_5$ | $c_6$ |
|---|---|---|---|---|---|---|---|
| Trane CVHF 2799 | 0.35161 | 0.00921 | -2.382325E-05 | 0.12232 | -0.18201 | -0.00784 | 0.68849 |
| CH1-30H | 19.06210 | -1.33277 | 2.30658 E-02 | 9.77271 | -2.12435 | -0.24626 | 1.30724 |
| CH1-7D | -0.59745 | 0.02880 | -2.32380 E-04 | 1.51642 | -0.45829 | -0.01089 | 0.19651 |
| CH1-10D | -6.96597 | 0.48961 | -8.48258 E-03 | -1.73432 | -0.77935 | 0.10189 | 0.17410 |
| CH1-14D | 0.425461 | -0.00551 | -9.48600 E-05 | 0.38709 | 0.09060 | 0.01593 | -0.14964 |
| CH1-21D | 1.40462 | 0.01898 | -2.06077 E-03 | -2.02660 | -1.46201 | 0.13174 | 0.32790 |
| CH1-28D | 1.94517 | -0.01389 | -1.49532 E-03 | -1.91033 | -1.53332 | 0.12419 | 0.46424 |
| CH2-1D | 13.53640 | -1.05093 | 2.03286 E-02 | 2.27129 | 2.28096 | -0.13296 | -0.49633 |
| CH2-7D | 2.33977 | -0.08433 | 6.53170 E-04 | -1.91995 | -0.10428 | 0.07856 | 0.03295 |
| CH2-10D | 1.41009 | -0.02335 | -3.97950 E-04 | -2.10914 | -0.42073 | 0.09222 | 0.14380 |
| CH2-14D | 8.75129 | -0.45837 | 5.93953 E-03 | -0.58359 | -0.84720 | 0.06192 | 0.24894 |
| CH2-21D | 10.74070 | -0.57270 | 7.47873 E-03 | -0.22867 | -1.14377 | 0.06158 | 0.33336 |
| CH2-28D | 12.86780 | -0.70446 | 9.53311 E-03 | 0.15227 | -1.02804 | 0.04728 | 0.30031 |

Table C.4: Coefficients for the electric power input models for chillers, $d_0$ to $d_5$ – existing York & Cappiello model

| Set name | $d_0$ | $d_1$ | $d_2$ | $d_3$ | $d_4$ | $d_5$ |
|---|---|---|---|---|---|---|
| CH1-30H | -121425 | 84.553 | 3599.280 | 20842.40 | 9.36407 E-07 | 22.2139 |
| CH1-7D | -34174 | 15.667 | 952.645 | 6129.97 | 3.43740 E-05 | -1.1631 |
| CH1-10D | -5664 | 0.820 | 14.050 | 1629.03 | 2.23514 E-05 | -1.3097 |
| CH1-14D | -9665 | 1.517 | 59.640 | 2609.11 | 1.97104 E-05 | -0.5389 |
| CH1-21D | -14925 | 5.600 | 405.399 | 2726.63 | 2.77382 E-05 | -3.2874 |
| CH1-28D | -18533 | 10.909 | 605.179 | 2967.64 | 3.28715 E-05 | -3.0989 |
| CH2-1D | -13860 | -3.296 | 41.018 | 3773.35 | 4.03397 E-06 | -0.3261 |
| CH2-7D | -48285 | 33.093 | 1579.170 | 7521.84 | 3.94222 E-05 | 5.7517 |
| CH2-10D | -44955 | 32.408 | 1474.740 | 7005.15 | 3.51244 E-05 | 4.2943 |
| CH2-14D | -30485 | 25.708 | 991.470 | 4756.36 | 2.91392 E-05 | 5.3648 |
| CH2-21D | -41553 | 38.963 | 1377.730 | 6448.54 | 2.89060 E-05 | 3.5309 |
| CH2-28D | -13700 | 15.200 | 535.864 | 1741.90 | 2.58396 E-05 | 3.0212 |
| CH2-1WW | 6915 | -0.002 | 272.648 | -3222.38 | 1.60953 E-05 | -0.3919 |
| CH2-1WEH | -10682 | 7.204 | 479.196 | 1137.69 | 3.19120 E-05 | -1.9564 |
| CH2-2WW | -49769 | 45.401 | 1646.520 | 7726.21 | 3.11948 E-05 | 8.0153 |
| CH2-2WEH | 2547 | -8.578 | -211.881 | 74.86 | 2.94375 E-05 | -1.1209 |

Table C.5: Coefficients for the electric power input models for chillers, $d_6$ to $d_{10}$ – existing York & Cappiello model

| Set name | $d_6$ | $d_7$ | $d_8$ | $d_9$ | $d_{10}$ |
|---|---|---|---|---|---|
| CH1-30H | -20.700 | -2.97423 | -12.54540 | -722.082 | 4.42106 E-01 |
| CH1-7D | -174.215 | -0.55130 | -2.31787 | -131.701 | 8.17863 E-02 |
| CH1-10D | -139.677 | -0.03186 | -0.10136 | 9.327 | 4.46411 E-03 |
| CH1-14D | -182.165 | -0.05224 | -0.20870 | -4.230 | 7.66351 E-03 |
| CH1-21D | -130.203 | -0.19608 | -0.83166 | -32.854 | 2.94983 E-02 |
| CH1-28D | -84.241 | -0.38733 | -1.61674 | -63.781 | 5.77056 E-02 |
| CH2-1D | -254.707 | 0.15159 | 0.49230 | -4.408 | -2.18083 E-02 |
| CH2-7D | 65.680 | -1.13230 | -4.95945 | -286.067 | 1.69973 E-01 |
| CH2-10D | 41.546 | -1.11302 | -4.85331 | -257.949 | 1.67029 E-01 |
| CH2-14D | 73.655 | -0.87849 | -3.84827 | -194.866 | 1.31944 E-01 |
| CH2-21D | 32.026 | -1.34809 | -5.81057 | -236.341 | 2.01478 E-01 |
| CH2-28D | 104.84 | -0.51863 | -2.26451 | -106.402 | 7.77564 E-02 |
| CH2-1WW | 326.063 | 0.00117 | -0.01258 | -38.473 | 9.31737 E-04 |
| CH2-1WEH | 36.873 | -0.25031 | -1.07724 | -55.316 | 3.78368 E-02 |
| CH2-2WW | 109.143 | -1.56796 | -6.79427 | -315.464 | 2.35053 E-01 |
| CH2-2WEH | -86.495 | 0.30910 | 1.29831 | 41.285 | -4.63336 E-02 |

*Table C.6: Coefficients for the electric power input models for chillers – existing Gordon & Ng model*

| Set name | $e_1$ | $e_2$ | $e_3$ |
|---|---|---|---|
| CH1-30H | 0.85195 | -2398.68 | 0.00660 |
| CH1-7D | 0.46488 | -526.92 | 0.00806 |
| CH1-10D | 0.52266 | -817.55 | 0.00815 |
| CH1-14D | 0.56725 | -1002.46 | 0.00802 |
| CH1-21D | 0.54212 | -884.92 | 0.00833 |
| CH1-28D | 0.46665 | -552.17 | 0.00867 |
| CH2-1D | 0.59389 | -1119.25 | 0.00937 |
| CH2-7D | 0.21374 | 434.77 | 0.01022 |
| CH2-10D | 0.32000 | 0.64 | 0.00989 |
| CH2-14D | 0.37813 | -223.85 | 0.00957 |
| CH2-21D | 0.50599 | -780.04 | 0.00930 |
| CH2-28D | 0.51724 | -838.29 | 0.00934 |
| CH2-1WW | 0.50248 | -780.12 | 0.00964 |
| CH2-1WEH | 0.62023 | -1250.67 | 0.00928 |
| CH2-2WW | 0.36045 | -179.73 | 0.00954 |
| CH2-2WEH | 0.54012 | -862.27 | 0.00926 |

*Table C.7: Coefficients for the coefficient of performance for chiller – Existing Swider model*

| Set name | $f_1$ | $f_2$ | $f_3$ |
|---|---|---|---|
| CH1-30H | 1.38768 E-03 | -0.37782 | 0.271301 |
| CH1-7D | 5.86066 E-04 | -0.02232 | 0.166573 |
| CH1-10D | 1.39000 E-04 | 0.28252 | 0.068173 |
| CH1-14D | 1.82409 E-04 | 0.28186 | 0.065769 |
| CH1-21D | 1.61620 E-04 | 0.20301 | 0.096527 |
| CH1-28D | 3.87480 E-04 | 0.05607 | 0.140090 |
| CH2-1D | -2.45130 E-04 | 0.32783 | 0.062889 |
| CH2-7D | -3.35160 E-04 | 0.23111 | 0.110382 |
| CH2-10D | -3.33850 E-04 | 0.23188 | 0.109850 |
| CH2-14D | -1.89340 E-04 | 0.19172 | 0.117681 |
| CH2-21D | 1.78660 E-04 | 0.06517 | 0.144667 |
| CH2-28D | 8.28700 E-04 | -0.15894 | 0.194756 |
| CH2-1WW | -1.38336 E-04 | 0.21619 | 0.099014 |
| CH2-1WEH | -9.75356 E-04 | 0.40104 | 0.076834 |
| CH2-2WW | 2.71566 E-04 | 0.02233 | 0.160078 |
| CH2-2WEH | -4.09633 E-04 | 0.24192 | 0.106742 |

# Appendix D: ANN models

For all tables, the light grey cells represent the results that are part of both the classic static and augmented window approach. The results in bold have been selected as the most accurate results and are presented in section 5.5.

*Table D.1: Results for chiller CH-1, classic static and augmented window - proposed ANN models*

| Set name | Power - $Q_E/Q_{Edesign}$, $T_{CNDS}$, $T_{O/A}$ | | | | | COP - $Q_E/Q_{Edesign}$, $T_{CNDS}$, $T_{O/A}$ | | | | |
| | Training set | | Testing set | | | Training set | | Testing set | | |
| | CV, % | RMSE, kW | CV, % | RMSE, kW | MBE, kW | CV, % | RMSE | CV, % | RMSE | MBE |
|---|---|---|---|---|---|---|---|---|---|---|
| **CH1-30H-1H3N** | **3.2** | **9.6** | **2.4** | **7.0** | **0.75** | **3.2** | **0.2** | **2.3** | **0.1** | **-0.03** |
| CH1-30H-1H4N | 3.0 | 9.2 | 3.2 | 9.5 | -2.93 | 2.8 | 0.2 | 2.6 | 0.2 | -0.02 |
| CH1-30H-1H5N | 2.7 | 8.2 | 2.8 | 8.2 | -0.32 | 2.5 | 0.1 | 2.7 | 0.2 | -0.01 |
| CH1-30H-1H6N | 2.6 | 7.9 | 2.8 | 8.1 | -1.34 | 2.3 | 0.1 | 2.8 | 0.2 | 0.06 |
| CH1-30H-1H7N | 2.5 | 7.7 | 2.9 | 8.5 | -0.45 | 2.3 | 0.1 | 2.7 | 0.2 | 0.00 |
| CH1-30H-1H8N | 2.5 | 7.6 | 2.8 | 8.1 | -1.91 | 2.3 | 0.1 | 2.7 | 0.2 | 0.04 |
| CH1-30H-1H9N | 2.4 | 7.3 | 3.1 | 9.0 | -2.77 | 2.2 | 0.1 | 3.0 | 0.2 | 0.04 |
| **CH1-7D-1H3N** | **3.9** | **12.3** | **4.1** | **9.8** | **0.33** | **3.9** | **0.2** | **5.8** | **0.3** | **0.12** |
| CH1-7D-1H4N | 3.8 | 12.2 | 4.1 | 9.7 | 0.12 | 3.9 | 0.2 | 5.6 | 0.3 | 0.12 |
| CH1-7D-1H5N | 3.7 | 11.6 | 4.7 | 11.2 | 0.72 | 3.7 | 0.2 | 4.3 | 0.2 | 0.10 |
| CH1-7D-1H6N | 3.5 | 11.2 | 5.1 | 12.3 | 0.60 | 3.6 | 0.2 | 8.1 | 0.4 | 0.17 |
| CH1-7D-1H7N | 3.5 | 11.3 | 7.8 | 18.6 | 4.45 | 3.5 | 0.2 | 6.0 | 0.3 | 0.11 |
| CH1-7D-1H8N | 3.5 | 11.0 | 6.1 | 14.5 | 2.66 | 3.5 | 0.2 | 8.0 | 0.4 | 0.15 |
| CH1-7D-1H9N | 3.4 | 10.9 | 5.1 | 12.3 | 0.72 | 3.5 | 0.2 | 8.4 | 0.4 | 0.16 |
| **CH1-10D-1H3N** | **3.8** | **11.2** | **4.2** | **10.1** | **-3.53** | **3.8** | **0.2** | **4.0** | **0.2** | **0.07** |
| CH1-10D-1H4N | 3.9 | 11.4 | 4.6 | 11.0 | -3.65 | 3.7 | 0.2 | 3.9 | 0.2 | 0.06 |
| CH1-10D-1H5N | 3.7 | 10.6 | 4.5 | 10.9 | -2.44 | 3.6 | 0.2 | 4.5 | 0.2 | 0.04 |
| CH1-10D-1H6N | 3.6 | 10.5 | 6.1 | 14.7 | -2.21 | 3.6 | 0.2 | 5.7 | 0.2 | 0.04 |
| CH1-10D-1H7N | 3.5 | 10.2 | 6.8 | 16.5 | -2.45 | 3.5 | 0.2 | 6.1 | 0.3 | 0.05 |
| CH1-10D-1H8N | 3.5 | 10.1 | 6.5 | 15.8 | -2.24 | 3.4 | 0.2 | 6.1 | 0.3 | 0.04 |
| CH1-10D-1H9N | 3.4 | 10.0 | 8.4 | 20.4 | -1.27 | 3.4 | 0.2 | 7.2 | 0.3 | 0.03 |
| **CH1-14D-1H3N** | **3.8** | **10.7** | **4.0** | **12.3** | **-7.49** | **3.7** | **0.2** | **3.5** | **0.2** | **0.11** |
| CH1-14D-1H4N | 3.8 | 10.6 | 4.7 | 14.4 | -8.94 | 3.7 | 0.2 | 4.1 | 0.2 | 0.14 |
| CH1-14D-1H5N | 3.7 | 10.6 | 35.6 | 15.4 | -9.54 | 3.7 | 0.2 | 4.0 | 0.2 | 0.13 |
| CH1-14D-1H6N | 10.1 | 3.6 | 3.9 | 12.0 | -6.55 | 3.5 | 0.2 | 3.8 | 0.2 | 0.11 |
| CH1-14D-1H7N | 3.6 | 10.2 | 4.1 | 12.6 | -7.37 | 3.6 | 0.2 | 3.9 | 0.2 | 0.12 |
| CH1-14D-1H8N | 3.6 | 10.1 | 4.1 | 12.7 | -7.17 | 3.5 | 0.2 | 3.9 | 0.2 | 0.11 |
| CH1-21D-1H3N | 3.6 | 10.6 | 2.8 | 9.3 | -0.57 | 3.6 | 0.2 | 2.9 | 0.2 | 0.02 |
| CH1-21D-1H4N | 3.5 | 10.3 | 2.8 | 9.3 | -0.86 | 3.5 | 0.2 | 2.9 | 0.2 | 0.02 |
| CH1-21D-1H5N | 3.5 | 10.2 | 2.8 | 9.3 | -1.40 | 3.5 | 0.2 | 2.9 | 0.2 | 0.03 |
| CH1-21D-1H6N | 3.5 | 10.1 | 2.8 | 9.2 | -1.58 | 3.5 | 0.2 | 2.9 | 0.2 | 0.03 |
| CH1-21D-1H7N | 3.4 | 10.0 | 2.9 | 9.7 | -1.74 | 3.5 | 0.2 | 3.0 | 0.2 | 0.03 |
| CH1-21D-1H8N | 3.4 | 10.0 | 2.9 | 9.9 | -2.00 | 3.5 | 0.2 | 3.0 | 0.2 | 0.04 |
| **CH1-21D-1H9N** | **3.4** | **9.7** | **3.0** | **9.9** | **-1.88** | **3.4** | **0.2** | **3.0** | **0.2** | **0.04** |
| CH1-28D-1H3N | 3.4 | 10.4 | 4.4 | 13.9 | 6.13 | 3.3 | 0.2 | 4.7 | 0.3 | -0.11 |
| CH1-28D-1H4N | 3.2 | 9.8 | 4.2 | 13.4 | 5.94 | 3.3 | 0.2 | 4.7 | 0.3 | -0.11 |
| CH1-28D-1H5N | 3.2 | 9.8 | 4.2 | 13.4 | 6.03 | 3.3 | 0.2 | 4.8 | 0.3 | -0.09 |
| CH1-28D-1H6N | 3.2 | 9.7 | 4.2 | 13.3 | 5.97 | 3.2 | 0.2 | 4.6 | 0.3 | -0.11 |
| CH1-28D-1H7N | 3.2 | 9.7 | 4.1 | 13.2 | 5.89 | 3.2 | 0.2 | 4.6 | 0.3 | -0.11 |
| CH1-28D-1H8N | 3.1 | 9.6 | 4.0 | 12.9 | 5.77 | 3.2 | 0.2 | 4.6 | 0.3 | -0.11 |
| **CH1-28D-1H9N** | **3.1** | **9.5** | **4.1** | **12.9** | **5.56** | **3.1** | **0.2** | **4.6** | **0.2** | **-0.11** |

*Table D.2: Results for chiller CH-2, classic static and augmented window – proposed ANN models*

| Set name | Power - $Q_E/Q_{Edesign}$, $T_{CNDS}$, $T_{O/A}$ | | | | | COP - $Q_E/Q_{Edesign}$, $T_{CNDS}$, $T_{O/A}$ | | | | |
|---|---|---|---|---|---|---|---|---|---|---|
| | Training set | | Testing set | | | Training set | | Testing set | | |
| | CV, % | RMSE, kW | CV, % | RMSE, kW | MBE, kW | CV, % | RMSE | CV, % | RMSE | MBE |
| CH2-1D-1H3N | 3.0 | 8.6 | 4.0 | 13.8 | 7.95 | 2.5 | 0.1 | 3.4 | 0.2 | 0.05 |
| CH2-1D -1H4N | 2.8 | 8.0 | 3.7 | 12.7 | -3.81 | 2.5 | 0.1 | 3.8 | 0.2 | 0.07 |
| CH2-1D -1H5N | 2.8 | 8.0 | 3.3 | 11.2 | -2.15 | 2.5 | 0.1 | 3.9 | 0.2 | 0.07 |
| CH2-1D -1H6N | 2.8 | 8.0 | 3.1 | 10.7 | -1.61 | 2.5 | 0.1 | 3.9 | 0.2 | 0.07 |
| CH2-1D -1H7N | 2.8 | 8.0 | 3.1 | 10.5 | -1.40 | 2.5 | 0.1 | 4.0 | 0.2 | 0.07 |
| CH2-1D -1H8N | 2.8 | 8.0 | 3.0 | 10.3 | -1.30 | 2.5 | 0.1 | 4.0 | 0.2 | 0.08 |
| **CH2-1D -1H9N** | **2.8** | **8.0** | **3.0** | **10.3** | **-1.24** | **2.5** | **0.1** | **4.0** | **0.2** | **0.08** |
| CH2-7D-1H3N | 3.6 | 12.3 | 3.5 | 11.3 | -3.44 | 3.7 | 0.2 | 3.4 | 0.2 | 0.05 |
| CH2-7D-1H4N | 3.5 | 11.8 | 3.6 | 11.6 | -3.60 | 3.7 | 0.2 | 3.5 | 0.2 | 0.05 |
| CH2-7D-1H5N | 3.3 | 11.2 | 3.3 | 10.6 | -0.65 | 3.4 | 0.2 | 3.6 | 0.2 | 0.07 |
| CH2-7D-1H6N | 3.2 | 10.9 | 3.2 | 10.2 | 0.46 | 3.5 | 0.2 | 3.2 | 0.2 | 0.04 |
| CH2-7D-1H7N | 3.1 | 10.3 | 3.4 | 10.9 | 1.77 | 3.1 | 0.2 | 3.6 | 0.2 | 0.02 |
| CH2-7D-1H8N | 2.9 | 9.8 | 3.4 | 10.8 | 2.60 | 3.2 | 0.2 | 3.2 | 0.2 | -0.03 |
| **CH2-7D-1H9N** | **2.8** | **9.5** | **3.7** | **11.8** | **2.74** | **3.1** | **0.2** | **3.6** | **0.2** | **-0.02** |
| CH2-10D-1H3N | 3.7 | 12.4 | 3.3 | 10.7 | -1.43 | 4.0 | 0.2 | 3.5 | 0.2 | 0.02 |
| CH2-10D-1H4N | 4.0 | 13.2 | 3.6 | 11.9 | 1.91 | 3.6 | 0.2 | 3.5 | 0.2 | 0.04 |
| CH2-10D-1H5N | 3.3 | 10.8 | 3.0 | 9.9 | -0.78 | 3.4 | 0.2 | 3.2 | 0.2 | 0.04 |
| CH2-10D-1H6N | 3.1 | 10.4 | 2.8 | 9.3 | 1.24 | 3.3 | 0.2 | 2.9 | 0.2 | -0.01 |
| CH2-10D-1H7N | 3.2 | 10.5 | 3.2 | 10.6 | 1.41 | 3.3 | 0.2 | 3.3 | 0.2 | 0.01 |
| CH2-10D-1H8N | 2.9 | 9.8 | 2.8 | 9.3 | -0.78 | 3.2 | 0.2 | 3.1 | 0.2 | 0.02 |
| **CH2-10D-1H9N** | **2.9** | **9.6** | **3.0** | **9.9** | **-1.70** | **3.1** | **0.2** | **3.4** | **0.2** | **0.03** |
| CH2-14D-1H3N | 3.6 | 11.8 | 4.3 | 13.3 | -0.94 | 3.6 | 0.2 | 3.8 | 0.2 | 0.01 |
| CH2-14D-1H4N | 3.3 | 11.0 | 4.1 | 12.7 | -0.31 | 3.5 | 0.2 | 3.7 | 0.2 | 0.01 |
| CH2-14D-1H5N | 3.3 | 10.8 | 3.7 | 11.7 | -0.41 | 3.4 | 0.2 | 4.1 | 0.2 | 0.02 |
| CH2-14D-1H6N | 3.1 | 10.2 | 3.8 | 11.7 | -0.32 | 3.3 | 0.2 | 3.9 | 0.2 | 0.02 |
| CH2-14D-1H7N | 3.0 | 9.8 | 3.9 | 12.3 | 0.97 | 3.0 | 0.2 | 3.9 | 0.2 | 0.01 |
| CH2-14D-1H8N | 2.9 | 9.6 | 3.7 | 11.6 | 0.99 | 3.0 | 0.2 | 3.8 | 0.2 | 0.01 |
| **CH2-14D-1H9N** | **2.9** | **9.5** | **3.7** | **11.6** | **0.38** | **3.1** | **0.2** | **3.9** | **0.2** | **0.01** |
| CH2-21D-1H3N | 3.7 | 11.9 | 5.7 | 12.9 | 0.66 | 3.7 | 0.2 | 4.3 | 0.2 | 0.02 |
| CH2-21D-1H4N | 3.6 | 11.7 | 5.4 | 12.2 | 0.45 | 3.6 | 0.2 | 4.2 | 0.2 | 0.02 |
| CH2-21D-1H5N | 3.2 | 10.5 | 4.6 | 10.4 | -1.26 | 3.4 | 0.2 | 4.3 | 0.2 | 0.02 |
| CH2-21D-1H6N | 3.3 | 10.6 | 4.4 | 10.0 | -1.63 | 3.4 | 0.2 | 4.3 | 0.2 | 0.03 |
| CH2-21D-1H7N | 3.0 | 9.8 | 4.1 | 9.2 | -1.16 | 3.3 | 0.2 | 4.1 | 0.2 | 0.02 |
| CH2-21D-1H8N | 3.0 | 9.7 | 4.4 | 9.9 | -1.17 | 3.2 | 0.2 | 4.2 | 0.2 | 0.02 |
| **CH2-21D-1H9N** | **3.0** | **9.8** | **4.1** | **9.3** | **-0.76** | **3.2** | **0.2** | **4.0** | **0.2** | **0.02** |
| CH2-28D-1H3N | 4.0 | 12.8 | 3.7 | 15.7 | -12.56 | 4.0 | 0.2 | 3.6 | 0.2 | 0.14 |
| CH2-28D-1H4N | 3.7 | 11.7 | 4.2 | 17.6 | -14.16 | 3.7 | 0.2 | 3.4 | 0.2 | 0.13 |
| CH2-28D-1H5N | 3.5 | 11.3 | 3.7 | 15.7 | -12.53 | 3.5 | 0.2 | 2.8 | 0.1 | 0.10 |
| CH2-28D-1H6N | 3.3 | 10.5 | 3.4 | 14.5 | -11.36 | 3.4 | 0.2 | 3.0 | 0.1 | 0.12 |
| CH2-28D-1H7N | 3.3 | 10.3 | 3.1 | 13.0 | -9.39 | 3.4 | 0.2 | 3.1 | 0.2 | 0.11 |
| CH2-28D-1H8N | 3.1 | 9.9 | 2.5 | 10.5 | -7.94 | 3.3 | 0.2 | 2.5 | 0.1 | 0.09 |
| **CH2-28D-1H9N** | **3.1** | **9.9** | **2.5** | **10.3** | **-7.52** | **3.2** | **0.2** | **2.5** | **0.1** | **0.08** |

*Table D.3: Results for chiller CH-2, split static – proposed ANN models*

| Set name | Power - $Q_E/Q_{Edesign}$, $T_{CNDS}$, $T_{O/A}$ | | | | | COP - $Q_E/Q_{Edesign}$, $T_{CNDS}$, $T_{O/A}$ | | | | |
| | Training set | | Testing set | | | Training set | | Testing set | | |
| | CV, % | RMSE, kW | CV, % | RMSE, kW | MBE, kW | CV, % | RMSE | CV, % | RMSE | MBE |
|---|---|---|---|---|---|---|---|---|---|---|
| **CH2-1WW-1H3N** | **3.2** | **10.7** | **8.6** | **27.6** | **18.89** | **3.0** | **0.2** | **8.9** | **0.5** | **-0.36** |
| CH2-1WW -1H4N | 2.6 | 8.6 | 11.6 | 37.4 | 29.62 | 2.8 | 0.1 | 10.7 | 0.6 | -0.47 |
| CH2-1WW -1H5N | 2.5 | 8.2 | 9.2 | 29.4 | 19.92 | 2.5 | 0.1 | 8.9 | 0.5 | -0.34 |
| CH2-1WW -1H6N | 2.4 | 8.1 | 9.9 | 31.9 | 22.53 | 2.5 | 0.1 | 9.5 | 0.5 | -0.38 |
| CH2-1WW -1H7N | 2.3 | 7.8 | 9.3 | 30.0 | 19.70 | 2.5 | 0.1 | 8.9 | 0.5 | -0.34 |
| CH2-1WW -1H8N | 2.3 | 7.9 | 10.2 | 32.7 | 24.40 | 2.4 | 0.1 | 8.9 | 0.5 | -0.37 |
| CH2-1WW -1H9N | 2.3 | 7.8 | 9.6 | 30.8 | 21.18 | 2.4 | 0.1 | 9.8 | 0.6 | -0.41 |
| **CH2-1WEH-1H3N** | **2.5** | **8.4** | **2.6** | **8.7** | **0.58** | **2.4** | **0.1** | **2.2** | **0.1** | **-0.004** |
| CH2-1WEH -1H4N | 2.4 | 8.0 | 2.6 | 8.9 | 2.52 | 2.4 | 0.1 | 2.4 | 0.1 | -0.02 |
| CH2-1WEH -1H5N | 2.4 | 7.9 | 2.8 | 9.6 | 1.88 | 2.3 | 0.1 | 2.4 | 0.1 | -0.01 |
| CH2-1WEH -1H6N | 2.4 | 7.9 | 2.9 | 9.8 | 3.15 | 2.3 | 0.1 | 2.4 | 0.1 | -0.02 |
| CH2-1WEH -1H7N | 2.3 | 7.8 | 3.5 | 11.7 | 4.13 | 2.2 | 0.1 | 2.7 | 0.1 | -0.03 |
| CH2-1WEH -1H8N | 2.3 | 7.6 | 3.4 | 11.4 | 4.00 | 2.2 | 0.1 | 2.7 | 0.1 | -0.03 |
| CH2-1WEH -1H9N | 2.3 | 7.6 | 3.3 | 11.0 | 3.72 | 2.2 | 0.1 | 2.7 | 0.1 | -0.03 |
| CH2-2WW-1H3N | 3.6 | 11.9 | 3.4 | 12.4 | -2.16 | 3.7 | 0.2 | 3.3 | 0.2 | -0.01 |
| CH2-2WW -1H4N | 3.6 | 11.7 | 3.6 | 13.1 | -1.54 | 3.6 | 0.2 | 3.4 | 0.2 | -0.02 |
| CH2-2WW -1H5N | 3.3 | 10.8 | 3.3 | 12.0 | -0.21 | 3.4 | 0.2 | 3.2 | 0.2 | -0.02 |
| CH2-2WW -1H6N | 3.1 | 10.2 | 3.1 | 11.0 | 0.09 | 3.2 | 0.2 | 3.1 | 0.2 | -0.02 |
| CH2-2WW -1H7N | 3.0 | 9.8 | 3.1 | 11.0 | 1.27 | 3.2 | 0.2 | 3.1 | 0.2 | -0.01 |
| **CH2-2WW -1H8N** | **2.8** | **9.1** | **3.0** | **10.8** | **0.95** | **3.0** | **0.2** | **3.0** | **0.2** | **-0.01** |
| CH2-2WW -1H9N | 2.7 | 8.8 | 3.1 | 11.1 | 1.88 | 2.9 | 0.2 | 3.0 | 0.2 | -0.01 |
| CH2-2WEH-1H3N | 2.4 | 8.1 | 9.6 | 22.1 | 8.99 | 2.5 | 0.1 | 5.6 | 0.3 | -0.10 |
| CH2-2WEH -1H4N | 2.5 | 8.2 | 8.5 | 19.5 | 6.65 | 2.5 | 0.1 | 6.1 | 0.3 | -0.15 |
| CH2-2WEH -1H5N | 2.4 | 7.9 | 7.3 | 16.8 | 9.26 | 2.4 | 0.1 | 5.4 | 0.3 | -0.13 |
| CH2-2WEH -1H6N | 2.4 | 7.9 | 8.9 | 20.5 | 10.97 | 2.4 | 0.1 | 5.0 | 0.2 | -0.13 |
| CH2-2WEH -1H7N | 2.3 | 7.7 | 6.1 | 13.9 | 6.57 | 2.4 | 0.1 | 4.8 | 0.2 | -0.12 |
| **CH2-2WEH -1H8N** | **2.3** | **7.7** | **6.1** | **14.1** | **6.88** | **2.4** | **0.1** | **4.9** | **0.2** | **-0.12** |
| CH2-2WEH -1H9N | 2.3 | 7.7 | 6.2 | 14.4 | 7.28 | 2.4 | 0.1 | 4.9 | 0.2 | -0.12 |

*Table D.4: Results for chiller CH-1, classic static and augmented window – Y&C ANN models*

| Set name | Power - $Q_E$, $T_{CNDR}$, $T_{CHWS}$ | | | | | COP - $Q_E$, $T_{CNDR}$, $T_{CHWS}$ | | | | |
|---|---|---|---|---|---|---|---|---|---|---|
| | Training set | | Testing set | | | Training set | | Testing set | | |
| | CV, % | RMSE, kW | CV, % | RMSE, kW | MBE, kW | CV, % | RMSE | CV, % | RMSE | MBE |
| CH1-30H-1H3N | 2.8 | 8.6 | 2.6 | 7.5 | -1.58 | 2.7 | 0.2 | 2.1 | 0.1 | 0.01 |
| CH1-30H-1H4N | 2.6 | 7.9 | 2.5 | 7.4 | -1.83 | 2.4 | 0.1 | 2.1 | 0.1 | 0.02 |
| CH1-30H-1H5N | 2.6 | 7.9 | 2.5 | 7.3 | -1.86 | 2.4 | 0.1 | 2.1 | 0.1 | 0.02 |
| CH1-30H-1H6N | 2.5 | 7.5 | 2.4 | 7.1 | -1.61 | 2.4 | 0.1 | 2.1 | 0.1 | 0.02 |
| CH1-30H-1H7N | 2.4 | 7.4 | 2.4 | 6.9 | -0.77 | 2.4 | 0.1 | 2.1 | 0.1 | 0.01 |
| **CH1-30H-1H8N** | **2.4** | **7.2** | **2.3** | **6.7** | **-0.42** | **2.3** | **0.1** | **2.0** | **0.1** | **-0.003** |
| CH1-30H-1H9N | 2.1 | 6.5 | 2.2 | 6.5 | 0.52 | 2.1 | 0.1 | 2.0 | 0.1 | -0.03 |
| CH1-7D-1H3N | 4.1 | 13.1 | 4.1 | 9.7 | -0.71 | 4.2 | 0.2 | 6.3 | 0.3 | 0.16 |
| CH1-7D-1H4N | 4.1 | 13.1 | 4.3 | 10.3 | 0.84 | 4.2 | 0.2 | 6.6 | 0.3 | 0.16 |
| CH1-7D-1H5N | 4.1 | 13.1 | 4.1 | 9.8 | 0.56 | 4.2 | 0.2 | 6.4 | 0.3 | 0.16 |
| CH1-7D-1H6N | 3.5 | 11.1 | 4.4 | 10.6 | 2.23 | 3.5 | 0.2 | 7.2 | 0.3 | 0.13 |
| CH1-7D-1H7N | 3.5 | 11.1 | 4.6 | 11.0 | 2.62 | 3.5 | 0.2 | 4.1 | 0.2 | 0.04 |
| **CH1-7D-1H8N** | **3.4** | **10.7** | **5.2** | **12.4** | **3.33** | **3.4** | **0.2** | **4.6** | **0.2** | **0.06** |
| CH1-7D-1H9N | 3.2 | 10.3 | 5.0 | 11.9 | 1.97 | 3.3 | 0.2 | 6.3 | 0.3 | 0.08 |
| CH1-10D-1H3N | 3.9 | 11.5 | 4.2 | 10.1 | -3.31 | 3.9 | 0.2 | 3.9 | 0.2 | 0.06 |
| CH1-10D-1H4N | 3.9 | 11.4 | 4.2 | 10.2 | -3.68 | 3.9 | 0.2 | 3.9 | 0.2 | 0.07 |
| CH1-10D-1H5N | 3.5 | 10.1 | 4.5 | 10.8 | -2.48 | 3.4 | 0.2 | 4.0 | 0.2 | 0.05 |
| CH1-10D-1H6N | 3.4 | 9.7 | 4.4 | 10.6 | -2.61 | 3.3 | 0.2 | 4.0 | 0.2 | 0.05 |
| CH1-10D-1H7N | 3.3 | 9.6 | 3.6 | 8.7 | -2.68 | 3.3 | 0.2 | 3.4 | 0.2 | 0.05 |
| **CH1-10D-1H8N** | **3.3** | **9.5** | **3.4** | **8.3** | **-2.64** | **3.3** | **0.2** | **3.4** | **0.2** | **0.06** |
| CH1-10D-1H9N | 3.3 | 9.5 | 3.5 | 8.5 | -2.50 | 3.2 | 0.2 | 3.3 | 0.2 | 0.05 |
| CH1-14D-1H3N | 4.0 | 11.2 | 4.7 | 14.5 | -10.41 | 3.9 | 0.2 | 4.5 | 0.2 | 0.18 |
| CH1-14D-1H4N | 3.6 | 10.2 | 4.2 | 13.2 | -8.26 | 3.5 | 0.2 | 3.9 | 0.2 | 0.13 |
| CH1-14D-1H5N | 3.5 | 10.0 | 38.1 | 15.4 | -9.99 | 3.4 | 0.2 | 4.1 | 0.2 | 0.15 |
| CH1-14D-1H6N | 3.4 | 9.7 | 4.5 | 13.9 | -8.18 | 3.4 | 0.2 | 3.8 | 0.2 | 0.12 |
| CH1-14D-1H7N | 3.3 | 9.4 | 4.5 | 14.0 | -8.45 | 3.3 | 0.2 | 3.9 | 0.2 | 0.13 |
| **CH1-14D-1H8N** | **3.3** | **9.3** | **4.5** | **13.9** | **-8.38** | **3.2** | **0.2** | **3.9** | **0.2** | **0.13** |
| CH1-14D-1H9N | 3.2 | 9.2 | 4.1 | 12.6 | -7.72 | 3.2 | 0.2 | 3.9 | 0.2 | 0.12 |
| CH1-14D-1H10N | 4.1 | 11.9 | 4.3 | 13.5 | -7.88 | 4.2 | 0.2 | 4.0 | 0.2 | 0.12 |
| CH1-21D-1H3N | 3.9 | 11.3 | 3.4 | 11.4 | -2.04 | 3.8 | 0.2 | 3.0 | 0.2 | 0.04 |
| CH1-21D-1H4N | 3.4 | 10.0 | 3.2 | 10.6 | -1.59 | 3.4 | 0.2 | 3.0 | 0.2 | 0.03 |
| CH1-21D-1H5N | 3.3 | 9.7 | 3.1 | 10.4 | -1.82 | 3.3 | 0.2 | 3.1 | 0.2 | 0.03 |
| CH1-21D-1H6N | 3.3 | 9.5 | 6.5 | 21.6 | -2.41 | 3.3 | 0.2 | 5.0 | 0.3 | 0.04 |
| CH1-21D-1H7N | 3.3 | 9.4 | 4.1 | 13.9 | -1.50 | 3.3 | 0.2 | 3.9 | 0.2 | 0.03 |
| **CH1-21D-1H8N** | **3.3** | **9.5** | **3.3** | **11.0** | **-1.12** | **3.2** | **0.2** | **3.2** | **0.2** | **0.02** |
| CH1-21D-1H9N | 3.2 | 9.4 | 4.3 | 14.4 | -1.34 | 3.2 | 0.2 | 3.7 | 0.2 | 0.03 |
| CH1-21D-1H10N | 3.2 | 9.2 | 3.8 | 12.6 | -1.36 | 3.2 | 0.2 | 3.9 | 0.2 | 0.02 |
| CH1-21D-1H11N | 3.1 | 9.1 | 3.3 | 11.1 | -1.31 | 3.2 | 0.2 | 3.3 | 0.2 | 0.03 |
| CH1-21D-1H12N | 3.1 | 9.1 | 4.1 | 13.7 | -1.35 | 3.2 | 0.2 | 4.1 | 0.2 | 0.03 |
| CH1-28D-1H3N | 3.6 | 11.0 | 4.9 | 25.5 | 6.98 | 3.6 | 0.2 | 5.3 | 0.3 | -0.13 |
| CH1-28D-1H4N | 3.3 | 10.1 | 4.4 | 14.1 | 5.96 | 3.2 | 0.2 | 4.8 | 0.3 | -0.11 |
| CH1-28D-1H5N | 3.2 | 9.9 | 4.2 | 13.4 | 5.91 | 3.2 | 0.2 | 4.7 | 0.3 | -0.11 |
| CH1-28D-1H6N | 3.2 | 9.7 | 4.2 | 13.5 | 5.89 | 3.2 | 0.2 | 4.8 | 0.3 | -0.11 |
| CH1-28D-1H7N | 3.1 | 9.6 | 4.2 | 13.4 | 5.72 | 3.1 | 0.2 | 4.7 | 0.3 | -0.11 |
| **CH1-28D-1H8N** | **3.1** | **9.5** | **4.2** | **13.2** | **5.61** | **3.1** | **0.2** | **4.7** | **0.3** | **-0.11** |
| CH1-28D-1H9N | 3.1 | 9.5 | 4.2 | 13.4 | 5.81 | 3.1 | 0.2 | 4.7 | 0.3 | -0.11 |

*Table D.5: Results for chiller CH-2, classic static and augmented window – Y&C ANN models*

| Set name | Power - $Q_E$, $T_{CNDR}$, $T_{CHWS}$ | | | | | COP - $Q_E$, $T_{CNDR}$, $T_{CHWS}$ | | | | |
|---|---|---|---|---|---|---|---|---|---|---|
| | Training set | | Testing set | | | Training set | | Testing set | | |
| | CV, % | RMSE, kW | CV, % | RMSE, kW | MBE, kW | CV, % | RMSE | CV, % | RMSE | MBE |
| CH2-1D-1H3N | 2.9 | 8.4 | 3.2 | 11.0 | -1.36 | 2.4 | 0.1 | 2.6 | 0.1 | -0.01 |
| CH2-1D -1H4N | 2.8 | 8.0 | 3.3 | 11.3 | -1.67 | 2.3 | 0.1 | 2.7 | 0.1 | -0.01 |
| CH2-1D -1H5N | 2.7 | 7.7 | 3.5 | 12.0 | -1.43 | 2.3 | 0.1 | 2.7 | 0.1 | -0.01 |
| CH2-1D -1H6N | 2.7 | 7.6 | 3.4 | 11.5 | -1.23 | 2.2 | 0.1 | 2.7 | 0.1 | -0.01 |
| CH2-1D -1H7N | 2.7 | 7.6 | 3.3 | 11.4 | -1.14 | 2.2 | 0.1 | 2.7 | 0.1 | -0.01 |
| **CH2-1D -1H8N** | **2.7** | **7.6** | **3.3** | **11.2** | **-1.05** | **2.2** | **0.1** | **2.7** | **0.1** | **-0.01** |
| CH2-1D -1H9N | 2.7 | 7.6 | 3.2 | 11.0 | -0.96 | 2.2 | 0.1 | 2.7 | 0.1 | -0.01 |
| CH2-7D-1H3N | 5.8 | 19.5 | 4.9 | 15.7 | -11.28 | 6.0 | 0.3 | 4.9 | 0.3 | 0.20 |
| CH2-7D-1H4N | 5.6 | 18.8 | 5.3 | 17.1 | -7.01 | 5.7 | 0.3 | 4.9 | 0.3 | 0.15 |
| CH2-7D-1H5N | 4.7 | 15.8 | 4.3 | 13.8 | -5.19 | 4.9 | 0.3 | 4.6 | 0.2 | 0.13 |
| CH2-7D-1H6N | 4.8 | 16.1 | 4.1 | 13.0 | -2.64 | 5.0 | 0.3 | 4.5 | 0.2 | 0.07 |
| CH2-7D-1H7N | 4.7 | 15.7 | 4.2 | 13.3 | -2.07 | 5.0 | 0.3 | 4.5 | 0.2 | 0.08 |
| **CH2-7D-1H8N** | **4.4** | **14.8** | **4.4** | **14.0** | **-3.23** | **4.7** | **0.2** | **4.7** | **0.2** | **0.09** |
| CH2-7D-1H9N | 4.7 | 16.0 | 4.4 | 14.2 | -2.71 | 4.9 | 0.3 | 4.5 | 0.2 | 0.07 |
| CH2-10D-1H3N | 5.5 | 18.2 | 4.3 | 14.0 | -2.64 | 5.8 | 0.3 | 4.8 | 0.3 | 0.06 |
| CH2-10D-1H4N | 5.1 | 16.8 | 4.4 | 14.4 | -0.19 | 5.1 | 0.3 | 4.3 | 0.2 | 0.01 |
| CH2-10D-1H5N | 4.7 | 15.5 | 4.1 | 13.5 | -1.33 | 4.9 | 0.3 | 4.6 | 0.2 | 0.03 |
| CH2-10D-1H6N | 4.5 | 14.8 | 4.1 | 13.6 | -0.27 | 4.7 | 0.2 | 4.3 | 0.2 | 0.01 |
| CH2-10D-1H7N | 4.3 | 14.3 | 4.1 | 13.3 | -0.61 | 4.6 | 0.2 | 4.3 | 0.2 | 0.005 |
| **CH2-10D-1H8N** | **4.2** | **14.0** | **4.2** | **13.6** | **-0.42** | **4.5** | **0.2** | **4.5** | **0.2** | **0.01** |
| CH2-10D-1H9N | 4.2 | 13.9 | 4.2 | 13.6 | -0.53 | 4.5 | 0.2 | 4.5 | 0.2 | 0.02 |
| CH2-14D-1H3N | 5.4 | 17.9 | 4.2 | 13.0 | -2.98 | 5.8 | 0.3 | 3.7 | 0.2 | 0.06 |
| CH2-14D-1H4N | 5.4 | 17.8 | 4.6 | 14.4 | -3.33 | 5.6 | 0.3 | 4.1 | 0.2 | 0.06 |
| CH2-14D-1H5N | 4.8 | 15.9 | 4.6 | 14.3 | -2.76 | 5.0 | 0.3 | 4.4 | 0.2 | 0.06 |
| CH2-14D-1H6N | 4.7 | 15.4 | 4.5 | 14.0 | -1.14 | 4.9 | 0.3 | 4.1 | 0.2 | 0.04 |
| CH2-14D-1H7N | 4.3 | 14.1 | 4.3 | 13.5 | -2.16 | 4.7 | 0.2 | 4.4 | 0.2 | 0.05 |
| **CH2-14D-1H8N** | **4.2** | **14.0** | **4.2** | **13.2** | **-1.37** | **4.6** | **0.2** | **4.3** | **0.2** | **0.04** |
| CH2-14D-1H9N | 4.3 | 14.1 | 4.3 | 13.4 | -1.54 | 4.6 | 0.2 | 4.4 | 0.2 | 0.04 |
| CH2-21D-1H3N | 4.8 | 15.6 | 3.8 | 8.5 | -1.04 | 5.1 | 0.3 | 3.5 | 0.2 | 0.02 |
| CH2-21D-1H4N | 4.8 | 15.4 | 3.4 | 7.8 | -0.82 | 5.1 | 0.3 | 3.5 | 0.2 | 0.02 |
| CH2-21D-1H5N | 4.4 | 14.3 | 4.5 | 10.1 | -0.69 | 4.7 | 0.2 | 4.0 | 0.2 | 0.02 |
| CH2-21D-1H6N | 4.2 | 13.7 | 3.4 | 7.8 | -0.92 | 4.6 | 0.2 | 3.6 | 0.2 | 0.02 |
| CH2-21D-1H7N | 4.3 | 13.8 | 4.2 | 9.4 | 0.16 | 4.6 | 0.2 | 3.9 | 0.2 | -0.0001 |
| **CH2-21D-1H8N** | **4.2** | **13.6** | **4.2** | **9.4** | **0.09** | **4.5** | **0.2** | **4.1** | **0.2** | **-0.002** |
| CH2-21D-1H9N | 4.2 | 13.6 | 4.5 | 10.2 | 0.09 | 4,5 | 0.2 | 4.4 | 0.2 | -0.002 |
| CH2-28D-1H3N | 4.8 | 15.2 | 2.7 | 11.4 | -6.31 | 5.0 | 0.3 | 3.3 | 0.2 | 0.11 |
| CH2-28D-1H4N | 4.7 | 15.0 | 4.0 | 17.0 | -12.57 | 4.7 | 0.2 | 4.4 | 0.2 | 0.16 |
| CH2-28D-1H5N | 4.5 | 14.3 | 2.7 | 11.4 | -8.10 | 4.7 | 0.2 | 3.0 | 0.2 | 0.10 |
| CH2-28D-1H6N | 4.2 | 13.2 | 2.5 | 10.3 | -5.77 | 4.4 | 0.2 | 3.2 | 0.2 | 0.09 |
| CH2-28D-1H7N | 4.3 | 13.5 | 2.8 | 11.8 | -7.72 | 4.5 | 0.2 | 3.6 | 0.2 | 0.11 |
| **CH2-28D-1H8N** | **4.2** | **13.2** | **2.5** | **10.4** | **-5.48** | **4.5** | **0.2** | **3.4** | **0.2** | **0.09** |
| CH2-28D-1H9N | 4.1 | 13.2 | 2.4 | 10.3 | -6.04 | 4.4 | 0.2 | 3.2 | 0.2 | 0.10 |

*Table D.6: Results for chiller CH-2, split static – Y&C ANN models*

| Set name | Power - $Q_E$, $T_{CNDR}$, $T_{CHWS}$ | | | | | COP - $Q_E$, $T_{CNDR}$, $T_{CHWS}$ | | | | |
|---|---|---|---|---|---|---|---|---|---|---|
| | Training set | | Testing set | | | Training set | | Testing set | | |
| | CV, % | RMSE, kW | CV, % | RMSE, kW | MBE, kW | CV, % | RMSE | CV, % | RMSE | MBE |
| CH2-1WW-1H3N | 3.8 | 12.7 | 11.9 | 38.3 | 27.68 | 3.7 | 0.2 | 11.6 | 0.7 | -0.50 |
| CH2-1WW -1H4N | 2.6 | 8.8 | 12.6 | 40.4 | 26.51 | 3.0 | 0.2 | 11.9 | 0.7 | -0.47 |
| CH2-1WW -1H5N | 2.6 | 8.8 | 13.3 | 42.7 | 26.88 | 3.0 | 0.1 | 12.3 | 0.7 | -0.48 |
| CH2-1WW -1H6N | 2.6 | 8.6 | 12.5 | 40.2 | 27.09 | 2.9 | 0.1 | 12.0 | 0.7 | -0.48 |
| CH2-1WW -1H7N | 2.4 | 8.2 | 12.8 | 41.2 | 24.81 | 2.7 | 0.1 | 11.8 | 0.7 | -0.42 |
| **CH2-1WW -1H8N** | **2.2** | **7.5** | **15.7** | **50.4** | **23.41** | **2.3** | **0.1** | **15.7** | **0.9** | **-0.40** |
| CH2-1WW -1H9N | 2.2 | 7.3 | 12.9 | 41.5 | 22.17 | 2.2 | 0.1 | 12.3 | 0.7 | -0.37 |
| CH2-1WEH-1H3N | 2.4 | 8.0 | 2.4 | 8.1 | 1.73 | 2.3 | 0.1 | 2.0 | 0.1 | -0.02 |
| CH2-1WEH -1H4N | 2.4 | 8.0 | 2.3 | 7.8 | 1.79 | 2.3 | 0.1 | 2.0 | 0.1 | -0.02 |
| CH2-1WEH -1H5N | 2.4 | 8.1 | 2.4 | 8.0 | 1.89 | 2.3 | 0.1 | 2.0 | 0.1 | -0.02 |
| CH2-1WEH -1H6N | 2.4 | 8.0 | 2.3 | 7.8 | 1.89 | 2.3 | 0.1 | 2.0 | 0.1 | -0.02 |
| CH2-1WEH -1H7N | 2.4 | 8.1 | 2.4 | 8.0 | 1.88 | 2.3 | 0.1 | 2.0 | 0.1 | -0.02 |
| **CH2-1WEH -1H8N** | **2.4** | **8.1** | **2.4** | **8.0** | **1.72** | **2.3** | **0.1** | **2.0** | **0.1** | **-0.02** |
| CH2-1WEH -1H9N | 2.4 | 8.1 | 2.1 | 8.0 | 1.72 | 2.3 | 0.1 | 2.0 | 0.1 | -0.02 |
| CH2-2WW-1H3N | 3.8 | 12.5 | 3.5 | 12.6 | -3.22 | 4.0 | 0.2 | 3.6 | 0.2 | 0.03 |
| CH2-2WW -1H4N | 3.6 | 12.0 | 3.5 | 12.6 | -2.94 | 3.8 | 0.2 | 3.6 | 0.2 | 0.03 |
| CH2-2WW -1H5N | 3.4 | 11.2 | 3.5 | 12.4 | -1.14 | 3.8 | 0.2 | 3.6 | 0.2 | 0.03 |
| CH2-2WW -1H6N | 3.4 | 11.2 | 3.3 | 11.8 | -1.35 | 3.8 | 0.2 | 3.5 | 0.2 | 0.03 |
| CH2-2WW -1H7N | 3.2 | 10.5 | 3.2 | 11.4 | -1.08 | 3.5 | 0.2 | 3.4 | 0.2 | 0.03 |
| **CH2-2WW -1H8N** | **3.3** | **10.8** | **3.1** | **11.3** | **-1.30** | **3.6** | **0.2** | **3.4** | **0.2** | **0.04** |
| CH2-2WW -1H9N | 3.2 | 10.5 | 3.4 | 12.1 | -1.59 | 3.4 | 0.2 | 3.6 | 0.2 | 0.02 |
| CH2-2WEH-1H3N | 2.4 | 7.8 | 8.5 | 19.5 | 4.15 | 2.3 | 0.1 | 6.5 | 0.3 | 0.04 |
| CH2-2WEH -1H4N | 2.4 | 7.8 | 9.1 | 21.0 | 8.57 | 2.3 | 0.1 | 5.3 | 0.3 | -0.05 |
| CH2-2WEH -1H5N | 2.3 | 7.8 | 9.1 | 20.9 | 8.67 | 2.3 | 0.1 | 5.3 | 0.3 | -0.06 |
| CH2-2WEH -1H6N | 2.3 | 7.8 | 7.3 | 16.9 | 4.88 | 2.3 | 0.1 | 5.5 | 0.3 | -0.02 |
| CH2-2WEH -1H7N | 2.3 | 7.8 | 7.8 | 18.1 | 5.61 | 2.3 | 0.1 | 5.3 | 0.3 | -0.04 |
| **CH2-2WEH -1H8N** | **2.3** | **7.8** | **7.8** | **18.0** | **5.56** | **2.3** | **0.1** | **5.3** | **0.3** | **-0.04** |
| CH2-2WEH -1H9N | 2.3 | 7.8 | 7.9 | 18.2 | 5.90 | 2.3 | 0.1 | 5.4 | 0.3 | -0.03 |

214

*Table D.7: Results for chiller CH-1, classic static and augmented window –G&Ng and Swider ANN models*

| Set name | Power - $Q_E$, $T_{CNDR}$, $T_{CHWR}$ | | | | | COP - $Q_E$, $T_{CNDR}$, $T_{CHWR}$ | | | | |
|---|---|---|---|---|---|---|---|---|---|---|
| | Training set | | Testing set | | | Training set | | Testing set | | |
| | CV, % | RMSE, kW | CV, % | RMSE, kW | MBE, kW | CV, % | RMSE | CV, % | RMSE | MBE |
| CH1-30H-1H3N | 2.8 | 8.5 | 2.3 | 6.6 | -0.17 | 2.8 | 0.2 | 2.0 | 0.1 | -0.001 |
| CH1-30H -1H4N | 2.7 | 8.4 | 2.3 | 6.8 | -0.47 | 2.8 | 0.2 | 2.1 | 0.1 | 0.003 |
| CH1-30H -1H5N | 2.6 | 7.9 | 2.6 | 7.6 | 0.47 | 2.6 | 0.2 | 2.3 | 0.1 | -0.02 |
| CH1-30H -1H6N | 2.6 | 7.8 | 2.7 | 7.9 | -1.03 | 2.3 | 0.1 | 2.4 | 0.1 | 0.01 |
| CH1-30H -1H7N | 2.3 | 7.0 | 2.7 | 8.0 | -1.68 | 2.3 | 0.1 | 2.5 | 0.1 | 0.03 |
| **CH1-30H -1H8N** | **2.3** | **6.9** | **2.7** | **7.8** | **-1.18** | **2.3** | **0.1** | **2.4** | **0.1** | **0.02** |
| CH1-30H -1H9N | 2.3 | 7.0 | 2.6 | 7.6 | -0.99 | 2.3 | 0.1 | 2.4 | 0.1 | 0.02 |
| CH1-7D-1H3N | 4.2 | 13.3 | 3.5 | 8.5 | -1.47 | 4.3 | 0.2 | 6.6 | 0.3 | 0.17 |
| CH1-7D-1H4N | 4.2 | 13.3 | 3.5 | 8.3 | -1.61 | 4.3 | 0.2 | 6.5 | 0.3 | 0.16 |
| CH1-7D-1H5N | 3.5 | 11.2 | 3.8 | 9.0 | -3.47 | 3.6 | 0.2 | 5.9 | 0.3 | 0.13 |
| CH1-7D-1H6N | 3.5 | 11.0 | 4.3 | 10.4 | 2.37 | 3.5 | 0.2 | 5.3 | 0.3 | 0.08 |
| CH1-7D-1H7N | 3.4 | 10.8 | 4.4 | 10.6 | 3.08 | 3.4 | 0.2 | 4.7 | 0.2 | 0.07 |
| **CH1-7D-1H8N** | **3.3** | **10.5** | **3.5** | **8.4** | **-1.15** | **3.4** | **0.2** | **6.8** | **0.3** | **0.12** |
| CH1-7D-1H9N | 3.3 | 10.6 | 5.8 | 14.0 | 2.86 | 3.4 | 0.2 | 6.6 | 0.3 | 0.07 |
| CH1-10D-1H3N | 4.0 | 11.6 | 4.6 | 11.3 | -3.12 | 3.9 | 0.2 | 4.1 | 0.2 | 0.06 |
| CH1-10D-1H4N | 4.0 | 11.5 | 4.6 | 11.2 | -3.16 | 3.9 | 0.2 | 4.1 | 0.2 | 0.06 |
| CH1-10D-1H5N | 3.4 | 10.0 | 4.3 | 10.4 | -2.08 | 3.4 | 0.2 | 3.9 | 0.2 | 0.05 |
| CH1-10D-1H6N | 3.4 | 9.9 | 4.4 | 10.8 | -2.01 | 3.4 | 0.2 | 4.0 | 0.2 | 0.04 |
| CH1-10D-1H7N | 3.3 | 9.7 | 4.4 | 10.7 | -2.86 | 3.3 | 0.2 | 3.9 | 0.2 | 0.06 |
| **CH1-10D-1H8N** | **3.2** | **0.4** | **4.5** | **10.9** | **-1.74** | **3.2** | **0.2** | **4.0** | **0.2** | **0.03** |
| CH1-10D-1H9N | 3.2 | 9.4 | 4.4 | 10.7 | -1.52 | 3.2 | 0.2 | 3.9 | 0.2 | 0.03 |
| CH1-14D-1H3N | 4.0 | 11.4 | 5.2 | 16.2 | -11.71 | 3.9 | 0.2 | 4.1 | 0.2 | 0.17 |
| CH1-14D-1H4N | 4.0 | 11.3 | 4.7 | 14.4 | -10.59 | 3.0 | 0.2 | 4.4 | 0.2 | 0.18 |
| CH1-14D-1H5N | 3.5 | 9.9 | 32.9 | 13.3 | -7.78 | 3.4 | 0.2 | 3.8 | 0.2 | 0.12 |
| CH1-14D-1H6N | 3.4 | 9.7 | 4.6 | 14.4 | -8.58 | 3.4 | 0.2 | 4.0 | 0.2 | 0.13 |
| CH1-14D-1H7N | 3.4 | 9.6 | 4.2 | 13.0 | -7.91 | 3.3 | 0.2 | 4.2 | 0.2 | 0.14 |
| **CH1-14D-1H8N** | **3.3** | **9.3** | **4.2** | **13.0** | **-7.65** | **3.2** | **0.2** | **4.2** | **0.2** | **0.13** |
| CH1-14D-1H9N | 3.3 | 9.4 | 4.4 | 13.6 | -8.17 | 3.3 | 0.2 | 4.2 | 0.2 | 0.13 |
| CH1-21D-1H3N | 3.9 | 11.2 | 3.4 | 11.4 | -2.13 | 3.8 | 0.2 | 3.0 | 0.2 | 0.04 |
| CH1-21D-1H4N | 3.7 | 10.8 | 3.5 | 11.6 | -2.04 | 3.7 | 0.2 | 3.0 | 0.2 | 0.03 |
| CH1-21D-1H5N | 3.4 | 9.9 | 3.1 | 10.4 | -1.87 | 3.4 | 0.2 | 3.0 | 0.2 | 0.03 |
| CH1-21D-1H6N | 3.7 | 10.7 | 3.1 | 10.5 | -2.19 | 3.6 | 0.2 | 3.2 | 0.2 | 0.04 |
| CH1-21D-1H7N | 3.3 | 9.6 | 3.1 | 10.2 | -1.48 | 3.3 | 0.2 | 3.0 | 0.2 | 0.03 |
| **CH1-21D-1H8N** | **3.3** | **9.7** | **3.0** | **10.2** | **-1.36** | **3.3** | **0.2** | **2.9** | **0.2** | **0.03** |
| CH1-21D-1H9N | 3.2 | 9.4 | 3.6 | 12.1 | -1.71 | 3.3 | 0.2 | 3.7 | 0.2 | 0.03 |
| CH1-28D-1H3N | 3.6 | 11.0 | 4.9 | 15.5 | 6.93 | 3.6 | 0.2 | 5.3 | 0.3 | -0.13 |
| CH1-28D-1H4N | 3.6 | 11.0 | 4.8 | 15.2 | 6.94 | 3.6 | 0.2 | 5.4 | 0.3 | -01.3 |
| CH1-28D-1H5N | 3.3 | 10.0 | 4.2 | 13.3 | 5.78 | 3.2 | 0.2 | 4.7 | 0.3 | -0.11 |
| CH1-28D-1H6N | 3.2 | 9.8 | 4.3 | 13.6 | 6.09 | 3.2 | 0.2 | 4.7 | 0.3 | -0.11 |
| CH1-28D-1H7N | 3.2 | 9.9 | 4.3 | 13.8 | 6.07 | 3.2 | 0.2 | 4.8 | 0.3 | -0.11 |
| **CH1-28D-1H8N** | **3.1** | **9.6** | **4.1** | **13.1** | **5.78** | **3.1** | **0.2** | **4.7** | **0.3** | **-0.11** |
| CH1-28D-1H9N | 3.1 | 9.6 | 4.2 | 13.2 | 5.77 | 3.1 | 0.2 | 4.6 | 0.3 | -0.10 |

*Table D.8: Results for chiller CH-2, classic static and augmented window – G&Ng and Swider ANN models*

| Set name | Power - $Q_E$, $T_{CNDR}$, $T_{CHWR}$ | | | | | COP - $Q_E$, $T_{CNDR}$, $T_{CHWR}$ | | | | |
| | Training set | | Testing set | | | Training set | | Testing set | | |
| | CV, % | RMSE, kW | CV, % | RMSE, kW | MBE, kW | CV, % | RMSE | CV, % | RMSE | MBE |
| CH2-1D-1H3N | 2.8 | 8.0 | 2.8 | 9.7 | -0.49 | 2.4 | 0.1 | 2.8 | 0.1 | -0.01 |
| CH2-1D -1H4N | 2.8 | 7.9 | 3.0 | 10.2 | -0.39 | 2.4 | 0.1 | 2.8 | 0.1 | -0.01 |
| CH2-1D -1H5N | 2.8 | 7.9 | 2.9 | 9.9 | -0.26 | 2.4 | 0.1 | 2.8 | 0.1 | -0.01 |
| CH2-1D -1H6N | 2.8 | 7.9 | 2.8 | 9.7 | -0.12 | 2.4 | 0.1 | 2.9 | 0.1 | -0.01 |
| CH2-1D -1H7N | 2.8 | 7.9 | 2.8 | 9.6 | -0.02 | 2.4 | 0.1 | 2.9 | 0.1 | -0.01 |
| **CH2-1D -1H8N** | **2.8** | **7.9** | **2.8** | **9.6** | **0.05** | **2.4** | **0.1** | **2.9** | **0.1** | **-0.01** |
| CH2-1D -1H9N | 2.8 | 7.9 | 2.8 | 9.5 | 00.3 | 2.4 | 0.1 | 2.7 | 0.1 | -0.01 |
| CH2-7D-1H3N | 5.6 | 19.1 | 4.4 | 13.9 | -9.37 | 6.1 | 0.3 | 4.5 | 0.2 | 0.18 |
| CH2-7D-1H4N | 4.8 | 16.4 | 4.5 | 14.4 | -5.60 | 5.1 | 0.3 | 4.4 | 0.2 | 0.11 |
| CH2-7D-1H5N | 4.4 | 14.8 | 4.2 | 13.3 | -4.45 | 4.7 | 0.2 | 4.3 | 0.2 | 0.09 |
| CH2-7D-1H6N | 4.5 | 15.2 | 4.6 | 14.7 | -3.31 | 4.8 | 0.2 | 4.3 | 0.2 | 0.08 |
| CH2-7D-1H7N | 4.4 | 14.8 | 4.1 | 13.0 | -3.00 | 4.6 | 0.2 | 4.3 | 0.2 | 0.09 |
| **CH2-7D-1H8N** | **4.3** | **14.4** | **4.3** | **13.7** | **-3.42** | **4.5** | **0.2** | **4.3** | **0.2** | **0.09** |
| CH2-7D-1H9N | 4.1 | 13.9 | 4.1 | 13.1 | -3.54 | 4.4 | 0.2 | 4.4 | 0.2 | 0.09 |
| CH2-10D-1H3N | 5.4 | 18.0 | 4.3 | 13.9 | -2.80 | 5.8 | 0.3 | 4.8 | 0.3 | 0.06 |
| CH2-10D-1H4N | 4.7 | 15.5 | 4.1 | 13.3 | 0.44 | 4.9 | 0.3 | 4.4 | 0.2 | 0.01 |
| CH2-10D-1H5N | 4.4 | 14.6 | 3.9 | 12.7 | -1.11 | 4.7 | 0.2 | 4.2 | 0.2 | 0.02 |
| CH2-10D-1H6N | 4.5 | 14.8 | 4.1 | 13.5 | -0.27 | 4.7 | 0.2 | 4.3 | 0.2 | 0.01 |
| CH2-10D-1H7N | 4.5 | 14.8 | 4.2 | 13.6 | -0.41 | 4.6 | 0.2 | 4.4 | 0.2 | 0.01 |
| **CH2-10D-1H8N** | **4.2** | **14.0** | **4.0** | **13.1** | **-0.30** | **4.5** | **0.2** | **4.4** | **0.2** | **0.02** |
| CH2-10D-1H9N | 4.2 | 14.1 | 4.0 | 13.2 | -0.58 | 4.5 | 0.2 | 4.3 | 0.2 | 0.02 |
| CH2-14D-1H3N | 5.3 | 17.4 | 3.8 | 11.9 | -2.54 | 5.7 | 0.3 | 3.6 | 0.2 | 0.06 |
| CH2-14D-1H4N | 5.4 | 17.7 | 4.6 | 14.2 | -3.36 | 5.6 | 0.3 | 4.0 | 0.2 | 0.06 |
| CH2-14D-1H5N | 4.8 | 15.9 | 4.8 | 15.0 | -3.26 | 5.0 | 0.3 | 4.5 | 0.2 | 0.06 |
| CH2-14D-1H6N | 4.4 | 14.7 | 4.2 | 13.0 | -2.10 | 4.8 | 0.3 | 4.3 | 0.2 | 0.05 |
| CH2-14D-1H7N | 4.4 | 14.4 | 4.4 | 13.6 | -1.46 | 4.8 | 0.2 | 4.2 | 0.2 | 0.04 |
| **CH2-14D-1H8N** | **4.3** | **14.1** | **4.2** | **13.1** | **-1.28** | **4.7** | **0.2** | **4.2** | **0.2** | **0.04** |
| CH2-14D-1H9N | 4.3 | 14.1 | 4.3 | 13.3 | -1.32 | 4.7 | 0.2 | 4.2 | 0.2 | 0.04 |
| CH2-21D-1H3N | 4.8 | 15.6 | 3.7 | 8.5 | -1.05 | 5.1 | 0.3 | 3.5 | 0.2 | 0.02 |
| CH2-21D-1H4N | 4.8 | 15.4 | 3.5 | 7.8 | -0.81 | 5.1 | 0.3 | 3.5 | 0.2 | 0.02 |
| CH2-21D-1H5N | 4.5 | 14.6 | 4.5 | 10.2 | -0.37 | 4.7 | 0.2 | 4.0 | 0.2 | 0.01 |
| CH2-21D-1H6N | 4.3 | 13.8 | 3.6 | 8.3 | 0.36 | 4.6 | 0.2 | 3.6 | 0.2 | -0.003 |
| CH2-21D-1H7N | 4.4 | 14.2 | 4.9 | 11.1 | -1.44 | 4.6 | 0.2 | 4.3 | 0.2 | 0.03 |
| **CH2-21D-1H8N** | **4.1** | **13.3** | **5.0** | **11.3** | **-1.1** | **4.4** | **0.2** | **4.3** | **0.2** | **0.02** |
| CH2-21D-1H9N | 4.1 | 13.3 | 5.1 | 11.6 | -1.21 | 4.4 | 0.2 | 4.2 | 0.2 | 0.02 |
| CH2-28D-1H3N | 4.8 | 15.2 | 2.7 | 11.2 | -6.02 | 5.0 | 0.3 | 3.3 | 0.2 | 0.11 |
| CH2-28D-1H4N | 4.7 | 15.0 | 2.5 | 10.4 | -7.37 | 5.0 | 0.3 | 3.1 | 0.2 | 0.11 |
| CH2-28D-1H5N | 4.3 | 13.7 | 3.0 | 12.5 | -7.82 | 4.5 | 0.2 | 3.8 | 0.2 | 0.12 |
| CH2-28D-1H6N | 4.1 | 13.2 | 2.5 | 10.3 | -5.43 | 4.4 | 0.2 | 3.2 | 0.2 | 0.09 |
| CH2-28D-1H7N | 4.2 | 13.4 | 2.8 | 11.6 | -8.37 | 4.5 | 0.2 | 3.5 | 0.2 | 0.12 |
| **CH2-28D-1H8N** | **4.2** | **13.4** | **2.7** | **11.3** | **-6.72** | **4.5** | **0.2** | **3.5** | **0.2** | **0.10** |
| CH2-28D-1H9N | 4.1 | 13.2 | 2.6 | 10.8 | -6.99 | 4.4 | 0.2 | 3.2 | 0.2 | 0.10 |

*Table D.9: Results for chiller CH-2, split static – G&Ng and Swider ANN models*

| Set name | Power - $Q_E$, $T_{CNDR}$, $T_{CHWR}$ | | | | | COP - $Q_E$, $T_{CNDR}$, $T_{CHWR}$ | | | | |
|---|---|---|---|---|---|---|---|---|---|---|
| | Training set | | Testing set | | | Training set | | Testing set | | |
| | CV, % | RMSE, kW | CV, % | RMSE, kW | MBE, kW | CV, % | RMSE | CV, % | RMSE | MBE |
| CH2-1WW-1H3N | 2.9 | 9.6 | 17.6 | 56.5 | 20.73 | 3.2 | 0.2 | 14.8 | 0.8 | -0.39 |
| CH2-1WW -1H4N | 2.7 | 8.9 | 12.8 | 41.0 | 25.94 | 3.0 | 0.2 | 12.1 | 0.7 | -0.46 |
| CH2-1WW -1H5N | 2.6 | 8.6 | 13.1 | 42.0 | 24.46 | 2.9 | 0.1 | 12.0 | 0.7 | -0.43 |
| CH2-1WW -1H6N | 2.5 | 8.4 | 12.5 | 40.2 | 23.72 | 2.8 | 0.1 | 11.6 | 0.7 | -0.42 |
| CH2-1WW -1H7N | 2.4 | 8.1 | 13.1 | 42.2 | 24.01 | 2.7 | 0.1 | 12.1 | 0.7 | -0.41 |
| **CH2-1WW -1H8N** | **2.3** | **7.6** | **13.9** | **44.6** | **22.25** | **2.3** | **0.1** | **12.7** | **0.7** | **-0.38** |
| CH2-1WW -1H9N | 2.2 | 7.2 | 13.6 | 43.6 | 21.43 | 2.2 | 0.1 | 12.6 | 0.7 | -0.37 |
| CH2-1WEH-1H3N | 2.5 | 8.6 | 2.4 | 8.0 | 1.08 | 2.2 | 0.1 | 1.9 | 0.1 | -0.01 |
| CH2-1WEH -1H4N | 2.4 | 8.0 | 2.2 | 7.5 | 1.20 | 2.2 | 0.1 | 2.0 | 0.1 | -0.01 |
| CH2-1WEH -1H5N | 2.4 | 8.0 | 2.2 | 8.0 | 1.53 | 2.2 | 0.1 | 2.0 | 0.1 | -0.01 |
| CH2-1WEH -1H6N | 2.4 | 7.9 | 2.3 | 7.6 | 1.65 | 2.2 | 0.1 | 2.0 | 0.1 | -0.01 |
| CH2-1WEH -1H7N | 2.4 | 7.9 | 2.3 | 7.6 | 1.63 | 2.2 | 0.1 | 2.0 | 0.1 | -0.01 |
| **CH2-1WEH -1H8N** | **2.4** | **7.9** | **2.2** | **7.6** | **1.62** | **2.2** | **0.1** | **2.0** | **0.1** | **-0.01** |
| CH2-1WEH -1H9N | 2.4 | 7.9 | 2.2 | 7.6 | 1.62 | 2.2 | 0.1 | 2.0 | 0.1 | -0.01 |
| CH2-2WW-1H3N | 5.9 | 19.5 | 3.6 | 13.0 | -5.71 | 6.3 | 0.3 | 3.8 | 0.2 | 0.11 |
| CH2-2WW -1H4N | 5.2 | 17.2 | 4.8 | 17.1 | -6.05 | 5.2 | 0.3 | 4.7 | 0.2 | 0.07 |
| CH2-2WW -1H5N | 4.7 | 15.5 | 4.0 | 14.3 | -3.24 | 5.1 | 0.3 | 4.4 | 0.2 | 0.06 |
| CH2-2WW -1H6N | 4.6 | 15.2 | 3.9 | 13.9 | -2.39 | 5.0 | 0.3 | 4.3 | 0.2 | 0.06 |
| CH2-2WW -1H7N | 4.7 | 15.3 | 3.9 | 13.9 | -2.99 | 5.0 | 0.3 | 4.3 | 0.2 | 0.07 |
| **CH2-2WW -1H8N** | **4.4** | **14.3** | **3.6** | **13.0** | **-1.22** | **4.7** | **0.2** | **4.1** | **0.2** | **0.04** |
| CH2-2WW -1H9N | 4.4 | 14.4 | 3.9 | 13.8 | -2.25 | 4.7 | 0.2 | 4.3 | 0.2 | 0.05 |
| CH2-2WEH-1H3N | 2.4 | 7.9 | 10.7 | 24.6 | 11.12 | 2.3 | 0.1 | 5.4 | 0.3 | -0.08 |
| CH2-2WEH -1H4N | 2.4 | 7.9 | 9.7 | 22.3 | 9.45 | 2.3 | 0.1 | 5.4 | 0.3 | -0.07 |
| CH2-2WEH -1H5N | 2.4 | 7.9 | 9.4 | 21.7 | 8.86 | 2.3 | 0.1 | 5.4 | 0.3 | -0.07 |
| CH2-2WEH -1H6N | 2.3 | 7.8 | 7.9 | 18.1 | 5.57 | 2.3 | 0.1 | 5.8 | 0.3 | -0.02 |
| CH2-2WEH -1H7N | 2.3 | 7.7 | 8.0 | 18.4 | 5.53 | 2.3 | 0.1 | 5.8 | 0.3 | -0.02 |
| **CH2-2WEH -1H8N** | **2.3** | **7.8** | **7.7** | **17.8** | **5.10** | **2.2** | **0.1** | **5.8** | **0.3** | **-0.01** |
| CH2-2WEH -1H9N | 2.3 | 7.8 | 7.8 | 17.9 | 4.96 | 2.2 | 0.1 | 5.9 | 0.3 | -0.01 |

# Appendix E: TRNSYS default model coefficients

*Table E.1: Data of chiller capacity to cooling capacity at design conditions and COP to COP at design conditions*

| Water Temperature | | TRNSYS default coefficients | | New TRNSYS coefficients | |
|---|---|---|---|---|---|
| CHWS, °C | CWT, °C | Capacity ratio, kW/kW | COP ratio | Capacity ratio, kW/kW | COP ratio |
| 5 | 16 | 1.0403 | 1.3348 | **0.8942** | **1.1508** |
| 5 | 20 | 1.0161 | 1.1843 | 0.8709 | 1.1146 |
| 5 | 25 | 0.9859 | 1.0742 | 0.9003 | 0.9549 |
| 5 | 30 | 0.9556 | 0.9596 | 0.8799 | 0.8610 |
| 5 | 35 | 0.9250 | 0.8629 | 0.8538 | 0.7761 |
| 5 | 40 | 0.8951 | 0.7775 | | |
| 6 | 16 | 1.0623 | 1.3573 | 0.9171 | 1.2876 |
| 6 | 20 | 1.0381 | 1.2292 | **0.8938** | **1.2738** |
| 6 | 25 | 1.0081 | 1.0944 | 0.9234 | 1.0895 |
| 6 | 30 | 0.9778 | 0.9798 | 0.9030 | 0.9955 |
| 6 | 35 | 0.9475 | 0.8809 | 0.8772 | 0.9084 |
| 6 | 40 | 0.9175 | 0.7978 | | |
| 7 | 16 | 1.0843 | 1.3820 | 0.9987 | 1.2627 |
| 7 | 20 | 1.0601 | 1.2517 | 0.9754 | 1.2468 |
| 7 | 25 | 1.0301 | 1.1169 | **1.0050** | **1.0624** |
| 7 | 30 | 1.0000 | 1.0000 | 0.9848 | 0.9661 |
| 7 | 35 | 0.9699 | 0.9011 | 0.9592 | 0.8791 |
| 7 | 40 | 0.9397 | 0.8157 | | |
| 8 | 16 | 1.1061 | 1.4045 | 1.0304 | 1.3059 |
| 8 | 20 | 1.0821 | 1.2742 | 1.0073 | 1.2899 |
| 8 | 25 | 1.0521 | 1.1371 | 1.0369 | 1.1238 |
| 8 | 30 | 1.0222 | 1.0202 | **1.0169** | **1.0069** |
| 8 | 35 | 0.9921 | 0.9191 | 0.9913 | 0.9177 |
| 8 | 40 | 0.9621 | 0.8337 | | |
| 9 | 16 | 1.1281 | 1.4270 | 1.0569 | 1.3402 |
| 9 | 20 | 1.1041 | 1.2966 | 1.0338 | 1.3241 |
| 9 | 25 | 1.0743 | 1.1573 | 1.0636 | 1.1353 |
| 9 | 30 | 1.0444 | 1.0404 | 1.0436 | 1.0390 |
| 9 | 35 | 1.0143 | 0.9393 | **1.0180** | **0.9497** |
| 9 | 40 | 0.9845 | 0.8517 | | |
| 10 | 16 | 1.1501 | 1.4494 | | |
| 10 | 20 | 1.1261 | 1.3191 | | |
| 10 | 25 | 1.0963 | 1.1798 | | |
| 10 | 30 | 1.0666 | 1.0607 | | |
| 10 | 35 | 1.0367 | 0.9573 | | |
| 10 | 40 | 1.0069 | 0.8697 | | |

*Table E.2: TRNSYS default data of chiller electric PWR versus part-load cooling load PLR*

| PLR | Fraction of Full Load Power |
|---|---|
| 0.0 | 0.0000 |
| 0.25 | 0.2497 |
| 0.50 | 0.4956 |
| 0.75 | 0.6902 |
| 1.00 | 1.0000 |